

DEGLACIATION DYNAMICS
OF THE FEEGLETSCHER NORD, SWITZERLAND:
IMPLICATIONS FOR GLACIO-FLUVIAL SEDIMENT TRANSFER

Martin J Smart

Submitted to the University of Hertfordshire
in partial fulfilment of the requirements of the degree of
Doctor of Philosophy

September 2015

Abstract

Understanding of the processes of sediment transfer within, and from, glaciated catchments is of fundamental importance in order to establish rates of sediment transfer and resultant landscape evolution. Rates of glacio-fluvial sediment transfer are strongly controlled by glacier meltwater runoff and the availability of sediments for entrainment. However, it is becoming apparent that recently deglaciated forefields can modify the patterns of suspended sediment transfer. Glacier shrinkage exposes areas of unstable glacial sediments that can be subject to reworking and redistribution, and, as these environments become ice-free, heightened levels of geomorphological activity (so-called 'paraglacial' activity) are also likely to have a significant impact on both sediment and water yields from deglaciating catchments. Consequently, questions are raised as to the impacts of deglaciation upon contemporary and future rates of suspended sediment transfer, and the resultant fluvial sediment loads and rates of landscape adjustment. Therefore, the aim of this research was to present an integrated study of how sediment transfer in a glaciated catchment functions during, and is responding to, deglaciation. A variety of techniques were employed to examine the hydrological functioning of an Alpine glacier, the Feegletscher Nord, Switzerland, and the resultant temporal and spatial patterns of sediment transfer in light of catchment hydrology, ablation processes and forefield geomorphology. Data was collected over two field campaigns in 2010 and 2012 to capture the inputs, throughputs and outputs of meltwater and sediment. This research found that patterns of sediment transfer were modified within the proglacial zone, reinforcing previous findings that the location of proglacial monitoring is important in determining the observed patterns of sediment transfer. These patterns of sediment transfer were attributed to variations in forefield sediment availability, which appeared to demonstrate marked spatial variability. This variability was hypothesised to be influenced by the geomorphological characteristics of the forefield, including rock fall debris that appeared to limit sediment availability, and glacial sediments that enhanced the availability of in-channel and channel-marginal sediments. These findings suggest that the investigation of rates of sediment transfer and paraglacial sedimentation may be complicated in catchments that have experienced complex geomorphological responses to deglaciation. In addition, the investigation of sediment transfer processes and the development of a glacier runoff model enabled the exploration of future suspended sediment loads with progressive deglaciation and a changing climate. Suspended sediment loads were predicted to experience rapid declines until the end of the 21st Century due to reductions in meltwater runoff as glacier extent is reduced. However, it is suggested that uncertainties in future sediment availability limit the usefulness of such forecasts. Consequently, this research highlights how the understanding of both sedimentary and hydrological processes in glaciated catchments may be enhanced by consideration of the changes that can occur in these environments associated with glacier shrinkage and a changing climate.

Acknowledgements

There are many people to whom I owe thanks for their support. The most thanks are owed to my supervisor Dr Phil Porter. The project builds upon and, in many ways, is the culmination of a programme of research Phil conceived at the Feegletscher, where he has not only undertaken considerable research but has done so whilst providing excellent opportunities for undergraduate and postgraduate students to engage with his research and that of his fellow researchers. The original inspiration for this project came from his dedication to engaging his students in his research and fieldwork, of which I was fortunate to benefit from as an undergraduate and postgraduate student. The academic guidance, support and expertise I have received from Phil has been tremendous and I have been incredibly lucky to have been so well supervised with such dedication and attention. I am also thankful to Phil for his personal support in many ways and I am very proud for this project to have given me the opportunity to pursue an academic career and contribute to the small but excellent glaciological research that is undertaken at the University of Hertfordshire, which clearly has a bright future ahead.

A debt of gratitude is also owed to Dr Tris Irvine-Fynn for the time and effort he has given me as my second supervisor. His unrivalled knowledge of glaciological literature and the current research themes across the breadth of the subject has made Tris invaluable to the success of this project. Tris has made invaluable contributions in guiding the strategic course of this research and through his encouragement in keeping it on track. His advice and support, particularly in the modelling aspects of the research, were tremendous and I thank him for delivering it with good humour and sincere encouragement and enthusiasm for this research.

Thanks is also due to Dr Tim Sands who acted as my second supervisor in the early stages of this research programme. His insights into the project and advice in the field were very helpful and he has been a thoroughly supportive colleague throughout this project, which has been very appreciated.

There are a number of other individuals to whom sincere thanks is due. First and foremost, to Charlotte Wilkes for providing wonderful company in the field and for giving up her summer in 2012 to volunteer and support me with assistance in data collection. Her dedication to this research and good humour made a long and challenging field season a joy and I am in her debt for that. Thanks are also due to Iain Cross for his excellent company and humour in the field and for showing us what culinary wonders can be achieved on a camping stove. Andy Lowe is thanked for providing excellent advice regarding glacier melt models, and his own glacier melt model formed the basis for the runoff modelling workshop taught to me by Phil when I was an undergraduate, which first introduced me to the topic. Thanks with field assistance are also due to Simon Cook, Craig Wilkinson, Owen Courtney, Victoria Kirkwood, Carina Spooner, and

Harriet Loughman, who all helped in many ways during the two field campaigns, and not least are thanked for their excellent company, hard work and cooking skills.

On a more personal note, Rebecca Edwards is thanked for her friendship and company during this project, and for making working in our small windowless office ('the cupboard') for all those years so much fun with so many great memories.

Thanks are also due for the excellent technical support I have received over the course of this project. Peter Coates, Joanna Elvy, Aiden Bygrave, Di Francis and Jamie Stone are all owed thanks for their help in many varied tasks from the ordering and preparation of field equipment, to laboratory assistance, to the printing of this thesis.

Thanks and gratitude are also owed to MeteoGroup who kindly provided meteorological data. Funding for the fieldwork in 2012 from the Dudley Stamp Memorial Fund is gratefully acknowledged. In addition, funding was gratefully received for fieldwork from the School of Life and Medical Sciences, University of Hertfordshire.

Finally, my parents are owed the most thanks for their love and unending support, without which this project would never have been possible.

Contents

List of Figures.....	viii
Life of Tables.....	xii
Glossary of terms and abbreviations.....	xv
1 Introduction.....	1
1.1 Context.....	1
1.2 Research Aim and Objectives.....	4
1.3 Thesis Structure.....	6
2 Glacio-Fluvial Sediment Transfer: A Review.....	8
2.1 Introduction.....	8
2.2 Glacier Thermal Regime.....	10
2.3 Glacier Hydrology.....	10
2.3.1 Hydrological System Morphology.....	10
2.3.2 Water Flow in Glacier Drainage Systems.....	13
2.3.3 Drainage System Dynamics.....	15
2.3.4 Controls on Glacier Runoff.....	17
2.4 Sediment Transfer.....	23
2.4.1 Sediment Production.....	23
2.4.2 Mechanisms of Sediment Transfer.....	27
2.4.3 Proglacial Sediment Transfer.....	44
2.5 Geomorphological responses to Deglaciation.....	48
2.5.1 Models of Landscape response to Deglaciation.....	48
2.5.2 Paraglacial activity.....	52
2.6 Summary.....	59
3 Field Site and Data Collection.....	62
3.1 Introduction.....	62
3.2 The Alps.....	62
3.2.1 Geological and Glacial History.....	62
3.2.2 Contemporary Climate.....	65
3.3 The Feegletscher.....	66
3.3.1 Geometry and Mass Balance.....	66
3.3.2 Glacier Hydrology.....	75
3.3.3 Feegletscher Geology and Geomorphology..	76
3.3.4 Proglacial Hydrology.....	79
3.4 Data Collection.....	82
3.4.1 Monitoring sites.....	82
3.4.2 Meteorology.....	82
3.4.3 Glacier surveying.....	86

	3.4.4	Proglacial Stream Monitoring.....	89
	3.4.4.1	Discharge.....	92
	3.4.4.2	Suspended Sediment Concentration.....	94
	3.4.5	Dye tracing.....	95
4		Hydrometeorological Data Series.....	98
	4.1	Introduction.....	98
	4.2	Meteorology.....	98
	4.2.1	Time-series.....	98
	4.2.2	Lapse rates.....	102
	4.3	Glacier ablation.....	105
	4.4	Proglacial stream data.....	106
	4.5	Dye tracing.....	115
	4.6	Summary.....	117
5		Characteristics of Runoff and Suspended Sediment Transfer from the Feegletscher Nord.....	119
	5.1	Introduction.....	119
	5.2	Overview of analytical techniques.....	120
	5.3	Cross-correlations.....	122
	5.3.1	Discharge.....	122
	5.3.2	Suspended Sediment Concentrations.....	127
	5.4	Recession Analysis.....	130
	5.4.1	Hydrograph recession analysis.....	131
	5.4.1.1	Hydrograph Recession Results.....	132
	5.5	Classification Procedure.....	138
	5.5.1	Hydrograph Classification Method.....	139
	5.5.1.1	Hydrograph Classification Results... ..	140
	5.5.2	SSC curve Classification Method.....	148
	5.5.2.1	SSC curve Classification Results.....	149
	5.6	Summary.....	169
6		Modelling Glacier Ablation and Runoff.....	172
	6.1	Introduction.....	172
	6.2	Outline to runoff modelling.....	173
	6.3	Energy Balance Models.....	175
	6.4	Temperature-Index Models.....	178
	6.4.1	Introduction.....	178
	6.4.2	Degree-day models.....	179
	6.5	Development and Application of the Feegletscher Temperature-Index Model (FTIM).....	183
	6.5.1	Model Outline.....	183
	6.5.1.1	Temperature Component.....	184

	6.5.1.2	Threshold Temperature Component	185
	6.5.1.3	Precipitation Component.....	187
	6.5.1.4	Spatial Distribution.....	187
	6.5.1.5	Degree-Day Factors.....	188
	6.5.2	Modelled Runoff from the Feegletscher Nord....	197
	6.5.3	Meltwater Routing.....	203
	6.6	Summary of FTIM.....	211
7		Glacio-Fluvial Suspended Sediment Transfer and Deglaciation...	213
	7.1	Introduction.....	213
	7.2	Outline to approach.....	215
	7.3	Suspended Sediment and Discharge Relationships.....	217
	7.4	Rainfall and SSC.....	233
	7.5	Forward Modelling of Sediment Transfer.....	247
	7.5.1	Forward Modelling Approach.....	249
	7.5.2	Future Perspectives for Glacier Runoff and Suspended Sediment Transfer.....	256
	7.6	Summary.....	262
8		Synthesis and Conclusion.....	266
	8.1	Introduction.....	266
	8.2	Research Synthesis.....	269
	8.2.1	Hydrology of the Feegletscher Nord.....	269
	8.2.1.1	Hydrological System.....	270
	8.2.1.2.	Meltwater Storage.....	274
	8.2.1.3	Simulation of Glacier Ablation and Runoff.....	277
	8.2.2	Glacio-Fluvial Sediment Transfer.....	281
	8.2.2.1	Patterns and Trends in Proglacial SSC.....	283
	8.2.2.2	Controls on Proglacial SSC.....	285
	8.2.3	Glacio-Fluvial Sediment Transfer and Deglaciation..	295
	8.3	Future Research Priorities.....	299
	8.4	Thesis Summary Conclusion.....	306
		Bibliography.....	308

List of Figures

2.1	Schematic diagram of the model of glacier hydrological networks.....	11
2.2	Typical diurnal relationship between meltwater runoff, air temperature and incoming solar radiation from Gregory (1987).....	18
2.3	Relationship between suspended sediment yield and annual discharge volume for 43 basins.....	25
2.4	Scatter plot of suspended sediment concentration and discharge observations from Glacier de Tsijiore Nouve, Switzerland.....	31
2.5	Diurnal hysteresis plots between discharge and suspended sediment concentration.....	33
2.6	Sediment yield during the paraglacial period.....	49
2.7	Specific sediment yield during the paraglacial period as a function of basin size	52
3.1	Photograph of the Feegletscher Nord taken on DOY 210, 2012.....	93
3.2	2011 Satellite image of Feegletscher Nord.....	67
3.3	Cumulative length variation of the Feegletscher Nord from 1883 to 2014.....	68
3.4	Lateral moraine marking Little Ice Age of Feegletscher Nord.....	69
3.5	Feegletscher Nord in 1918 close to maximum Little Ice Age extent.....	70
3.6	Aerial images of the proglacial zone of the Feegletscher Nord in 1941, 1946 and 1968.....	71
3.7	Aerial images of the proglacial zone of the Feegletscher Nord in 1972, 1980 and 1990.....	72
3.8	Aerial images of the proglacial zone of the Feegletscher Nord in 1995, 1999 and 2000.....	73
3.9	Aerial images of the proglacial zone of the Feegletscher Nord in 2011.....	74
3.10	Aerial image of the proglacial zone of the Feegletscher Nord highlighting hydrological features.....	79
3.11	2009 photograph of the upper proglacial lake at the Feegletscher Nord.....	81
3.12	2012 photograph of the upper proglacial lake at the Feegletscher Nord following sedimentation.....	81
3.13	Catchment map indicating locations of monitoring sites utilised in field campaigns.....	84
3.14	Map of Feegletscher Nord proglacial zone with monitoring stations.....	85
3.15	Photograph of installation and location of ablation Stake A.....	87
3.16	Photograph of installation and location of ablation Stake B.....	87
3.17	Photograph of location of ablation Stake C.....	88
3.18	Photograph of location of ablation Stake D.....	88
3.19	Photograph of Station A.....	90

3.20	Photograph of Station B.....	91
3.21	Photograph of Station C.....	91
3.22	Photograph of Station D.....	92
4.1	Meteorological data recorded at Saas Fee weather Station in 2012.....	100
4.2	Charts of air temperature recorded at three altitudes with elevation of 0°C isotherm calculated with environmental lapse rate.....	101
4.3	Time series of air temperature at three monitoring stations with calculated lapse rates between the stations and mean daily air temperatures at the three stations...	104
4.4	Glacier ablation recorded at four ablation stakes plotted against time and cumulative positive degree intervals.....	105
4.5	SSC and discharge recorded at Station B along with air temperature and precipitation recorded at Saas Fee weather Station during 2012.....	110
4.6	SSC and discharge recorded at Station C along with air temperature and precipitation recorded at Saas Fee weather Station during 2012.....	111
4.7	SSC and discharge recorded at Station D along with air temperature and precipitation recorded at Saas Fee weather Station during 2012.....	111
4.8	Discharge time-series at Station A during 2012.....	112
4.9	Discharge and SSC time-series at Station A during DOY 224.....	112
4.10	Suspended sediment load at stations B, C and D during 2012.....	114
4.11	Results of dye tracing through subterranean drainage pathways draining the upper proglacial lake.....	116
4.12	Dye tracing performed through upper proglacial lake.....	116
4.13	Second dye trace performed through upper proglacial lake.....	117
5.1	Results of cross-correlation analysis showing a) the daily lag between peak discharge and maximum air temperature and minimum discharge and minimum air temperature and b) the daily lag between air temperature and proglacial discharge.....	125
5.2	Results of cross-correlation analysis for proglacial SSC at Stations B, C and D...	129
5.3	<i>K</i> -values derived from the analysis of 37 hydrograph recessions.....	137
5.4	Plot of the Principal Component scores for the four identified components of the diurnal hydrographs.....	141
5.5	Six representative hydrograph forms obtained by hydrograph classification according to shape and magnitude.....	144
5.6	Plots of temporal patterns in hydrograph shape and magnitude and meteorological periods along with mean daily proglacial discharge.....	145
5.7	Plot of PC scores at the three proglacial suspended sediment gauging Stations...	154
5.8	Composite SSC curve classification classes for Station B.....	160
5.9	Composite SSC curve classification classes for Station C.....	161

5.10	Composite SSC curve classification classes for Station D.....	162
5.11	Composite plots for Station B of mean daily discharge and total daily suspended sediment load, daily rainfall total and mean daily air temperature, with SSC shape and magnitude classifications.....	166
5.12	Composite plots for Station C of mean daily discharge and total daily suspended sediment load, daily rainfall total and mean daily air temperature, with SSC shape and magnitude classifications.....	167
5.13	Composite plots for Station D of mean daily discharge and total daily suspended sediment load, daily rainfall total and mean daily air temperature, with SSC shape and magnitude classifications.....	168
6.1	Correlations between threshold temperature for melt and observed ablation at each ablation stake.....	186
6.2	Trends in degree-day factors at the four ablation stakes over the 2012 monitoring period.....	190
6.3	Plot of observed ablation and simulated ablation using optimised scaling degree-day factors.....	187
6.4	Time-series of hourly measured discharge and predicted potential runoff.....	200
6.5	Plot of residuals in the OLS regression of measured runoff, simulated ablation and rainfall.....	201
6.6	Time-series plots of the daily water budget, daily total discharge and simulated potential runoff, and cumulative daily total discharge and simulated runoff.....	202
6.7	Plot of simulated potential runoff and net storage.....	208
6.8	Time-series of optimised modelling runoff incorporating routing parameters along with discharge and a time-series of simulated runoff incorporating predicted net storage.....	209
7.1	Plot of measured total proglacial SSC for DOY 202-232 and predicted proglacial SSC from the multivariate regression model.....	230
7.2	Plot of 2-minute total proglacial discharge and SSC along with hourly air temperature and precipitation and residual SSC from the pooled MRM of total proglacial SSC.....	231
7.3	Plot of residual log SSC and air temperature for DOY 203-231.....	232
7.4	Proglacial SSC and discharge responses at Station D to the rainfall event on DOY 184.....	242
7.5	Proglacial SSC and discharge responses at Stations B and C to the rainfall event on DOY 210.....	243
7.6	Proglacial SSC and discharge responses at Stations B and C to the rainfall event on DOY 217.....	244

7.7	Proglacial SSC and discharge responses at Stations B and C to the rainfall event on DOY 218.....	245
7.8	Proglacial SSC and discharge responses at Stations B and C to the rainfall event on DOY 219.....	246
7.9	Proglacial SSC and discharge responses at Station B to the rainfall event on DOY 233.....	247
7.10	Hypsometric curve of the Feegletscher Nord glacier area and the possible future area changes applied to the model.....	255
7.11	Modelled total suspended sediment loads for DOY 180-251 from the reference period (1980-2009) and 2012 to the end of the 21 st Century.....	262

List of Tables

2.1	Mechanisms of glacier erosion and their associated processes.....	27
3.1	Calibration curves to transfer stage to discharge.....	80
3.2	Calibration curves to transfer turbidity to SSC.....	95
4.1	Descriptive statistics of meteorological time-series.....	102
4.2	Descriptive statistics for discharge and SSC time-series.....	107
4.3	Correlation and cross-correlation analysis of 2012 discharge, SSC and air temperature time-series.....	113
5.1	Descriptive statistics of <i>K</i> -values derived from hydrograph recession curve analysis	136
5.2	Summary of the PCA performed on the 2012 discharge hydrographs along with the cluster identified from the Principal Component (PC) loadings.....	140
5.3	Daily means of the four bulk flow indices used to classify hydrograph magnitude cluster.....	142
5.4	Summary statistics for the four meteorological periods identified by the cluster analysis.....	146
5.5	Summary statistics for proglacial discharge for the four meteorological periods identified by the cluster analysis.....	147
5.6	Summary of the PCA performed on the proglacial SSC time-series.....	151
5.7	Summary statistics of the magnitude clusters for each station identified from the cluster analysis.....	157
5.8	Average suspended sediment indices for high and low magnitude classes for each gauging station.....	159
5.9	Suspended sediment indices during the four meteorological periods identified by cluster analysis.....	164
6.1	Components of the energy balance equation and their physical principles.....	177
6.2	Overview of degree-day factors at various locations and glaciers.....	181
6.3	Elevation zones of the Feegletscher Nord in FTIM.....	188
6.4	Average degree-day factors over the 2012 ablation season.....	189
6.5	Degree-day factors for snow and ice at each ablation stake.....	189
6.6	Percentage of simulated ablation compared to measured ablation at each of the four ablation stakes for a range of degree-day factors.....	193
6.7	Percentage of total modelled runoff compared to measured runoff for a range of degree-day factors.....	193
6.8	Comparative summary of ablation and runoff simulations with a range of scaling degree-day factors applied according to glacier elevation.....	195
6.9	Comparative summary of ablation and runoff simulation at hourly time-steps with four sets of scaling degree-day factors.....	196

6.10	Pearson correlation coefficients between discharge and air temperature indices.....	199
6.11	Optimised routing parameters utilised in FTIM.....	207
7.1	Simple regression models of proglacial SSC.....	220
7.2	Multivariate regression models of proglacial SSC constructed with discharge-based predictor variables.....	221
7.3	Multivariate regression model of proglacial SSC constructed with pooled observations from Stations B and C.....	227
7.4	Descriptions of the three climate change emission scenarios used in the generation of regional projections for Switzerland in the Swiss Climate Scenarios CH2011 project.....	250
7.5	Comparison of temperature increase estimates in 2100 above pre-industrial levels for SRES scenarios and RCPs by Rogelj <i>et al.</i> (2012).....	251
7.6	Mean additive temperature and multiplicative precipitation changes for the three emissions scenarios for DOY 180-251 for the future projection periods.....	253
7.7	Mean average air temperature and total precipitation for DOY 180-251 in the shifted time-series of temperature and precipitation for the three future time periods and emissions scenarios.....	253
7.8	Summary statistics of modelled changes in suspended sediment transfer and meltwater runoff for DOY 180-251 according to predicted 21 st Century climate changes.....	260
7.9	Summary statistics of modelled changes in suspended sediment transport and meltwater runoff for DOY 180-251 with $\pm 25\%$ changes in degree-day factors.....	261

List of Abbreviations and Acronyms

A1B	Climate change scenario belonging to A1 scenario group
A2	Climate change scenario belonging to A2 scenario group
ASL	Above sea level
CA	Cluster Analysis
CCF	Cross correlation function
DDF	Degree-day Factor
DEM	Digital Elevation Model
DOY	Numerical day of year beginning on 1 st January
DW	Durbin-Watson statistic
EBM	Energy Balance Model
EC	Electrical conductivity
F	F-test statistic
FTIM	Feegletscher Temperature Index Melt Model
GCM	Global Climate Model
GLR	Global (short-wave) radiation
GPR	Ground penetrating radar
GPS	Global position system
η^2	Nash-Sutcliffe coefficient of efficiency
HCA	Hierarchical Cluster Analysis
IPCC	Intergovernmental Panel on Climate Change
LIA	Little Ice Age
K	Reservoir storage coefficient
μ	Mean
μ_Q	Discharge weighted mean
Δ_d	Mean daily range
M	Snow or ice melt
MRM	Multivariate regression model
n	Number of observations
nM	Nanometers (wavelength)
OLS	Ordinary Least Squares regression
P	Probability measure of confidence
PC	Principal Component
PCA	Principal Components Analysis
Φ	Krumbein scale of particle size
$hQ!$	Hours since discharge was last equalled or exceeded
ΣQ	Cumulative discharge
Q	Discharge
ΔQ	Rate of change of discharge
Q_b	Baseflow discharge
Q_C	Heat through conduction
Q_E	Turbulent flux of latent heat
Q_H	Turbulent flux of sensible heat
Q_L	Long wave radiation
Q_M	Net energy
Q_o	Discharge at t_0
Q_p	Daily peak discharge
Q_P	Heat supplied by rain

Q_s	Net short-wave radiation
Q_{std}	Daily standard deviation of discharge
Q_t	Discharge at time t
r	Correlation coefficient
r^2	Coefficient of determination (simple regression)
R^2	Coefficient of determination (multivariate regression)
RCM	Regional Climate Model
RCP3PD	Climate change stabilisation scenario
RMSE	Root mean square error
σ	Standard Deviation
S	Siemens
S_0	SSC at t_0
S_t	SSC at time t
SD	Standard Deviation
σ	Standard Deviation
σ_d	Mean daily Standard Deviation
SE	Standard error
SF	Saas Fee
SQR	Standardised discharge range
SSL	Suspended sediment load
SSC	Suspended sediment concentration
t	Time
t_p	Time to peak
T	Air Temperature
T^{+ve}	Positive air temperature
TIM	Temperature Index Model
W	Modelled potential water available for runoff
WMO	World Meteorological Organisation
Z	Elevation

1 1 Introduction

1.1 Context

Glaciated catchments are among the most erosive environments on the planet (Dedkov & Moszherin, 1992) with estimates of the effective rates of glacier erosion ranging from 0.01 mm yr^{-1} in polar latitudes to $10\text{-}100 \text{ mm yr}^{-1}$ for large temperate glaciers (Hallett *et al.*, 1996). The global flux of glacial sediment delivery to oceans is $0.8\text{-}50 \times 10^{12} \text{ kg}$ annually (Murray *et al.*, 1993), with significant implications for marine ecosystems (e.g. Hay, 1998; Sugden *et al.*, 2009; Bhatia *et al.*, 2013; Hood *et al.*, 2015). The high rates of erosion in glaciated catchments are principally attributed to processes of sediment production, entrainment and transport by ice and meltwater at the ice-bed interface (Hallett *et al.*, 1996; Alley *et al.*, 1997). Erosive processes and sediment yields have been demonstrated to be dominated by the presence and passage of meltwater through a subglacial drainage system over all other processes (Collins, 1979; Hallett *et al.*, 1996; Alley *et al.*, 1997; Swift *et al.*, 2002; Swift *et al.*, 2005a). Research that has focussed upon Alpine glaciers has shown that strong coupling exists between meltwater discharge and the amount of sediment transferred in suspension over a wide range of timescales (Gurnell, 1987; Fenn, 1989). However, a range of glacial hydrological processes are capable of significantly modifying this relationship, which can result in irregular patterns of sediment transfer, particularly at short time-scales (Collins, 1979; Souchez & Lorrain, 1987; Willis *et al.*, 1996; Swift *et al.*, 2002; Swift *et al.*, 2005a). The morphology and evolution of the subglacial drainage network (and the associated variability of subglacial water pressure) is implicated as a primary control for many of these mechanisms by determining both sediment availability and the rate of fluvial sediment evacuation (e.g. Collins, 1979; Willis *et al.*, 1996; Hubbard *et al.*, 1995;

Hubbard & Nienow, 1997; Swift *et al.*, 2002; Swift *et al.*, 2005a; 2005b). Recently deglaciated forefields have been shown to subsequently modify suspended sediment transfer patterns and yields due to the storage and release of proglacial sediments (Gurnell, 1982; Warburton, 1990; Hodgkins *et al.*, 2003; Richards & Moore, 2003; Orwin & Smart, 2004; Leggat *et al.*, 2015). The presence of these typically unstable stores of sediment are hypothesised to result in elevated suspended sediment yields from glaciated catchments, which are expected to be highest during and immediately following deglaciation (Church & Ryder, 1972). A changing climate is predicted to continue the already pronounced deglaciation that is occurring in the cryosphere (e.g. Ramillien *et al.*, 2006; Rignot *et al.*, 2008; Farinotti *et al.*, 2009; Van De Broeke *et al.*, 2009). The loss of snow and ice may enhance summer meltwater flows due to increased air temperatures and a longer melt season, but as mass loss continues, meltwater discharge is likely to be significantly reduced (Alcamo *et al.*, 2007). This will create disequilibria in the water cycle with resultant impacts on the sediment flux within, and from, Alpine catchments, a process which is strongly determined by meltwater inputs, throughputs and outputs (Hodgkins *et al.*, 2003; Swift *et al.*, 2005b). However, uncertainties regarding the controls on processes of proglacial sediment storage and release (e.g. Hodgkins *et al.*, 2003; Orwin & Smart, 2004a; Diodato *et al.*, 2013) raise questions as to the impacts of glacier shrinkage upon fluvial suspended sediment yields. In addition, as progressive deglaciation continues, heightened levels of geomorphological activity (so-called 'paraglacial' activity) are also likely to have a significant impact on both sediment and water yields from deglaciating catchments (Church & Ryder, 1972; Ballantyne, 2002a; Porter *et al.*, 2010), raising the possibility that sediment yields may increase. The enhanced geomorphological activity associated with deglaciation is hypothesised to significantly impact patterns of sediment transfer due to the exposure and mobilisation of unstable forefield and ice-marginal sediments

(Lukas *et al.*, 2005; Porter *et al.*, 2010; Carrivick *et al.*, 2013), and the development and decay of ice-marginal landforms, such as proglacial lakes (Carrivick & Tweed, 2013; Bogen *et al.*, 2015). However, research focussed upon the mechanisms, rates and impacts of this enhanced geomorphological activity remains limited (Sletten *et al.*, 2001). This suggests that sediment transfer processes in deglaciating environments are likely to result from complex slope-fluvio-glacio linkages, with a dominance of meltwater in transporting and cascading sediments downstream coupled with an increasing importance of forefields as potential sources and sinks of glacial sediments. However, the understanding of these linkages is limited and requires attention, particularly if the impacts upon rates of sediment transfer are to be quantified and subsequently used for the forecasting of suspended sediment yields, the interpretation of sedimentary records and landforms, or the prediction of landscape response to deglaciation (Lønne & Lyså, 2005; Lukas *et al.*, 2005; Warburton, 2007). Furthermore, the understanding of processes of glacio-fluvial sediment transfer is challenged by recent research that has raised questions regarding the suitability of using proglacial records of meltwater and suspended sediment to explain the functioning of glacio-fluvial hydrological and sedimentary systems (e.g. Orwin & Smart, 2004a; Porter *et al.*, 2010; Covington *et al.*, 2012; Gulley *et al.*, 2012a). This has potential implications for studies utilising proglacial records of meltwater and suspended sediments to infer glacial hydrological processes through the so-called ‘inverse approach’, as uncertainties may arise in studies that fail to capture a whole-catchment view of the inputs, throughputs and outputs of meltwater and sediment.

Therefore, it is hypothesised that coupling between glacier surface melt and meltwater outflow characteristics may be critical in explaining the associated sediment transfer dynamics at short temporal scales, particularly due to the importance of

subglacial water pressure in determining sediment loads and patterns. Specifically, research is needed to address the extent to which the timing of supraglacial melt generation is linked to the resultant proglacial hydrograph form; and how, subsequently, meltwater input and throughput determines the patterns and magnitudes of sediment transfer. Furthermore, improved understanding of the extent to which sediment transfer patterns are modified in the proglacial zone is needed due to the potential influence of paraglacial sedimentation on suspended sediment availability, and the possible coupling between paraglacial activity and the glacio-fluvial hydrological and sedimentary systems. Specifically, research is needed to address whether, and to what extent, sediment transfer dynamics can be reliably attributed to glacial or non-glacial activity. Therefore, to understand how sediment-transfer in glacial systems functions during, and is responding to, deglaciation, it is necessary to examine the hydrological functioning of glaciers under enhanced climate forcing and the resultant temporal and spatial patterns of sediment transfer in light of a range of potential glacial, non-glacial and glacially-conditioned processes, which may significantly alter the input, storage, and output of sediments within, and from, glaciated catchments. By undertaking an integrated, catchment-scale approach that utilises a combination of methods to understand the glacio-fluvial transfer of meltwater and sediment (e.g. Richards *et al.*, 1996), this research provides a unique understanding of the processes controlling sediment transfer in light of catchment hydrology, ablation processes and forefield dynamics.

1.2 Research Aim and Objectives

Information of the functioning of glacio-fluvial hydrological and sedimentary systems has typically been provided by the inverse approach to extract information on aspects of the configuration, functioning and dynamics of glacial drainage systems from proglacial time-series of discharge and suspended sediment concentrations. However,

given the high sediment yields of temperate glacial environments and their predicted and observed sensitivity to climate warming, it is surprising that there are limited examples of fully integrated studies seeking to understand the controls on glacio-fluvial sediment transfer in light of deglaciation. Integrated approaches have been demonstrated to enable the successful characterisation and understanding of glacier hydrology (e.g. Richards *et al.*, 1996; Irvine-Fynn *et al.*, 2005a) and are followed as a template in this research. Significant uncertainties in the melt-related controls on sediment transfer through glaciers and the subsequent proglacial modification of water and sediment loads create a compelling impetus to understand and characterise processes of water and sediment transfer in glaciated catchments in light of progressive deglaciation. Furthermore, the correct interpretation of relict landforms and the ability to predict landscape evolution is dependent on the understanding of both the rates of glacio-fluvial sediment transfer and the potentially complex interactions between meltwater, geomorphology and sediment transfer in deglaciating environments.

Therefore, the aim of the research presented in this thesis was to accurately quantify sediment transfer processes and hydrology at the Feegletscher Nord, Switzerland, to develop an understanding of how sediment loads are coupled to glacial, fluvial, climatic and non-glacial processes. This aim was achieved through an integrated study of water and sediment transfer at an Alpine glaciated catchment to reliably characterise the nature of, and controls on, the hydrological and sedimentary systems through detailed consideration of the inputs, throughput, and outputs of meltwater and sediment in space and time.

The following objectives were formulated in order to achieve this aim:

- To scrutinise proglacial stream discharge hydrographs and suspended sediment records to establish the dominant controls on suspended sediment entrainment and transport and the nature of spatial and temporal variability in these records.
- To investigate water and suspended sediment transfer through the proglacial environment in order to identify the controls on proglacial discharge and suspended sediment concentrations.
- To simulate glacier runoff through the creation of a glacier melt model in order to establish the controls on meltwater production and routing and subsequently, predict meltwater generation under a range of climate change scenarios.
- To compare the simulated runoff time-series to measured proglacial discharge in order to elucidate the functioning of the glacier hydrological system, with consideration of the implications for sediment entrainment and evacuation by meltwater.
- To combine the characterisation of glacio-fluvial suspended sediment transfer processes with the glacier runoff model in order to explore potential future changes in proglacial sediment loads under future climate change scenarios.

1.3 Thesis Structure

This thesis is presented in eight chapters that, together, address the aim and objectives of the research programme. A review of the literature into the research topic is presented in Chapter 2, with particular attention to temperate Alpine glacier hydrology, glacio-fluvial sediment transfer, and the potential range of hydrological and geomorphological responses to deglaciation that can occur in these environments. A summary of the research priorities in light of the wider literature is then presented. Chapter 3 introduces the study site, the Fee catchment, Switzerland, with a particular

focus upon the Feegletscher Nord as the location focussed upon in the field campaigns. This chapter also includes a description of the methods adopted in this research. Chapter 4 then details the two field campaigns in 2010 and 2012 and the meteorological, hydrological and glaciological data that was collected is presented. The temporal and spatial variability in meltwater and sediment transfer is investigated in Chapter 5 to inform the subsequent analyses undertaken in Chapters 6 and 7. Chapter 6 then presents the development of a glacier melt model, capable of simulating runoff at a high temporal resolution, in order to further investigate the hydrology of the Feegletscher Nord and facilitate the exploration of future trends in meltwater runoff and suspended sediment transfer under a changing climate. Chapter 7 presents analyses undertaken in order to investigate and characterise the controls on the suspended sediment transfer patterns revealed in Chapter 5, the results of which are then coupled with the glacier runoff model developed in Chapter 6 to explore possible future changes in suspended sediment loads under a range of climate change scenarios. The key findings of these three chapters are then discussed and summarised in Chapter 8, and avenues for future research are identified in light of the questions raised in this research.

2 Glacio-Fluvial Sediment Transfer: A Review

2.1 Introduction

The overall aim of this research was to examine and understand the hydrological and geomorphological impacts of deglaciation upon processes generating and transferring sediment within a glaciated Alpine catchment with a view to characterising the glacio-fluvial sedimentary and hydrological system. Consequently, it is necessary to understand glacier thermal regimes, which are briefly reviewed in Section 2.2. A more detailed review of glacier hydrology is undertaken in Section 2.3, with particular attention to the subglacial hydrology of temperate glaciers, as meltwater discharge is typically the dominant transport mechanism of the products of glacial (and non-glacial) erosion in glaciated catchments. Subsequently, Section 2.4 considers the processes and patterns of glacio-fluvial sediment transfer, with attention to the dynamics of glacio-fluvial sediment transfer in deglaciating environments (Section 2.4.4). A range of potential hydrological and geomorphological responses to deglaciation are considered in Section 2.5, and Section 2.6 summarises the key areas of uncertainty in the current understanding of glacio-fluvial sediment transfer.

2.2 Glacier Thermal Regime

The thermal condition of glacier ice is a fundamental determinant on the processes controlling meltwater inputs, throughputs and outputs within a glacier body. The heat balance will determine the thermal condition of ice at the glacier bed and can be represented by the following balance equation:

$$\Delta H_B = H_A + H_S + H_F + H_G \quad (2.1)$$

where H_B is the heat balance, H_A is the heat exchange between the atmosphere and ice or snow, H_S is the heat from the temperature of accumulating snowfall, H_F is the heat generated by frictional forces opposing ice deformation and flow, and H_G is the heat from geothermal sources. Thermal regimes can be classified across a continuum with temperate and cold-based glaciers marking each extreme (Benn & Evans, 2014). Temperate glaciers are those composed almost entirely of ice at or close to the pressure melting point (Paterson, 1994; Fountain & Walder, 1998). Such glaciers will be characterised by the presence of ice in a liquid phase and will typically have an ice-bed at the pressure melting point, whereby the pressure of the overlying ice is sufficient to generate melting of the ice at the base of the glacier, which may in turn facilitate glacier motion (Hubbard & Nienow, 1997). Large-scale permeability in the form of crevasses and moulins is generally associated with such thermal regimes due to high rates of glacier activity, which causes crevasses to form in response to ice deformation (Weertman, 1973; Fountain & Walder, 1998). Such permeability will permit surface meltwater to penetrate the glacier and result in the steady drainage of meltwater as ice drains via englacial and subglacial pathways (Flowers & Clarke, 2002; Fountain *et al.*, 2005). Such glaciers are typically found in Alpine mid-latitude settings and are in direct contrast to cold-based glaciers, characterised by ice below the pressure melting point throughout all or most of their body and does not contain liquid phase water (Hodgkins, 1997). Such glaciers are typically found in polar and High-Arctic regions and are often characterised by low permeability due to low rates of glacier activity and similarly low rates of ice deformation (Hodgkins, 1997; Bingham *et al.*, 2006). However, a significant proportion of glaciers lie between these extremes, particularly those found in sub-polar regions at high latitudes. So-called ‘polythermal’ glaciers experience both cold and temperate ice at their base, with often complex spatial distribution and resultant hydrology (Irvine-Fynn *et al.*, 2011). In addition, the formation of superimposed ice

layers as meltwater percolates through the snowpack and refreezes possesses the capability to limit the permeability of glacier ice and can result in greater volumes of supraglacially stored meltwater, which can drain rapidly over the ice (Wadham & Nuttall, 2002). Therefore, it is apparent that the nature of the thermal regime in existence at the glacier bed results in a different set of processes governing meltwater routing through a glacier.

2.3 Glacier Hydrology

The hydrology of glaciers has been extensively reviewed by a number of authors (e.g. Hodgkins, 1997; Hubbard & Nienow, 1997; Fountain & Walder, 1998; Singh & Singh, 2001; Jansson *et al.*, 2003; Benn & Evans, 2014), and therefore, the following Section provides a summary and review of glacier hydrology with respect to temperate Alpine glaciers. Section 2.3.1 reviews the morphologies of glacier hydrological systems. Section 2.3.2 then details the principles governing water flow through englacial and subglacial conduits and channels. Section 2.3.3 considers the dynamics of glacier drainage systems, including the seasonal evolution of channelised subglacial drainage networks. Section 2.4 then outlines the range of controls on glacier runoff.

2.3.1 Hydrological System Morphology

The inputs of energy to the surface of a glacier will increase during the summer, generating melt, which is delivered from the snow and ice-pack to the subglacial drainage network via supraglacial and englacial pathways (Figure 2.1) (Hock, 2005). Features such as moulins and crevasses permit this entry and passage of water and such features may be perennial or develop during the ablation system by meltwater or by glacier motion fracturing the ice (Fountain *et al.*, 2005). Meltwater that reaches the bed will continue to flow or become stored according to the morphology of the glacial drainage network. As such, the inputs of water to a glacier hydrological system will

comprise surface melt, melt generated at the ice-bed, and releases from englacial or subglacial stores.

Water is routed through glaciers via supraglacial, englacial and subglacial drainage systems. Subglacial drainage systems for Alpine glaciers are, at the simplest conceptualisation, characterised by two morphologies: a hydraulically inefficient ‘winter’ subglacial drainage system characterised by a positive relationship between water pressure and discharge, and a discrete, hydraulically efficient channelised drainage system that develops in the summer melt season, with an inverse relationship between water pressure and discharge (Hubbard & Nienow, 1997; Fountain & Walder, 1998; Nienow *et al.*, 1998; Swift *et al.*, 2002). The morphology of the subglacial drainage network is not normally spatially or temporally static and has been shown to be subject to re-organisation and evolution (Collins, 1979; Willis *et al.*, 1996; Hubbard & Nienow, 1997; Nienow *et al.*, 1998; Swift *et al.*, 2002; 2005a).

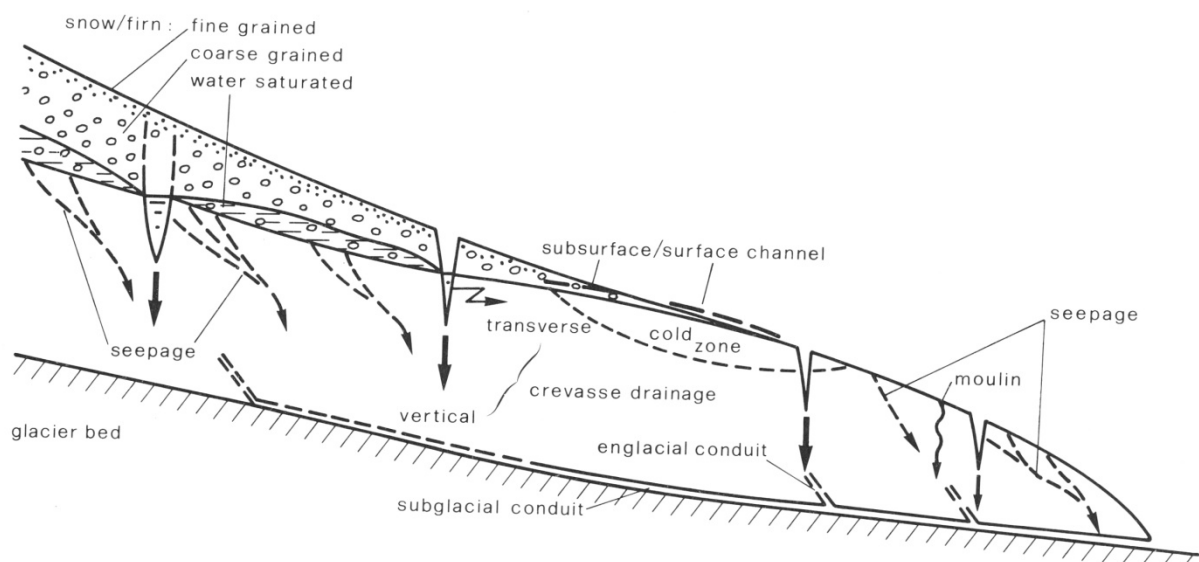


Figure 2.1: Schematic diagram of the model of glacier hydrological networks (Rothlisberger & Lang, 1987)

Distributed subglacial drainage systems are comprised of hydraulically resistive or inefficient flowpaths that cover a large proportion of the glacier bed. Such networks can be composed of several types of morphology: linked networks of cavities exist where water pressure is large enough for cavities to develop (for example on the lee-side of protrusions from the bed) (Kamb, 1987). These cavities may store both water and sediment during winter as they become isolated. Networks of braided canals are associated with glaciers overlying soft sediments (Walder & Fowler, 1994). They comprise wide, shallow canals distributed along the basal interface either through or over areas of soft basal sediment (Clark & Walder, 1994). Water may also flow through sediments via Darcian flow if the sediments at the ice-bed interface have sufficient permeability to permit the passage of water (Hubbard *et al.*, 1995). Similarly, where the basal geomorphology comprises bedrock, films of flowing water under high pressure may also transport water beneath the glacier. These are typically a few millimetres in depth and may extend over large areas of the bed (Shreve, 1972; Weertman, 1972; Souchez & Lorrain, 1987). Water flow via sediments is likely to be highly dependent on the basal geomorphology comprising permeable substrate or till and any volumes of water transported are not generally considered significant compared to flow in discrete network morphologies. Typical flow velocities have been reported for distributed networks, such as linked cavity systems, of 0.025 ms^{-1} (Nienow *et al.*, 1998; Swift *et al.*, 2002).

Hydraulically efficient drainage systems comprise channels and conduits that can be routed through ice, bedrock or sediments. Röthlisberger channels (R-channels) and Nye channels (N-channels) are those located at the ice-bed interface. R-channels may be closed by the processes of ice creep and deformation, or by the forward movement of ice that can obstruct their passage. The size, and therefore, water capacity of these

channels reflects a balance between channel enlargement by frictional melting from the passage of water and closure by ice deformation (Hooke *et al.*, 1990; Hubbard & Nienow, 1997). Where stable channel morphology exists, N-channels are products of subglacial erosion by streams and are carved into the bed, making them more permanent features of the drainage network (Souchez & Lorrain, 1987). The profiles of R- and N-channels are usually described as semi-circular but N-channels may form as a V-shaped groove in the bedrock (Röthlisberger & Lang, 1987). Such channels, where bedrock or substratum form part of their structure, can have a significantly higher hydraulic roughness compared to a smooth ice pipe (Röthlisberger & Lang, 1987; Gulley *et al.*, 2012a). Typical flow velocities for such networks have been reported in the region of $0.2 - 0.8 \text{ ms}^{-1}$, an order of magnitude greater than velocities reported for distributed networks (e.g. Nienow *et al.*, 1998; Swift *et al.*, 2002).

2.3.2 Water Flow in Glacier Drainage Systems

Water that reaches the bed will be transported through a network of englacial and subglacial channels and conduits. The hydraulic efficiency of the drainage network is largely determined by its cross sectional area and hydraulic potential. The size of these channels is governed by the competing forces of ice deformation and turbulent heating. Water flowing in these water-filled and ice-bounded conduits is driven by gravity acting on the water and the surrounding ice (Hubbard & Nienow, 1997). For water flowing at the base of a glacier the hydraulic potential will be a function of both water pressure and elevation. Hydraulic potential in a subglacial conduit is given by:

$$\varphi = \varphi_0 + \varphi_e + P_w \quad (2.2)$$

where φ is the hydraulic potential, φ_0 is a constant depending on the shape and size of the conduit, φ_e is the potential due to elevation (defined as $\varphi_e = \rho_w g z$ where ρ_w is the

density of water, g is acceleration due to gravity, and z is elevation), and P_w is water pressure (Shreve, 1972; Flowers & Clarke, 1999). Water flowing through englacial and subglacial conduits is also under pressure from the overlying ice. For water-filled conduits under steady-state conditions, the water pressure will be controlled by the balance between water flow (producing melt through frictional heat generation) and ice deformation (in response to the pressure gradient between water pressure and ice overburden pressure). The result of these competing forces is that water-filled conduits may not always follow the direction of the maximum local bedslope and may flow up or across subglacial slopes (Hubbard & Nienow, 1997). Pressure conditions in subglacial drainage networks are higher in inefficient configurations than discrete channels. However, steady state conditions are unlikely to exist, and it is common for conduits to be at atmospheric pressure under many circumstances due to the longer time it takes for channels to enlarge rather than contract (Hooke, 1984; Röthlisberger & Lang, 1987).

Shreve (1972) described how water pressures in channels or conduits will be lower than the ice over-burden pressures in the surrounding ice due to the pressure decrease associated with the frictional melting of the channel walls. This effect increases with the channel diameter, with larger channels experiencing lower water pressures. Therefore, the channels with larger diameters are able to compete more successfully with smaller channels in capturing water. This leads to branching and capture resulting in the development of arborescent drainage networks. Sharp *et al.* (1993) describe how rates of subglacial drainage channel growth and closure will rarely reflect the steady-state conditions described by Shreve (1972) and Hooke (1984) but will fluctuate with variations in meltwater flux, ice thickness, ice surface slope, basal sliding velocity and substrate composition. Therefore, the variability in subglacial conditions is a strong determinant of drainage system structure, with resultant configurations that are likely to

be spatially and temporally dynamic, resulting in the possible coexistence of both distributed and discrete drainage configurations (Hubbard *et al.*, 1995).

2.3.3 Drainage System Dynamics

A seasonal evolution of an efficient drainage system has been observed by researchers (e.g. Collins, 1979; Willis *et al.*, 1996; Hubbard & Nienow, 1997; Swift *et al.*, 2002; Swift *et al.*, 2005a). Experiments by Nienow *et al.* (1998) at Haut Glacier D'Arolla, Switzerland demonstrated that there is a significant glacier-wide seasonal evolution of the drainage system morphology whereby a system of hydraulically efficient channels extends up-glacier over the course of each melt season at the expense of an inefficient distributed drainage system. Increases in ablation at the surface of a glacier over the ablation season increase runoff which destabilises the spatially extensive but inefficient 'slow' network into forming hydraulically efficient 'fast' channels that cover a relatively smaller proportion of the glacier bed. As this hydraulically efficient configuration evolves upglacier, sources of subglacially stored water, for example in cavities, may be tapped by the migrating and evolving channels and conduits (Nienow *et al.*, 1998). Kamb (1987) proposed that distributed linked-cavity systems may collapse into channelised systems if water pressure perturbations occur above a steady-state value. This would lead to the development of tunnels between the cavities with the final morphology depending on glacier surface slope and presence and strength of underlying sediments. The majority of these efficient conduits are then closed before the start of the next ablation season due to the reduction in wall melting from frictional heat generation and closure by ice deformation. Nienow *et al.* (1998) calculated that subglacial channels at the Gornergletscher, Switzerland, would not survive the winter except beneath a short section of the glacier, extending to approximately 200-700m from the snout.

The headward evolution of an efficient drainage network has been inferred from tracer studies, typically from aquilots of dye injected into supraglacial drainage features such as moulins. Increases in tracer transit velocity and decreased dispersal of dyes have been suggested to indicate a shift from distributed to discrete drainage networks (e.g. Nienow *et al.*, 1998; Swift *et al.*, 2005a). The correlation between the rate of headward expansion of the channelised system and the rate of retreat of the transient snowline implies that surface meltwater generation is a significant contributing component to this evolution. Hydrographs and dye trace return curves have been found to become increasingly peaked over the ablation season, highlighting the interdependence between surface ablation and subglacial hydrological processes (Nienow *et al.*, 1998; Swift *et al.*, 2005a). Surface meltwater would access the subglacial drainage network according to the presence of moulins and crevasses (Fountain and Walder, 1998). The irregular location of these recharge points leads to an episodic pattern of subglacial channel growth. Recent research has suggested that the distribution of such features may be the dominant control of subglacial conduit distribution (e.g. Gulley *et al.*, 2012b).

In addition, factors other than meltwater production, routing and storage have been shown to affect the rate of seasonal evolution of the drainage network. For example, heavy rainfall events were found by Nienow *et al.* (1998) to be a possible cause of high discharges assisting in the development of channel formation. In addition, the rate of channel extension to the upper part of a glacier may be slowed due to the presence of patchy firn on the glacier surface acting as an aquifer and permitting only slow percolation of meltwater to the bed (Fountain & Walder, 1998). This could delay the transfer of meltwater to the subglacial drainage system, although this is likely to only be a significant factor for glaciers with large areas of firn (Nienow *et al.*, 1998).

Deglaciation is also likely to impact on the dynamics of the subglacial drainage network through the increased potential for the preservation of conduits due to reduced capacities for creep-closure as glaciers thin causing lower ice-overburden pressures (Flowers, 2008). Consequently, the rate of subglacial channel growth and closure can fluctuate with variations in meltwater flux, ice thickness, ice surface and bed slope, basal sliding velocity and substrate composition (Hubbard & Nienow, 1997; Flowers, 2008), highlighting that the configuration and dynamics of glacier drainage systems can vary considerably between glaciers.

2.3.4 Controls on Glacier Runoff

Glacial hydrological processes are dominated by changes of diurnal and seasonal duration with discharge in Alpine areas exhibiting substantial variability in comparison to Arctic basins (Gurnell *et al.*, 1994). There is a seasonal pattern of low flows or no flow during the winter months, which is followed by higher flows during the summer ablation season (Collins, 1989; 2008). The summer discharge will reflect factors driving snow and ice melt, as well as variations in the radiation balance in receipt at the glacier surface and air temperature (Figure 2.2) (Gregory, 1987). Incoming solar radiation and the associated pattern of air temperature variations are the primary controls of glacier runoff at the diurnal and annual scales (Hock, 2005). Figure 2.2 illustrates the typical summer diurnal relationship between glacier and basin runoff with air temperature and incoming solar radiation. When hydrographs from glaciers are further examined, there is a considerable base flow component upon which a diurnal cycle of runoff is superimposed with a lag of a few hours after the daily melt maximum (e.g. Richards *et al.*, 1996). The ratio of daily minimum to maximum flow will decrease with increasing basin and glacier size. The superimposed diurnal cycles of runoff consist of rapidly draining components of the day's meltwater:

- Meltwater from the lowest parts of the glacier basin, draining via supra- and subglacial pathways to the proglacial streams and;
- Meltwater from the snow-free part of the glacier which drains along short connections to the main subglacial conduits.

Thus, the shape and magnitude of a hydrograph will reflect the dominant processes controlling their modification (e.g. Elliston, 1973).

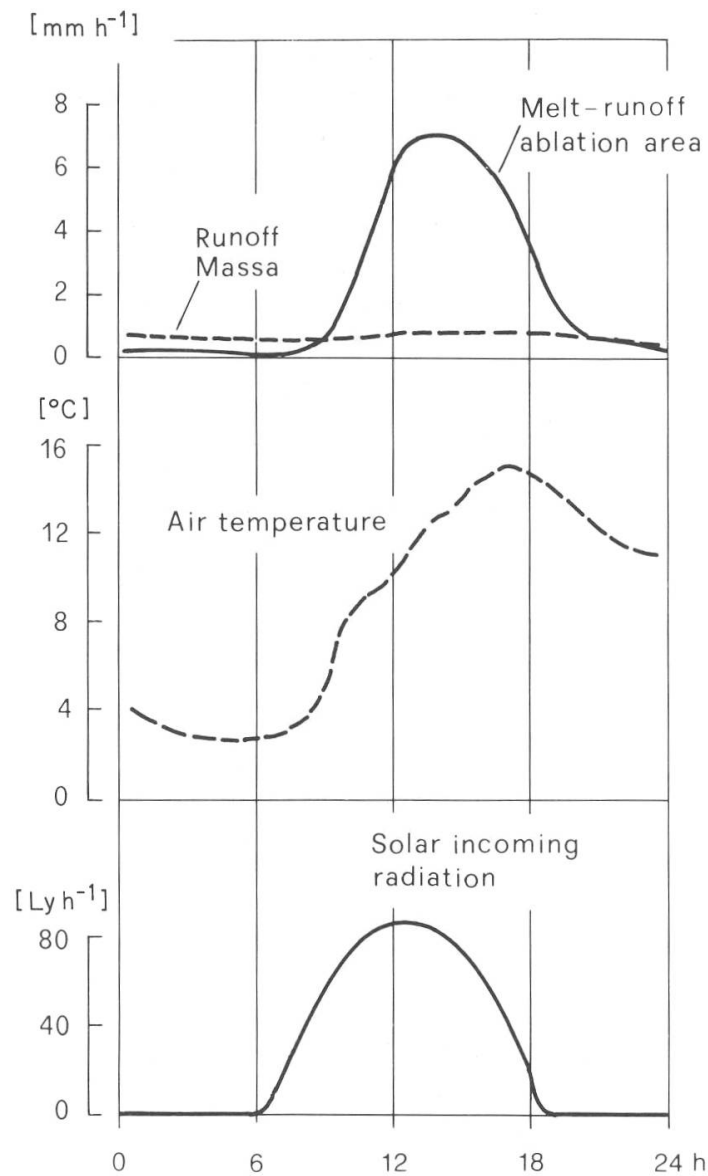


Figure 2.2: Typical diurnal relationship between meltwater runoff, air temperature and incoming solar radiation from Gregory (1987)

The competing influence of meltwater generation and subglacial flow competency in the determination of output hydrograph characteristics has been investigated (e.g. Gurnell *et al.*, 1992; Richards *et al.*, 1996; Flowers, 2008; Covington *et al.*, 2012; Gulley *et al.*, 2012a). A time-lag between air temperature and runoff of a few hours is typically evident at Alpine glaciers (e.g. Richards *et al.*, 1996) and reflects the distance the water has to travel through the drainage system and the hydraulic efficiency of the drainage network (Hock & Hooke, 1993). As such, these time lags would be expected to decrease over the ablation season as a ‘fast’ channelised subglacial drainage system develops (e.g. Willis *et al.*, 1990; Swift *et al.*, 2002). These controls on the hydrograph form have formed the basis for a number of so-called ‘inverse’ approaches to hydrological investigation, whereby glacier drainage system characteristics are inferred from the shape and magnitude of outflow hydrographs (e.g. Collins, 1979; Brown *et al.*, 1990; Collins; 1995; Swift *et al.*, 2005a). However, the competing influence of surface meltwater inputs versus subglacial drainage system competency in determining the resultant hydrograph form is well debated (e.g. Flowers & Clarke, 2002; Flowers, 2008; Covington *et al.*, 2012), raising the possibility that subglacial hydrological processes may have a reduced role in the modification of hydrographs when conduit subglacial drainage configuration exists, due to a lack of water storage and constriction in such networks (e.g. Covington *et al.*, 2012). Instead, the dominant control on proglacial hydrograph form may be surface meltwater inputs and, as such, proglacial hydrographs may principally represent the rates of surface melt and meltwater input to the subglacial hydrological system. This suggests that hydrographs cannot be used conclusively to infer changes in either morphology or efficiency of hydrological systems without detailed knowledge of surface ablation and the resultant meltwater inputs to the glacier hydrological system.

Importantly, a range of features can store meltwater within glaciers, which can modify runoff patterns. This storage and release can occur at a wide range of timescales during the ablation season (Richards *et al.*, 1996; Hubbard & Nienow, 1997; Fountain & Walder, 1998; Jansson *et al.*, 2003). Storage reservoirs can comprise supraglacial channels and ponds, snow and firn, the active layer of surface ice, englacial pockets and conduits, and subglacial cavities and conduits (Jansson *et al.*, 2003). This storage of water has been interpreted from hydrographs through examination of hydrograph recession limbs to identify breaks in slope, which are interpreted as reflecting outflow from a reservoir until it drains (e.g. Gurnell, 1993; Hannah & Gurnell, 2001). However, the interpretation of the physical basis for these reservoirs is problematic in the absence of *in situ* observations, and as such, storage reservoirs have been conceptualised and applied as a number of linear flow reservoirs (often one to four), analogous to physical reservoirs of differing residence time (e.g. firn, snow, ice and groundwater) (e.g. Hannah & Gurnell, 2001). Knowledge and understanding of storage reservoirs has subsequently been applied in glacier hydrological modelling to predict runoff by defining the storage and routing that occurs within the glacier between meltwater generation at the surface and discharge processes at the portal (e.g. Hock & Noetzli, 1997; Hock, 1999; Farinotti *et al.*, 2011).

A further possible cause of hydrograph modification is meteorological forcing as meteorological conditions are a fundamental driver of ablation, and precipitation can influence both runoff and ablation processes. The component of meteorological conditions that determine rainfall, snowfall and surface melt processes are characterised by a stochastic nature, which can result in variability in runoff patterns. Precipitation in the European Alps may fall in both solid and liquid form throughout the year, and can, therefore, contribute to mass storage and glacier runoff. Röthlisberger and Lang (1987)

state that the percentage of precipitation falling as snow is approximately 100% at elevations of 3500-4000 m asl. However, the 0°C isotherm has been regularly observed to exceed 4500 m in the European Alps in subsequent studies (e.g. Collins, 1998), highlighting how climatic warming may result in complex relationships between ablation, precipitation and runoff. Due to the wide elevation range of most alpine glacier basins, very few storms will provide liquid precipitation over the whole of a glacier's elevation range, although the elevation of the transient snow line will provide an approximate indicator of elevations likely to experience solid precipitation. When precipitation falls as rain onto the glacier surface, it may become temporarily stored in the snowpack or flow supraglacially to the subglacial drainage network via moulins and crevasses (e.g. Richards *et al.*, 1996; Nienow *et al.*, 1998). Extreme discharge events in glacier basins may be caused by extreme melt rates and storm precipitation. In Europe, major rainfall induced floods due to storms tend to occur during the second half of the ablation season (Collins, 1998). Such storms generally result in pronounced and peaked runoff from the glacier due to the small extent of the snow pack and an efficient subglacial drainage network. Storm precipitation induced floods are rare and the resultant discharge hydrograph will be representative of the delivery of significant amounts of rainfall in conjunction with reduced meltwater generation due to reduced solar radiation delivery (Röthlisberger & Lang, 1987). If the rainfall is heavy, prolonged and warm it can constitute a significant mechanism of ablation due to advection of heat to the surface (Hock, 2005). Similarly, events associated with extreme melt rates resulting from maximum glacier surface heat fluxes have been observed (e.g. Marcus *et al.*, 1985). Whilst extreme melt rates in the European Alps are considered rare, the probable maximum hourly melt rates are reported by Röthlisberger and Lang (1987) for the Aletschgletscher, Switzerland, as between 10mm and 93mm water equivalent on mid-summer days in the ablation area. Therefore, the largest discharge events will

more-likely occur in mid-to-late summer when significant liquid precipitation falls in conjunction with maximum surface melt rates which is then transported by an efficient subglacial drainage network.

To summarise, runoff from glaciated basins will be dominated by discharge of meltwater from the glacier, the patterns and magnitude of which may be modified by a number of factors. These include factors such as the nature and dynamics of the glacier drainage system (e.g. Nienow *et al.*, 1998; Swift *et al.*, 2005a), the storage and release of meltwater within the glacier (Jansson *et al.*, 2003), and meteorological variables (Röthlisberger & Lang, 1987; Collins, 1989). At temperate Alpine glaciers, meltwater generated during the summer ablation season will typically flow within a subglacial drainage network and continue downstream through the proglacial zone. Meltwater that has access to the subglacial environment has the capacity to erode and entrain sediments stored at the ice-bed, and as such, rates of sediment transfer in glaciated catchments are strongly determined by meltwater discharge (Alley *et al.*, 1997).

2.4 Sediment Transfer

The glacial sedimentary system has been extensively reviewed (e.g. Clark, 1987; Alley *et al.*, 1997; Harbor & Warburton, 1993) and the processes responsible for erosion, transport and deposition of sediment in these systems has been widely studied (e.g. Collins, 1979; Maizels, 1979; Boulton & Hindmarsh, 1987; Fenn, 1987; Gurnell, 1987; Souchez & Lorrain, 1987; Fenn & Gomez, 1989; Willis *et al.*, 1996; Hubbard & Nienow, 1997; Hodgkins, 1999; Hodson & Ferguson, 1999; Hodgkins *et al.*, 2003; Orwin & Smart, 2004a; Swift *et al.*, 2002; Swift *et al.*, 2005a). This section provides a description of the mechanisms and sources of sediment in the Alpine sedimentary system, followed by a comprehensive review of the processes and dynamics of sediment transfer in glaciated catchments.

2.4.1 Sediment Production

Glaciated catchments are among the most erosive environments on the planet. The rate of erosion has been effectively monitored from the amount and concentration of sediment transported in meltwater rivers (e.g. Bogen & Bønsnes, 2003). This glacial erosion of material has been quantified into the total sediment yield, the amount of sediment eroded from the glacier over a given year. The major controls on spatial and temporal variability in sediment yields from a glaciated region are lithology, relief and climate, each operating at various timescales (Evans, 1997). Early attempts to explain the global patterns of sediment yield showed that they were not simply a product of latitude and altitude as the relatively low yields of arctic glaciers compared to the higher yields of Alpine glaciers was subject to high internal variation within the two groups (Figure 2.3) (Bogen & Bønsnes, 2003). Much of this internal variation has been shown

to be dependent on the dynamics and efficacy of glacial processes, with the thermal regime of a glacier (Section 2.3.1) being a fundamental determinant of sediment yield (Hallet *et al.*, 1996; Knudsen *et al.*, 2007).

There are three principle sources of sediment in a glaciated basin; subaerial, subglacial and proglacial. Sediment production and routing processes are described by Fenn (1987) as operating interdependently, differentially and intermittently, and as such, the processes are emphasised as operating at various temporal and spatial resolutions that can result in complex sediment transfer patterns and relationships (Alley *et al.*, 1997). Sediments that are produced can then be transported by glacial, fluvial and mass movement processes along five paths; subaerial, supraglacial, englacial, subglacial and proglacial (Benn & Evans, 2014). The sediment-transfer system comprises stages of erosion, transport and sedimentation and can be expressed as a balance equation:

$$\Delta S_s = G_p + F_p + W_p - G_t - F_t - M_t \quad (2.4)$$

where the term S_s describes sediments stored in the basin, the terms G , F , W and M denote, respectively, glacial, fluvial, weathering and mass movement processes with the terms p in the expression referring to sediment production and t as sediment transport (Fenn, 1987). The result of these sediment production and transport processes is the presence of rock debris at the base of most glaciers that forms the principal source of sediments which can be entrained and mobilised by meltwater (e.g. Boulton, 1979; Boulton & Hindmarsh, 1987; Alley, 1992; Alley *et al.*, 1997; Fountain & Walder, 1998). However, Equation 2.4 simplifies a complex system of sediment production and

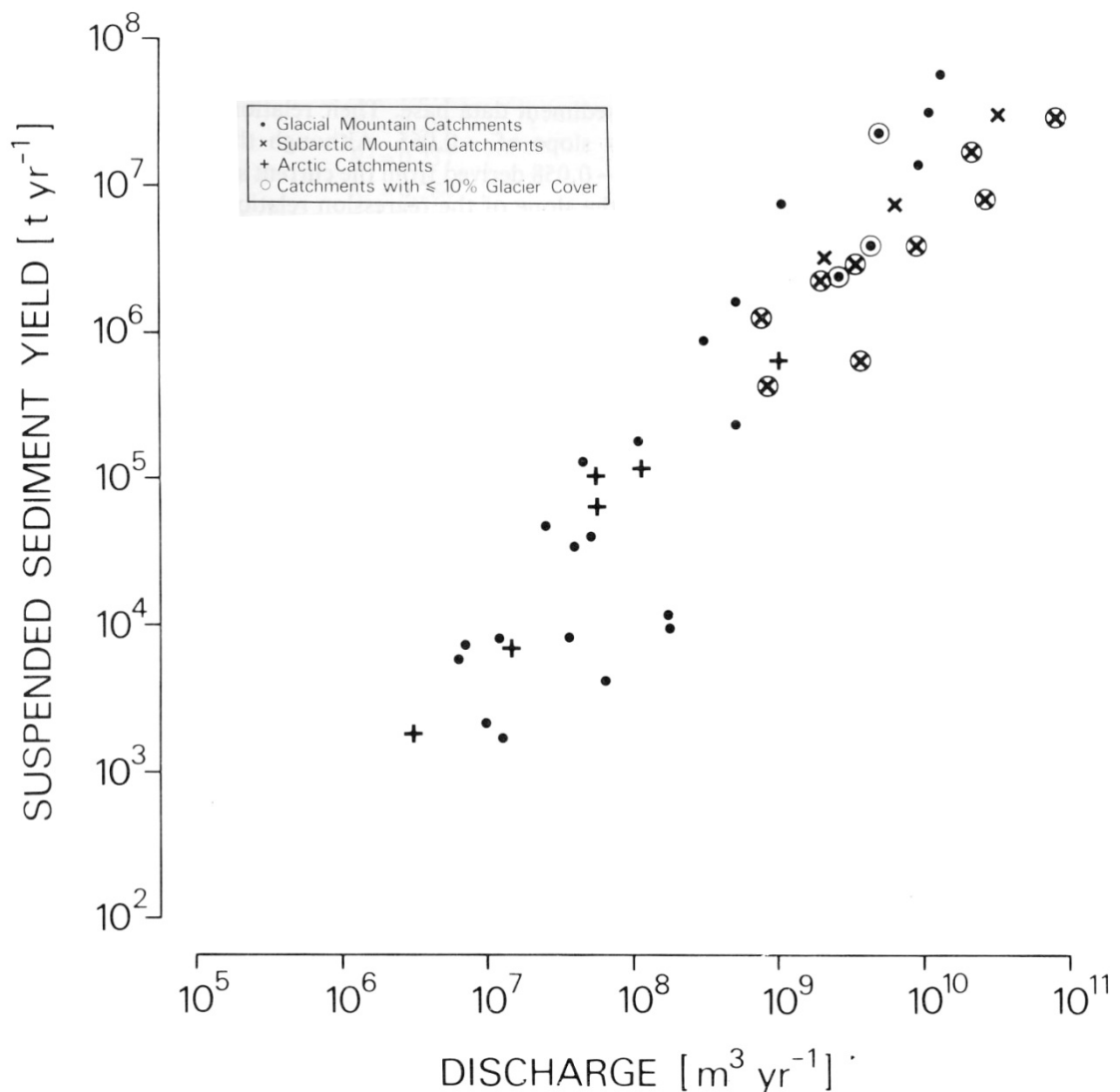


Figure 2.3: Relationship between suspended sediment yield and annual discharge volume for 43 basins highlighting the highest suspended sediment yields are associated with catchments with $\leq 10\%$ glacier cover (Gurnell, 1987)

transport, which is elaborated upon further in this Chapter.

The glacial processes producing sediment can be described as primary production processes that are able to break down rock under their own actions, these include; plucking, cavitation, gelifraction, and hydrolysis (Boulton, 1982; Fenn, 1987). Secondary production processes are those that rely on another process to provide the necessary circumstances to achieve erosion, these include; abrasion, shearing, and corrosion. The principle mechanisms of glacial erosion are outlined in Table 2.1. Sediments are therefore likely to be produced according to variations in the efficacy of erosion processes in relation to the resistance of the bed materials (Fenn, 1987). It is most often sediments that are present, either through production or storage, at the base of a glacier that are of most interest as they usually represent the processes of glacial erosion and comprise the major sediment source for evacuation by meltwater. The composition of sediments at the ice-bed interface has been documented from glacial retreat and subglacial investigations (e.g. Dowdeswell *et al.*, 1985; Boulton & Hindmarsh, 1987; Hambrey *et al.*, 1997; Hambrey *et al.*, 1999; Evans *et al.*, 2006), in addition to examination of sediments carried in proglacial streams (e.g. Bogen, 1989; Lenzi *et al.*, 2003; Haritashya *et al.*, 2010). Observations in natural subglacial cavities of glaciers and areas exposed by glacial retreat, show that most of the subglacial surface is veneered by a thin layer of basal till, not generally exceeding a few centimetres in depth and only occasionally reaching decimetres (Souchez & Lorrain, 1987). The beds of temperate glaciers have been described as consisting of mixed or patchy interfaces that alternate between bedrock and sediments (e.g. Harper & Humphrey, 1995; Iverson *et al.*, 1995). Observations made within subglacial conduits beneath a cold based glacier, Rieperbreen, Svalbard, described large boulders on a floor of sorted sediments that were surrounded by walls of poorly sorted, fine-grained till (Gulley *et al.*, 2012a).

Grain-size distributions of subglacial tills do not typically conform to log-normal distributions, highlighting their dependence on local factors such as geology and erosive processes (Boulton, 1978; Haldorsen, 1981; Clarke, 1987; Hooke & Iverson, 1995; Evans *et al.*, 2006). Therefore, the beds of glaciers are likely to comprise significant stores of sediment which are diverse in composition and characteristics, reflecting both the geological characteristics of the basin and the nature and efficacy of erosive processes. At temperate Alpine glaciers, these subglacial stores of sediment typically represent the dominant source of sediment transferred downstream by meltwater, as such, it is necessary to examine the mechanisms of sediment transfer.

Table 2.1: Mechanisms of glacier erosion and their associated processes. Adapted from Fenn (1987).

Mechanism of erosion	Processes
Plucking and quarrying	Block removal by ice deforming around it plucking block out. Failure of block under pressure from overriding rock particles and becomes wedged out. Block is lifted by freezing to basal ice.
Crushing and shearing	Failure due to overburden pressure on roof of obstacles or on upstream face of obstacle leading to dislodgement or disintegration
Abrasion	Indentation and grinding due to contact, leading to abrasive wear. Cracking due to loading and unloading of a brittle surface during basal sliding leading to brittle fracture.
Fluvial erosion	Flowing water as sheet-wash or channel flow causes wash, scour, corrasion, abrasion, cavitation, bank collapse, network extension or change, or leaching causing erosion of materials.
Chemical weathering	Decomposition of minerals through solution, hydrolysis, carbonation, hydration, oxidation, reduction or cation exchange
Physical weathering	Gravitation, expansion or hydraulic forces lead to the mechanical disintegration of rock into finer grade debris through pressure release, gelifraction, hydration shattering or impact shattering.

2.4.2 Mechanisms of Sediment Transfer

Basal sediment evacuation by subglacial meltwater dominates all other sediment transfer processes for temperate glaciers (Swift *et al.*, 2005b). In subglacial streams, water discharge has strong high-frequency variations that occur over a typically short

melt-season and exhibit a strongly diurnal pattern (Section 2.3.4). This high temporal variability makes the glacio-fluvial environment particularly effective in transporting sediment (Alley *et al.*, 1997). Sediment yields and erosive processes have been demonstrated to be dominated by the presence and passage of subglacial meltwater through a subglacial drainage system over all other processes (Alley *et al.*, 1997; Swift *et al.*, 2005b). Swift *et al.* (2005b) report subglacial sediment evacuation to be dependent on the availability of meltwater during the ablation season due to:

- The accumulation of sediment at the bed over winter;
- Increased surface runoff causing enhanced ice-bed separation and increased basal sliding;
- Subglacial flowpath instabilities and;
- The inception of a channelised subglacial drainage system.

The ability of a glacial system to erode and transfer sediment is therefore crucially linked to the morphology of the basal drainage network of the glacier and thus, the hydraulic capacity of the drainage network. Sediment that has been entrained by meltwater can be transported as suspended sediment load or bedload. Bedload and suspended load have been reported as typically sub-equal in glacial meltwaters with bedload dominating glacial streams (Gurnell, 1987). The magnitude of both suspended load and bedload (and the portioning between them) are strongly controlled by the size distribution of the sediment supplied to the stream, as finer particles are more readily suspended and transported (Alley *et al.*, 1997). Gurnell (1987) found that bedload transport at a variety of temperate glaciers was between 30% and 60% of total sediment load whereas, Østrem and Olsen (1987) report that 80-90% of the total sediment load was most often carried as suspended load. This highlights how sediment-transfer conditions between glaciers and even within glacial environments can be quite different.

In their review of empirical evidence for portioning bedload and suspended load, Turowski *et al.* (2010) describe how the fraction of suspended load carried in a mountain stream in a glaciated Austrian catchment varied from zero to one, whereas, the associated fraction of bedload was highly scattered. It was emphasised that control parameters on bedload portion were not able to be conclusively defined due to a lack of available data, reinforcing the complexity of sediment transfer processes for larger particles. Hammer and Smith (1983) suggest the importance of supraglacial debris as a source of bedload. At Hilda Glacier, Canada, material from rockfalls and avalanches formed an “ablation till” that was deficient in fine sized material. The supraglacial material was supplied by supraglacial meltwater channels through sloughing and the melting out of englacial debris along the upper parts of channel walls, which was likely enhanced due to the glacier receding. This ablation till was estimated to be the source of 46% of bedload and 24% of the total proglacial sediment load, emphasising the importance of sediment sources in the determination of sediment loads. In other work, stream power (the rate of energy dissipated in the channel) has been used to predict the amount of bedload transport and the relationship between bedload capacity and discharge has been shown to display a greater-than-linear increase of bedload capacity with water discharge (Gomez & Church, 1989).

Current relationships between subglacial sediment transport and meltwater are empirically derived from the amount of surface melt reaching the ice-bed interface (Swift *et al.*, 2002). The amount of sediment transported is strongly determined by the proportion of the bed that meltwater flowing in turbulent streams has access to. Therefore, basal sediment fluxes will be negligible for glaciers with low rates of subglacial water flow. Downstream increases in transport capacity are predicted to occur for subglacial streams due to a steepening of hydraulic gradients down glacier

which often results in increased ability of the channel to erode bedrock or erodible stream banks and channel sides (Alley *et al.*, 1997). When the available basal sediment is removed and the subglacial water flows over bedrock then erosion of the bedrock will occur, as the sediments that are carried in the water can constitute an effective mechanism of subglacial erosion. The coarse fraction of sediment carried in suspension, which will increase with discharge, determines the erosive capability of subglacial meltwater (Souchez & Lorrain, 1987). This demonstrates the coupling between processes of sediment production and erosion, with potential implications for the availability of subglacial sediments.

Sediment that is entrained in the meltwater will be transported and maintained within the flow by turbulent mixing, and as long as the meltwater is characterised as such, the tendency of the particles to settle out of the flow due to gravity will be resisted. The sediment transport capacity of a stream is dependent on shear stress which is, in part, dependent on the velocity. Links between suspended sediment concentration (SSC) and discharge can be examined, at their simplest level, through the use of suspended sediment rating curves. Suspended sediment rating curves are derived by applying linear regression analysis to concurrent suspended sediment concentration and discharge observations for the same site (Gurnell, 1987; Fenn, 1989). Figure 2.4 shows a sediment rating curve for the proglacial stream of Glacier de Tsidjiore Nouve, Switzerland, in the ablation season of 1984. Assumptions of the regression used to produce suspended sediment rating curves are that the residuals in the dependent variable (SSC) are random, have zero mean, are normally distributed with constant variance and exhibit no serial autocorrelation (Gurnell, 1987). However, mean water flow velocity in streams and rivers increases more slowly than the driving shear stress. Therefore, sediment transport capacity increases with water flow velocity with a

greater-than-linear dependence of suspended sediment flux on water flow velocity (Alley *et al.*, 1997). Studies have shown that sediment transport in streams fed by glacial meltwater increases more rapidly than discharge (e.g. Swift *et al.*, 2002).

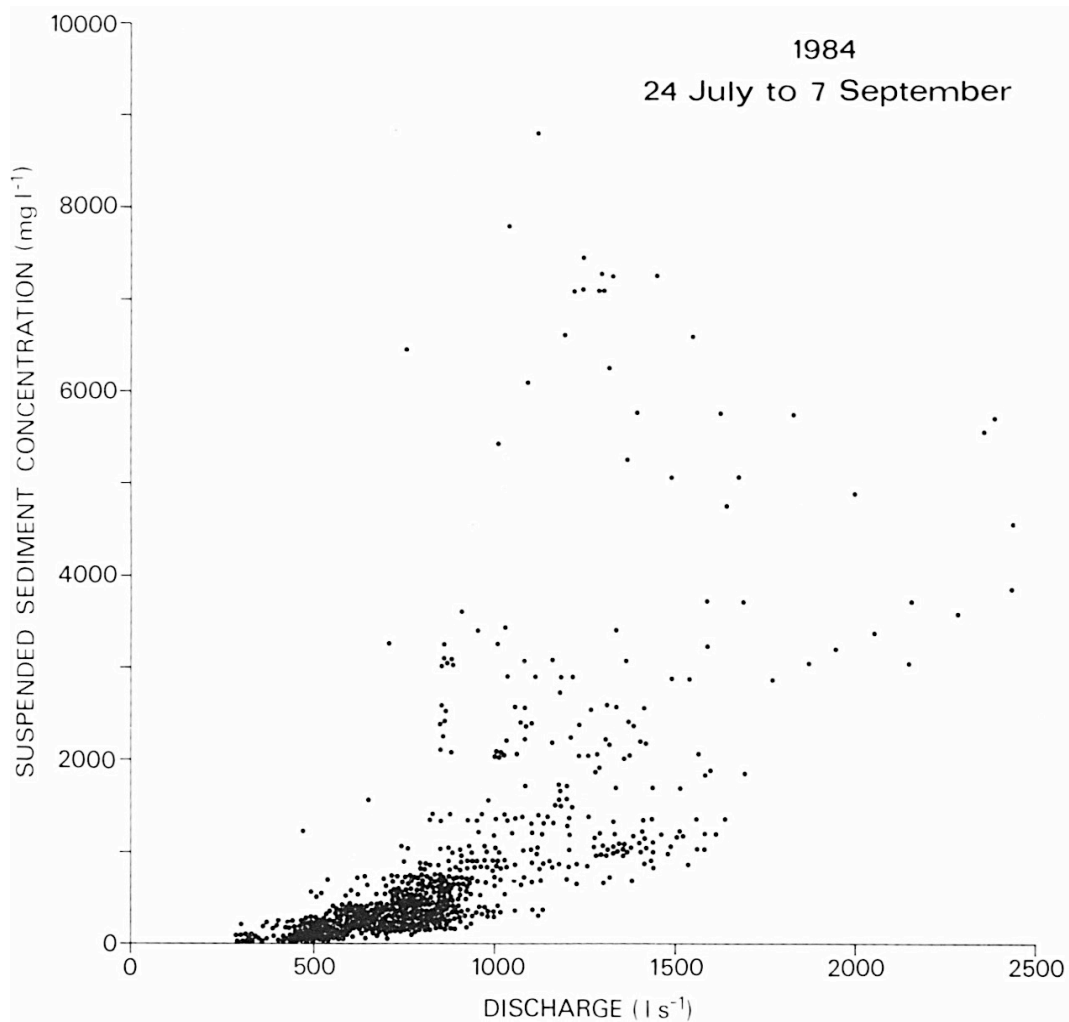


Figure 2.4: Scatter plot of suspended sediment concentration and discharge observations for part of the 1984 ablation season for the proglacial stream of Glacier de Tsijiore Nouve, Switzerland. (Gurnell, 1987). Note how a linear or power/exponential curve could be fitted to relate SSC to discharge.

Observations of variability in sediment loads for similar discharges at some glaciers suggest that sediment transport is limited more by sediment availability than stream capacity (e.g. Gurnell, 1987; Collins, 1989; Hasnain 1996; Haritashya *et al.*, 2006). The temporal variations of sediment evacuation by subglacial meltwater during the ablation

season have been characterised by peak discharges in meltwater accompanied by low concentrations of suspended sediment each day (e.g. Collins, 1979; Swift *et al.*, 2005a). The irregularity of the suspended sediment concentrations suggested rapid injection or pickup of sediment into subglacial streams following by exhaustion, recurring apparently independent of the variations of diurnal discharge. Therefore, the relationship between suspended sediment transfer and discharge in glaciated catchments is unlikely to solely reflect instantaneous entrainment and mobilisation by discharge, and instead, is also strongly dependent on sediment availability. This makes the use of sediment rating curves problematic for predicting SSC from discharge, as curves showing a strong linear fit have been rare (Gurnell & Fenn, 1984; Fenn, 1989). In particular, it is evident that considerable scatter is inherent to most sediment rating curves, indicating that the relationship between suspended sediment concentration and discharge is not simple, particularly at short timescales (e.g. Haritashya *et al.*, 2006). Sediment rating curves derived for different time periods may be very different in form and serial autocorrelation has been shown to create bias in the relationship (e.g. Fenn *et al.*, 1985). Therefore, considerable investigation has taken place in order to elucidate possible causes of scatter in SSC rating curves.

Hysteresis in the relationship between suspended sediment concentration and discharge has been shown to have a daily looped relationship over the ablation season (Figure 2.5). This is caused by a lag between the peaks in the time series of observations of suspended sediment concentration and discharge at the diurnal scale (Hodson & Ferguson, 1999). Gurnell (1987) describes how peaks in SSC normally occur in advance of the peak in discharge with this relationship being observed at diurnal and seasonal scales during the ablation season. This relationship indicates that, despite sufficient transport capacity in the streams to transport suspended sediment, there is

exhaustion in the supply of sediment at a range of temporal scales (e.g. Richards & Moore, 2003; Swift *et al.*, 2005b). The discharge history of the stream is therefore important in determining sediment available for transport as it accounts for the extent to which sediment may have been exhausted by a previous peak discharge event. Therefore, the exhaustion of sediment available for transport in suspension is one cause of the scatter in SSC rating curves.

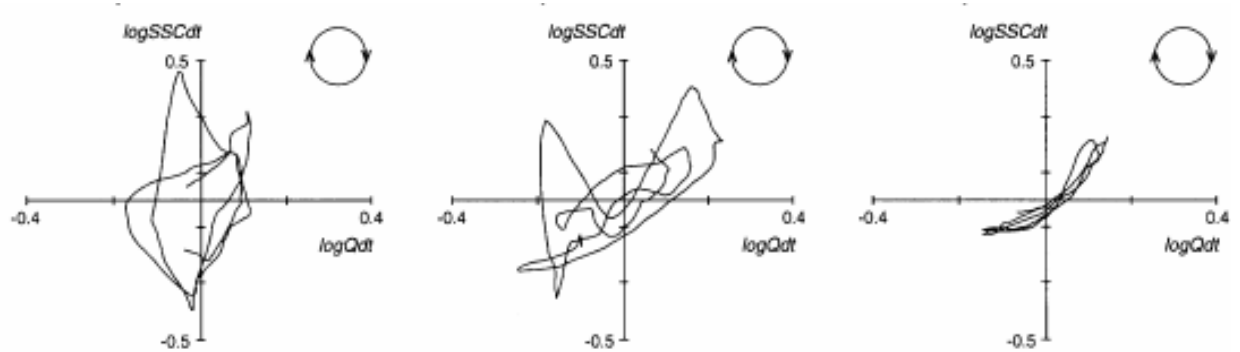


Figure 2.5: Diurnal hysteresis plots between discharge and suspended sediment concentration at Austre Broggerbreen, Finsterwalderbreen and Erdmannbreen, respectively. The open circles show the direction of the hysteresis between discharge and suspended sediment concentration. (Hodson & Ferguson, 1999).

The processes of sediment exhaustion have been investigated through a so-called ‘inverse approach’ whereby, sediment availability can be inferred from statistical models of SSC (e.g. Sharp *et al.*, 1998; Hodgkins 1999; Hodson & Ferguson, 1999; Richards & Moore, 2003). Such approaches have focussed on temporal changes in SSC, and in particular, those changes that appear uncorrelated to discharge should a simple rating curve approach be utilised. Three sets of processes that determine sediment exhaustion have been sought to be understood through this approach: sediment availability; sediment supply and; meltwater pathway. The application of this approach has centred around the construction and application of a range of discharge-based predictor variables that theoretically account for changes in sediment supply in order to explain changes in SSC through examination of the nature and strength of each predictor coefficient in the regression equation (e.g. Willis *et al.*, 1996; Hodson, 1999;

Hodson & Ferguson, 1999; Richards & Moore, 2003; Irvine-Fynn *et al.*, 2005a; Swift *et al.*, 2005b; Stott & Mount, 2007). The discharge-based predictors used in such studies to explain changes in sediment availability at a range of temporal scales include:

- The rate of change in discharge has been used to account for short-term sediment supply changes associated with the rapid entrainment of material during rising and falling discharges which results in the exhaustion or flushing of material (e.g. Willis *et al.*, 1996; Hodgkins, 1999; Hodson & Ferguson, 1999; Irvine-Fynn *et al.*, 2005a).
- The discharge history of the stream has been used to account for medium-term changes in sediment supply associated with entrainment of sediments during high discharges that was deposited during the falling limb of previous high discharges (e.g. Willis *et al.*, 1996; Hodgkins, 1999; Irvine-Fynn *et al.*, 2005a).
- Cumulative discharge has been used to account for seasonal supply exhaustion caused by the evacuation or limitation of sediment available for transport during the melt season (e.g. Hodson & Ferguson, 1999; Richards & Moore, 2003; Irvine-Fynn *et al.*, 2005a).

Multivariate regression approaches are required to be interpreted in light of the autocorrelation structures in the residuals from the models as studies have shown SSC values to be strongly dependent on past values (e.g. Ferguson, 1984; Fenn, 1989). The presence of autocorrelation can indicate the tapping of sediment stores throughout the melt season that took a period of hours to deplete, in addition to the large difference between the settling and entrainment velocities of such sediments (Fenn *et al.*, 1985; Willis *et al.*, 1996; Hodgkins, 1999; Hodson & Ferguson, 1999).

The process-based insights of the hydrological studies into suspended sediment transfer have yielded considerable insight into the functioning of particular glacial

systems and it is apparent that the availability of sediment supplies is a significant factor in determining the amount of suspended sediment transported in meltwater. Consequently, integrated approaches have incorporated a set of empirically and theoretically grounded processes into a method for robustly explaining patterns in SSC-discharge relationships that may have previously been attributed to scatter or random controls (e.g. Richards *et al.*, 1996; Hodson & Ferguson, 1999; Hodgkins *et al.*, 2003; Swift *et al.*, 2005b). However, whilst sediment availability may be significant in determining the amount of sediment transported in suspension, the ability of glacial systems to potentially increase and rapidly vary sediment supply has also been documented (e.g. Collins, 1989; Gurnell & Warburton, 1990; Willis *et al.*, 1996; Swift *et al.*, 2005b). Such patterns, often seen as pulses of sediment that maybe uncorrelated with discharge, have been associated with the morphology and dynamics of subglacial drainage networks.

The dynamics of sediment transfer patterns highlight the importance for consideration of sediment storage and release processes. As such, studies seeking to investigate sediment transfer dynamics must first consider the mechanisms of subglacial sediment entrainment. Sediment produced or transported at the ice-bed interface may become stored within the subglacial environment (Boulton, 1978; Collins, 1989; Alley *et al.*, 1997). The decrease in discharge towards the end of the ablation season will result in a diminishing capacity of subglacial discharges to entrain and transport sediments, resulting in the storage of sediments in subglacial conduits and cavities during the winter. Therefore, it is common for high sediment loads to occur at the start of the ablation season as the first meltwater reaching the sediment rich ice-bed interface is able to entrain significant amounts of stored material (e.g. Hooke *et al.*, 1985; Collins, 1990). This is particularly evident during the first major discharge event of the ablation

season (such as a spring event or precipitation induced flood) whereby, large amounts of stored sediments can be accessed by meltwater reaching the glacier bed (e.g. Collins 1990). Sediment loads during spring events are most likely limited only by transport capacity, as the sediment transport that accompanies these outbursts far exceeds the level predicted by any relationship between discharge and suspended sediment concentration (e.g. Anderson *et al.*, 1999; Swift *et al.*, 2005b). Such significant sediment transport events are in contrast to the episodic releases associated with the release of sediments stored in isolated subglacial pockets and cavities. These stores of sediment are tapped as water pressure increases and drainage pathways connect and integrate the cavities to the subglacial drainage network (e.g. Kamb, 1987). The rate and extent of such sediment flushes is strongly linked to subglacial water pressure increases whereby, as meltwater or rainfall reaches the bed there may be an increase in the number of subglacial cavities becoming linked which would input sediment to the system by tapping new sediment sources (e.g. Mair *et al.*, 2002). The release of sediment and water from these cavities is capable of generating high temporal variability in the concentration of sediment in the meltwater and can result in a large proportion of total annual sediment transport occurring in a few days (Souchez & Lorrain, 1987). The integration of isolated drainage features is a characteristic process of drainage network rationalisation. Flushes of sediment from the tapping of cavities will be representative of the sudden release of stored water and sediments in addition to a greater overall capacity for sediment transport.

Attempts to explain the variability in sediment evacuation have also been linked with the extent and pattern of the seasonal snowline (see Section 2.3.3). It has been hypothesised that the retreat and pattern of the snowline will account for much short-term variability in the rates of sediment evacuation and erosion due to determining the

location and timing of inputs of surface melt to the drainage system (Nienow *et al.*, 1998; Swift *et al.*, 2002). Part of this variability may arise due to the removal of the snowpack resulting in an increasing and progressively earlier diurnal peak in the daily hydrographs (Swift *et al.*, 2005a). In their study of sediment evacuation by an evolving drainage network at Haut Glacier d’Arolla, Swift *et al.* (2002) found that during the winter, low melt rates resulted in low discharges and low rates of flow through a subglacial drainage system, which is likely to be spatially distributed. Swift *et al.* (2005b) found that the form of diurnal runoff cycles was critical in determining basal sediment evacuation at Haut Glacier d’Arolla. When a predominantly inefficient subglacial drainage network was in operation the suspended sediment load (SSL, expressed in tonnes day⁻¹ or kg hr⁻¹) increased with discharge in the form $SSL \propto Q^{2.3}$. However, when an efficient channelized system became dominant, the relationship was $SSL \propto Q^{3.2}$. This highlights that the sediment transporting capacity of the flow increases at a greater rate than discharge. When the drainage network was predominantly distributed and inefficient, the sediment transport increased slowly with discharge and rates of basal sediment evacuation were generally low. Sediment availability increased as the drainage network channelised as diurnal water pressure within subglacial channels increased. This increase in diurnal variation of water pressure was coupled with increased ice-bed interaction that elevated subglacial erosion rates and the breakdown of larger sediment into more easily transported sizes, leading to efficient evacuation of basal sediment during the melt season. Thus, as higher flow velocities through larger pathways took place, there was an increase in basal sediment entrainment and evacuation, resulting in increased sediment load over the melt season. Sediment evacuation was expected to diminish over the melt season as a channelised system covers an increasingly restricted area of the bed. However, this was not observed as sediment evacuation continued to increase highlighting that additional mechanisms

were allowing meltwater to access previously untapped sediment. Such mechanisms were postulated to include the deformation of basal till into subglacial conduits and increased subglacial erosion by ice-motion, both of which could be controlled by increasing diurnal water pressure variations over the melt season.

The example of an unusual increase in seasonal sediment load has potentially important implications for studies seeking to link short-term episodic deliveries of sediment to subglacial meltwaters. Large pulses of suspended sediment concentration that are unrelated to discharge are known to occur throughout the ablation season (e.g. Willis *et al.*, 1996; Swift *et al.*, 2005a). Such pulses have been correlated with enhanced glacier motion. Research by Willis *et al.* (1996) on suspended sediment dynamics at Midtdalsbreen, Norway, found 57% of observed pulses in suspended sediment concentration that occurred during the ablation season were correlated with episodes of enhanced glacier motion. Six possible mechanisms for the generation of the sediment pulses were postulated:

1. Higher subglacial water pressures would cause increased basal sliding and enhanced subglacial erosion which would be more likely to occur in a distributed hydrological system;
2. Higher subglacial water pressures would steepen hydraulic gradients within the drainage system leading to increased water velocities and mobilisation and transport of sediment;
3. Increased pore water pressures may decrease sediment strength and lead to sediment deformation into subglacial channels;
4. Increased subglacial water pressures in a linked-cavity system leading to an increase in the number of linked cavities and the tapping of new sediment in newly tapped cavities;

5. Increased subglacial water pressure and glacier sliding may cause the drainage network to extend onto new areas of the bed and tap sediment;
6. High subglacial water pressures may cause part of the distributed drainage network to collapse into a channelised system.

Willis *et al.* (1996) state that whilst combinations of any of these potential mechanisms may generate sediment flushes, most of the flushes are likely to be caused by increased subglacial erosion, increased mobilisation and transport of sediment within an existing drainage network, or increased mobilisation and transport of sediment from new areas of the bed; all of which were facilitated by enhanced glacier motion. Similar findings have been obtained from research into glacier surge mechanisms whereby, outbursts of turbid meltwater during periodic flow instabilities have been linked to changes in the morphology of subglacial drainage systems (Björnsson *et al.*, 2003). Mechanisms responsible for such pulses in SSC have been postulated to be related to the reorganisation of the subglacial drainage network causing the release of stored water (Eisen *et al.*, 2005). For example, during a surge event at Kuannersuit glacier, Greenland, sediment discharge during the surge was considerably higher than during quiescence, and the total sediment yield during the 3-year surge could be as high as the total yield during the quiescent period of at least 100 years (Knudsen *et al.*, 2007). It has also been postulated that pulses of turbid meltwater that coincided with mini-surges at Variegated Glacier, Alaska, could have been caused by either the input of sediment through due to increased erosion at the ice-bed interface, or through the exposure of new areas of the bed to meltwater which would allow stored sediments to be entrained and transported (Humphrey *et al.*, 1986). Upon review of these mechanisms of enhanced sediment availability associated with glacier motion, it is apparent that

subglacial water pressure exerts a critical control on the processes resulting in sediment flushes.

In light of the apparent significance of subglacial water pressures in both facilitating sediment transport and generating anomalies in SSC, it is clear that the hydraulic efficiency of the subglacial drainage network is likely to be the overarching control on subglacial sediment evacuation through its control over flow competence, capacity and routing. Studies have shown that the availability of basal sediment for transport is determined by the morphology of the basal drainage network, as it influences the mechanisms by which sediment can be accessed and entrained (e.g. Swift *et al.*, 2005b). When a distributed drainage network is dominant, high water pressures are sustained over large parts of the bed where large quantities of sediments can be stored and are available for evacuation. When the network evolves so that an efficient network is dominant, this sediment is able to be accessed and entrained by a limited number of channelised conduits such that sediment availability declines and becomes exhausted over the melt season. However, although channelised networks access a smaller proportion of the bed compared to the distributed network, they may be capable of maintaining high availability of sediment over the melt season due to increasing diurnal water pressure variation in the subglacial channels. Studies have documented that variations in basal water pressure, controlled by the diurnal input of meltwater, have resulted in ice-bed separation (Willis *et al.*, 1996; Mair *et al.*, 2003; Swift *et al.*, 2005b). Ice-bed separation is one mechanism governing sediment availability as it would lead to extra-channel flow excursions and the possibility of deformation of high-pressure basal sediment towards the low-pressure conduits (Hubbard *et al.*, 1995; Swift *et al.*, 2005b). This is likely to be significant where glaciers overly till. Where soft deformable beds or layers of till underlay a glacier, basal till may extrude into the subglacial conduits and

be removed by high stream discharges (Boulton & Hindmarsh, 1987; Hubbard *et al.*, 1995). Willis *et al.* (1996) suggest that there will be an increase in sediment deformation into subglacial channels that are incised into the sediment when pore water pressures increase. An increase in subglacial water pressures was hypothesised as responsible for an increase in deformation of high-pressure basal sediment into lower pressure subglacial channels by Swift *et al.* (2005b) at Haut Glacier d'Arolla, Switzerland. Should a subglacial channel experience a pressure drop, till creep may be induced, which would be resisted by the viscosity and yield strength of the till. Therefore, the intrusion of sediment into conduits will be associated with subglacial morphologies and drainage dynamics that have the capacity to permit high basal water pressures which also experience dynamic variability. However, if sufficient meltwater is present and flowing through a channel to remove the till supplied to it and remain open, then the till will thin in the narrow zone at the channel edge, isolating the channel from till farther away over the course of a melt season and potentially contributing to seasonal sediment supply exhaustion. This would imply that any long-lived channels will have very little or no deforming till (Alley, 1992). Walder and Fowler (1994) describe how in subglacial channels that are incised into sediment, the flow in the centre of the stream will exert the greatest shear stress acting on the bed and will lead to greater erosion there, in turn creating a higher suspended load than at the banks. Thus, the mechanisms of subglacial sediment extraction may have implications for conduit formation and morphology, as a subglacial conduit can only experience a steady-state if the net erosion balances the creep of till into the channel. It is interesting to note that high basal water pressures may be localised in discrete drainage configurations where subglacial conduits are recharged by moulins (Nienow *et al.*, 1996; Gulley *et al.*, 2012a). Conduits fed by moulins have been hypothesised to result in both higher water pressures and more temporally dynamic changes in the hydraulic head of the conduits

when compared to the expected diurnal variability in water pressures. Hydraulic head and water pressures would increase rapidly in the conduits as the moulin recharges, which would subsequently propagate into the conduit system. It is conceivable that these localised variations in high water pressures could result in increased sediment entrainment and evacuation, particularly if the conduits and surrounding ice overly till, which may be observed as pulses of sediment. Therefore, it is likely that the variability in sediment availability for entrainment due to changes in water pressure is representative of both the general temporal patterns of variability associated with discharge through the subglacial conduits in addition to the variability in water pressure associated with meltwater recharge through moulins and crevasses and the subsequent propagation of waves of water pressure through spatially localised areas of the subglacial drainage network.

Significant releases of stored water have also been shown to be capable of transporting large quantities of suspended sediment (e.g. Maizels, 1997; Roberts *et al.*, 2001; Marren *et al.*, 2002; Rushmer, 2006; Russell *et al.*, 2006). Glacier outburst floods or jokulhlaups occur when an englacial or ice marginal lake is suddenly drained (Tweed & Russell, 1999). Such stores of water may be seasonal or perennial features but the release of water is usually unpredictable. Subglacial erosion has been found to play a major role in outburst events (Röthlisberger & Lang, 1987; Roberts *et al.*, 2001). Gornersee is a lake at the junction of the Gorner and Grenz glaciers, Switzerland, that develops annually and drains every year between the end of June and early September yielding discharges of up to $200 \text{ m}^3\text{s}^{-1}$. The discharge was found to increase at a steady rate over three days then recede rapidly until it reached the normal rate of glacial discharge (Bezinge, 1987; Collins, 1979). Collins (1979) observed suspended sediment concentrations of up to around 12 g l^{-1} during the drainage of the Gornersee which, in

1974, transported around 25 000 m³ of sediment in four days compared to the total ablation season transport of 67 000 m³. The draining of the lake was thought to have triggered a major change in the morphology of the subglacial drainage network with the probable creation of new channels, which permitted increased contact of waters with the bed and sediments that sustained the increase in sediment concentration throughout the rising flow of the lake drainage event.

Therefore, it is apparent that the morphology and water pressure of subglacial drainage networks exerts a critical control on both availability and transfer by meltwater of sediments produced and stored at the glacier bed. This is because network morphology, along with the input of meltwater, is the primary determinant of subglacial water pressure variability, which has been widely observed to be the critical control on the availability of sediment for entrainment at a range of temporal scales. Variations in sediment availability are fundamental in determining observed sediment loads and patterns, particularly as it is common for glacial streams to experience excess sediment transfer capacity. However, the relationship is complex, as subglacial water pressure also exerts controls on a range of glacier dynamics. Sediment availability may increase due to process such as ice-bed separation, motion, till deformation and the extension of conduits, and this may subsequently result in short-lived increases in sediment loads. Other dynamics such as the rationalisation of the subglacial drainage network and increases to hydraulic gradients can result in meltwater having restricted access to sources of sediment, particularly at the seasonal scale. Therefore, the scale of temporal variability in subglacial water pressure is fundamental to defining its impact on sediment availability. It can be concluded that rapid variability in subglacial water pressure, characteristic of short-term increases associated with meltwater inputs (or rainfall), can result in the action and interaction of a range of processes which cause

similarly short-lived increases in sediment availability which are manifested as pulses of SSC. This is further complicated by the inaccessibility of glacial hydrological systems resulting in a paucity of *in situ* observations. As such, data collected in studies seeking to understand the structure and functioning of subglacial systems is most often obtained in the proglacial zone. However, hydrological and sedimentological data can be subject to significant modification in proglacial zones, owing to their high energy and dynamic characteristics.

2.4.3 Proglacial Sediment Transfer

Proglacial zones are well documented and described as high energy environments that comprise significant stores of sediment exposed by glacier shrinkage which can be subject to rapid reworking due to high geomorphological and fluvial activity (e.g. Maizels, 1979; Hammer & Smith, 1983; Gregory, 1987; Gurnell, 1987; Warburton, 1990; Hodgkins *et al.*, 2003; Orwin & Smart, 2004a; Carrivick *et al.*, 2013). Early attempts to investigate the patterns of sediment transfer from glaciers revealed that records of suspended sediment concentration obtained in proglacial zones may be subject to significant temporal and spatial variation which is non-glacial in origin (e.g. Gurnell, 1982; Gurnell & Warburton, 1990; Gurnell *et al.*, 1992). In particular, it is the short-term storage and release of sediments in proglacial channels that may exert strong controls suspended sediment concentration variability (Warburton, 1990). Research from Arctic and Alpine catchments has highlighted the apparent significance of proglacial zones as a source of sediment transported in proglacial streams, which has been indicated by increases in the non-glacial component of sediment load as distance from the glacier snout increases (Gurnell & Warburton, 1990; Gurnell *et al.*, 1992, Orwin & Smart, 2004a). The theoretical basis for this was, as distance from the snout increased, as would the total number of sediment sources that could be readily subject to rapid subaerial or fluvial reworking. For example, Hammer and Smith (1983) measured

suspended sediment concentrations at ice-proximal and distal proglacial locations to ascertain that channel banks contributed 47% of the observed suspended sediment load with channel bank inputs creating the highest variability over short timescales. In addition, Orwin and Smart (2004a) found the proglacial area of Small River Glacier, Canada, to be the source for up to 80% of the total suspended sediment yield with release from proglacial channels dominating the observed transfer patterns. Hodson *et al.* (1998) monitored suspended sediment concentrations in a proglacial zone of an arctic glacier, revealing the proglacial zone to be both a source and sink of sediment over an ablation season. Over consecutive ablation seasons, proglacial zones have been found to act as a source and sink, with the runoff regime determining changes in sediment storage (Maizels, 1979; Hodgkins *et al.*, 2003). Flood events and high discharges caused by enhanced ablation and storms (Section 2.3.4) can be particularly important in enhancing sediment redistribution within, and from, glaciated catchments (e.g. Bogen, 1995; Gurnell, 1995). For example, discrete discharge events were found to be associated with high rates of sediment evacuation at Finsterwalderbreen, Svalbard (Hodgkins *et al.*, 2003). In addition, the disintegration of proglacial landforms such as moraines has been documented in Arctic forefields (Lønne & Lyså, 2005; Lukas *et al.*, 2005), highlighting the role of such landforms as transient stores of sediment, which can be reworked and redistributed by glacio-fluvial processes. Such fluvial controls on sediment production, storage and transport draw comparisons to similar relationships described in Section 2.4.2 in attempts to explain the exhaustion and varying availability of glacial sediment sources, raising questions as to the sources of sediments transported in proglacial channels. Therefore, it is apparent from the storage and release of sediment in proglacial channels that proglacial zones in both Alpine and Arctic settings can function as both sources and sinks of sediment (e.g. Hammer & Smith, 1983;

Warburton, 1990; Holmund *et al.*, 1996; Hodson *et al.*, 1998; Hodgkins *et al.*, 2003; Orwin & Smart, 2004a).

The role of proglacial zones as sinks and sources of sediment is complicated when the age of surfaces in modern proglacial zones are considered (Ballantyne, 2002a; Orwin & Smart, 2004b; Carrivick *et al.*, 2013). The youngest, most recently exposed surfaces in a proglacial zone, will be most susceptible to mobilisation (Ballantyne, 2002). Young surfaces result in the rapid transfer of fine sediments through debris flow, rainfall and fluvial processes (e.g. Orwin & Smart, 2004b). As recently exposed surfaces age, there is a decrease in sediment transfer that is largely due to an exhaustion of fine sediment for mobilisation (Church & Ryder, 1972). Stabilisation subsequently occurs due to surface armouring as vegetation colonises (Gurnell *et al.*, 2000). This lack of supply will be shown in the suspended sediment records of an environment that has recently become ice-free through an elevation in suspended sediment transport (from the younger surfaces), resulting from the rapid and episodic removal of easily mobilised fine sediments (Orwin & Smart, 2004b). Furthermore, sediment transfer has been shown to become increasingly restricted to fluvial processes with increasing distance from the snout highlighting the significance of geomorphological activity in redistributing glacio-fluvial sediments in more recently ice-free areas (Carrivick *et al.*, 2013). Therefore, terrain age in proglacial environments highlights the importance of consideration of the transformation that occurs as environments become ice-free and switch from systems dominated by glacial and glacially-conditioned processes of sediment transfer to those dominated by fluvial processes and paraglacial activity (Church & Ryder, 1972).

The dominance of coupled glacio-fluvial processes in Alpine sedimentary systems can be complicated by the presence of paraglacial activity in glaciated basins (e.g. Mercier & Laffly, 2005; Mercier *et al.*, 2009; Porter *et al.*, 2010). The presence of such activity has the potential to link the glacio-fluvial system to ice-marginal and slope processes, resulting in potentially complex slope-fluvio-glacio linkages (e.g. Etzelmüller *et al.*, 2000). For example, in attempting to explain observed variability in proglacial stream sediment fluxes at Austre Brøggerbreen, Svalbard, Porter *et al.* (2010) linked short-term, stochastic pulses in SSC to ice-marginal sediment sources, whereby ice-margin and valley-side sediments thaw and result in water-saturated debris flows. These sediments can be delivered to the glacier surface where they may enter supraglacial streams or moulins and be observed in proglacial SSC records. The implications of ice-marginal inputs are two-fold: First, they represent enhanced sediment delivery which has the capacity to significantly enhance sediment yields as progressive deglaciation occurs, raising the potential for ice-marginal sediment sources to become greater components of sediment yields as warming continues. Second, the variability extra-glacier sources may induce in proglacial suspended sediment records may complicate the already challenging interpretation of such records, particularly in studies utilising proglacial records to infer the functioning and controls on glacier dynamics. Thus, it is conceivable that deglaciation results in a fundamental adaption to the alpine model of glacio-fluvial sediment transfer by coupling ice-marginal slope processes to the glacio-fluvial sediment transfer system. Therefore, a slope-glacio-fluvial sedimentary system during deglaciation would result in increased complexity in sediment transfer processes and introduce complexity in the determination of rates and controls on sediment transfer. As such, records of suspended sediment obtained in proglacial zones of thinning glaciers must be interpreted in light of paraglacial conditioning and progressive deglaciation.

2.5 Geomorphological responses to Deglaciation

The preceding section has demonstrated that it is becoming apparent that the loss of glacier ice results in a landscape susceptible to rapid geomorphological change. This landscape modification results from a set of geomorphological processes termed 'paraglacial' (Church & Ryder, 1972). Landscapes which become exposed due to the withdrawal of glacier ice have been characterised by authors as being in an unstable or metastable condition (e.g. Ballantyne, 2002a; Orwin & Smart, 2004a; Mercier, 2009) owing to the rapid and extensive modification of such landscapes by '*nonglacial processes that are directly conditioned by glaciation*' (Church & Ryder, 1972, p. 3059). Church and Ryder (1972) suggested that after deglaciation the dominant component of sediment supply in fluvial transport systems will shift from glacial sources to secondary sources comprising reworked sediments. Those surfaces most recently exposed through deglaciation will be most vulnerable to rapid reworking and modification.

2.5.1 Models of Landscape response to Deglaciation

Church and Ryder (1972) suggested that landscapes experience a paraglacial period which is determined by the sediment yield of the landscape (Figure 2.6). The paraglacial period commences at the start of deglaciation and continues until the release of sediment returns to the background rate as determined by the geological characteristics of the landscape. The asymptotic decline in sediment yield represents the availability of glacially conditioned sediment, as it is this sediment which forms the sediment yield above background levels. This temporal analysis of paraglacial sediment release can therefore be approximated to an exhaustion model whereby the rate of paraglacial sediment release is represented as:

$$S_t = S_0 e^{-\lambda t} \quad (2.5)$$

where t is time elapsed since deglaciation, S_t is the proportion of ‘available sediment remaining for reworking at time t , S_0 is the total ‘available’ sediment at $t=0$, and λ is the rate of loss of ‘available’ sediment by either release or stabilisation (Ballantyne, 2002).

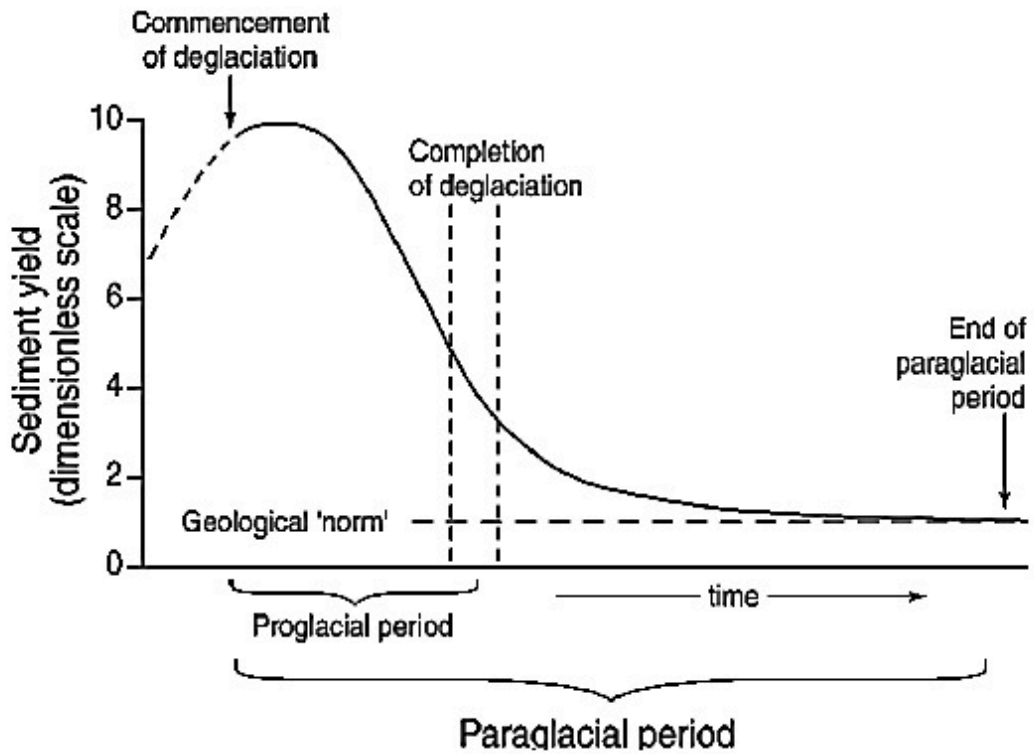


Figure 2.6: Sediment yield during the paraglacial period (Ballantyne, 2002a)

This exhaustion model assumed that the availability of potentially unstable sediment is the only constraint on the rate of paraglacial sediment release or reworking, that there are no further perturbations to the paraglacial system such as those caused by glacier readvance, and that sediment release is reduced by the system becoming stable or sediment sources become depleted (Ballantyne, 2002). A distinction is made between systems in which sediment release is directly conditioned by glaciation, termed primary paraglacial systems, and those in which rates of release is conditioned by the release of *in situ* glacial sediment in addition to releases by reworking of stored paraglacial sediments, termed secondary paraglacial systems (Ballantyne, 2002a). In primary

paraglacial systems it is possible calculate the length of the period of paraglacial sediment release if it is assumed that the total available sediment at the start of deglaciation (S_0 in Equation 2.5) is equal to 1. Therefore, from Equation 2.5, if $S_0 = 1$ at $t = 0$, then the rate of loss (λ) of available sediment can be expressed as:

$$\lambda = \ln(S_t)/-t \quad (2.6)$$

demonstrating the dependence of sediment release on the proportion of remaining sediment, resulting in the exponential decline shown in Figure 2.6 (Ballantyne, 2002a). In this model it is assumed that the availability of glacially conditioned sediment that exists in a potentially unstable state is the sole determinant on the rate of (paraglacial) sediment release.

In secondary paraglacial systems, fluvial processes are acknowledged as the primary processes remobilising paraglacial sediment through the reworking of paraglacial sediment stores in addition to the release of *in situ* glacial sediment (Ballantyne, 2002a). This model presents a positive relationship between specific sediment yield and basin size and, for studies in large basins, is a nearly linear function of downstream distance (e.g. Church & Slaymaker, 1989). The specific sediment yield is theorised to increase downstream due to the increasing mobilisation of glacial sediment (Ashmore, 1993) in addition to fluvial reworking and remobilisation of paraglacial sediment stores (Church & Ryder, 1972). Thus, drawing comparisons to increases in sediment loads in proglacial zones discussed in Section 2.4.3 (e.g. Gurnell & Warburton, 1990; Gurnell *et al.*, 1992, Orwin & Smart, 2004a). This downstream increase in specific sediment yield has been interpreted as a delayed peak in sediment yield and has been represented by a series of curves (Figure 2.7) (Harbor & Warburton,

1993). In small basins reworked sediments are removed and not replenished whilst in medium and larger basins the supply of reworked glacial sediment is replenished from upstream tributaries causing a delayed peak in sediment yield, and as such, form waves or cascades of reworked sediment through the catchment, typically over timescales in the order of centuries. Whilst this conceptualisation of sediment cascades is unlikely to be representative of the rate and efficacy of paraglacial processes during the paraglacial period, which are likely to be most active immediately after deglaciation (and therefore, before the peak in sediment yield proposed in the model of secondary paraglacial systems), this does allow the exhaustion model of primary paraglacial systems to be explored as a function of basin size. If the rate of sediment transfer is largest immediately after deglaciation and declines approximately exponentially, then small basins will have the greatest specific sediment yields immediately after deglaciation followed by medium and large basins. This is because the (exponential) rate of decline in sediment transfer is controlled by sediment input which will decrease with increasing catchment size. This model assumes that, in contrast to smaller basins, larger basins are characterised by:

- A larger decline in the rate of change in sediment removal;
- A more rapid decline in initial sediment availability and;
- A more rapid decline in initial rates of sediment release.

These assumptions are based on a system experiencing steady state conditions and whilst it is possible that progressive downstream sediment cascades will delay a peak in specific sediment yield, there is a compelling case for interpreting contemporary sediment yields in light of enhanced coupling of slope-glacio-fluvial during deglaciation.

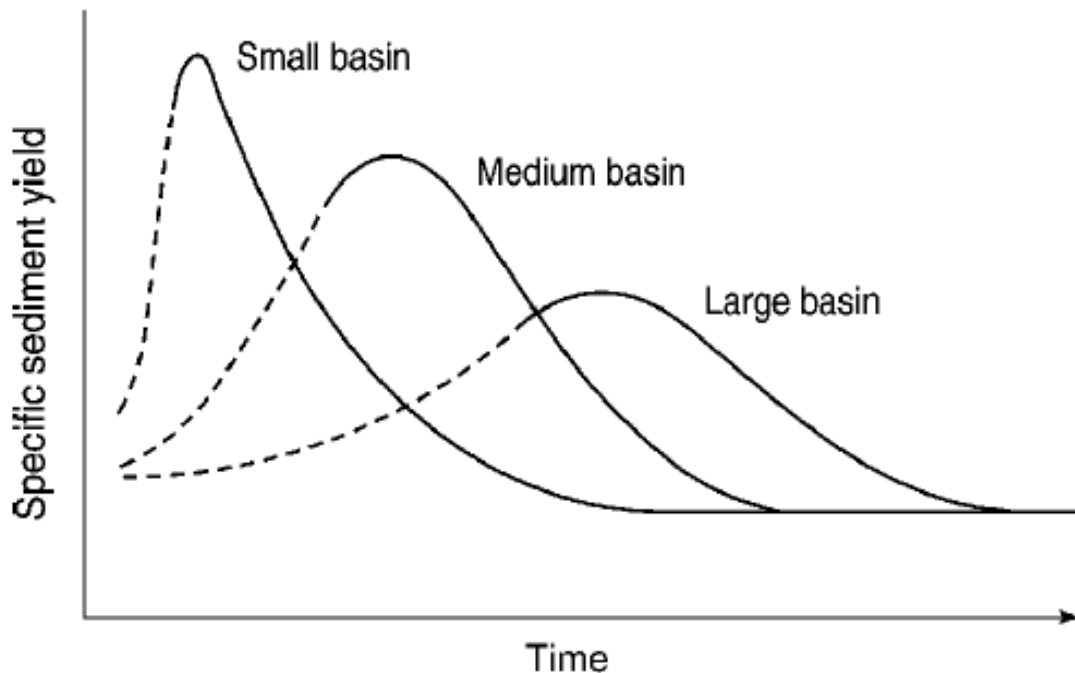


Figure 2.7: Specific sediment yield during the paraglacial period as a function of basin size (Harbor & Warburton, 1993; Ballantyne, 2002a)

2.5.2 Paraglacial activity

Enhanced sediment delivery over shorter timescales may occur due to periods of enhanced or renewed sediment reworking due to fluvial or forefield and ice-marginal non-glacial activity (Etzelmüller, 2000; Lukas *et al.*, 2005; Etienne *et al.*, 2008; Curry *et al.*, 2009; Porter *et al.*, 2010), with implications for predicting landscape response to deglaciation. Questions regarding the functioning of the slope-glacio-fluvial sediment transfer system in landscapes experiencing a changing climate have focussed on the heightened levels of geomorphological activity, due to the potential for such activity to impact upon sediment fluxes and yields in deglaciating environments. The enhanced geomorphological activity is usually a direct result of the exposure of unstable

sediments exposed by glacial down-wasting, but may also be brought about due to processes forced by climate such as the thawing of permafrost, enhanced runoff from glacier melt or altered precipitation patterns (e.g. Orwin & Smart, 2004b; Lukas *et al.*, 2005; Porter *et al.*, 2010; Carrivick *et al.*, 2013). Paraglacial activity associated with valley slopes and ice-marginal zones has been shown to deliver sediments to glacial systems (e.g. Ballantyne, 2002; Porter *et al.*, 2010; Cook *et al.*, 2013; Uhlmann *et al.*, 2013). These sediments may be delivered directly to the surface of glaciers and impact surface ablation rates (Lukas *et al.*, 2005) and be subsequently entrained and transported through the glacial hydrological network, raising suspended sediment concentrations (Porter *et al.*, 2010). This activity can be associated with thermal erosion that triggers the mobilisation or failure of ice-marginal sediments as progressive down-wasting of ice occurs (e.g. Porter *et al.*, 2010). Furthermore, rock slope failures due to glacial debuitressing have been postulated to affect rates of erosion and sediment transfer (Cossart *et al.*, 2008). Delivery of material to glaciers and forefields through slope failures may enhance sediment yields (Uhlmann *et al.*, 2013), however, such events may also inhibit sediment transfer due to the higher strength of rock avalanche material compared to glacio-fluvial deposits, which may inhibit processes of erosion and reworking (Cook *et al.*, 2013). Therefore, the relationships between paraglacial activity and sediment transfer patterns are likely to be complex. However, such slope-glacio-fluvial linkages have important implications for sediment storage and transfer in proglacial zones because, in addition to creating further temporal and spatial variability in sediment fluxes, it questions the dominant controls on sediment transfer in deglaciating environments, because contemporary rates of sediment transfer may be influenced from the recent or historical occurrence of paraglacial activity (e.g. Diodato *et al.*, 2013).

Glacial shrinkage can have a variety of geomorphic implications, reflecting the complex relationships between glacial, slope and valley-floor systems. The formation of proglacial lakes is one possible impact of glacial shrinkage (e.g. Hasholt *et al.*, 2000; Richardson & Reynolds, 2000; Hubbard *et al.*, 2005; Korup & Tweed, 2007; Carrivick & Tweed, 2013; Bogen *et al.*, 2015). Such lakes are usually located at the margins of glaciers in small depressions or overdeepened basins (Cook & Swift, 2012; Bogen *et al.*, 2015), and are often dammed between the frontal glacier margin and moraine material or other debris deposited in the forefield, such as landslide debris (Korup, 2002; Harrison *et al.*, 2006; Korup & Tweed, 2007; Rubensdotter & Rosqvist, 2009). The life-cycle of proglacial lakes is strongly coupled to glacier behaviour, in particular, glacial hydrological processes (Carrivick & Tweed, 2013), and can serve as indicators for historical glacier and ice-sheet behaviour (e.g. Teller, 1995). During periods of glacier shrinkage, proglacial lakes tend to grow as meltwater inputs generally increase and act as sediment traps reducing downstream sediment delivery (e.g. Bogen *et al.*, 2015). Sedimentation processes will be controlled according to the proximity of the lake to the ice-margin and lake water density stratification (Carrivick & Tweed, 2013). Sedimentation rates within lakes are affected by a range of sediment dynamics associated with glacial and geomorphological controls on sediment transfer. These include the vertical position of meltwater input streams relative to the total water depth with the thickness of delta sediments reflecting the vertical range of meltwater input. In addition, changes in lake stage, which may be abrupt, episodic or cyclical can have a significant impact on the rate of sedimentation. The role of proglacial lakes as water and sediment storage elements in glaciated catchments is well documented (e.g. Marshall & Clarke 1999; Hasholt *et al.*, 2000; Liermann *et al.*, 2012; Bogen *et al.*, 2015). Proglacial lakes interrupt meltwater passage through the proglacial zone, due to reduced flow velocities causing significant sedimentation. These lakes are particularly effective for

trapping coarse material forming the bedload component of glacio-fluvial sediment loads. Hasholt *et al.* (2000) estimated that 100% of the coarse-fraction of material was trapped in two small arctic proglacial lakes, with $90 \pm 10\%$ of fine-grained material becoming trapped; the primary source of which was found to be proglacial slopes. Similarly, Hicks *et al.* (1990) found 95% of the sediment yield in a glaciated basin in New Zealand was trapped by a proglacial lake, with 60% of the sediment originating from surrounding slopes. Liermann *et al.* (2012) report similar findings from a small proglacial lake in western Norway, whereby 80 to 85% of incoming suspended sediments were trapped during an ablation season. Therefore, the presence of proglacial lakes is likely to impact upon rates of glacio-fluvial sediment transfer due to their capacity to interrupt the downstream sediment cascade through processes of sedimentation, however, uncertainties regarding the life-cycles of such lakes raises the possibilities that sediment yields may be enhanced by the presence of sedimented former lakes which act as sediment sources. Furthermore, episodic downstream sediment delivery and reworking is a possible consequence of the development of proglacial lakes as they tend to be unstable and prone to catastrophic drainage or outburst floods through failure of their dam (Richardson & Reynolds, 2000). This raises uncertainties as to the impact of proglacial lakes upon rates of sediment transfer due to their potential role in storing and mobilising contemporary or previously sequestered glacial sediments (Carrivick & Tweed, 2013).

Processes of deglaciation have been invoked to explain and predict landscape response to deglaciation, particularly as understanding of the processes controlling the development and decay of landforms in high-latitudes is limited (e.g. Holmund *et al.*, 1996; Sletten *et al.*, 2001; Lønne & Lyså, 2005; Lukas *et al.*, 2005). Sediment reworking and redistribution by meltwater and fluvial processes is a fundamental

control on landscape modification (e.g. Lønne & Lyså, 2005; Lukas *et al.*, 2005), however, the rates and controls on these processes is poorly understood (Sletten *et al.*, 2001). Furthermore, questions remain as to whether deglaciated proglacial landscapes are representative of sediment accumulation or erosion and whether the source of sediments is subglacial, supraglacial or ice-marginal (e.g. Hodgkins *et al.*, 2003). It is suggested that reconstructions of landscape erosional history (and likewise, predictions of landscape change) are difficult due to the influence of paraglacial sedimentation on landscape adjustment (Orwin & Smart, 2004b). As areas become ice-free, the recently exposed surfaces will be unstable and subject to rapid reworking which will result in an elevation of suspended sediment yield as extra-channel sediments are input into proglacial streams. Slope processes and mobilisation by rainfall (in addition to in-channel fluvial processes) may be responsible for much of this sediment transfer, which has been shown to create variable transfer patterns between surfaces and proglacial streams (Orwin & Smart, 2004b). These transfer processes are most active within decades of deglaciation because sediment yields will decrease as sources of readily-mobilised fine sediment are exhausted and surfaces are colonised by vegetation resulting in surface armouring (Church & Ryder, 1972; Ballantyne, 2002). Therefore, stronger mobilisation processes are required in order to transfer sediments from older sources. Because the youngest surfaces will scale with the retreating ice margin, the area of older surfaces will increase over time, implying that the stabilisation of surfaces should result in a decline in sediment yield within decades of deglaciation. However, the release and storage in proglacial channels may sustain enhanced paraglacial sediment yields due to deposits of sediment in channels and extra-channel surfaces from previous glaciations (Ballantyne, 2002). If sediment yields in a deglaciating environment are representative of both paraglacial sedimentation in addition to the remobilisation of previously sequestered sediment, then interpretation of contemporary

landscape response to deglaciation and the resultant impacts on sediment yields and transfer patterns may be difficult, particularly over longer timescales. Therefore, uncertainties in the rates of sediment transfer during any 'paraglacial period' question what constitutes 'normal' sediment yields during deglaciation (Orwin & Smart, 2004a), and as such, the quantification of contemporary rates of sediment transfer is likely to be challenging, with important implications for inferring rates of landscape adjustment (e.g. Collins, 1998).

Attempts have been made to interpret the impact of a warming climate on water and sediment loads in streams and rivers draining glaciated catchments (e.g. Syvitski, 2002; Morehead *et al.*, 2003; Warburton *et al.*, 2007; Collins, 2008; Kettner & Syvitski, 2008; Huss *et al.*, 2014; Pralong *et al.*, 2015), albeit with a paucity of long-term data. Significant warming is expected to occur in Europe with most regions already experiencing more pronounced warming in summer than in winter (Alcamo *et al.*, 2007; CH2011, 2011), with significant implications for Alpine glaciers (e.g. Paul *et al.*, 2004; Zemp *et al.*, 2006; Bauder *et al.*, 2007; Paul *et al.*, 2007; Huss, 2011; Bliss *et al.*, 2014; Huss *et al.*, 2014). Climatic warming is also likely to change the seasonality of precipitation with the frequency of intense precipitation events also likely to increase (CH2011, 2011). Glaciated regions of the European Alps will be particularly sensitive to changes in temperature and precipitation whereby, small glaciers are likely to disappear while larger glaciers are likely to experience volume reductions of between 30% and 70% by 2050 (Zemp *et al.*, 2006; Huss, 2011). As glaciers retreat, the spring and summer discharge that is generated from the melting of surface snow and ice will decrease in the long term. Initially, the retreat will enhance summer flows but as more mass is lost from glaciers this discharge is likely to be significantly reduced (Collins, 2008), raising questions as the resultant impacts upon glacio-fluvial sediment transfer.

Despite several decades of glacier retreat, there is a paucity of data into long-term changes in the sediment loads of rivers draining glaciated catchments with unknown future trends (Syvitski, 2002; Warburton *et al.*, 2007; Diodato *et al.*, 2013; Pralong *et al.*, 2015). The dependence of geomorphological processes on climate, particularly in glaciated regions and catchments (Syvitski, 2002; Diodato *et al.*, 2013), provides one opportunity to explore the consequences of climate change through the modelling of *in situ* sediment transfer processes under the current climate (Morehead *et al.*, 2003; Stott & Mount, 2007; Warburton, 2007; Warburton *et al.*, 2007; Diodato *et al.*, 2013; Pralong *et al.*, 2015), through climate-runoff-sediment modelling chains that predict sediment loads from inputs of temperature and precipitation (e.g. Syvitski, 2002; Diodato *et al.*, 2013; Pralong *et al.*, 2015). Such simulations have forecast declines in sediment loads to occur with future changes in climate due to reductions in glacier runoff with deglaciation (Pralong *et al.*, 2015). However, when tested against past observations, sediment loads in glaciated catchments have been found to be poorly associated with glacier size due to apparently complex interactions between glacial, paraglacial and nonglacial processes (Diodato *et al.*, 2013), raising questions as to the dominant controls on sediment transfer during enhanced deglaciation. Furthermore, such models have suggested that temporal shifts in the timing of sediment transfer will occur towards the end of the Century, whereby maximum sediment loads will occur in early summer rather than late summer (Pralong *et al.*, 2015). However, improved understanding of how glacio-fluvial processes and sediment loads may respond to deglaciation is needed in order to make and refine such forecasts, particularly in light of the uncertainties in the rates of paraglacial sedimentation, which will be a critical control on the availability of sediment during deglaciation (Orwin & Smart, 2004b; Warburton, 2007). Therefore, it is apparent that examination of the functioning of glacio-fluvial systems is needed in light of the potential for enhanced processes of sediment mobilisation and transport if

better understanding of how sediment yields may vary during and after deglaciation is to be achieved. This has important implications for predicting landscape evolution and the interpretation of sedimentary records (e.g. Hambrey *et al.*, 2001; Lønne & Lysa, 2005; Lukas *et al.*, 2005; Knight & Harrison, 2009), due to the role of glacio-fluvial processes in reworking and redistributing glacial sediments (e.g. Warburton, 1990; Hodson *et al.*, 1998; Ballantyne, 2002; Hodgkins *et al.*, 2003; Orwin & Smart, 2004a; Barnard *et al.*, 2006; Leggat *et al.*, 2015).

2.6 Summary

This chapter has presented a review of the functioning of the glacial sedimentary system with particular attention to temperate alpine glaciers. The production and transfer of sediments in such glaciated catchments is strongly dependent on the ability for surface meltwater to access the subglacial environment where high rates of meltwater throughput often causes subglacial streams to experience excess transport capacity. The configuration of the subglacial drainage network is critical in facilitating access to subglacial sediments and determining the rate of fluvial sediment evacuation. However, the ability to distinguish between the competing controls of ablation inputs and subglacial drainage system morphology in determining the proglacial hydrograph (and thus, the nature of the proglacial SSC curve) remains illusive. Furthermore, the interpretation of SSC records obtained in proglacial zones are influenced by the nature of these forefields as high energy environments that are sensitive to change because they experience a complex set of interactions between glacial, fluvial and geomorphological processes. As climate change results in progressive deglaciation, expanding proglacial zones constitute significant stores of previously sequestered sediment raising the possibility that the scale of this storage may perhaps exceed that stored within and beneath the glacier. With continued deglaciation, it is becoming apparent that recently ice-free areas experience a range of fluvial, non-glacial and

paraglacial processes with the capacity to control the transfer of sediments within, and from, glaciated catchments. It is also becoming evident that such activity is not limited to the forefield, as sediment delivery from ice-marginal areas to glacial hydrological systems represents coupled slope-glacio-fluvial sediment transfer. The latter sections of this chapter have demonstrated that proglacial sediment loads can be influenced by the spatial organisation of geomorphological activity, the age of surfaces since deglaciation, and the nature of forefield hydrological processes. However, there is limited knowledge on the impacts of this diverse range of processes upon sediment transfer which, in addition to the uncertainties in rates of paraglacial sedimentation, raises questions centred upon understanding both contemporary sediment transfer patterns and processes of landform genesis and landscape evolution. In particular, this paucity of knowledge is likely to have significant implications for studies seeking to explain patterns of suspended sediment transfer in proglacial zones or in those which utilise proglacial records of suspended sediment transfer to investigate glacial processes and dynamics. Given the issues raised above, a number of key uncertainties can be summarised regarding the functioning of Alpine hydrological and sedimentary systems during deglaciation:

- It is becoming apparent that in order to understand hydrological and sediment transfer systems, integrated approaches that consider the inputs, throughputs and outputs of meltwater and sediment within a catchment are required in order to characterise the controls on proglacial hydrographs and SSC curves.
- The extent to which proglacial modification of SSC transfer patterns and loads occur requires attention through investigation of the extent to which any modifications can be robustly attributed to glacial, fluvial or non-glacial processes.

- A range of hydrological and geomorphological responses to deglaciation are likely to impact upon rates of glacio-fluvial sediment transfer, however, limited understanding of the extent and impacts of these responses in deglaciating environments is apparent, consequently, questions are raised as to the potential impacts of paraglacial activity upon processes of sediment transfer.

Given the variability in sediment transfer processes experienced in glaciated alpine catchments, it is likely that many of the processes responsible for determining sediment loads and patterns will manifest uniquely to the particular study system in question. However, if researchers seek to understand how such systems respond to deglaciation and predict the resultant landscape evolution, there is a clear impetus to quantify the importance of glacial, paraglacial and non-glacial processes in determining contemporary sediment loads and sediment transfer patterns in light of progressive deglaciation.

3 Field Site and Data Collection

3.1 Introduction

Chapter 2 highlighted the potential range of uncertainties associated with characterising processes of glacio-fluvial sediment transfer in deglaciating environments. Consequently, in order to understand the controls on, and processes of, suspended sediment transfer in glaciated basins, there is a need to observe processes of meltwater and sediment transfer in deglaciating Alpine glaciated catchments that experience characteristics such as recently deglaciating forefields, proglacial lakes, and potential paraglacial activity. The Feegletscher catchment, Switzerland, constitutes a compelling case study for such a programme of research, as a result of the glacial history, forefield geomorphology and hydrology of the catchment. The following chapter details these characteristics of the Feegletscher Nord catchment along with the research design of this programme of research. The geological and glaciological history of the Feegletscher Nord, is described in Section 3.2. Section 3.3 describes the glaciology of the Feegletscher and characteristics of the proglacial area, including descriptions of the geomorphology and proglacial hydrology. The methods adopted in this study are then presented in Section 3.4 along with the uncertainties associated with the data collection.

3.2 The Alps

3.2.1 Geological and Glacial History

The European Alps are a collision mountain belt created during the convergence between the African and European Plates (Schmid *et al.*, 1996; Bousquet *et al.*, 2002). Within this system of mountain chains and basins, the Swiss Alps form the transition

between the N-S oriented Western Alps of France and Italy and the E-W oriented Eastern Alps of Austria. There are two broad areas of high elevation within the Alps, the central part of the Swiss Alps comprises a number of granite peaks higher than 4000 m and stretches 200 km in an ENE-WSW orientation (Kühni & Pfiffner, 2001). The second is the Mont Blanc massif in the SW with a peak elevation of 4807 m at Mont Blanc and a number of peaks exceeding 4000 m. The Rhone and Rhine rivers form two large longitudinal valleys and mark a divide between the northern and southern main mountain ridges of the Swiss Alps. The Saaser valley lies in this southern ridge, in the Internal Zones of the Alps that consist of a stack of large thrust sheets comprised of crystalline rocks, ophiolitic rocks and Mesozoic sediments (Kühni & Pfiffner, 2001; Bousquet *et al.*, 2002).

The Feegletscher is set on the eastern flank of the Mishabel backfold where the geology is dominated by Bernard nappe mica-schists, with serpentinite, amphibolite and quartzite (Curry *et al.*, 2009). In line with the general pattern of retreat in the region, the Feegletscher Nord catchment was deglaciated by about 9 kaBP and subsequently repeatedly reoccupied by ice during the Holocene. Most glaciers in the Alps were no larger during most of the Holocene than during the Little Ice Age (Grove, 2001). In their chronology of Holocene glacier changes, Ivy-Ochs *et al.* (2009) chart patterns of glacier variations in this region from late Pleistocene to the Little Ice Age:

- 12 - 10.5 kaBP was marked by glacier advance due to the 1300 year-long Younger Dryas that is reflected by moraine construction. Increasingly dry conditions at the end of this period led to glacier shrinkage.
- 10.5 - 3.3 kaBP began with a shift towards warmer and likely drier conditions that lasted until about 3.3 kaBP. These climatic conditions resulted in glacier shrinkage with most glaciers smaller than their maximum

Little Ice Age extents. However, this period encountered a few, short phases of cooler conditions during which smaller glaciers may have reached their Little Ice Age extent.

- 3.3 ka to the Little Ice Age began with prolonged glacier advances, which led to the Little Ice Age advances from the 14th century until 1850. The largest glaciers advanced around 500-600 AD and possibly again around 800-900 AD, reaching sizes comparable to their Little Ice Age maximum extents. Most maximum Little Ice Age ice extents were achieved in the 14th, 17th and 19th centuries, with 1820-1850 AD marking the date of the final maximum extent of glaciers in the Western Alps.

This long history of advance and retreat has successively exposed significant quantities of glacial deposits, particularly from abandoned moraines that have subsequently been reworked and redistributed (e.g. Curry *et al.*, 2009; Lukas *et al.*, 2012). In addition, the history of glaciation and deglaciation since the late Pleistocene has directly conditioned rock mass stability through glacial erosion and debuttreasing resulting in a number of large-scale slope failures (e.g. Eberhardt *et al.*, 2004; Cook *et al.*, 2013).

Since around 1850, glacier retreat in the Swiss Alps has been pronounced and well reported (e.g. Grove, 1997; Haeberli & Beniston, 1998; Maisch *et al.*, 2000; Paul *et al.*, 2004; Bauder *et al.*, 2007; Farinotti *et al.*, 2009; SAS/VAW, 2009). Despite two periods of minor readvance around 1920-1925 and 1970-1980, half of the ice volume in the European Alps has been lost since 1850 (Haeberli & Beniston, 1998). Farinotti *et al.* (2009) estimated the ice volume of the Swiss Alps to be $74 \pm 9 \text{ km}^3$ in 1999, of which 12% was subsequently lost between 1999 and 2008. As of 2009 there are 5345 glaciers in the European Alps, found mostly at higher elevations of Switzerland, Italy, Austria, and France. Most of the glaciers are small, with 81% reported to be smaller than 0.5 km^2

and only 1% larger than 8.4km² (Zemp, 2006). Investigations into future changes have been attempted (e.g. Huss *et al.*, 2007; 2014) and there is strong consensus that ice mass loss in the 21st century will be significant (e.g. Solomon, 2007; Pachauri *et al.*, 2014).

3.2.2 Contemporary Climate

Westerly air masses are an important source of moisture in the Alps and low-pressure systems in the Mediterranean are an important source of prolonged cold and wet conditions. Due to the northern and southern ranges acting as topographic barriers, the inner alpine valleys, such as the Saaser, are relatively dry. The Feegletscher experiences the relatively dry, alpine climate of the Valais. Analysis of MeteoSwiss meteorological data for the region shows mean monthly rainfall of 74.3 mm and mean annual rainfall of 895 mm (2002-2012 data). Average May-September precipitation is slightly higher with a mean monthly total of 86.2 mm (2002-2012 data). The region experiences a mean annual temperature of 4.6 °C and a mean monthly average temperature for May to September of 11.3 °C. Farinotti (2010) calculated the environmental lapse rate in the region as -0.00056 °C m⁻¹ from 14 MeteoSwiss stations at elevations ranging from 273 to 3570 m asl.

3.3 The Feegletscher

3.3.1 Geometry and Mass Balance

The Feegletscher is located in the Saaser Valley, Valais Switzerland ($46^{\circ} 06' N.$, $7^{\circ} 54' E$). The glacier is fed from two high snow-field accumulation areas to the east of Alphubel (c. 4200m asl) and north of Allalinhorn (4027 m asl). The Langflüh ridge separates the glacier into two lobes. The Feegletscher Süd has an irregular terminus of c. 2.5 km frontal length, whereas the Feegletscher Nord (Figure 3.1) is constrained by steep rock walls as it descends from the ice-field, terminating behind a bedrock ridge.



Figure 3.1: Photo of the Feegletscher Nord taken on DOY 210, 2012. Black dotted line indicates approximate location of ice-flow divide between Feegletscher Nord and Feegletscher Süd.

The Feegletscher Nord is a small ice-field outlet glacier that descends from *c.* 4200 m asl to a terminus at 2169 m asl (Figure 3.2). The terminus of the Feegletscher Nord is located approximately 2 km from the village of Saas Fee. Analysis of a high resolution digital elevation model (swissALTI3D by SwissTopo, 2009) show the glacier length is 4.87 km across an elevation range of 2024 m. Glacier area was calculated from geocorrected satellite imagery as 7.56 km² and the mean glacier surface slope angle is steep at 29.1°. The Feegletscher Nord is oriented in a N-E direction and surrounded by the steep slopes of the peaks of the Mischabel chain, many of which exceed 4000m asl. It is heavily crevassed in the upper reaches but becomes constrained and narrowed by steep rock walled topography in its lower reaches (Figure 3.1). Most of the ablation zone of the glacier comprises sediment-covered ice. The lowermost trunk of the glacier appears to be becoming detached from the upper glacier at a short icefall and the lower parts of the glacier have significant quantities of surface debris (Whalley, 1979).

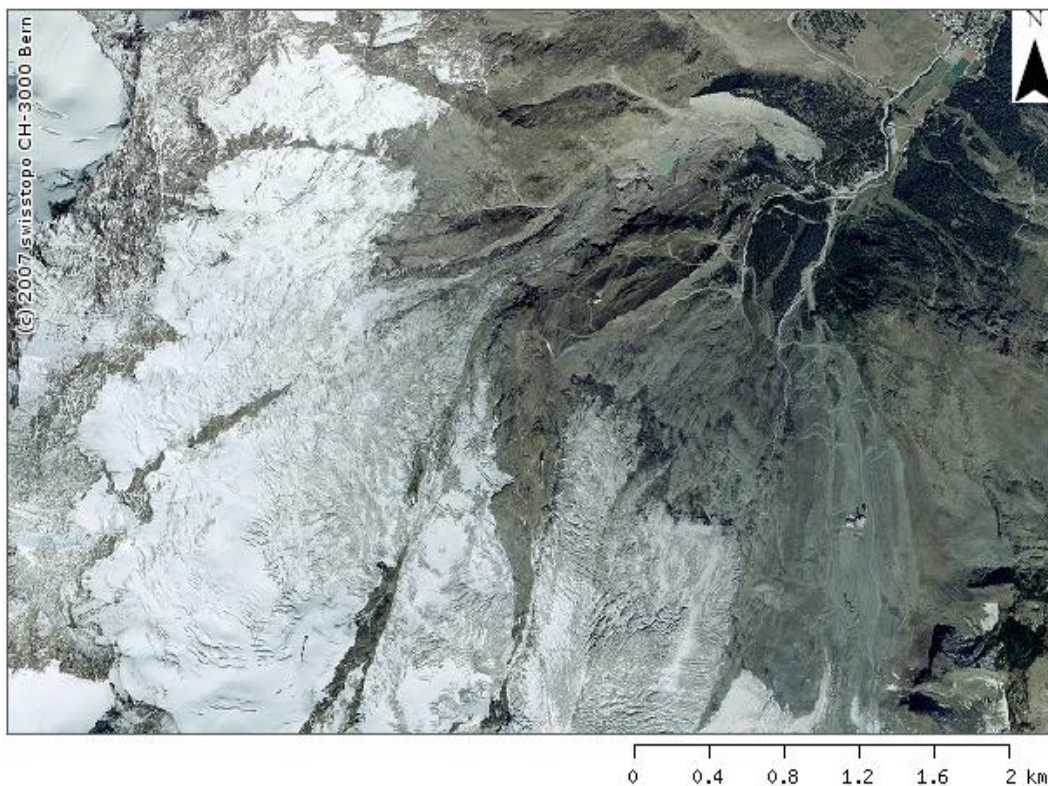


Figure 3.2: 2011 Satellite image of Feegletscher Nord indicating heavily crevassed mid and lower reaches. The terminal moraine is seen in the top right corner of the image. (SwissTopo, 2011).

Length variation data has been collected since 1883 and demonstrates retreat of the frontal position of the glacier of *c.* 1100 m to 2014 (Figure 3.3) (SAS/VAW, 2014). The Feegletscher Nord reached its Little Ice Age maximum position at AD 1818 as indicated by a *c.* 60 – 120 m high lateral moraine (Figure 3.4) (Bircher, 1982). Since the Little Ice Age, the glacier has retreated approximately 1100 m (SAS/VAW, 2009) and lowered approximately 90 m (Curry *et al.*, 2009). This trend of retreat has been interspersed by periods of minor advance and is highlighted in Figures 3.6, 3.7 and 3.8. There was a slight re-advance of the glacier during the 1970s and 1980s as it responded to climate cooling in line with other Alpine glaciers (Figure 3.7) (Beniston *et al.*, 1994). However, the glacier has been in sustained retreat since 1989 (Figures 3.8 and 3.9), with recession of *c.* 800 m (SAS/VAW, 2009). This rapid retreat has been accompanied by significant surface lowering and thinning which is apparent from the exposure of bedrock previously covered by glacier ice which extends throughout the elevation range of the glacier (Figure 3.1).

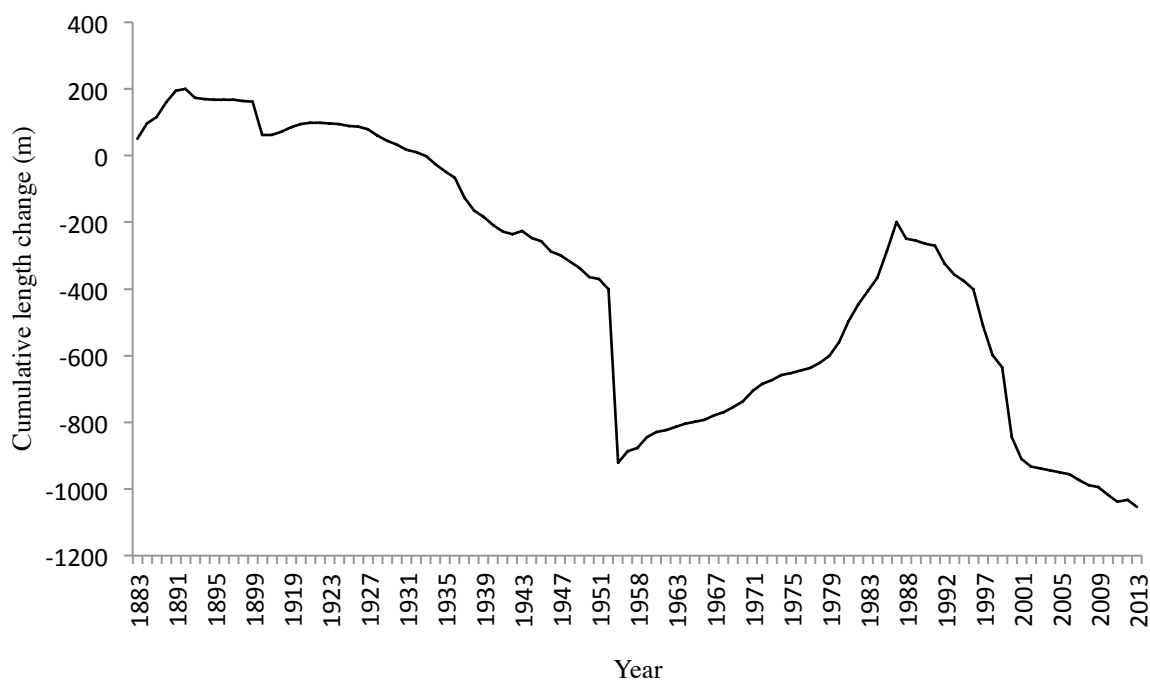


Figure 3.3: Cumulative length change of the Feegletscher Nord from 1883 to 2014 (SAS/VAW, 2014).



Figure 3.4: Lateral moraine marking Little Ice Age extent of Feegletscher Nord.



Figure 3.5: Feegletscher Nord in 1918 close to maximum Little Ice Age extent. Aspect is similar to Figure Figure 3.1. (ETH-Bibliothek, 2013)

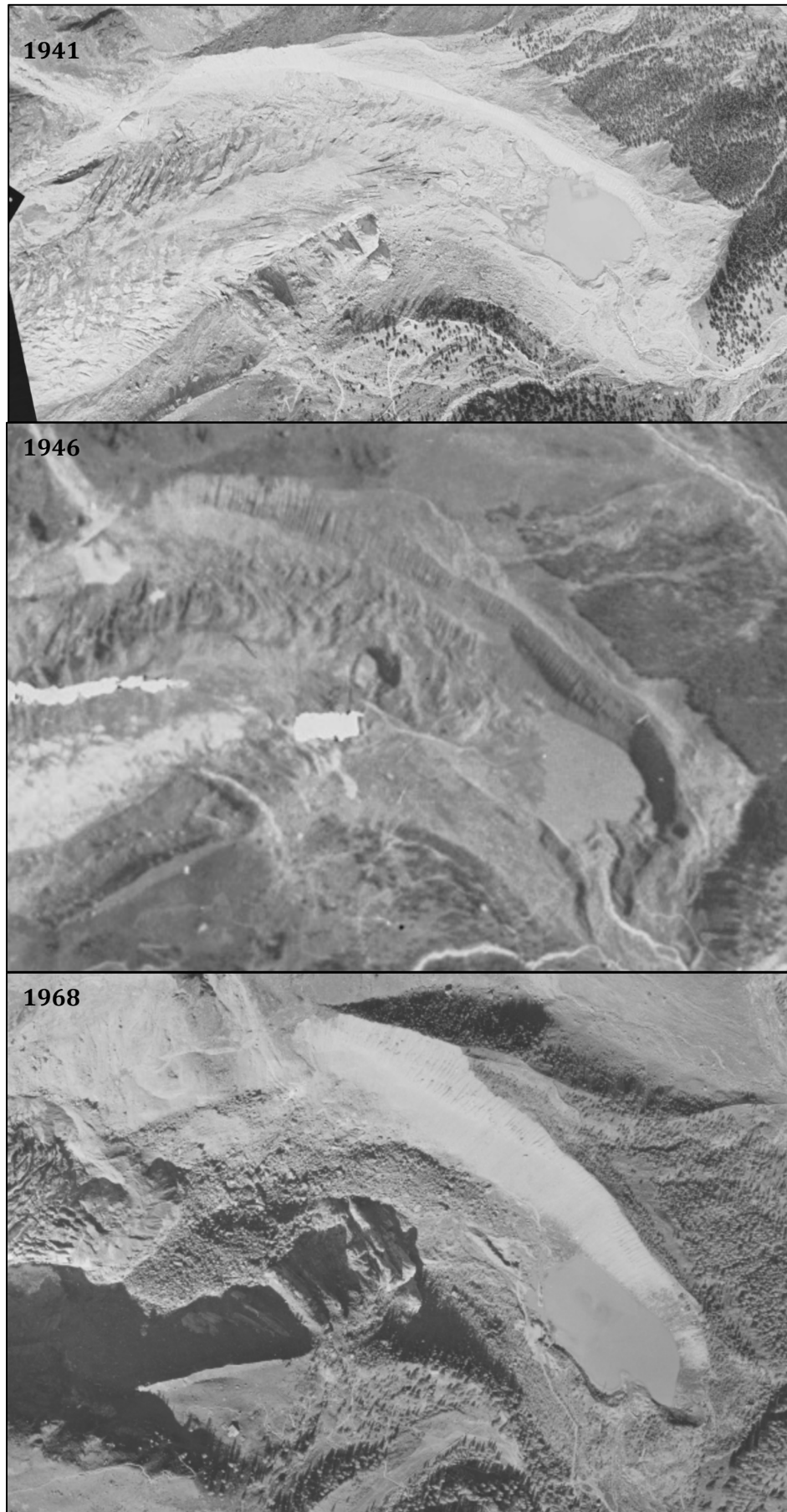


Figure 3.6: Feegletscher Nord proglacial zone aerial images in 1941, 1946 and 1968 showing the recession of the frontal position and highlighting the 1954 rock avalanche debris in 1968 image (SwissTopo, 2011).



Figure 3.7: Feegletscher Nord proglacial zone aerial images in 1972, 1980 and 1990 showing the re-advance of the frontal position (SwissTopo, 2011).

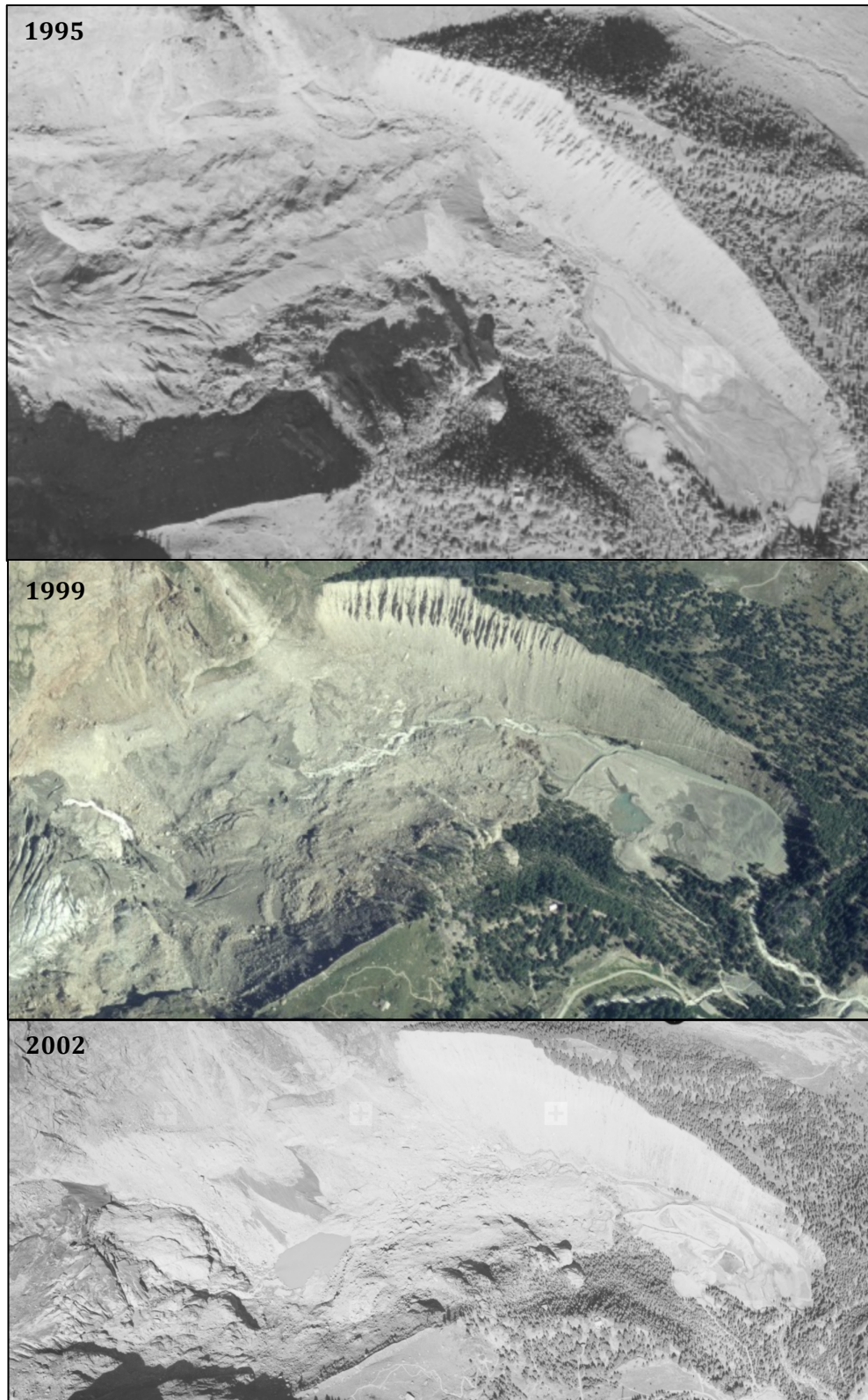


Figure 3.8: Feegletscher Nord proglacial zone aerial images in 1995, 1999 and 2002 charting the recession of the frontal position and showing the sedimentation of the lower proglacial lake and the formation of the upper proglacial lake in 2002 (SwissTopo, 2011).



Figure 3.9: Feegletscher Nord proglacial zone aerial image in 2011 highlighting the partial sedimentation of the upper proglacial lake and retreat of the frontal position of the glacier behind the bedrock ridge in bottom left of image (SwissTopo, 2011).

3.3.2 Glacier Hydrology

Despite a long history of tourism and development in the catchment, there is a paucity of published data on the Feegletscher Nord. Collins (1979) conducted hydrological and hydrochemical monitoring and analysis of the Feevispa river draining the Fee catchment. Total annual runoff between 1966-1972 is reported as around 37 to 54 x 10⁶ m³ with 88.7 % of the total runoff occurring between May and September and over 50% occurring in July and August. The drainage of englacial or subglacial stored water was hypothesised to occur in late September and 6 % of the total annual runoff was thought to be stored as liquid within the Feegletscher. The glacial hydrological system was inferred as readjusting very quickly to the inputs of snow and ice melt early in the ablation season. However, widely fluctuating individual daily flows suggested that meltwater outflow is limited to some extent in early summer by the drainage system, whereas late in the ablation season, conduits were able to effectively transmit meltwater. Small peaks on the falling limbs of diurnal hydrographs were postulated as resulting from the sudden releases of stored water.

Contemporary drainage conditions of the Feegletscher Nord are unknown. However, the thermal regime of the glacier is assumed to be temperate, as is commonly the case for other glaciers in the region and at similar alpine settings (e.g. Harbor *et al.*, 1997; Fountain & Walder, 1998; Swift *et al.*, 2005). Ground-penetrating radar detected conduits at the Feegletscher Sud located approximately 5-15 m below the ice surface at locations of ice depths of approximately 20-30 m (Urbini, 2012, *pers comms*; Urbini & Baskaradas, 2009). Because of their depth, they were described as superficial and sub-superficial meltwater pathways. Field observations indicate a lack of supraglacial streams at the Feegletscher Nord, likely owing to the steep and crevassed nature of the glacier surface. Meltwater streams flow between sections of glacier across areas of

exposed bedrock and along ice-margins. Short lags between the surface air temperature and meltwater discharge recorded in this research suggest a predominantly efficient or semi-efficient drainage system in operation by the end of the ablation season. Spring flood events associated with the sudden release of subglacially stored water have never been known to occur from the Feegletscher Nord and no outbursts of stored water have been recorded (Schnyder, 2012, *pers comms*). Field observations and satellite imagery indicates that meltwater exits the Feegletscher Nord from a single portal and flows over a deeply incised bedrock ridge via a waterfall and into a heavily braided proglacial lake before a network of proglacial streams transfer the meltwater to a single river, the Feevispa, at the proglacial boundary.

3.3.3 Feegletscher Geology and Geomorphology

The Feegletscher's surrounding and underlying topography is dominated by metamorphic rocks, with the Feegletscher Nord underlain by Palaeozoic mica-schists, along with others including muscovite gneiss, serpentinite, amphibolite and quartzite (Collins, 1979; Curry *et al.*, 2006; Cook *et al.*, 2013). The lowest altitude of permafrost in the region is *c.* 2650 for south-facing slopes and *c.* 2350 m for north-facing slopes (Curry *et al.*, 2009). The bedrock slopes surrounding the glacier are subject to frequent minor rock falls in addition to thaw-related activity.

The proglacial zone (Figures 3.9 & 3.10) is bounded by a large lateral moraine which was formed at the Little Ice Age glacial maximum. The forefield is characterised by two proglacial water bodies and deposits of rockfall material and glacial till. Curry *et al.*, (2009) describe the glacier forefield area as displaying marked within-valley asymmetry due to much larger lateral moraine volume on the northern side reflecting deposits from extensive active rockwalls on this side of the valley. The lateral moraine on the northern side marks the maximum vertical extent of the Feegletscher in 1818.

The moraine is steep and gullied with little vegetation on its active (proximal) slope and debris accumulation occurring at the foot of the moraine. The distal side is heavily vegetated and appears stable. Evidence of active paraglacial reworking of the moraine deposits has been previously described by Curry *et al.* (2006; 2009). The pattern of deglaciation has resulted in steep glacial deposits of stacked lateral moraines becoming exposed that have subsequently been reworked with deposits of reworked sediment accumulating at the foot of the slopes. Curry *et al.* (2006) report that the dominant agent of reworking of glacial material at the site is debris-flow activity and translational sliding, triggered by rainfall and snowmelt. The moraine is incised by the larger proglacial outlet stream and glacio-fluvial sediments have accumulated on the valley floor in the proglacial zone.

Cook *et al.* (2013) describe the forefield as characterised by the consequences of a large rock avalanche, known as the 'Guglen event', which occurred from a valley wall in July 1954. The rock avalanche involved the reported deposition of $> 1 \times 10^6 \text{ m}^3$ of rock, some of which was deposited on the glacier surface and the rest subsequently overridden and reworked by the glacier. The upper reaches of the proglacial zone are composed of much of the 1954 rockfall debris and Cook *et al.* (2013) describe the geomorphology of the proglacial zone as strongly conditioned by paraglacial activity comprising reworking of the lateral moraine and rock avalanche deposits. In seeking to explore the geomorphological consequences of the Guglen event, Cook *et al.* (2013) assessed the sedimentology of proglacial deposits to differentiate between glacial, rock avalanche and glacially modified deposits. It was found that the main proglacial stream (Point F, Figure 3.10) marks a divide between glacially reworked paraglacial debris from the lateral moraine, a gully-fed debris cone to the north, and areas of glacially overridden rock avalanche sediment and hummocky deposits forming an end moraine to

the south. These contrasting landform-sediment units were found to exhibit a significant difference in particle size characteristics with lateral moraine deposits comprising a greater proportion of fine sand to coarse silt with a mean particle size of 0.19 Φ , compared to hummocky moraine and reworked rock avalanche sediment, which comprised greater proportions of coarse grain sizes, with a mean particle size of 0.42 to 1.59 Φ . In general, the Guglen event rock avalanche debris and the glacially reworked avalanche debris were found to be dominated by gravel with a secondary component of sand, and only a very minor component of fine-grained material. This was in contrast to the more typical glacio-fluvial deposits in the vicinity of the lateral moraine. In addition, it was found that these sedimentological differences arise due to both the presence and reworking of rock avalanche debris. Much of the glacially-overridden rock avalanche sediments retained much of their angularity and contained a low proportion of faceted clasts, despite *c.* 40 years of glacial erosion. This was hypothesised to be a result of the large openblock nature of the avalanche deposits that resulted in high sheer stresses to limit glacial erosion and the ability to permit the efficient transfer of subglacial water which resulted in a lack of enhanced debris transfer as the rock avalanche was overridden and reworked (Cook *et al.*, 2013).

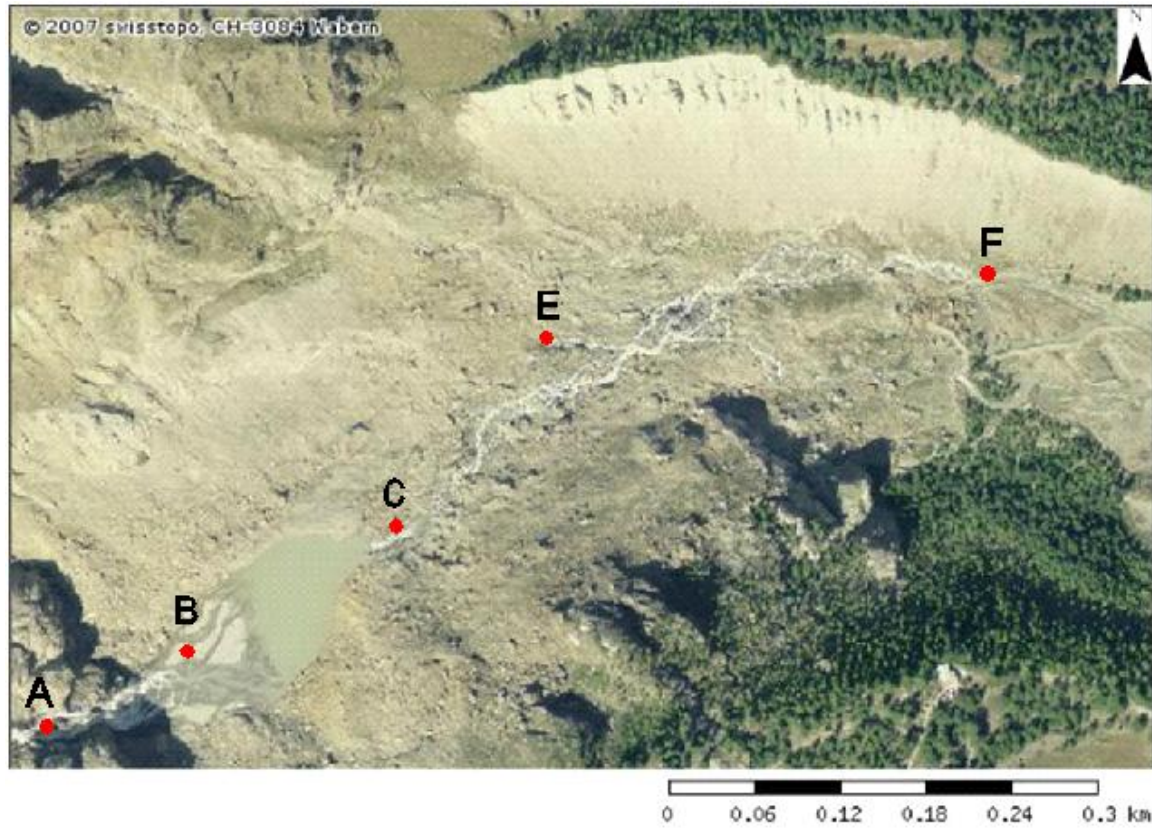


Figure 3.10: Aerial image of the proglacial zone of the Feegletscher Nord. Meltwaters flow from the glacier (out of view) in the SW corner of the image (A) into the proglacial lake via a braided delta (B). Meltwaters flow from the lake via a proglacial stream (C). Springs emerge approximately 185m downslope of the lake (E) and are suspected outlets of subterranean drainage from the lake. These streams converge to a main proglacial stream (F) in the east of the image which flows adjacent to the moraine. (Satellite imagery from SwissTopo, 2007)

3.3.4 Proglacial hydrology

The hydrology of the proglacial zone is characterised by a single braided proglacial stream and two proglacial water bodies that formed in response to glacier shrinkage. The upper proglacial lake at the Feegletscher Nord formed at an elevation of *c.* 2100 m during the ablation season of 2002 (Figures 3.8 & 3.11). Its dimensions were measured on 27th August 2008 and reported as 5,700 m² in area and 21,200 m³ in volume (Teyssere & Candolfi, 2008 cited in Hampel, 2009). Beneath the inlet to the lake there is a large delta that is composed of deposits of silt, sand, gravel and cobble sizes. There are several braided streams flowing through this delta. The lake is lined by fine sediments appearing similar to fine deposits in the delta. Field observations in 2010 indicated that lake stage varied on a diurnal scale, with variations of up to 2 m observed. This lake had become almost entirely sedimented by late June 2012 (Figure 3.13).

Meltwaters exit the upper lake through a discontinuous overspill channel that drains at high levels of lake stage and flows down-slope over relatively stable rock avalanche debris until it reaches the main proglacial stream at approximately 1900 m asl (Figure 3.10). Field observations suggest the lake may also drain through sub-surface seepage or flow through the dam, as sinkholes on the distal side of the lake shore were observed to be draining with no apparent proximate outflows. Springs approximately 185m downstream of the lake may be the outflow for any such sub-surface drainage, as the outflow from these springs appears substantial and continuous. The surface flow from these springs continues down-slope and joins the surface overspill flow from the lake to form a single proglacial stream. The single proglacial stream braids after coalescing at *c.* 1900 m asl and feeds a larger collection of shallow lakes. These lower lakes have been subject to sand and gravel extractions and their present morphology appears to

reflect this activity. The outflow from these shallow lakes joins the Feevispa stream from the Feegletscher Sud and flows down-valley.



Figure 3.11: 2009 photograph of the upper proglacial lake at the Feegletscher Nord. Note inlet streams to the lake flowing over bedrock through a braided delta to the main body of water (Schnyder, 2009).



Figure 3.12: Photograph of the upper proglacial lake in August 2012 following sedimentation (Schnyder, 2012).

3.4 Data collection

3.4.1 Monitoring sites

To achieve the aim of this study, a detailed programme of meteorological and hydrological data collected was undertaken in the catchment to characterise sediment transfer and hydrological processes. Field campaigns were conducted in 2010 and 2012. Proglacial fieldwork was undertaken in 2010 from 23rd June (DOY 174) to 4th July (DOY 185) and 10th to 19th September (DOY 253-262) as an exploratory campaign to investigate the hydrology and hydrogeomorphology of the forefield. An extended field campaign was undertaken in the ablation season of 2012 for ablation monitoring and proglacial fieldwork, which took place between 18th June (DOY 170) and 6th September 2012 (DOY 250). The 2012 field campaign was impacted by a storm event and resultant flood on DOY 183-184 that destroyed one gauging station with the loss of monitoring equipment and data. A further storm and flood occurred on DOY 233 that irreparably damaged one gauging station, however, data was retrievable. Figure 3.13 details the locations of monitoring stations within the catchment and Figure 3.14 presents the proglacial monitoring locations.

3.4.2 Meteorology

A programme of meteorological data collection was undertaken during the 2012 field season to facilitate the development of a distributed temperature-index melt model of the Feegletscher Nord. The most detailed meteorological data was provided by an automated weather station in Saas Fee operated by the Swiss Federal Office of Meteorology and Climatology (MeteoSwiss). The data comprised air temperature, rainfall and global radiation stored at 10-minute intervals and collected according to WMO standards. The station was located at 1796 m asl and 1.8km downvalley of the glacier terminus. A gap is present in the data from decimal day 184.9 to 191.6, as such,

air temperature and rainfall data was obtained from additional stations as follows: air temperature data was obtained from two temperature-only stations at two sites in the proglacial zone. These comprised Tinytag TGP-4020 data loggers with thermoelectric temperature probes enclosed in naturally aspirated radiation shields to ameliorate any bias introduced due to the influence of both direct radiation and air circulation. The accuracy of the sensors is ± 0.02 °C. The sensors measured air temperature continuously and stored data at 2-minute intervals. Hourly rainfall data during the missing period was obtained from a nearby automated weather station operated by MeteoSwiss located at 1535 m asl and 6.2 km downvalley of the glacier terminus. Further rainfall data was provided by a Campbell tipping bucket rain gauge that was installed in the proglacial zone on day 200 and operated until the monitoring station was damaged during a flood event on day 233. Precipitation was logged and totalled at two-minute intervals. Daytime cloud cover was estimated in okta by visual observations at two-hour intervals from DOY 198 to 250. In addition, observations of general weather conditions were made throughout this period.

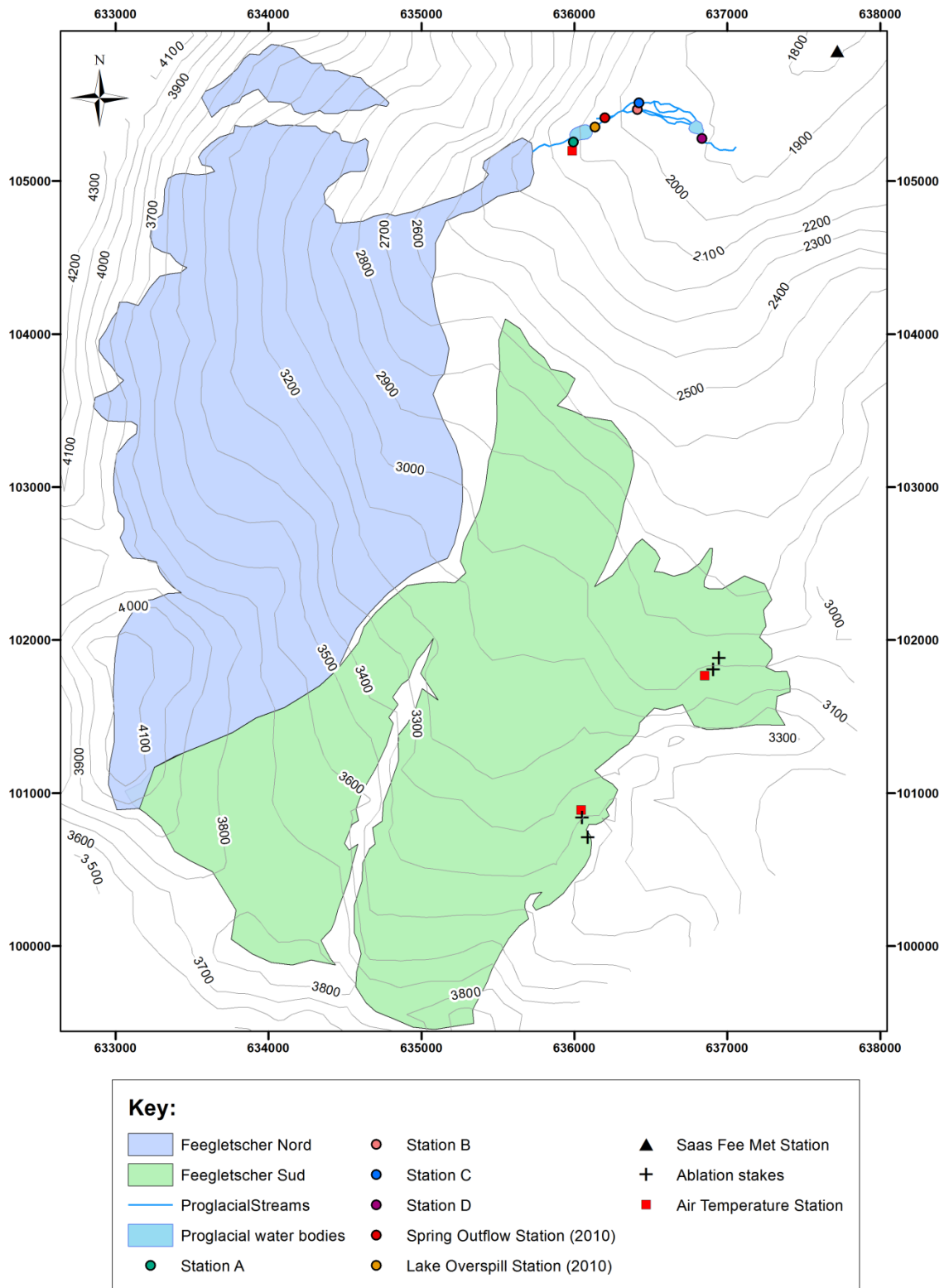


Figure 3.13: Map of monitoring sites utilised in 2012 field campaigns with additional 2010 sites highlighted in key.

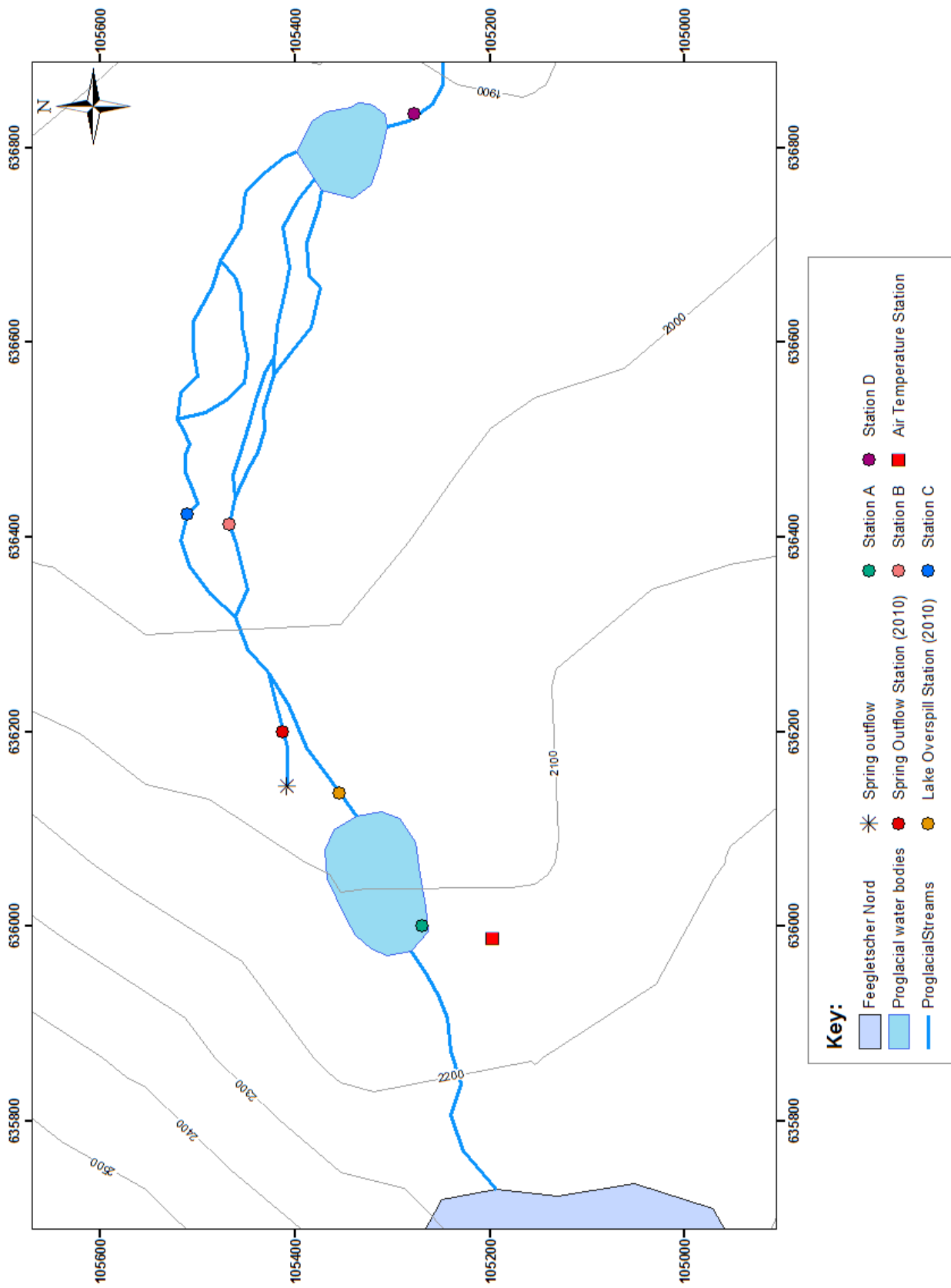


Figure 3.14: Map of Feegletscher Nord proglacial zone with hydrological features and monitoring stations indicated.

3.4.3 Glacier surveying

Four ablation stakes were distributed over the elevation range of the Feegletscher Sud owing to the lack of accessibility to the Feegletscher Nord surface during the 2012 field season (Figure 3.13). These were drilled into the ice to depths of 5 m. The locations for these stakes were selected to be representative of the surface ablation processes in the entire Fee catchment (Schnyder, 2012, *pers comms*), and such an approach is sufficient to monitor glacier ablation at a medium-sized glacier such as the Feegletscher (*e.g.* Østrem and Brugman, 1991). It is acknowledged that the use of more stakes would have desirable to ameliorate errors arising from the spatial and temporal variability that can occur in surface ablation rates (Fountain & Vecchia, 1999). However, the use of ablation stake transects was not possible due to crevasse fields and the use of the upper parts of the Feegletscher Sud for skiing routes. In addition, in order to maintain the skiing routes, snow is transferred daily from the accumulation area of the glacier in order to replenish these routes and fill crevasses at lower elevations, which would have resulted in erroneous ablation records.

In 2012, Stakes A and B were installed on DOY 180 (28th June) and stakes C and D on DOY 186 (4th July). The elevation range of the ablation stakes ranged from 3000m asl to 3450m asl. Ablation stake monitoring was undertaken using a standard tape measure (*e.g.* Hubbard & Glasser, 2005) at approximately weekly to fortnightly intervals until DOY 250 (6th September) (*e.g.* Richards *et al.*, 1996). To account for increased melting close to the base of the stake caused by the conduction of heat to the black plastic poles, a flat wooden measuring stick was used as a reference point for the glacier surface and measurements were made from this point to the top of each pole segment (*e.g.* Rutter *et al.*, 2011). The ablation stakes were assumed to be vertical in the ice and measurements were taken to within ± 0.01 m. In addition, GPS readings were

taken to monitor any elevation change due to ice flow. The retreat of the snowline was monitored either by direct observations at the ice-surface during ablation stake measurement using GPS records or through photographs of the glacier.



Figure 3.15: Installation and Location of ablation Stake A indicated by ranging pole in foreground.



Figure 3.16: Installation and location of ablation Stake B indicated by drilling equipment in foreground.



Figure 3.17: Location of ablation Stake C indicated by black circle.



Figure 3.18: Location of ablation Stake D.

3.4.4 Proglacial Stream Monitoring

Proglacial stream monitoring was undertaken in the 2010 and 2012 field campaigns. The monitoring of proglacial stream discharge and SSC was achieved through a network of gauging stations in the proglacial zone (Figure 3.14). These were comprised of Campbell CR10X or CR1000 data loggers to capture sensor data at 5 second intervals and record averages every 2-minutes.

During 2010, the aim of the field campaign was to characterise the hydrogeomorphology of the proglacial zone and the resultant control on suspended sediment transfer exerted by hydrological processes. Two periods of fieldwork for data collection were undertaken in the 2010 ablation season. The first was from 23rd June to 4th July, and the second was from 10th to 19th September. Three stations were established at stable channel cross sections in the proglacial zone to monitor discharge and SSC emerging at the two outlets of the upper proglacial lake, and discharge and SSC at the main proglacial stream adjacent to the lateral moraine. A further station monitored lake stage at the upper proglacial lake.

In 2012, the locations of gauging stations were selected upon the presence of a single channel with a stable cross section and further refined using three criteria: their siting should enable the total water and sediment loads and any downstream changes to be captured (minus any losses to groundwater), they should be located both up- and down-stream of proglacial water bodies, and they should, as a whole, give as wide a spatial representation of the hydrological and geomorphological characteristics of the proglacial zone as possible. Runoff routing during 2012 was similar to 2010, however, channel modification occurred after a significant flood event on DOY 184 of 2012. This event did not necessitate altering the gauging station locations. Field observations confirmed that the stream monitoring captured all fluvial flow from the Feegletscher Nord, minus any losses to groundwater. In 2012, Station A was installed within a

braided stream at the former upper proglacial lake (Figure 3.19). Station B was installed at a stream flowing through an area of hummocky moraine and rockfall debris (Figure 3.20). Station C was installed at the proglacial stream incising the lateral moraine (Figure 3.21). Station D was installed at the distal margin of the proglacial zone where meltwaters exit the forefield (Figure 3.22).



Figure 3.19: Station A on the margin of the former proglacial lake.



Figure 3.20: Station B in the proglacial zone.

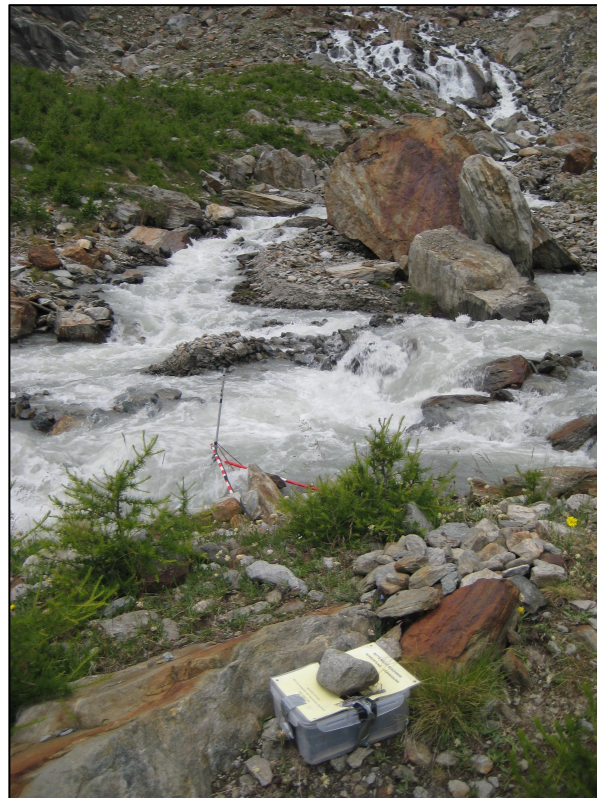


Figure 3.21: Station C in the proglacial zone.



Figure 3.22: Station D at the distal end of the proglacial zone.

3.4.4.1 Discharge

Meltwater discharge was monitored using standard methods (e.g. Hubbard & Glasser, 2005): Stream stage was recorded with the use of Druck pressure transducers (PDCR1730 or PDCR1830) at all gauging stations with accuracies of ± 0.25 (PDCR 1730) and ± 0.1 % (PDCR 1830). Stage-discharge relationships were developed at each gauging site using either velocity-area methods (e.g. Hodgkins *et al.*, 2003; Irvine-Fynn *et al.*, 2005) or salt dilution techniques (e.g. Moore, 2004; Orwin & Smart, 2004a), depending on the accessibility of the stream. These techniques were applied at a wide range of flow conditions to ensure robust stage-discharge relationships.

Stations A and B were calibrated using the velocity-area method as these streams were shallow enough to be accessed. A Valeport Model 002 flow-meter was used at the same channel cross-section for each site. The accuracy of the flow-meter is $\pm 2.5\%$ of readings above 0.5 ms^{-1} and $\pm 0.01 \text{ ms}^{-1}$ of readings below 0.5 ms^{-1} . Stations C and D required the use of salt dilutions ranging from 0.5 – 1.0 kg of salt, which was dissolved

in approximately 10 L of stream water and injected at distances of approximately 20 channel width upstream of the electrical conductivity (EC) probe at a flow constriction to ensure sufficient mixing (Moore, 2004; Hubbard & Glasser, 2005). Stream EC was measured in $\mu\text{S}/\text{cm}$ at 5 s intervals using a Hanna HI 8733 conductivity probe. The typical accuracy of the probe is reported as $\pm 2\%$ and a temperature coefficient of 2 % per $^{\circ}\text{C}$ was applied to compensate for the dependency of conductivity on temperature (e.g. Moore, 2004). A rating curve was applied to each time-series of stage using concurrent discharge values obtained from the aforementioned techniques against stage, these are summarised in Table 3.1. Calculated errors exhibit uncertainties in the region of 20% (with the exception of Station D, which was higher due to incomplete records for calibration). These errors are typical, with similar values given by Hodson and Ferguson (1999) and Irvine-Fynn *et al.* (2005a).

Table 3.1: Calibration curves to transform stage to discharge using non-linear regression. n is the number of concurrent observations of discharge and stage and SE is the standard error of the regression. All results were significant at $p \leq 0.05$.

<i>Gauging Location</i>	r^2	n	SE	SE as % of mean
Station A 2012	0.4	21	0.07	21.2
Station B 2012	0.6	12	0.15	17.9
Station C 2012	0.8	28	0.3	20
Station C 2010	0.6	9	0.3	
Station D 2012	0.4	15	0.65	29.7

Stage was monitored at two further locations during the 2010 field campaign. These were at the lake overspill channel and at springs where subterranean flow pathways emerged. Due to the nature of flow at these locations (for example, the lake overspill operated intermittently at high levels of lake stage) and the channel geometry, it was not

possible to obtain sufficiently reliable or numerous estimates of discharge through standard discharge gauging methods. However, dye traces (described in Section 3.5) gave indications of the nature of water flow from the springs. In addition, a time-series of lake stage at the upper proglacial lake was obtained during the June to July 2010 field campaign through the use of a Druck PDCR1830 pressure transducer submerged close to the lake shore.

3.4.4.2 *Suspended Sediment Concentration*

Turbidity monitoring was used to obtain continuous records of suspended sediment concentration (SSC) through the use of automated infra-red turbidity sensors calibrated with manually extracted “gulp” samples of stream water. This approach for determining turbidity-SSC relationships is well established in glaciological research (e.g. Willis *et al.*, 1996; Hodson & Ferguson, 1999; Hodgkins, 1999; Hodgkins *et al.*, 2003; Orwin & Smart, 2004a; Hubbard & Glasser, 2005; Irvine-Fynn *et al.*, 2005a; Orwin & Smart, 2005; Swift *et al.*, 2005a; Porter *et al.*, 2010). Turbidity was measured at each gauging station by infra-red Partech IR15C turbidity sensors with a typical range of 0 – 10,000 mg/l for suspended solids. SSC was measured from the filtering of 200 ml water samples through pre-weighed Whatman Grade no. 3 filter papers (6 μm particle retention). A sample of sediments lining the proglacial lake shore (likely to be representative of suspended sediment carried in the proglacial streams) was passed through a laser particle size analyser revealing only 6.4 % of sediments have a diameter $\leq 6.2 \mu\text{m}$, suggesting losses were small. Water samples were obtained for a wide range of flow conditions from a distance of approximately 25 % of the channel width. Sampling was aided with the use of a Manning VST automated vacuum water sampler at Stations B and C, which sampled at intervals ranging from 15 minutes to 2 hours. The filter papers were subsequently dried at 105 °C and weighed to derive SSC in g l^{-1} (e.g. Gurnell *et al.*, 1992). The analytical balance used to weigh the filtered papers is ± 0.001

g giving an error of $\pm 2\%$ at mean sediment content. Rating curves between turbidity and SSC were obtained using linear regression and are summarised in Table 3.2.

Table 3.2: Calibration curves to transform turbidity to SSC using linear regression. n is the number of concurrent observations of discharge and stage and SE is the standard error of the regression. a or b denotes the first and second 2010 field campaigns, respectively. All results were significant at $p \leq 0.05$.

<i>Gauging Location</i>	r^2	n	SE	SE as % <i>of mean</i>
Station B 2012	0.9	144	0.09	25
Station C 2012	0.8	133	0.07	25
Station C 2010a	0.8	37	0.03	
Station C 2010b	0.96	33	0.02	
Station D 2012	0.6	52	0.03	18.8
Lake Overspill 2010	0.9	60	0.02	
Spring Outflow 2010	0.8	46	0.02	

For both 2010 and 2012 data sets, missing values in the data series arose due to equipment maintenance when, for example, logger batteries were changed or sensors were checked for blockages. Missing values occurred over very short time-spans, typically several minutes. Missing values were filled by applying a five-point moving average to adjacent values in the time series.

3.4.5 Dye tracing

Dye tracing has been used extensively in glaciological research to investigate the nature and connectivity of surface and sub-surface flow pathways (e.g. Willis *et al.*, 1990; Sharp *et al.*, 1993; Nienow *et al.*, 1998; Gulley *et al.*, 2012a; Willis *et al.*, 2012). It has also been used to explore fluvial and groundwater flow through caverns and conduits (e.g. Smith & Atkinson, 1977; Smart, 1988; Mohammadi and Raeisi, 2007).

The purposes of undertaking dye tracing in this research were to establish the locations of inputs and outputs of subterranean flow pathways suspected of existing in paraglacial rock avalanche debris, and to describe the nature of flow through such pathways and the potential impact of this material on sediment transfer. In addition, dye tracing was undertaken following the sedimentation of the upper proglacial lake in 2012 to establish the nature of water throughput. The most commonly used tracers are fluorescent dyes such as Fluorescein and Rhodamine. Regulations in the Valais canton, Switzerland, do not allow Rhodamine dye to be used, consequently, Fluorescein dye was used in this study. Fluorescein emits a bright green fluorescence at 494 nm and is detectable at very low concentrations. It is also inert and non-toxic, which makes it an ideal tracer for use in natural environments. Fluorescein does suffer from photochemical degradation after several hours of exposure to sunlight (Smart & Laidlaw, 1977). However, as this study was investigating subterranean drainage pathways and the water flow through surface pathways of short distances, this effect was expected to be of negligible impact.

In 2010, dye tracings involved the injection of between 50ml and 150ml of liquid Fluorescein diluted at 1:10 ratio with stream water into suspected sub-surface drainage points close to the lake shore at the upper proglacial, which were first identified by visual observations of air bubbles being released through shallow fine-grained sediments. A Cyclops-7 fluorometer connected to a Campbell CR1000 data logger measured tracer return at a cluster of springs located approximately 185 m down-valley of the proglacial lake. A stage and turbidity gauging station was also installed at this location during the 2010 field campaign. The minimum detection limit of the fluorometer is 0.01 ppb. Due to the accessibility of injection locations, it was necessary to perform injections around the minimum levels of lake stage, typically at 07:00 which coincided with minimum discharge. Dye tracings were also performed in 2012

following the sedimentation of the proglacial lake in order to investigate meltwater routing and connectivity within the braided stream network occupying the former lake. 50ml of liquid Fluorescein diluted with stream water at a 1:10 ratio was injected close to the waterfall inlet to the lake and the same Cyclops-7 fluorometer was installed at the lake outlet.

4 Hydrometeorological Data Series

4.1 Introduction

This chapter presents the data collected in the Feegletscher catchment during two field campaigns: an exploratory field campaign was undertaken in 2010, which was followed by an extended and intensive campaign in the 2012 ablation season, the data collection from which forms the basis for the research undertaken in this thesis. Meteorological data is presented in Section 4.2 followed by glacier ablation data in Section 4.3. Proglacial time-series records for discharge and SSC are presented in Section 4.4 and the results of dye tracing undertaken in the proglacial zone are presented in Section 4.5.

4.2 Meteorology

4.2.1 Time-series

Meteorological data from the Saas Fee weather Station collected by MeteoSwiss is considered the principal data series and comprises precipitation, global radiation and air temperature measured to World Meteorological Organisation standards (Figures 4.1a, b & c). Additional data was provided by four temperature sensors installed in the catchment (Figures 4.2a, b & c) and a tipping bucket rain gauge located in the proglacial zone.

The Saas Fee weather Station was out of operation for a period of 5.65 days from DOY 185.94 to 191.6. As this data series was considered the principal meteorological record, temperature data was reconstructed from an air temperature sensor installed in the proglacial zone approximately 1 km upvalley from the Saas Fee weather station through linear regression ($r^2 = 0.8$, $n = 5352$, $p \leq 0.05$). This approach was justified (in

contrast to the use of the environmental lapse rate) as the record from the proglacial zone showed higher daily peak air temperatures suggesting that local environmental characteristics influenced air temperature at this location. Missing hourly rainfall records were obtained from an adjacent MeteoSwiss station in Saas Balen (distance = 6.1 km, elevation = 1461 m asl).

The air temperature record at the Saas Fee weather Station shows marked diurnal cyclicity and a slight seasonally decreasing trend. However, this general trend is influenced by a marked cool period over four days towards the end of the study period (Figure 4.1b, DOY 238 - 248). A mean air temperature of 12.6 °C is contrasted to the most frequent temperatures, which are between 8.8 °C and 10.8 °C, representing a positively skewed distributed (Table 4.1). Minimum station air temperature was 0.5 °C and maximum was 27.3 °C. Air temperature and global radiation are correlated with an r-value of 0.6 at $p \leq 0.01$. Similar diurnal variability is seen in the proglacial temperature records with a mean temperature of 9.8 °C. When the variability of the on-ice air temperature records is examined, a marked diurnal signal is dominant and mean air temperatures at 3000 m asl and 3448 m asl are 5.2 °C and 2.1 °C, respectively, indicating a marked downward shift as elevation increases. These temperature records also indicate that air temperatures were above 0 °C for a large proportion of the elevation range of the glacier for most of the ablation season, and tended to drop below zero mostly at higher elevations, typically overnight (Figure 4.2d).

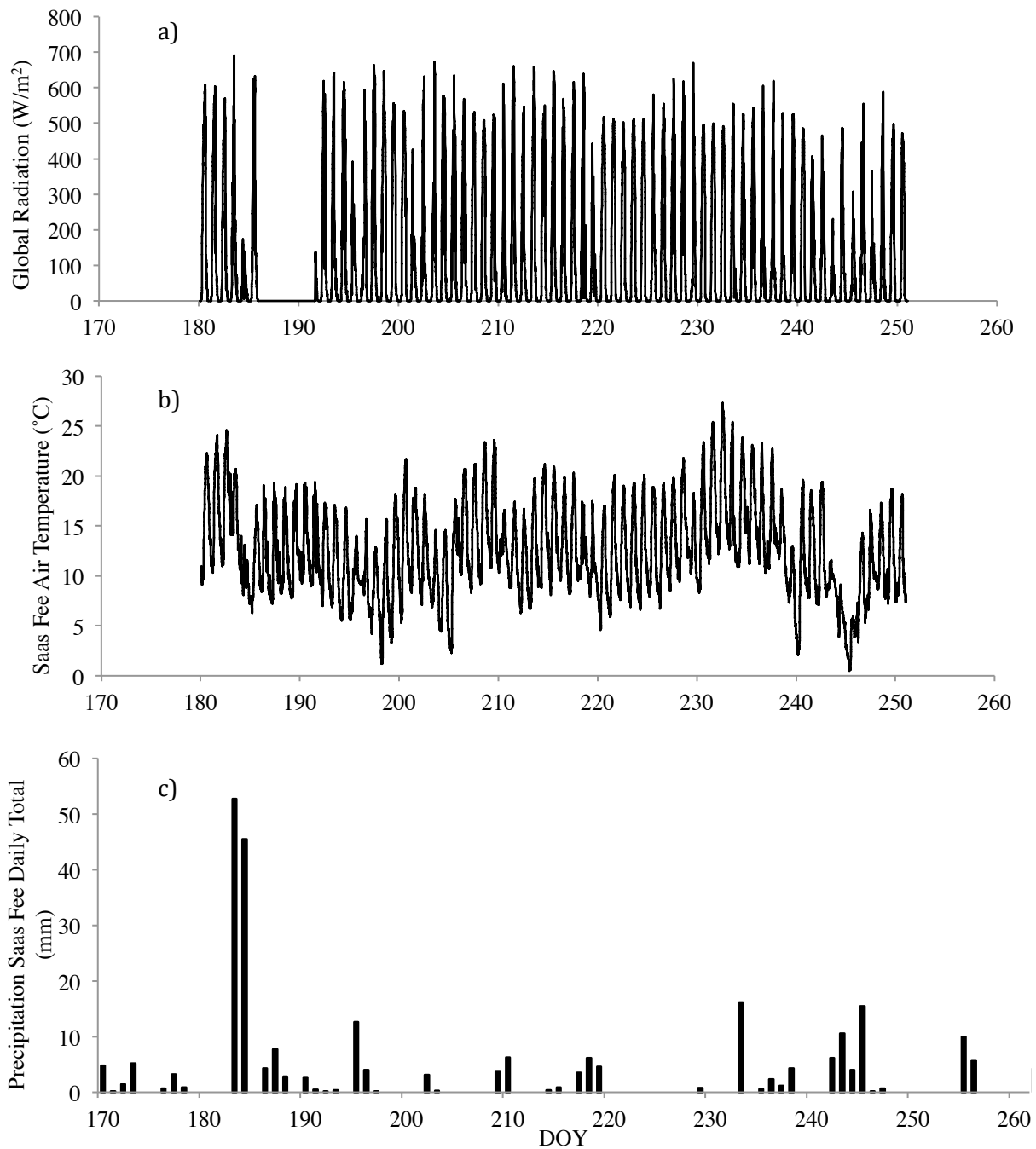


Figure 4.1: Meteorological data recorded at Saas Fee weather Station in 2012 of a) Global Radiation, with data gap from DOY 185.9 to 191.6. b) Air Temperature, with reconstructed data between DOY 185.9 to 191.6. c) Daily total precipitation.

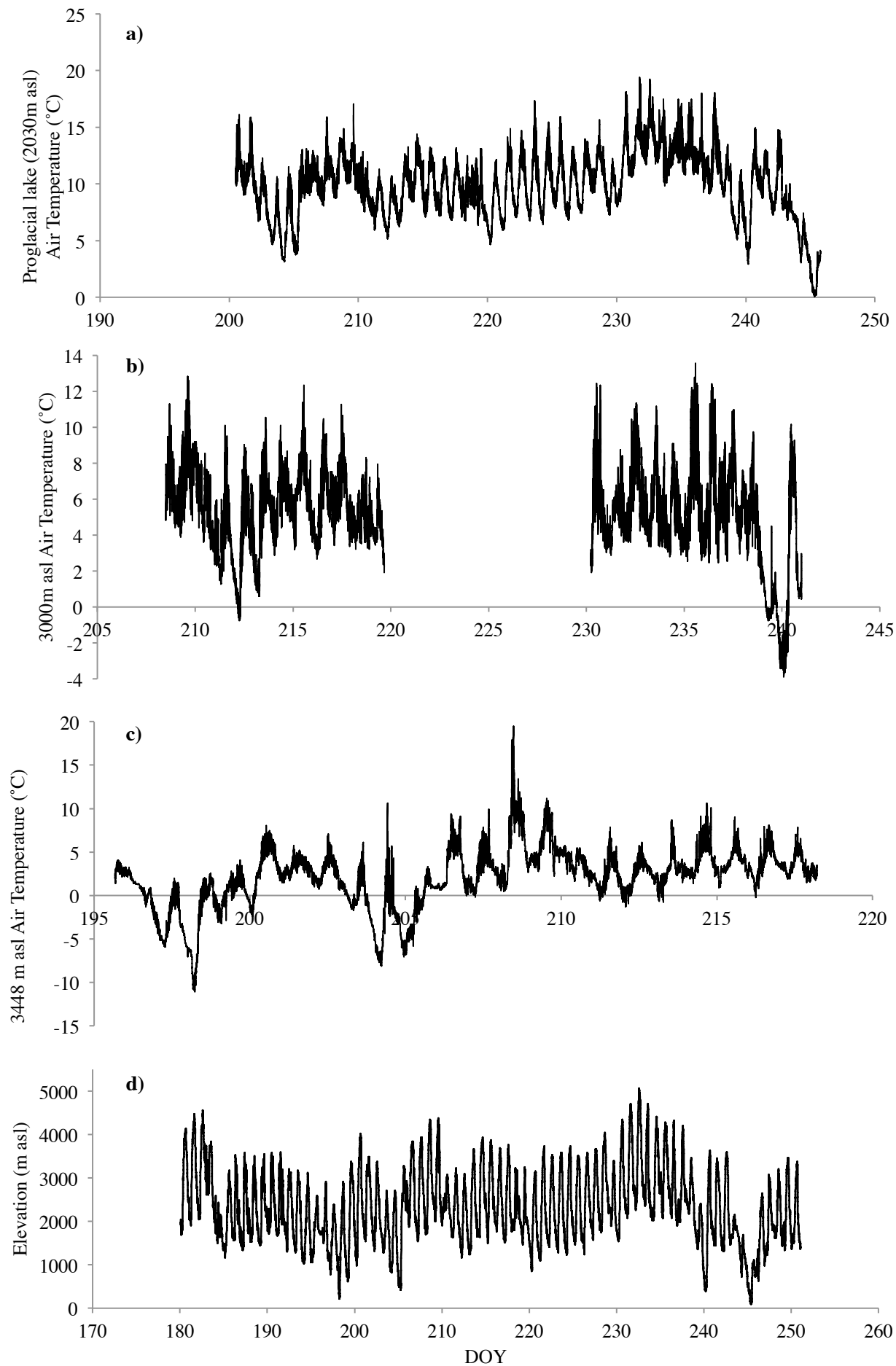


Figure 4.2: a) Air temperature at 2030 m asl. b) On-ice air temperature at 3448 m asl. c) On-ice air temperature at 3000 m asl. d) Elevation of 0°C isotherm calculated with environmental lapse rate

Table 4.1: Descriptive statistics of meteorological time-series

		SF weather Station (1790 m asl)	Proglacial zone (2030 m asl)	Stakes A & B (3000 m asl)	Stakes C & D (3448 m asl)
Air Temperature (°C)	Mean	12.6	9.8	5.2	2.1
	SD	4.6	2.8	2.5	3.4
	Mean daily SD	3.6	1.6	1.7	2
	Mean daily range	11.3	7	8.1	9.4
Global Radiation (w/m²)	Mean	125.5			
	SD	179.2			
	Mean daily SD	156			
	Mean daily range	499.2			

4.2.2 Lapse rates

The lapse rate at which air temperature varies as a function of elevation was investigated due to the potential for spatial and temporal variability in near-surface lapse rates in glaciated catchments (e.g. Hodgkins *et al.*, 2013b; Irvine-Fynn *et al.*, 2014). This was undertaken by establishing the mean lapse rate between three concurrent time-series of air temperature recorded at the Saas Fee weather Station (1790 m asl) and two temperature sensors installed at the locations of ablation stakes located at 3000 m asl and 3448 m asl, respectively (Figure 4.3a). The two sensors installed at the proglacial zone (c. 2000 m asl) were excluded from the lapse rate analysis, as examination of the time-series revealed they were likely significantly influenced by local topography and led to biased lapse rate values.

The mean lapse rate between the Saas Fee Station and the sensor at 3000 m asl was calculated as -0.0064 °C/m (Figure 4.3b) with a correlation of $r = 0.66$ ($n = 1353$, $p \leq 0.01$). The mean lapse rate between the two on-ice stations at 3000 m asl and 3448 m asl was calculated as -0.0044 °C/m (Figure 4.3b) with a correlation of $r = 0.76$ ($n =$

1353, $p \leq 0.01$). This lower lapse rate is a result of the temperature inversions highlighted in Figures 4.9. The occurrence of temperature inversions, when lapse rates are positive as air temperature increases with altitude, as shown during brief periods on Figure 4.3b, occurring on four days out of eight. Temperature inversions have been well-reported over many glaciers (e.g. Strasser *et al.*, 2004; Irvine-Fynn *et al.*, 2014) and result in the reduction of mean lapse rates, which can have significant implications for melt modelling, particularly if the resultant lapse rates do not compare well to published or realistic values.

To establish the suitability of the calculated lapse rates, the overall mean lapse rates were first established. The mean lapse rate between the Saas Fee weather Station and the upper most sensor at 3448 m asl was calculated as -0.0059 °C/m and the mean of the Saas Fee – 3000m asl lapse rate and 3000 – 3448 m asl lapse rate was calculated as -0.0054 °C/m. Despite the observed temperature inversions, both lapse rates are in good agreement with the lapse rate of -0.0056 °C/m calculated by Farinotti (2010) based on temperature records of 14 MeteoSwiss stations in the Swiss Alps with elevations ranging from 273 to 3580 m asl. Furthermore, the daily mean temperatures at each station (Figure 4.3c) indicate that, despite the observed temperature inversions, the use of a linear lapse rate is suited to define temperature as a function of elevation.

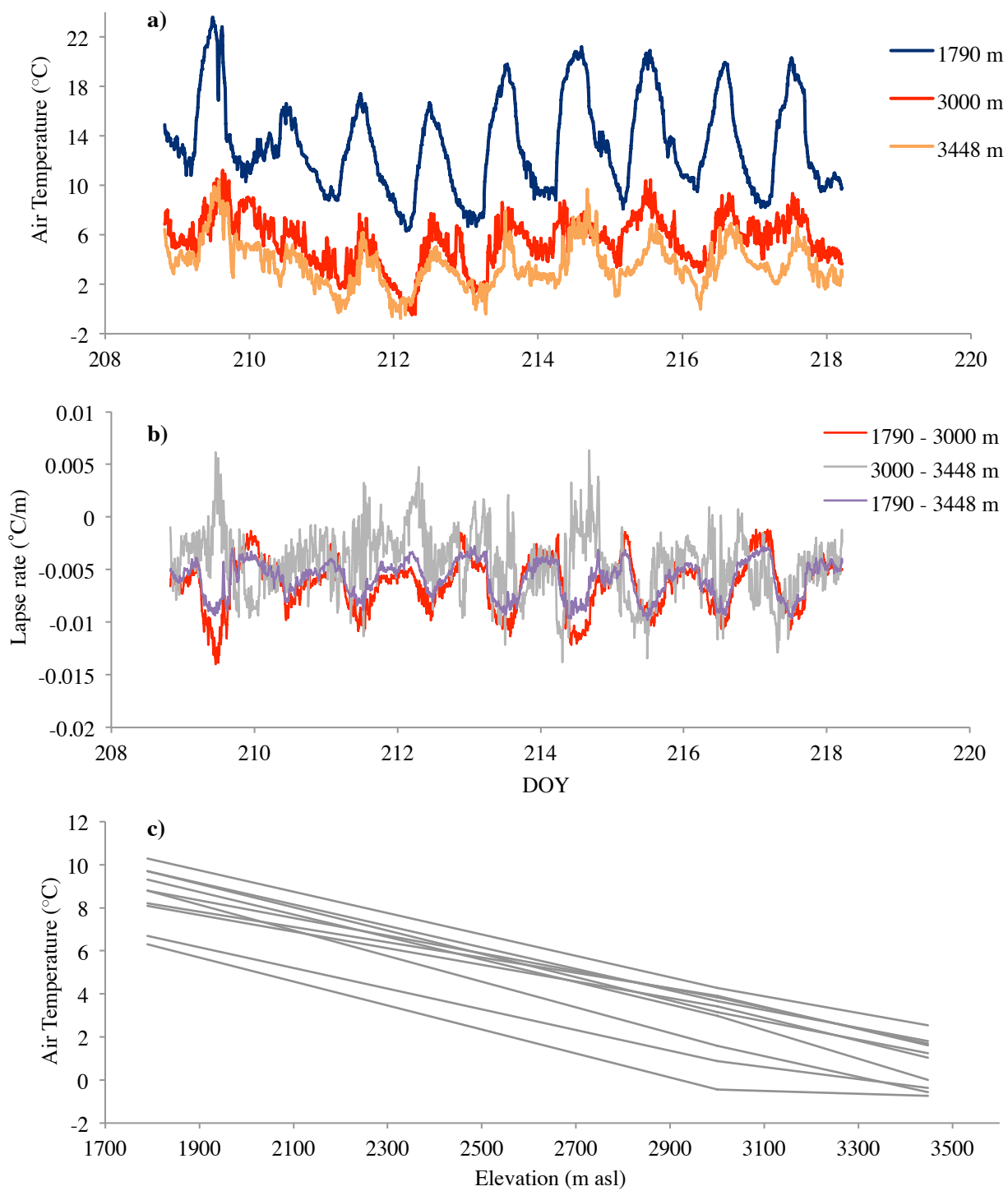


Figure 4.3: a) Time series of air temperature at three stations used to determine lapse rate. b) Calculated lapse rates between the three stations. c) Mean daily air temperatures at the three stations from DOY 209 to 217.

4.3 Glacier ablation

Glacier ablation was monitored during the 2012 field season through periodic surveys of four ablation stakes installed at the Feegletscher Sud. Observed ablation shows strong dependence with elevation, with stakes C and D (c. 3450 m asl) showing reduced amounts of ablation compared to stakes A and B (c. 3000 m asl) (Figure 4.4a). Cumulative positive air temperatures were calculated for each stake using the lapse derived in Section 4.2. A strong correlation exists between cumulative positive air temperatures and ablation, with $r > 0.6$ at all stakes ($p \leq 0.05$ except Stake D which was not significant at this level) (Figure 4.4b) suggesting a temperature-index approach to

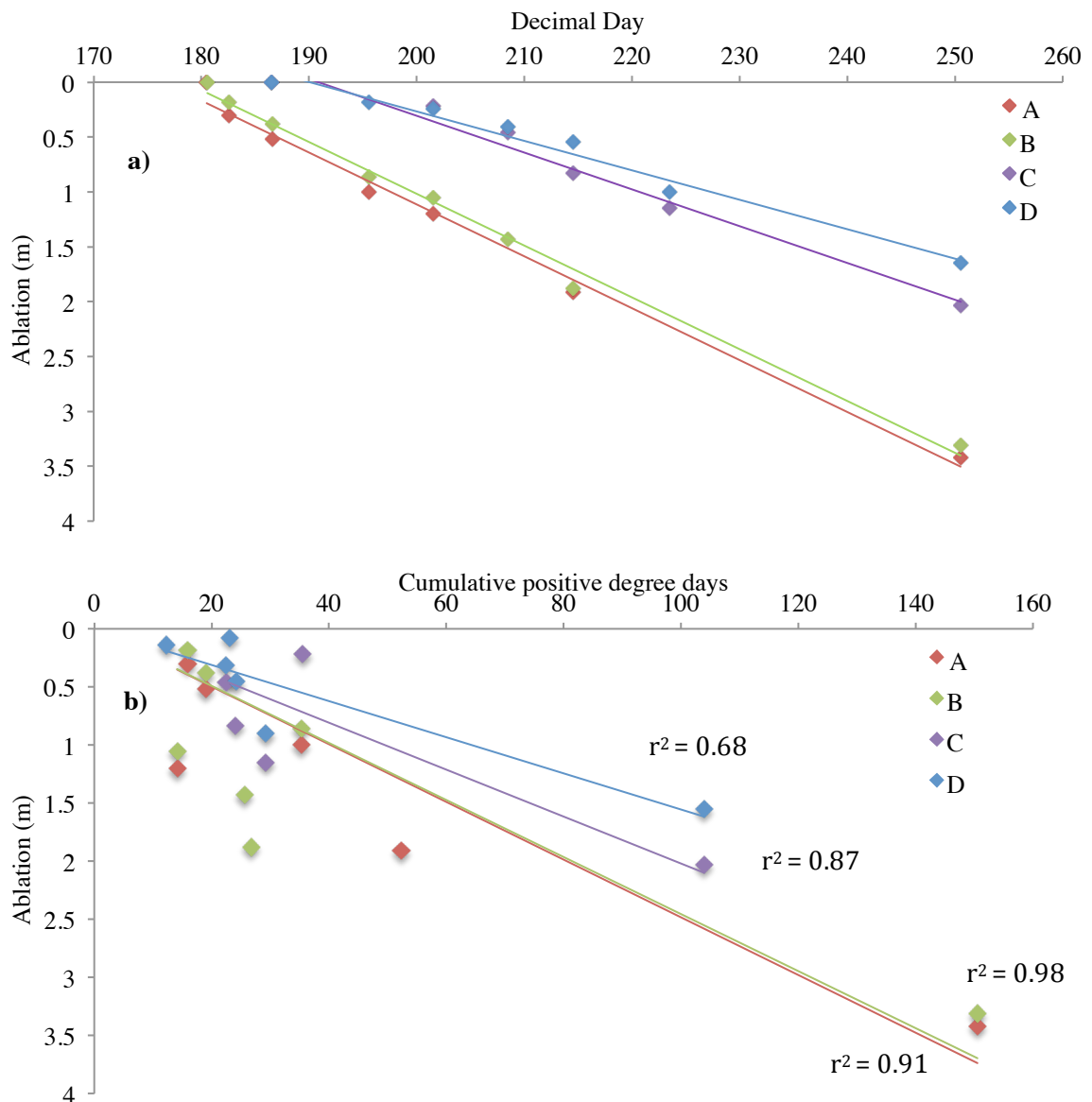


Figure 4.4: a) Glacier ablation at four ablation stakes A & B (c. 3000m asl) and C & D (c. 3450 m asl) plotted over time. b) Glacier ablation at four ablation stakes plotted against cumulative positive degree intervals (10 minute intervals). All relationships significant at $p \leq 0.05$ except for Stake D.

melt modelling is suitable. The mean rate of ablation over the study period is 0.05 m/day, although this reduces to 0.02 m/day for the stakes at higher elevation compared to 0.07m/day at lower elevations. Peak ablation of 0.14 m/day occurred at stake A over a period of two days in June. Average degree-day factors over the 2012 ablation were calculated as 5.5, 6, 7 and 8.4 mm d⁻¹ °C⁻¹ at stakes A, B, C and D, respectively, which are in good agreement with values reported elsewhere in the European Alps (e.g. Braithwaite & Zhang, 2000). Degree-day factors are further explored and analysed in Chapter 6.

4.4 Proglacial stream data

The general pattern of discharge at all gauged proglacial streams shows a strong diurnal signal, which is also present in the SSC, temperature and global radiation records (Figures 4.5, 4.6 & 4.7). Summary statistics for the discharge and SSC time-series are presented in Table 4.2. Discharge weighted mean SSC statistics were calculated as suspended sediment load (SSL) values divided by concurrent discharge values, and therefore differ from time-weighted averages as they account for the total mixing of sediment and water during the time interval. The patterns of discharge at the principal proglacial streams (B, C & D) show close similarity, with correlation coefficients between the stations ≥ 0.64 ($p \leq 0.001$) (Table 4.3). Stream D, draining the lower proglacial water body, shows highest mean Q followed by streams C and B (Table 4.2). The discharge at stream D, and the total discharge of streams C and B, is considered representative of total meltwater output from the Feegletscher Nord, minus any losses to groundwater or temporary storage in proglacial lakes, which were not quantified. Stream B carried approximately 50% of the runoff volume of the larger proglacial stream C. The total discharge of streams B and C is strongly correlated to the discharge at stream D ($r = 0.98$, $p \leq 0.001$), confirming that there are no significant inputs or outputs of water between the gauging locations. The continuous 34-day record

from DOY 202 to 233 for stations B & C shows a total runoff of $5.9 \times 10^6 \text{ m}^3$. This would suggest a total annual runoff for the Feegletscher Nord catchment of approximately $30 \times 10^6 \text{ m}^3$ using Collins (1979) calculation that over 50% of the total annual runoff occurs in July and August. This total annual runoff represents 62% of the mean total annual runoff reported by Collins (1979) for the period 1966–1976, which also included runoff from the larger Feegletscher Sud.

The time-series of stations B and C is considered most representative of trends during the study period owing to the most comprehensive data record, with Station C showing a marked increasing trend from DOY 198 to 233 reaching a peak Q of $4.9 \text{ m}^3/\text{s}$ (Figure 4.6) which aligns with a similar trend in air temperature. In contrast, Station B shows no clear trend and a peak Q of $2.1 \text{ m}^3/\text{s}$, suggesting this stream may be capacity-limited (Figure 4.5). The lack of continuous time-series from stations A and D prevents robust conclusions on long term flow characteristics from being drawn. However, Station A does have a strong diurnal pattern in discharge (Figure 4.8). Station D reached peak Q of $4.5 \text{ m}^3/\text{s}$ on two occasions (Figure 4.7). This value was exceeded during a significant rainfall event (98.2 mm over DOY 183-184) and a flood event on DOY 184. However, data for the event is limited as both stage and turbidity exceeded the measurable ranges of the sensors during the event for approximately 76 minutes.

Table 4.2: Descriptive statistics for discharge and SSC time-series. Values are number of observations (n), mean (μ), discharge weighted mean SSC (μ_Q) standard deviation (σ), mean daily standard deviation (σ_d) and mean daily range (Δ_d).

		A	B	C (2012)	D	C (2010a)	Outflow (2010a)	Overspill (2010a)
Q (m ³ /s)	n	7263	26828	25331	27681	3500	-	-
	μ	0.33	0.9	1.6	2.3	1.96	-	-
	σ	0.1	0.28	0.8	0.85	0.36	-	-
	σ_d	0.07	0.31	0.4	0.61	0.32	-	-
	Δ_d	0.27	1	1.66	2.1	1	-	-
SSC (g/l)	n	109	26955	25331	27683	3500	3500	3500
	μ	0.58	0.36	0.28	0.16	0.22	0.2	0.36
	μ_Q	-	0.4	0.37	0.18	0.23	0.21	0.38
	σ	0.46	0.9	0.49	0.28	0.26	0.18	0.5
	σ_d	0.38	0.13	0.18	0.09	0.2	0.15	0.41
Δ_d	1.6	0.49	0.92	0.47	0.77	0.59	1.6	

The pattern of SSC shows strong diurnal forcing, similar to discharge variability. A downstream decrease in mean SSC in the proglacial zone is apparent from the mean ranges for both field campaigns (Table 4.2), although, as with discharge, the lack of continuous turbidity monitoring at Station A prevents robust conclusions being drawn at this location. Station B shows the highest mean SSC including the highest discharge-weighted mean, despite this location showing a significantly lower mean daily range compared to Station C. Throughout the study-period there are significant high-magnitude SSC events, particularly at Station C, whereby SSC exceeds 1 g/l on nine occasions (Figure 4.6c). Rainfall events appear to coincide with some high SSCs, with the patterns also shown in the records for Station D and, to a lesser extent, Station B. It is also apparent that there is increased diurnal variability in the range of SSC at stations A and C compared to B and D (Table 4.2) which is explored further in Chapter 5. Despite the lack of continuous records at Station A, short-term variability in SSC, which appears unrelated to discharge, is apparent from the continuous manual SSC sampling undertaken on DOY 224 (Figure 4.9). Daily patterns of SSC that appear uncorrelated to

discharge are particularly evident at Station C, whereby multiple subsidiary peaks in SSC occur during the rising and falling hydrograph limbs. It is interesting to note that these appear largely absent in the records for stations B and D, which usually exhibit a single peak in SSC each day. Correlation analysis performed on the complete datasets revealed that SSC at Station A peaked before discharge, with the opposite occurring at stations B and C (Table 4.3). Discharge is correlated with SSC at Station D with a short negative time-lag. The results of further correlation analysis for meaningful time-series sub-periods are described in Chapter 5. Sediment loads during the 2012 monitoring period show considerable variability, particularly at Station C (Figure 4.10). Seven days of continuous data at stations B, C and D from DOY 215-221 show a cumulative sediment load of 94800 kg, 250000 kg and 266000 kg at these stations, respectively. This highlights a significant downstream decrease in sediment load from these locations. However, when the daily sediment loads are examined it is interesting to note that sediment load at Station D on DOY 221 slightly exceeds the combined load of stations B and C indicating a downstream increase.

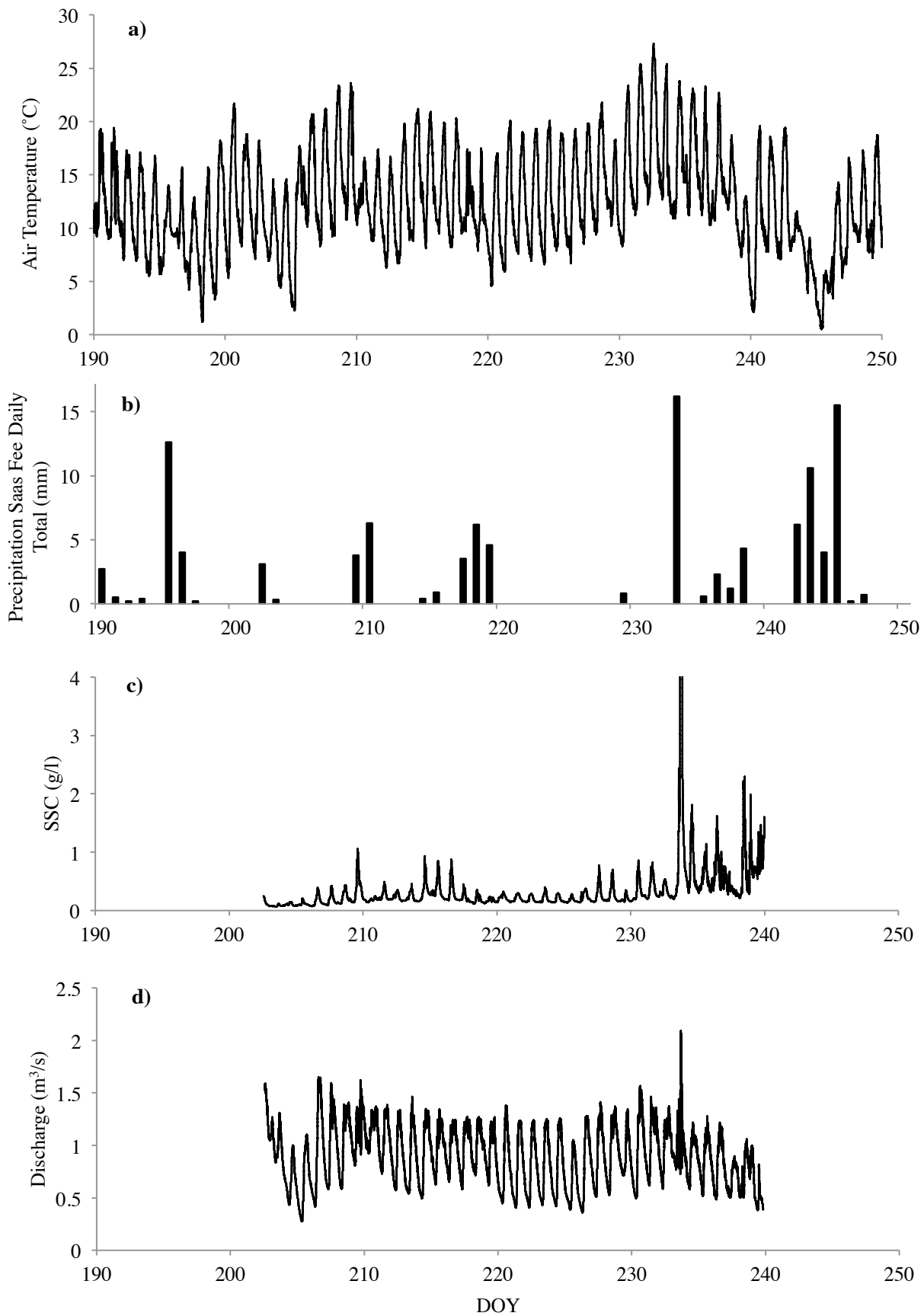


Figure 4.5: Time-series of air temperature (a) and precipitation (b) recorded at the Saas Fee weather station along with SSC (c) and discharge (d) at Station B during 2012. The y-axis on graph c) has been limited for clarity as the high-magnitude SSC on DOY 233 peaks in excess of 10 g/l.

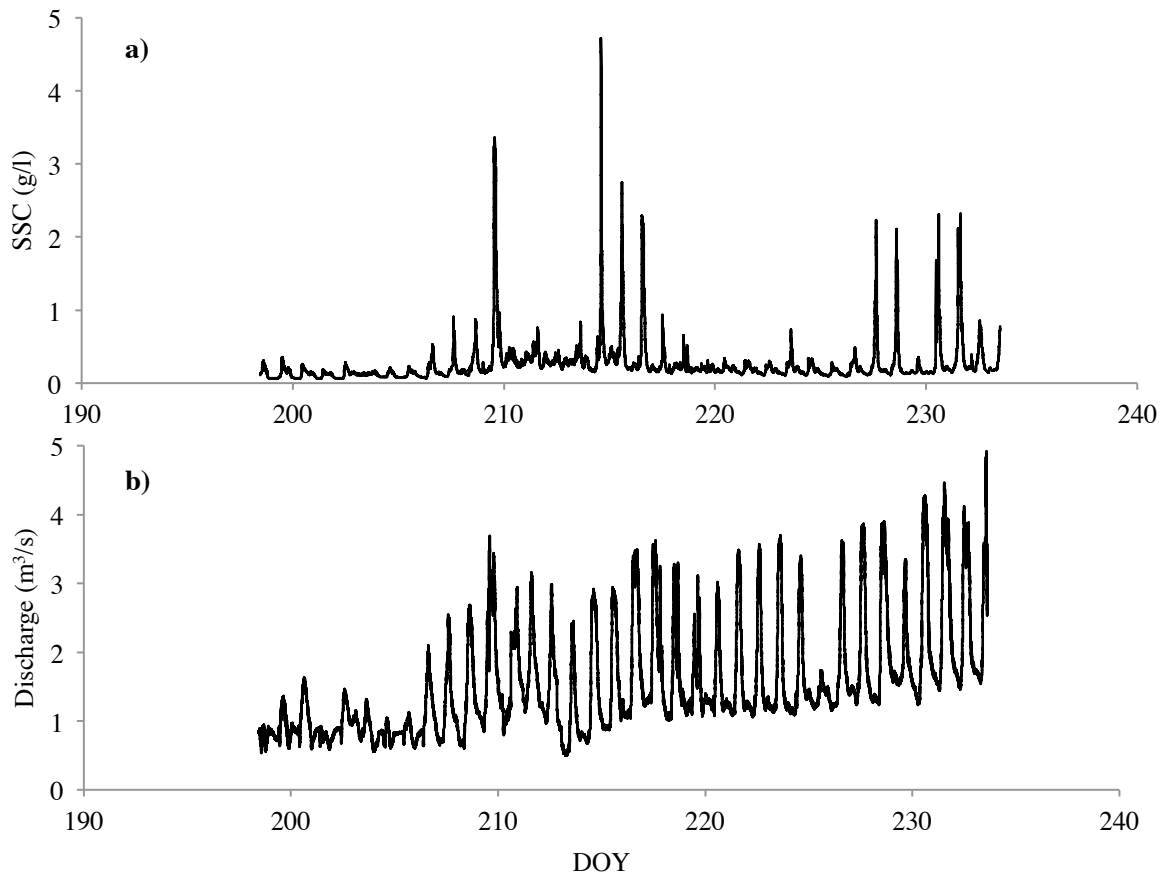


Figure 4.6: Time-series of a) SSC and b) discharge at Station C during 2012

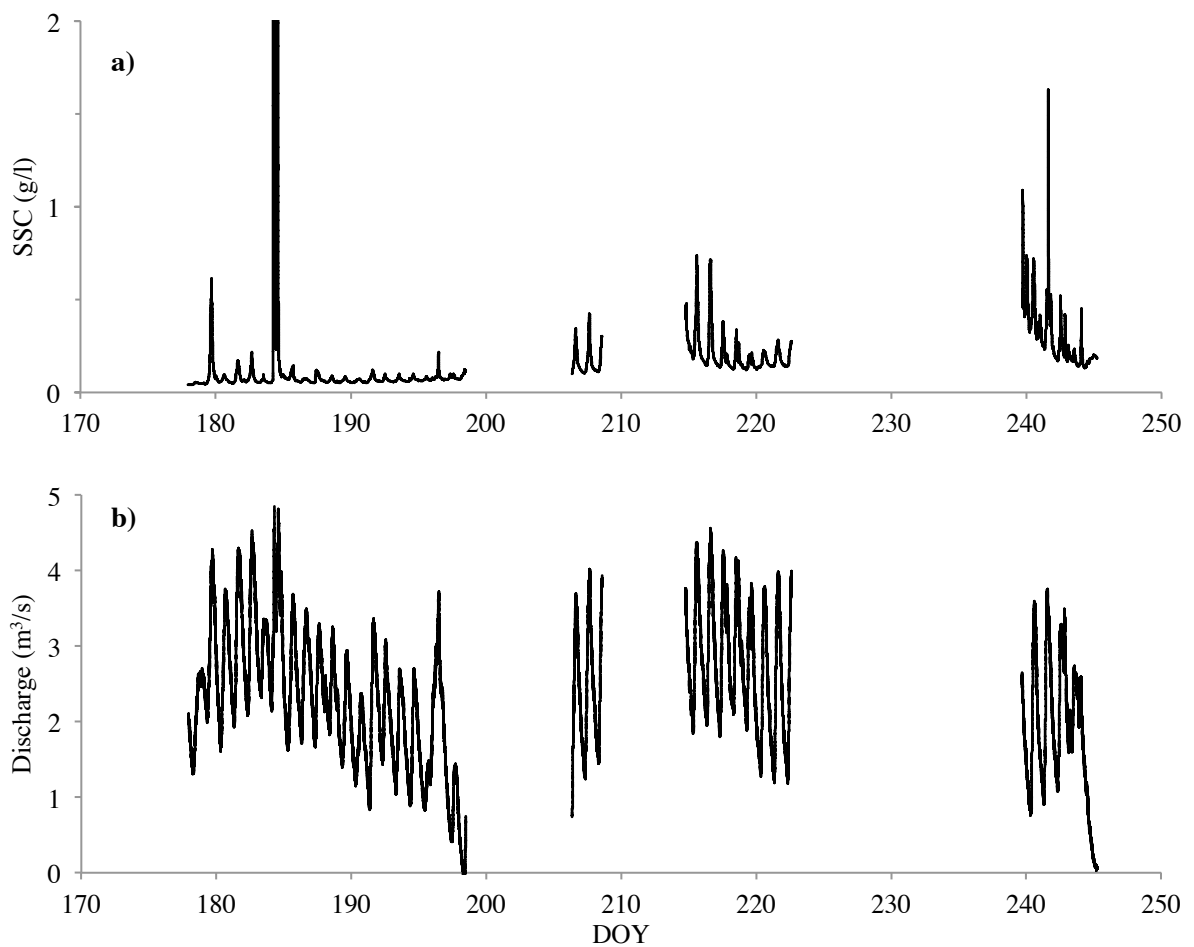


Figure 4.7: Time-series of a) SSC and b) discharge at Station D. Scale is adjusted in graph b) with the peak SSC on DOY 184 exceeding 10 g/l.

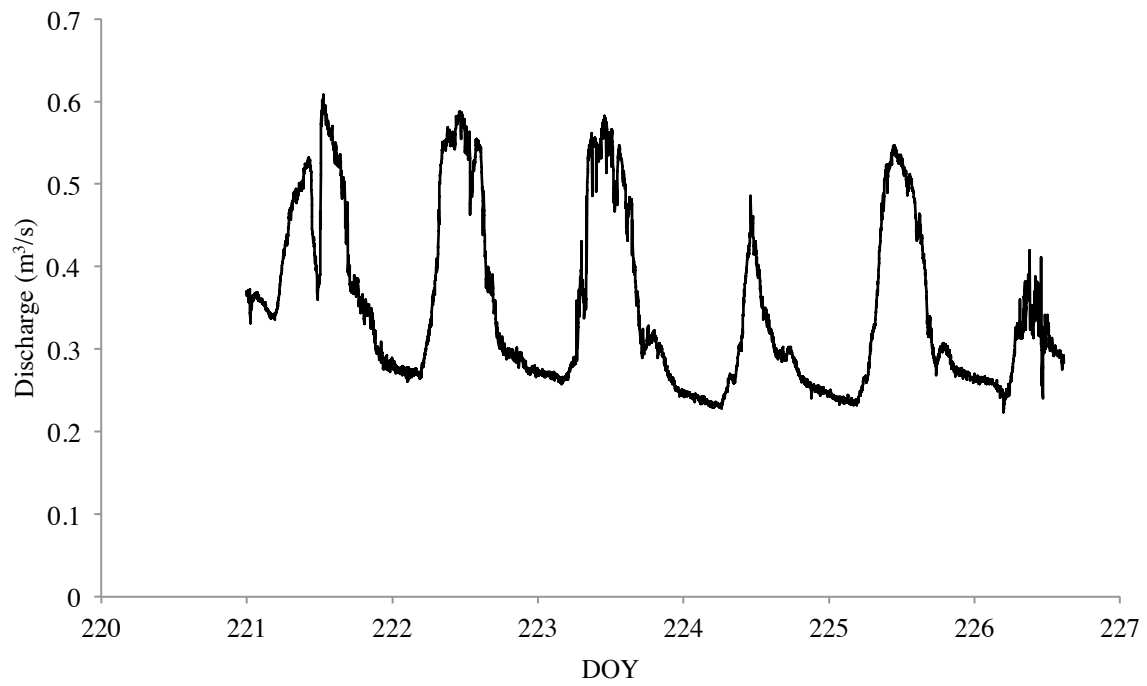


Figure 4.8: Discharge time-series at Station A.

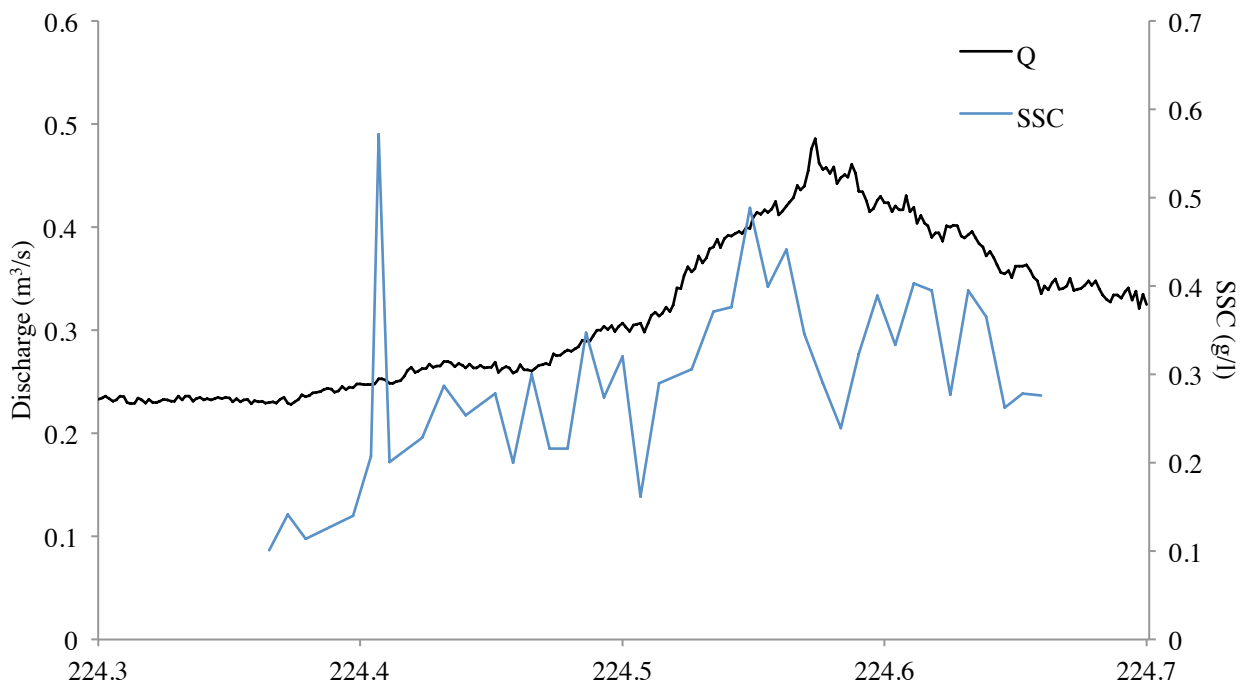


Figure 4.9: Discharge and SSC time-series at Station A during part of DOY 224.

Table 4.3: Correlation and cross-correlation analysis of 2012 time-series. Discharge (Q) was correlated against variables of temperature (T), suspended sediment concentration (SSC) at each station denoted SF , A , B , C , or D .

Var1	Var2	CCF lag=0	Lag (min)	CCF lagged
Q_A	T_{SF}	0.48	0	-
Q_A	Q_B	0.41	88	0.46
Q_A	SSC_B	0.25	-26	0.251
Q_A	Q_C	0.37	0	-
Q_A	SSC_C	0.13	-28	0.131
Q_A	Q_D	0.77	40	0.79
Q_A	SSC_D	0.8	0	-
Q_B	T_{SF}	0.69	-80	0.74
Q_B	SSC_B	0.138	14	0.142
Q_B	Q_C	0.63	-16	0.635
Q_B	SSC_C	0.23	-46	0.24
Q_B	Q_D	0.941	0	-
Q_B	SSC_D	0.5	-34	0.51
Q_C	T_{SF}	0.68	-20	0.69
Q_C	SSC_C	0.381	26	0.383
Q_C	Q_D	0.846	12	0.85
Q_C	SSC_D	0.613	0	-
Q_D	T_{SF}	0.67	-140	0.736
Q_D	SSC_D	0.176	-2	0.176

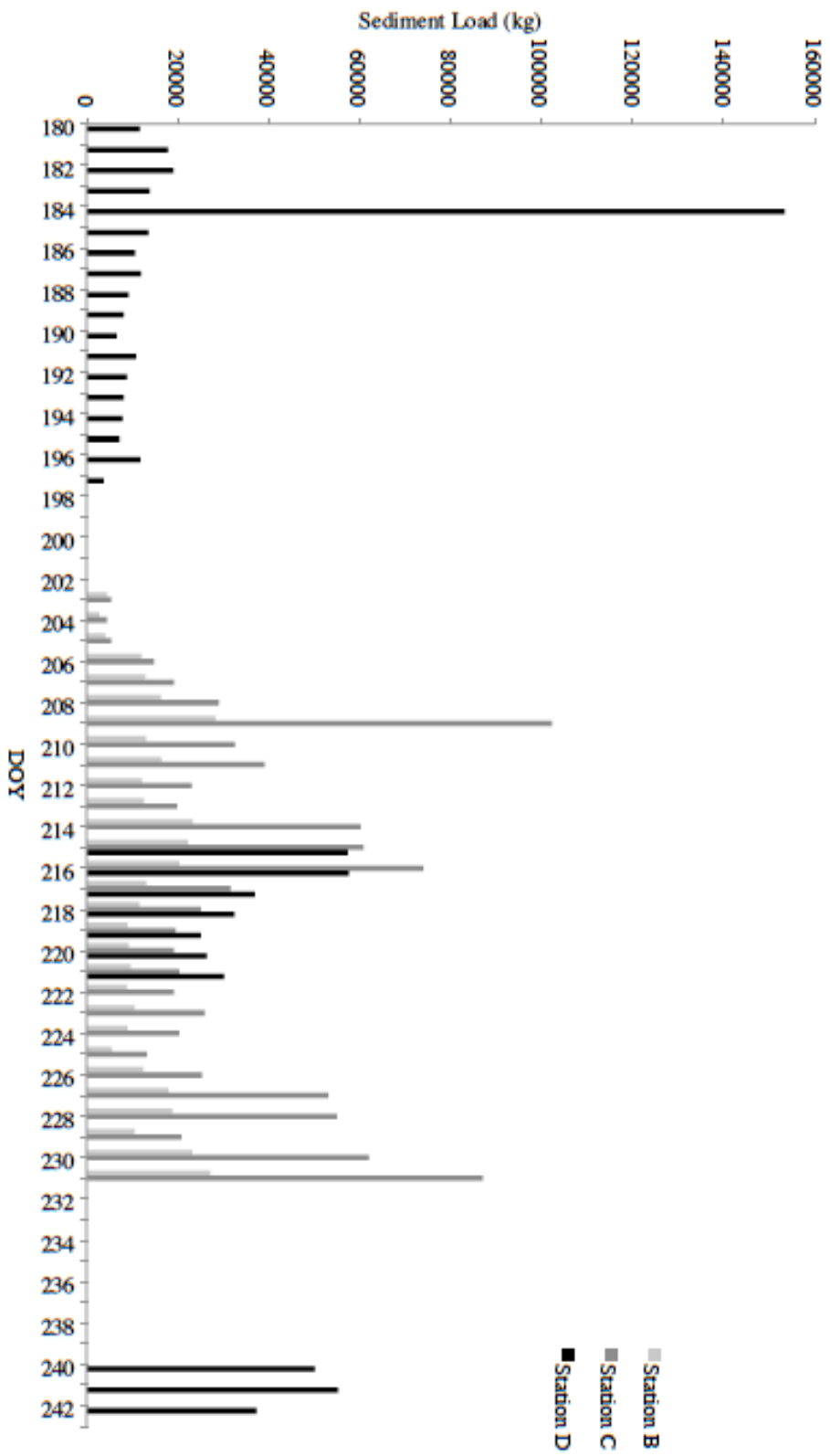


Figure 4.10: Suspended sediment load at Stations B, C and D during 2012. Note the large sediment load experienced at station D on DOY 184 due to a significant flood event. Seven days of continuous and simultaneous records occur at stations B, C and D from DOY 215-221.

4.5 Dye tracing

Tracer studies were conducted in 2010 to ascertain the nature of drainage through subterranean pathways draining the proglacial lake (Figure 4.11). These revealed that efficient drainage occurs through the moraine dam, shown by the discrete single peak returns with an absence of subsidiary peaks. Despite the efficient nature these return curves imply, the tracer velocities are low at 0.04 and 0.05 ms⁻¹, which suggests the pathways experience high conduit roughness.

The second set of tracer studies were performed in 2012 to ascertain the nature of drainage through the upper proglacial lake after significant sedimentation occurred between the 2010 and 2012 field campaigns. Field observations suggested that the upper proglacial lake was analogous to a braided delta with only a very small area of ponded water close to the lake outflow. Dye was injected close to the inflow and measured at the lake outlet. The dye return curves (Figures 4.12 and 4.13) exhibited a single flat peak, which is reached between 8 and 10 minutes after injection and declines rapidly after a further 4–6 minutes. The dye-trace in Figure 4.12 experiences a slight secondary peak that field observations suggested was caused by dye becoming pooled behind snow at the lake-margin.

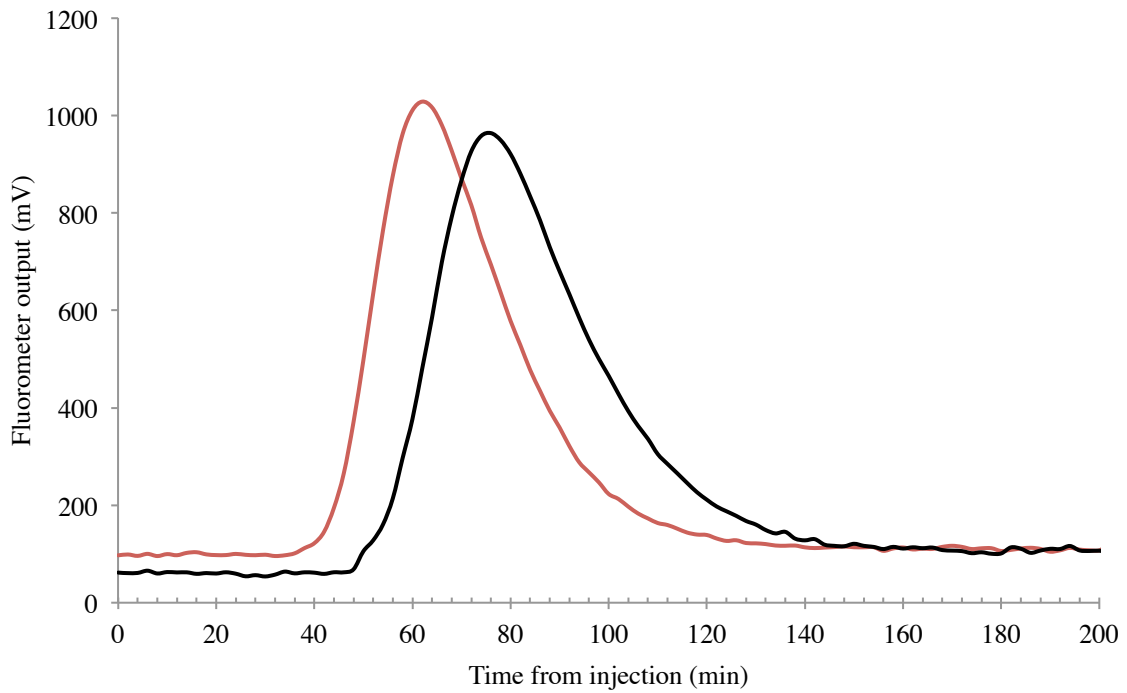


Figure 4.11: Results of dye tracing through subterranean drainage pathways drainage the upper proglacial lake.

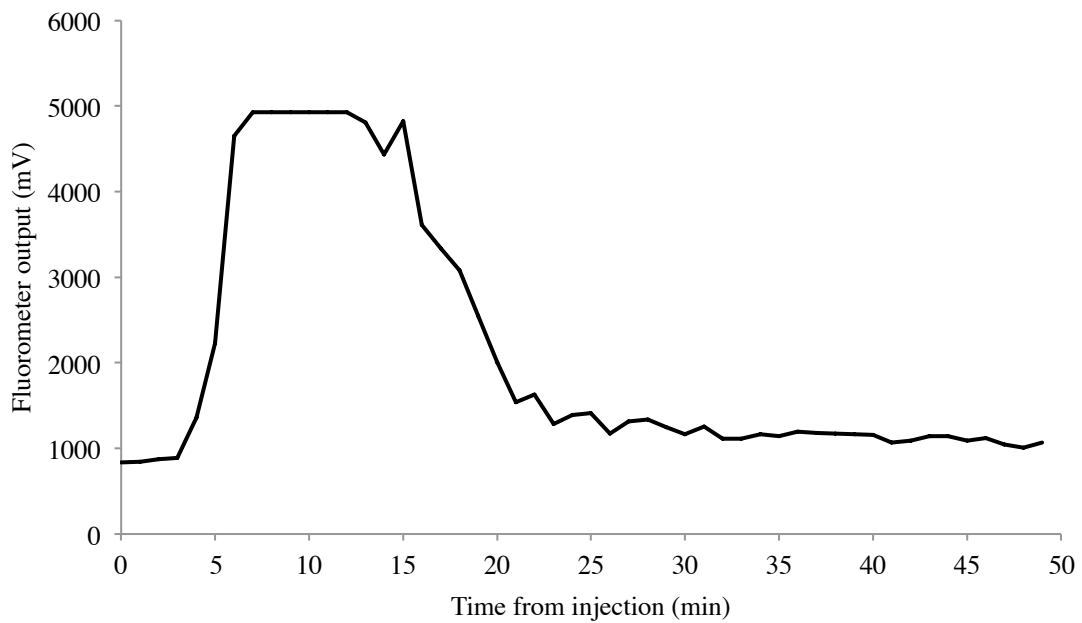


Figure 4.12: Dye trace performed through upper proglacial lake. Dye was injected close to lake inlet on 24/6/12 at 12:53. The presence of snow covering parts of the lake was hypothesised to trap dye resulting in the irregular patterns on the falling limb.

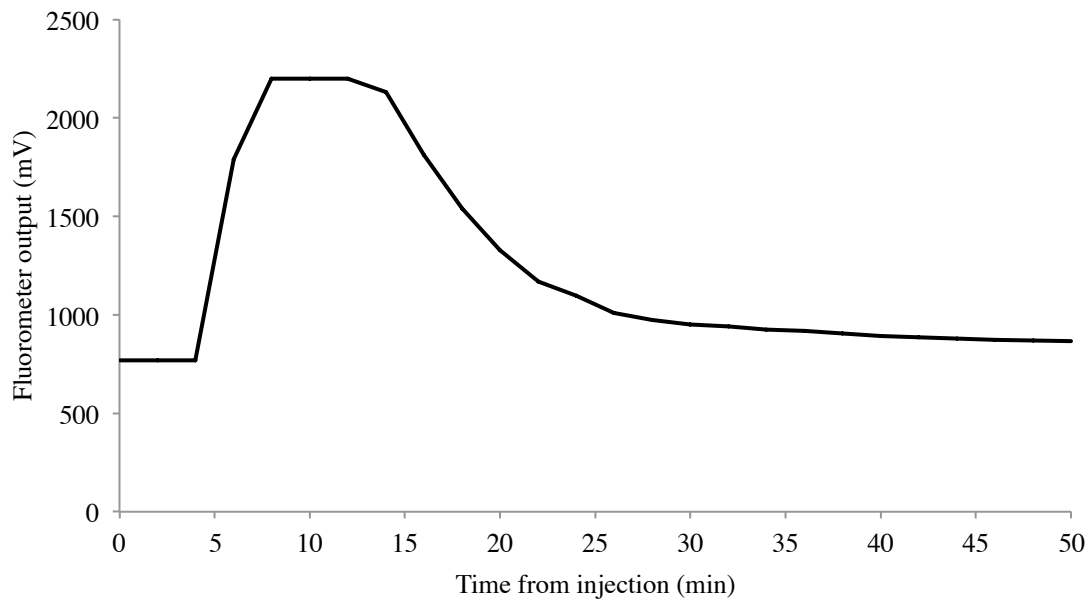


Figure 4.13: Second dye trace performed through upper proglacial lake. Dye was injected close to lake inlet on 17/8/12 at 08:42

4.6 Summary

This chapter has presented the field data collected at the Feegletscher Nord during 2010 and 2012. Prior to the analysis of this data in the subsequent chapters, the main aspects of the field data are summarised below:

- Glacier ablation was monitored at four locations over 70 days in 2012 and was strongly correlated to diurnal variations in air temperature and global radiation.
- A linear lapse rate of $-0.0054 \text{ }^{\circ}\text{C/m}$ was adopted that was calculated using air temperature time-series from a proglacial weather station and two on-ice temperature sensors. This value is in good agreement with other published lapse rates in the European Alps.
- Time-series discharge and SSC data was collected simultaneously and continuously at two-minute intervals for 29 days at stations B and C whilst 32 days of non-continuous data exists for Station D at the same resolution. A short

and incomplete data record of discharge exists at Station A due to logger failure.

However, 109 SSC samples were obtained over 3 days.

- The general pattern of discharge at all gauged proglacial streams shows a strong diurnal signal which is also present in the SSC, temperature and global radiation records. However, significant variability is apparent in the patterns and magnitudes of SSC.
- Throughout the 2012 study-period there are significant high-magnitude SSC events, particularly at Station C whereby SSC exceeds 1 g/l on nine occasions (mean is 0.28 g/l). Similar variability is seen in suspended sediment loads with Station C experiencing significant variability.
- Daily patterns of SSC that appear uncorrelated to discharge are particularly evident at Station C, whereby multiple subsidiary peaks in SSC occur during the rising and falling hydrograph limbs. These patterns appear largely absent in the records for stations B and D which usually display a single diurnal peak in SSC.
- Subterranean drainage pathways draining the upper proglacial lake were found to exist with an unusual combination of low flow velocities and an efficient dye return curve.
- By 2012, the upper proglacial lake had become almost entirely sedimented and dye tracing confirmed rapid meltwater throughflow.

5 Characteristics of Runoff and Suspended Sediment Transfer from the Feegletscher Nord

5.1 Introduction

In order to characterise the nature of and controls on temporal and spatial variability in meltwater and sediment transfer within the Feegletscher catchment, detailed examination of stream discharge and suspended sediment concentration records was undertaken. In this chapter, hydrographs and SSC curves are analysed to determine the nature and attributes of the glacio-fluvial hydrological and sedimentary systems. Section 2.3 illustrated how the transfer of sediments in suspension through glaciated catchments is strongly dependent on the transfer of meltwater through a subglacial drainage system that has access to the glacier bed. In light of the strong dependence of SSC on discharge, the transfer of suspended sediments from, and within, the Feegletscher Nord catchment is examined with a view to characterising the controls on the observed spatial and temporal variability in SSC. This will enable an understanding of how meltwater and SSC are transferred through the glacial hydrological system and the proglacial zone with consideration of how, subsequently, the proglacial zone potentially modifies the relationship between SSC and discharge. By undertaking an integrated, catchment-scale approach that utilises a combination of methods to understand the glacio-fluvial transfer of meltwater and sediment, the analysis presented in the following sections aims to elucidate understanding of controls on water and sediment transfer within, and from, the Feegletscher Nord catchment in both space and time.

Section 5.2 outlines the analytical approach adopted along with a review of the methods and their suitability in this research. The results of the cross-correlation

analysis on the discharge and SSC time-series are then presented in Section 5.3, and Section 5.4 details the findings with respect discharge recession curve analysis. The analysis of shape and magnitude of SSC and hydrographs are presented in Section 5.5, and Sections 5.6 and 5.7 discuss and summarise the results of the aforementioned suite of analytical techniques.

5.2 Overview of analytical techniques

Information on the functioning and nature of glacio-fluvial sediment transfer is typically gained from proglacial stream records of meltwater discharge and suspended sediment load owing to the inaccessibility of the subglacial hydrological system. With regards to glacier hydrology, it is the timing, shape and magnitude of the proglacial hydrograph, which can yield valuable information on the spatial and temporal controls on meltwater runoff. The overarching aim of this hydrograph analysis was to establish the nature and range of controls on observed discharge to inform the development of a runoff model. Three specific objectives emerge from this aim: to determine the strength and timing of discharge forcing by temperature; to determine the nature of storage processes that may account for delays between meltwater generation and runoff and; to investigate controls on observed spatial and temporal variations in hydrographs within the Feegletscher Nord catchment. With regards to suspended sediment transfer, entrainment and evacuation by meltwater dominates all other sediment transfer processes for temperate glaciers (Alley *et al.*, 1997; Swift *et al.*, 2005b). Therefore, in order to understand the links between discharge and SSC, the characteristics of suspended sediment concentration curves can be used to interpret controls on proglacial SSC such as the transport capacity of meltwater streams (e.g. Gurnell, 1987; Collins, 1989), sediment availability (e.g. Collins, 1979; Hodson & Ferguson, 1998), and the nature and origin of irregular patterns in suspended sediment transfer (e.g. Clifford *et al.*, 1995; Haritashya *et al.*, 2006). The overarching aim of the SSC analysis in this

chapter was to establish the nature and potential range of controls on observed proglacial SSC.

Here, this chapter follows analytical templates provided in Richards *et al.* (1996), Hannah *et al.* (2000), Orwin & Smart (2004a), Swift *et al.* (2005a), Irvine-Fynn (2008) and Leggat *et al.* (2015) so as to reproduce an appropriate and robust set of analytical procedures appropriate for both the dataset and aims of this research that result, as combined, in a comprehensive investigation of the hydrological and suspended sediment transfer processes at the Feegletscher Nord.

A detailed examination of outflow hydrographs and SSC curves from the Feegletscher Nord was undertaken in order to characterise the nature of, and controls on, the hydrological and sediment transfer systems in operation. Cross-correlation analysis can be applied to reveal the association between runoff and meteorological forcing as well as characteristics of meltwater throughput and the associated entrainment and exhaustion of sediments in glacial systems (e.g. Richards *et al.*, 1996). Water and sediment storage processes within glaciers can be investigated through examination of the recession limbs of hydrographs (e.g. Gurnell, 1993; Hannah *et al.*, 2000; Kido *et al.*, 2007) and a range of hydrological indices, such as peak discharge, time to peak, background flow and shape indexes can be used to differentiate hydrographs and SSC curves into similar classes (e.g. Hannah *et al.*, 2000; Harris *et al.*, 2000; Orwin & Smart, 2004a; Hannah *et al.*, 2005; Swift *et al.*, 2005a; Leggat *et al.*, 2015). These classes of hydrologically-similar periods can be used to either characterise hydrological processes (e.g. to examine the controls exerted by external influences such as weather patterns) or to normalise hydrological periods to investigate other processes such as patterns and controls on sediment transfer (e.g. Orwin & Smart, 2004a; Leggat

et al., 2015). In their review of hydrograph classification, Hannah *et al.* (2000) describe how such approaches to hydrograph classification can be thought of as subjective, as they rely on ‘hydrological judgment’ rather than an objective approach. In light of this, Hannah *et al.* (2000) developed an objective approach to classify diurnal hydrographs using statistical techniques, including principal component analysis (PCA) and cluster analysis (CA) applied to the aforementioned indices. Such techniques have subsequently been applied in studies seeking to isolate and characterise the controls on suspended sediment transfer patterns and magnitudes, as they are able to reduce large data sets to more manageable sizes, whilst retaining much of the underlying data structure (e.g. Orwin & Smart 2004a; Irvine-Fynn *et al.*, 2005a; Swift *et al.*, 2005a; Leggat *et al.*, 2015).

5.3 Cross-correlations

5.3.1 Discharge

Cross-correlation was undertaken to establish temporal patterns and trends in the daily lag times between air temperature and proglacial discharge (e.g. Richards *et al.*, 1996; Jobard & Dzikowski, 2006) in order to characterise the nature of meltwater transport in the Feegletscher Nord catchment. Cross correlations were determined for individual hydrological days (beginning at 07:00am which typically coincided with minimum discharge) that were free of significant precipitation events (due to the potential influence of rainfall in the magnitude and timings of peak discharges). In addition, the time lags between daily peak air temperature and peak proglacial discharge and between minimum air temperature and minimum peak discharge were also determined due to the asymmetric nature of many of the recorded hydrographs, which suggests air temperature may not be the sole driver of discharge and factors such as

drainage network capacity and competence or storage and release of meltwater may be important in controlling hydrograph form.

Figure 5.1a shows the daily lags between the peaks in discharge and air temperature and the minimum values of discharge and air temperature. It is apparent that the lags between minimum discharge and air temperature are generally greater than those between the maximum values. There is no clear seasonal pattern in the minimum lags, suggesting either no systematic pattern of change during the ablation season, or the absence of a strong correlation between minimum air temperature and minimum discharge. This might indicate that ablation may not be a significant factor driving discharges around the hydrograph minima. Lags between peak discharge and air temperature show a moderately declining trend, which is also evident in the daily cross-correlations between discharge and air temperature (Figure 5.1b). Daily lag times between discharge and air temperature ranged from 4.2 hours on DOY 191 to a negative lag of 40 minutes on DOY 203. It is problematic to deduce the physical processes responsible for a negative lag between discharge and air temperature. It may suggest the presence of more complex ablation processes, perhaps due to increased cloud cover reducing incoming short-wave radiation (Pellicciotti *et al.*, 2005), or due to cooling processes associated with katabatic winds or low humidity (Pellicciotti *et al.*, 2008). The negative lag may also suggest the influence of processes of meltwater storage and release, which have the capacity to modify the proglacial hydrograph form (Jansson *et al.*, 2003). Despite some scatter evident early in the ablation season, as shown in Figure 5.1b, it is evident that there is a declining trend in the time lag between discharge and air temperature. This observation has typically been interpreted to represent the decline of the supraglacial snowpack and an increasing efficiency of subglacial drainage networks over the course of an ablation season (e.g. Swift *et al.*, 2005a). It is interesting

to note that the majority of days in the mid-late ablation season exhibit no time lag between discharge and air temperature. This zero time lag can be further explored by examination of the time lags between the maximum and minimums in discharge and air temperature. It can be seen from Figure 5.1.a that from DOY 207 the peak in discharge frequently precedes the peak in air temperature, whilst the minimum in discharge generally continues to occur after the minimum air temperature. Thus, the zero lags noted between discharge and air temperature in Figure 5.1b may result when positive and negative lags occur between maximum and minimum pairs or may indeed represent transit times of meltwater through the glacial hydrological system raising the possibility of variable meltwater storage processes. The concept of linear storage reservoirs in glacial hydrological systems has been applied to explain the variation in meltwater throughput rates through glaciers (e.g. Hannah & Gurnell, 2001; Jansson *et al.*, 2003). This is explored further through analysis of hydrograph form in Section 5.4. Changes in the lag times may also arise from the variability in synoptic meteorological conditions. Field observations indicated no specific weather patterns or meteorological trends that could be related to the cross-correlation results. This may be due to the removal of periods with significant precipitation prior to cross-correlation analysis. However, the impact of meteorological conditions on discharge is further explored in Section 5.4.

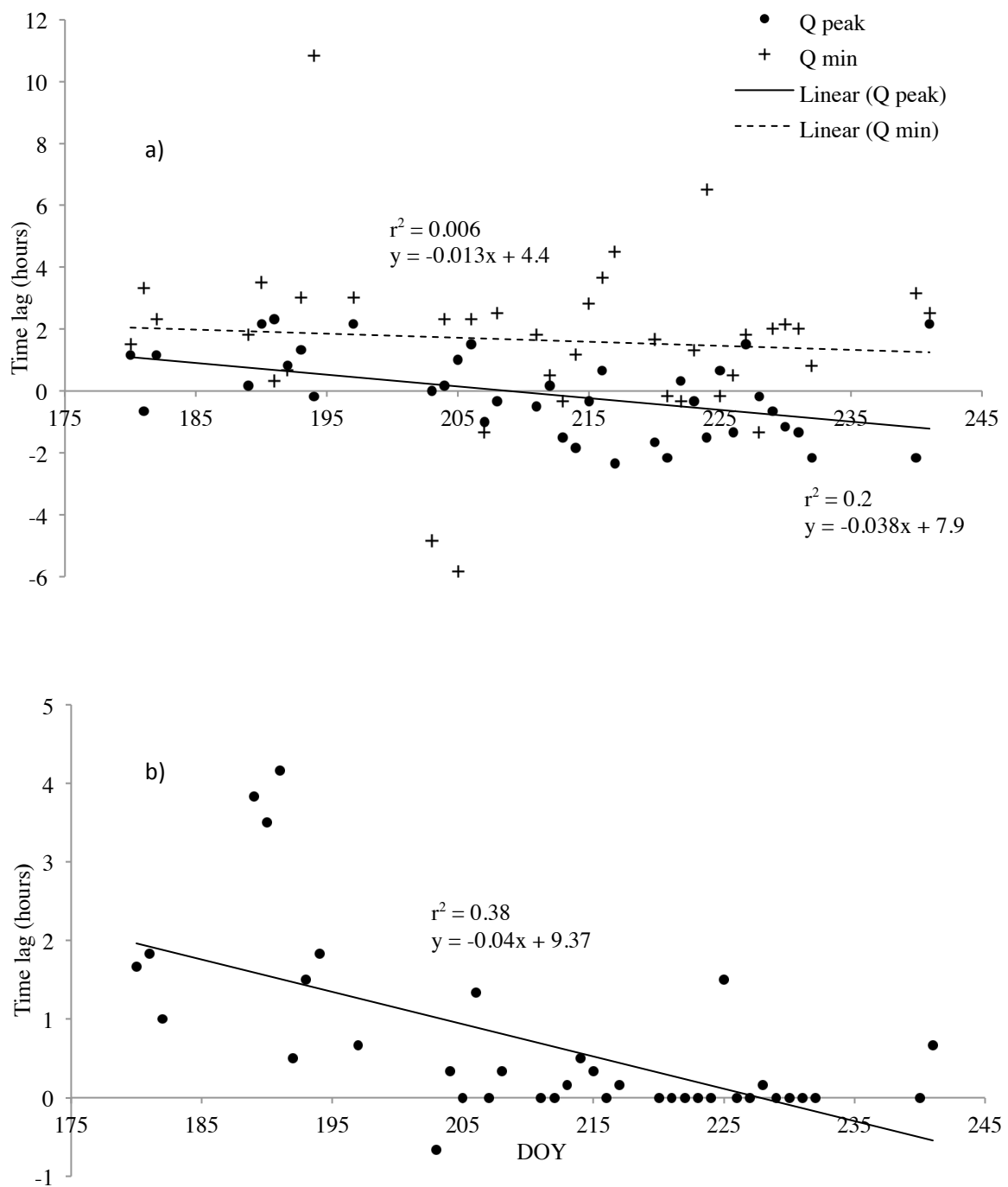


Figure 5.1: Results of cross-correlation analysis for a) the daily lag between peak discharge and maximum air temperature ($p \leq 0.01$) and minimum discharge and minimum air temperature (not significant at $p \leq 0.01$) and b) the daily lag between air temperature and proglacial discharge ($n = 38, p \leq 0.01$). Days with significant precipitation have been removed ($n = 13$).

When the time lags of discharge within the proglacial zone are considered (Table 4.3, Chapter 4), there was a short mean time lag of 12 min between discharge at Station D and Station C, suggesting the lower proglacial water body does not significantly dampen the hydrograph signal by acting as a buffer or store of meltwater over diurnal cycles. Interestingly, cross-correlation revealed that stage recorded at Station A from DOY 221 to DOY 226 (when the station was operational) peaks prior to discharge at stations B and C by 44 minutes, suggesting that proglacial hydrogeomorphology may be a factor determining meltwater throughput times. For example, dye tracing revealed the presence of subterranean drainage pathways draining the upper proglacial lake with a transit time of approximately 1 hour and slow tracer transit velocities of 0.05 and 0.04 ms^{-1} suggesting discharge through these pathways is a minor component of proglacial runoff.

Therefore, it is apparent that the short lags between air temperature and discharge, in addition to decreasing lag times over the ablation season, indicate that the hydrological functioning of the Feegletscher Nord presents some similarities with observations made at other temperate glaciers (e.g. Hubbard *et al.*, 1995; Richards *et al.*, 1996; Swift *et al.*, 2005a). However, cross-correlations between air temperature and discharge also show significant scatter amongst these overall trends, indicating that other factors may be influencing the hydrograph form. In particular, cross-correlations between minimum air temperatures and discharges suggest that storage processes may be operating within the glacial hydrological system at a range of timescales. Therefore, detailed examination of the hydrograph form to ascertain the nature of these storage processes is required to more accurately quantify the hydrology of the Feegletscher Nord and is described in Section 5.4.

5.3.2 Suspended Sediment Concentrations

Cross-correlation was undertaken to establish temporal patterns and trends in daily lag times between SSC and discharge. As reviewed in Section 2.3, the transport of suspended sediments from temperate glaciers is typically expected to peak before discharge due to the effects of subglacial sediment exhaustion because the transport capacity of subglacial streams normally exceeds available sediment supplies (Gurnell & Fenn, 1984; Clifford *et al.*, 1995; Richards & Moore, 2003). The seasonal exhaustion of subglacial sediment supplies can further influence this time lag, shown as increasing lag times between SSC and discharge over the ablation season.

Cross-correlations between SSC and discharge at each proglacial gauging station were undertaken for the 2012 data series (Figure 5.2). As for the cross-correlation performed on the discharge time-series in Section 5.3.1, cross correlations were determined for individual hydrological days (beginning at 07:00am which typically coincided with minimum discharge) that were free of significant precipitation events. Figure 5.2 shows the dominance of negative lags between SSC and discharge at all stations with seasonal mean lags of -1, -0.2 and -0.8 hours at stations B, C and D, respectively, indicating both the dominance of meltwater discharge in driving SSC and the high transport capacity of such discharges whereby sediment transport capacity exceeds sediment availability. In light of the potential proglacial modification of SSC transfer patterns, the examination of cross-correlations at the individual gauging stations shows Station C experienced the greatest variability in time lags with a standard deviation of 2 (compared to a standard deviation of 1.5 at Station B, and 1.2 at Station D) highlighting potentially higher variability in sediment availability at this location, potentially suggesting that the stream at Station C has access to a wider range of sediment sources than those at Stations B or D. However, despite the high standard

deviation at Station C, the short mean time lag and the frequency of time lags at or close to zero suggests that SSC at this location is strongly associated with instantaneous forcing by discharge. In-channel and channel-marginal sediment availability has been associated with variability in proglacial SSC (e.g. Maizels, 1979; Hammer & Smith, 1982; Warburton, 1990; Orwin & Smart, 2004a; Leggat *et al.*, 2015). Therefore, the increased variability at Station C could result from the higher availability of in-channel or channel-marginal fine sediments at this location, which are more readily entrained by discharge compared to stations B or D. It is interesting to note the absence of strong seasonal trends in the cross-correlations with all stations experiencing scatter, although heteroscedasticity decreases over the ablation season. The results of this analysis suggest that, whilst diurnal exhaustion of sediment sources occurs, there is little or no apparent seasonal exhaustion of sediment sources as has been observed elsewhere at temperate alpine glaciers (e.g. Collins, 1979; Gurnell, 1987; Fenn, 1989; Clifford *et al.*, 1995; Swift *et al.*, 2005b). This raises questions as to the processes responsible for the apparently sustained seasonal sediment loads as previous studies have attributed such unusual increases to subglacial hydrological processes creating increased ice-bed interaction (e.g. Swift *et al.*, 2002; 2005b). In addition, it is possible that the high degree of scatter observed at all stations may be associated with the storage and release of sediments within the Feegletscher Nord forefield. Areas that have recently become ice-free are likely to experience enhanced sediment availability due to the deposition and exposure of fine-grained and unstable glacio-fluvial sediments (Church & Ryder, 1972; Ballantyne, 2002a) that can be mobilised and redistributed by glacio-fluvial processes as observed in a variety of deglaciating environments (e.g. Orwin & Smart, 2004a; Leggat *et al.*, 2015). In light of these findings and the questions raised regarding the nature and functioning of the glacio-fluvial sediment system at the Feegletscher Nord,

Chapter 7 investigates the potential range of processes responsible for controlling the transfer of suspended sediments.

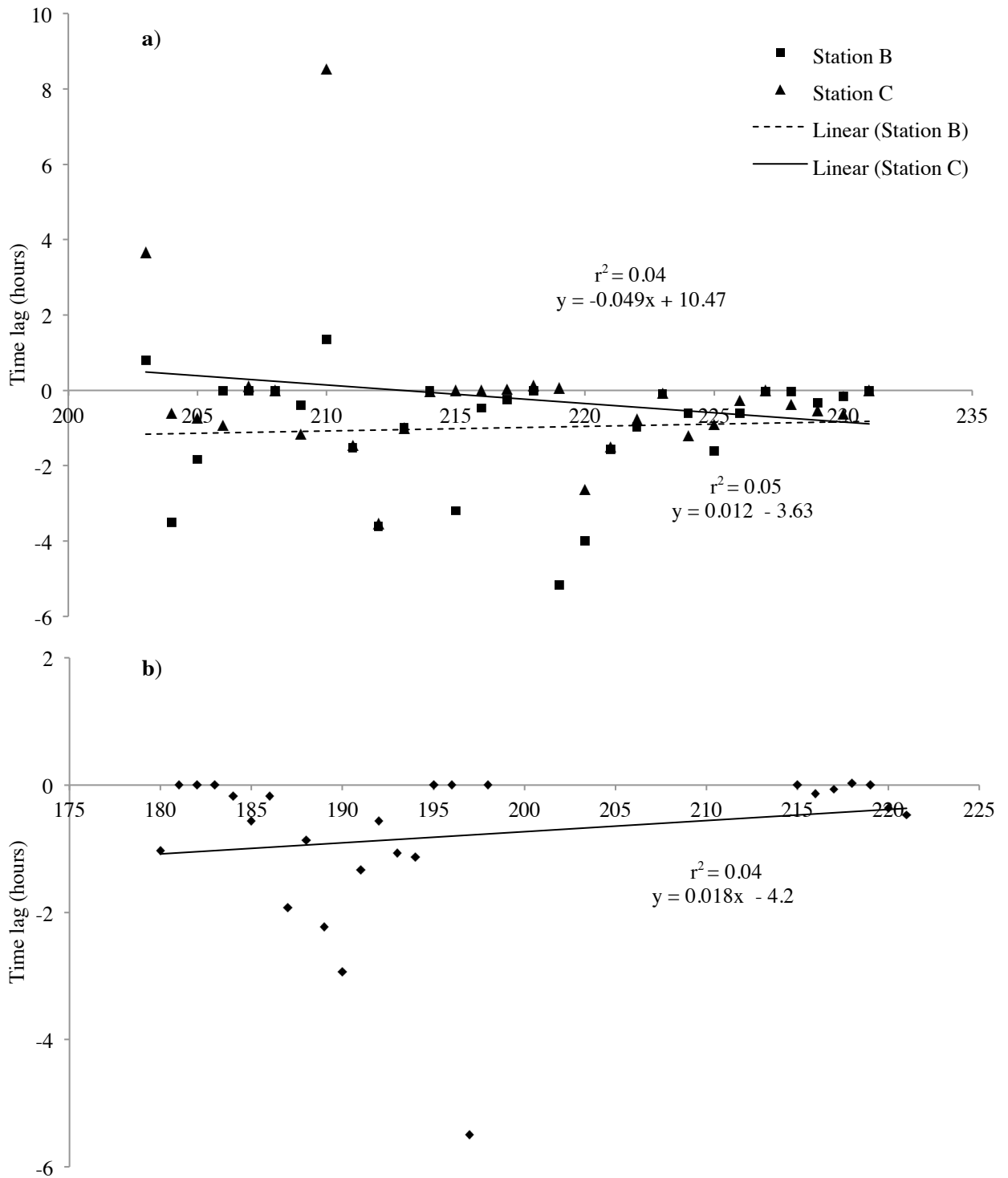


Figure 5.2: Results of cross-correlation analysis for proglacial SSC at Stations B and C (a) and station D (b). The relationships were not significant at $p \geq 0.01$.

5.4.1 Hydrograph recession analysis

Results of the cross-correlation analysis on the proglacial discharge time-series in Section 5.3.1 suggest that meltwater storage at a range of time-scales may be taking place within the Feegletscher Nord. The storage of meltwater by glaciers has been explored through examination of the receding limb of the diurnal hydrograph (*e.g.* Gurnell, 1993; Richards *et al.*, 1996; Hannah & Gurnell, 2001; Jansson *et al.*, 2003; Singh *et al.*, 2003; Sujono *et al.*, 2004; Irvine-Fynn, 2005a; Kido *et al.*, 2007; Rutter *et al.*, 2011; Hodgkins *et al.*, 2013). In this research, it is the extent to which water may be being stored in the short- and intermediate-term, over periods ranging from hours-days-months, which is likely to influence the form of the hydrograph (Jansson *et al.*, 2003). Water stored at this time scale may be located in surface snowpacks, crevasses, supraglacial pools, englacial pockets, subglacial cavities, englacial or subglacial drainage networks, and in basal sediments (Jansson *et al.*, 2003). Typically, storage occurs when inputs to the glacial hydrological system exceed outputs, due to the restricted capacity of the drainage network in the early ablation season to transmit this stored water, which is then released later in the ablation season. On a diurnal scale, the contribution of storage reservoirs to total daily runoff is expected to decrease over the ablation season, due to the decreasing amounts of snow and firn and the seasonal evolution of an efficient subglacial drainage network, which are both significant storage components (Jansson *et al.*, 2003). The concept of linear storage reservoirs has been employed to account for storage contributions from firn, snow and ice, particularly in the development of routing components to glacier runoff models (*e.g.* Hock, 1998; Hannah & Gurnell, 2001; Verbundt *et al.*, 2003; de Woul *et al.*, 2006; Hock & Jansson, 2005; Kido *et al.*, 2007; Magnusson *et al.*, 2011). These are typically applied as either fast reservoirs, representative of short-term water storage in ice, or slow reservoirs,

representative of medium to long-term storage in snow and firn, respectively. The highest storage coefficients are assigned to firn areas, as firn causes the largest delay due to delayed flow and storage in the snowpack as a result of low hydraulic conductivity and transmissivity. In contrast, the smallest coefficients are assigned to ice areas of rapid runoff where short delays are caused by the transit times of meltwater through typically englacial or subglacial drainage pathways (Hannah & Gurnell, 2001). Such reservoirs can be coupled in parallel or in series and the use of either two or three such reservoirs has been shown to perform well in runoff models (e.g. Hock, 1998; Hock & Jansson, 2006).

The determination of storage reservoirs, and hence, storage coefficients, is achieved through the analysis of recession hydrograph curves. Gurnell (1993) describes how the outflow from a linear reservoir (which is not recharged) can be expressed as

$$Q_t = Q_0 \left(e^{-\frac{t-t_0}{K}} \right) \quad (5.1)$$

where Q_t is discharge at time t ($\text{m}^3 \text{s}^{-1}$), Q_0 is initial discharge at t_0 ($\text{m}^3 \text{s}^{-1}$), and K is the reservoir storage coefficient (hours). Therefore, K may be estimated from the gradient of a semi-logarithmic plot of discharge over time. Breaks in slope of the recession curve are interpreted as recession flow from different linear storage reservoirs. Such breaks in slope are identified through a visual best fit to estimate the length and number of recessions and a least-squares regression was applied to these recessions. However, this approach can be subjective and, as such, least-squares regression was used to refine estimates of K through examination of the coefficient of determination at each apparently linear section of the time-series in order to identify the most probable start and end points. However, the initial identification of breaks in slope was determined

visually, and hence, remains somewhat subjective. The reservoir storage coefficient K was estimated by rearranging equation 5.1 such that

$$K = \frac{-t}{\ln\left(\frac{Q_t}{Q_0}\right)} \quad (5.2)$$

where Q_0 is the initial discharge and Q_t is discharge at time t . This highlights the assumption in this approach that following the initial discharge there was no further recharge due to meltwater runoff generation.

5.4.1.1 Hydrograph Recession Results

The above procedure was performed on 37 hydrographs from the 2012 ablations season. Days with precipitation were omitted from the analysis to eliminate recessions which may have had their shape modified by rainfall runoff. Four days without either clear breaks in slope or a discrete peak in discharge were excluded. In addition, a number of hydrographs displayed small short-lived peaks on the recession limb. These were not considered to be representative of a reservoir unless they were prolonged (i.e. $K \geq 1$ hour). Storage reservoir coefficients were successfully determined for 33 days in this period. The recessions showed significant variability over the ablation season ranging from 3 to 117 hours with an average of 22.3 hours (Table 5.1). Most recession curves displayed two breaks in slope indicating three reservoirs (e.g. Richards *et al.*, 1996), six days revealed a single break in slope indicating two reservoirs (e.g. Hannah & Gurnell, 2001), whilst three days displayed three breaks in slope, suggesting a fourth reservoir may exist which has been interpreted to represent a very slow reservoir (Richards *et al.*, 1996).

The summary statistics of the delineated K -values and their order on the recession curve are presented in Table 5.1. Most values were < 45 hours which is in the range reported by Hock and Jansson (2005) for ice reservoir storage (between 4 and 45 hours), suggesting that storage processes during, and up to, two preceding days may influence observed discharge. The low mean K -values determined for the three most frequently observed recessions (k_1 , k_2 and k_3) of 19, 24 and 27 are comparable with approximate average reservoir coefficients reported by Richards *et al.* (1996) of 12, 27 and 72 hours for the three most frequently observed recessions at Haut Glacier d'Arolla, Switzerland where some apparent dependence of the coefficients on the initial discharge was revealed. A small number of the identified reservoirs exceed this value and are comparable with storage in snow reservoirs (with a range between 30 and 120 hours). The absence of reservoirs identified in the range for firn storage (>120 hours) at the Feegletscher Nord is surprising given the presence of a high altitude snowfield at the glacier. The overall lack of longer term storage reservoirs could be attributed to the shrinkage and assumed negative mass balance of the glacier, which would potentially result in a depleted surface snowpack. The identified storage reservoirs may also be interpreted as water stored in subglacial sediments, the subglacial and englacial hydrological system or terrestrial groundwater flow (Fountain & Walder, 1998). However, the ability to define the physical basis for reservoirs identified through hydrograph recession analysis is problematic (e.g. Gurnell, 1993) and so any interpretation is necessarily subjective.

When the trends in K -values are considered, Figure 5.3 indicates a weak increasing trend over the 2012 ablation season, although the results are highly scattered. This is in contrast to the expected seasonal decrease in K -values associated with the evolution of an efficient glacial drainage network (e.g. Hannah & Gurnell, 2001; Jobard &

Dzikowski, 2006). This would appear to suggest that short-term storage is a dominant characteristic of the hydrology of the Feegletscher Nord, which is not dependent on seasonal changes in the configuration of the subglacial hydrological system. This finding is comparable to the results of the cross-correlation analysis, described in Section 5.3.1, which indicated that overnight discharge was poorly correlated with air temperature. Therefore, the observed overnight discharge may be related to the short or medium term storage of meltwater within the glacier. Furthermore, the lack of a seasonal trend in storage coefficients and the apparent overnight discharge variations raise questions as to the nature of the subglacial hydrological system. A decrease in storage coefficients would generally be expected owing to the reduced role of snow in storing water as the snowpack is removed and as the subglacial drainage system evolves into conduits. The presence of potentially significant contributions to runoff from subglacial storage suggests that the hydrological system may be, in part, described as a distributed drainage system, whereby meltwater becomes stored during the diurnal cycle in reservoirs, such as crevasses or sediments, due to limited flow capacity and competency, and is then transferred into conduits from these surrounding reservoirs, with the rate of transfer driven, in part, by variations in subglacial water pressures in the conduits (e.g. Hubbard *et al.*, 1995; Fountain & Walder, 1998; Swift *et al.*, 2002; Flowers, 2008). This interpretation would account for the lack of association between air temperature and discharge during the minima in the diurnal cycle, as discharge during these periods was instead being predominantly forced by the release of stored meltwater (e.g. Hubbard *et al.*, 1995). Furthermore, the seasonally decreasing lag times between air temperature and discharge presented in Section 5.3.1 may similarly be interpreted as representing either increasingly rapid surface inputs as the snowpack is removed or the evolution of the subglacial drainage network (e.g. Nienow *et al.*, 1998; Swift *et al.*, 2005). Taken together, these results highlight the competing processes of

surface meltwater inputs, meltwater storage and release, and drainage system capacity and competence which control the proglacial hydrograph (e.g. Flowers, 2008; *Swift et al.*, 2005a; Covington *et al.*, 2012; Gulley *et al.*, 2012a).

The extent to which the proglacial hydrograph is controlled and modified by either rates of surface meltwater input or the routing of meltwater through firn, snow and ice is well debated (e.g. Flowers, 2008; Covington *et al.*, 2012; Gulley *et al.*, 2012a). The decrease in lag times between air temperature and discharge may be reflective of the removal of the snowpack over the ablation season which would result in reduced proportions of surface melt being stored in slow draining reservoirs or low hydraulic conductivity (e.g. Richards *et al.*, 1996; Hannah & Gurnell, 2001; Swift *et al.*, 2002). Equally, the results of the cross-correlation analysis may reflect increases in the efficiency of the hydrological system, whereby conduits increased their transport capacity or extended upglacier (e.g. Nienow *et al.*, 1998). The lack of seasonal trends in storage coefficients of snow and ice reservoirs would tentatively support the former and would suggest the Feegletscher Nord experiences concurrent distributed and discrete drainage systems which did not exhibit discrete seasonal changes as would be comparable to other temperate Alpine glaciers (e.g. Fountain & Walder, 1998; Nienow *et al.*, 1998; Swift *et al.*, 2005a; Swift *et al.*, 2005a). However, it must be noted that the lack of field data from the early and late parts of the 2012 ablation season makes this interpretation speculative. In addition, one notable characteristic of the Feegletscher Nord with the capacity to influence drainage system dynamics is the pronounced glacier recession experienced. Flowers (2008) suggests that glacier thinning results in a reduced role for the conduit system in modulating the hydrograph because conduits are preserved under thin ice between years. These conduits would experience lower subglacial water pressure (than for conduits beneath thicker ice) and would transmit

meltwater in conjunction with a distributed system. Furthermore, the lack of longer duration storage reservoirs, such as those associated with firn storage, also suggests a reduced role for supraglacial storage, possibly as a result of the depleted snowpack extent and steep crevassed surface of the Feegletscher Nord. However, such interpretations as to the nature of the subglacial hydrological system at the Feegletscher Nord and the dominant controls on the proglacial hydrograph are unverifiable as subglacial conditions and drainage network morphologies beneath the glacier are unknown.

Table 5.1: Descriptive statistics of K -values derived from the analysis of hydrograph recession curves recorded at the Feegletscher Nord in 2012. The K -values are denoted by the order of appearance on the recession curve whereby K_1 represents the first part of the recession curve after peak discharge. Values are mean (μ), minimum and maximum values and standard deviation (σ) in hours.

	k1 (hours)	k2 (hours)	k3 (hours)	k4 (hours)
μ	18.6	23.6	26.7	26.5
Min	2.9	5.6	4.2	-
Max	63.9	117.3	57.9	-
n	33	33	17	1
σ	17	25.6	12.4	-

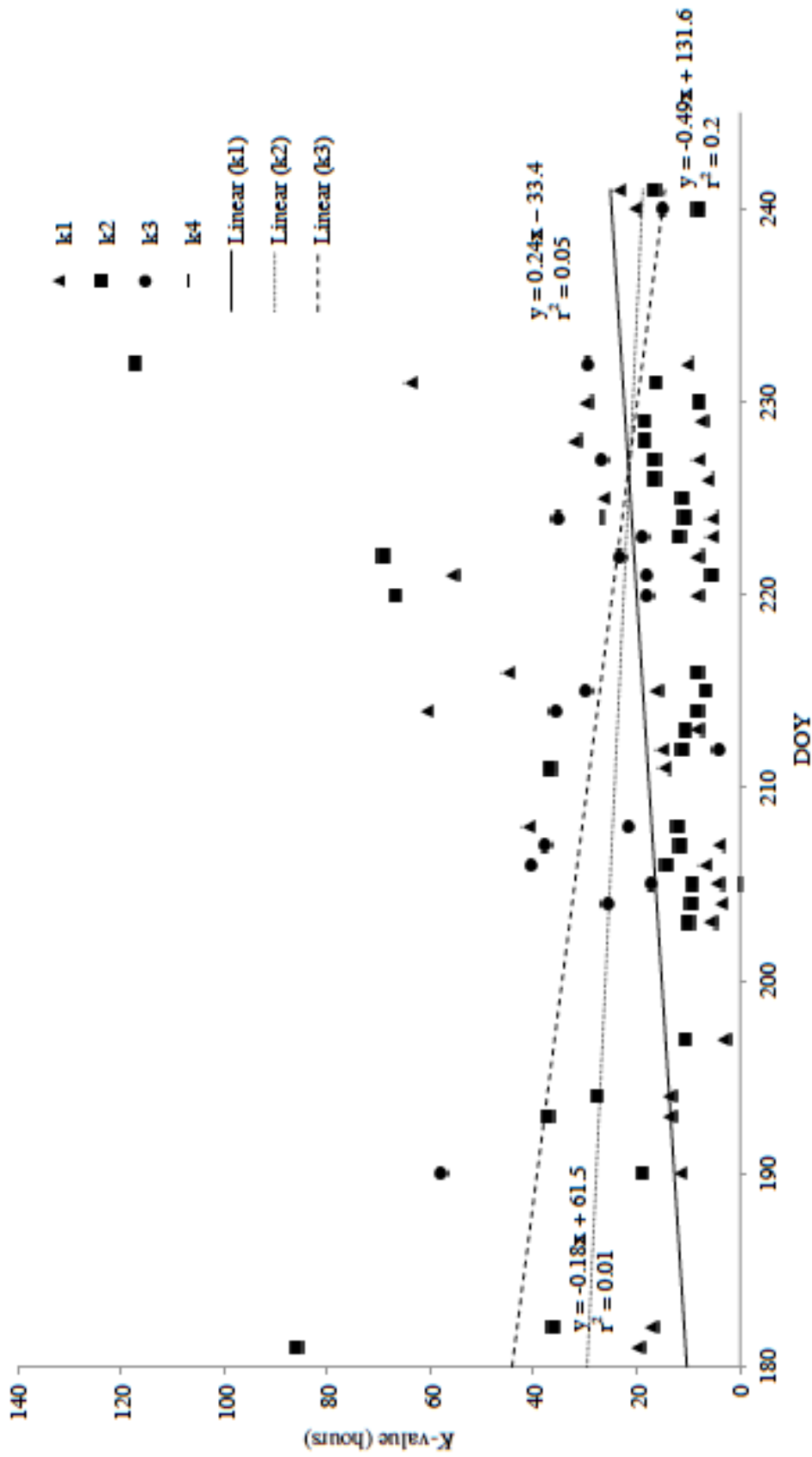


Figure 5.3: K-values derived from analysis of 37 hydrograph recessions over the 2012 ablation season. Reservoirs could not be identified for four hydrological days. The results are highly scattered with contrasting trends. Relationships were not significant at $p \geq 0.01$.

5.5 Classification Procedure

A procedure for the classification of diurnal hydrographs based on their shape and magnitude was proposed by Hannah *et al.* (2000) and has been applied to characterise the controls on, and explore seasonal changes in, the hydrology of glaciated catchments (e.g. Hannah *et al.*, 2000; Orwin & Smart, 2004; Hannah *et al.*, 2005; Irvine-Fynn *et al.*, 2005a; Swift *et al.*, 2005a; Leggat *et al.*, 2015). The procedure utilises principal component analysis (PCA) to reduce the discharge time-series data to a smaller number of underlying components which represent the variability of the data set as a series of generalised ‘shape’ models. Cluster Analysis (CA) is then performed on the retained components to identify days with similar diurnal discharge shapes. This allows the processes controlling the shape of these generalised clusters to be interpreted. The discharge flows are then classified according to their magnitude, using a range of diurnal bulk discharge indices including: mean daily flow, daily range, standard deviation, daily minimum and maximum and total load. Cluster analysis is performed on these indices and the dendrogram of like-magnitude days allows clusters to be determined and assigned a magnitude class. An assessment of processes controlling discharge is then undertaken based on the combined interpretation of the magnitude clusters and the generalised shape components.

Here, the aim of applying hydrograph classification techniques was to assess the nature and range of potential controls on discharge and SSC within the Feegletscher Nord catchment. Specifically, information on the potential glacial or non-glacial influences on the proglacial hydrograph and SSC curve is sought, in order to aid the development of a glacier runoff model and explore the hydrological controls on the transfer of suspended sediments.

5.5.1 Hydrograph Classification Method

For the classification of diurnal hydrographs, the procedure adopted here follows Hannah *et al.* (2000). The data series of bulk proglacial discharge was divided into hydrological days, again commencing at 07:00 which typically coincided with the hydrograph minimum.

To classify hydrograph shape, PCA was performed on N columns of days by n rows of discharge values. An orthogonal rotation was applied to maximise loadings on the variables and components with an Eigenvalue > 1 were retained. Hierarchical cluster analysis (HCA) was then performed on the loadings of the retained components to identify days with similar hydrograph shapes. HCA was performed using the average linkage algorithm and Euclidean distance measures as this method produced the most structured and interpretable cluster dendrograms (e.g. Hannah *et al.*, 2000; Swift *et al.*, 2005). The agglomeration schedule coefficients were used in conjunction with breaks in the dendrogram structure to determine the appropriate number of clusters.

To classify discharge hydrograph magnitude, a series of daily magnitude indices described by Hannah *et al.* (2000) were calculated comprising: mean daily discharge (Q_{mean}), daily discharge range (Q_{range}), the daily standard deviation of discharge observations (Q_{std}), baseflow discharge (Q_b), time to peak between daily peak and minimum flows (t_p), and SQR . SQR is the standardised discharge range and was calculated as:

$$SQR = \frac{(Q_p - Q_b)}{Q_b} \quad (5.3)$$

where Q_p is the daily peak flow and Q_b is the baseflow discharge. The indices were standardised as z -scores where mean = 0, and standard deviation = 1. The standardised daily magnitude indices were then classified using HCA using the average linkage method as per the ‘shape’ classification.

5.5.1.1 Hydrograph Classification Results

PCA undertaken on the proglacial discharge time series for 2012 retained four principal components which accounted for 88.8% of the variance in the time series (Table 5.2). Time plots of the principal component (PC) scores (Figure 5.4) support the interpretation of the four components:

- PC1: late peaked response,
- PC2: weak diurnal response with slow flow recession,
- PC3: variable response with variable baseflow and storage components,
- PC4: early peaked response with secondary flow components.

Table 5.2: Summary of the PCA performed on the 2012 discharge hydrographs along with the clusters identified from the PC loadings.

<i>Principle Components</i>	<i>Variance (%) explained</i>
PC1	33.4
PC2	23.6
PC3	20.7
PC4	11.1

Cluster analysis of the four retained component loadings resulted in three clusters which were interpreted into the following shape classes:

- Cluster 1: Peaked hydrographs which exhibit a strong diurnal signal and a later peak than those in cluster 3 (n = 13).
- Cluster 2: Variable hydrographs. The two days in this cluster exhibit unique hydrograph forms. DOY 195 experiences building discharge over the day with a subdued diurnal peak superimposed. DOY 206 exhibited a prolonged diurnal peak lasting much of the day with shallow rising and falling limbs (n = 2).
- Cluster 3: Peaked hydrographs which generally experience a steeper rising limb and an earlier peak than in the first cluster. In addition, some hydrographs in this group are influenced by rainfall (n = 20).

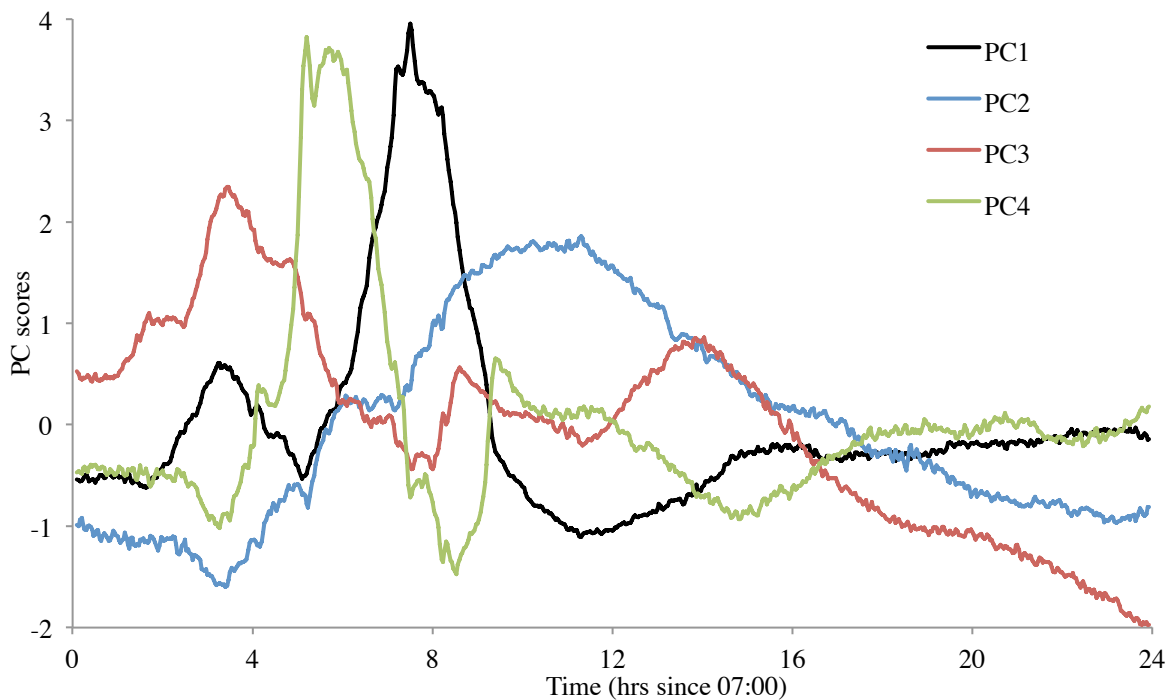


Figure 5.4: Plot of the PC scores for the four identified components of the diurnal hydrographs.

Cluster analysis on the daily magnitude indices revealed four clusters, which were interpreted into four magnitude classes (Table 5.4).

Table 5.3: Daily means of the four bulk flow indices used to classify hydrograph magnitude clusters for the 2012 discharge time-series

<i>Magnitude Cluster</i>	Q_{mean} ($m^3 s^{-1}$)	Q_{range} ($m^3 s^{-1}$)	SQR ($m^3 s^{-1}$)	Q_{std} ($m^3 s^{-1}$)	Q_b ($m^3 s^{-1}$)	n
1	1.278	1.836	2.481	0.533	0.841	8
2	2.241	3.127	4.525	0.934	0.699	5
3	2.710	2.770	1.913	0.842	1.498	19
4	1.900	3.533	10.852	1.046	0.325	2

The summary statistics (Table 5.3) were used to interpret the nature of the four clusters:

- Cluster 1: Low magnitude. The 8 days in this cluster exhibited the lowest average Q_{mean} , Q_{range} , and Q_{std} while average SQR and Q_b were low.
- Cluster 2: Intermediate magnitude. The 5 days in this cluster exhibited average Q_{mean} and Q_b between the low and high magnitude classes whilst average Q_{range} , SQR and Q_{std} were higher than for the low and high magnitude classes suggesting a greater degree of variability in diurnal discharge.
- Cluster 3: High magnitude. The 19 days in this cluster exhibited the highest average Q_{mean} and Q_b . Average Q_{range} and Q_{std} were between those for clusters 1 and 2, whilst average SQR was the lowest value suggesting a limited diurnal range and a considerable baseflow component.
- Cluster 4: Large range: The 2 days in this cluster exhibited average Q_{mean} between that for clusters 1 and 2 whilst average Q_b was the lowest. Average

Q_{range} , SQR and Q_{std} were all highest for this cluster suggesting significant diurnal variability.

The hydrograph shape and magnitude classifications were cross-tabulated by dividing the three shape classes by the four magnitude classes. The resulting composite hydrograph classification comprised 6 main hydrograph types (Figure 5.5). The hydrograph of DOY 195 represents a more anomalous event and was not considered a distinct hydrograph type in this procedure. The classes of hydrograph appear to represent more subtle changes in hydrological processes rather than distinct hydrological controls on proglacial discharge as observed by others (e.g. Hannah *et al.*, 2000). The shape classifications revealed the primary distinction between classes to be the timing of peak discharge and the seasonal distribution of classification classes is shown in Figure 5.6.

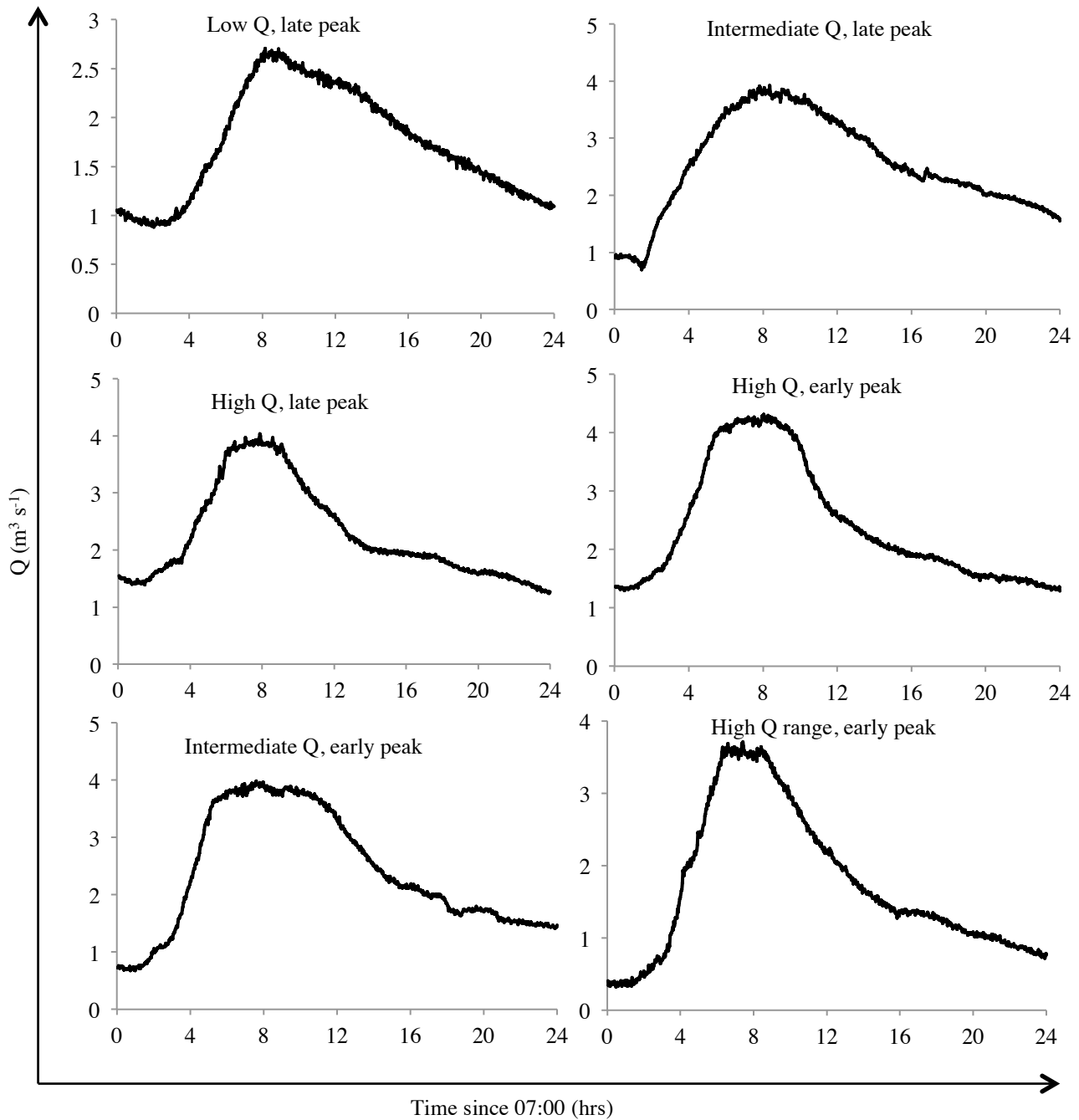


Figure 5.5: Six representative hydrograph forms obtained by hydrograph classification according to shape and magnitude.

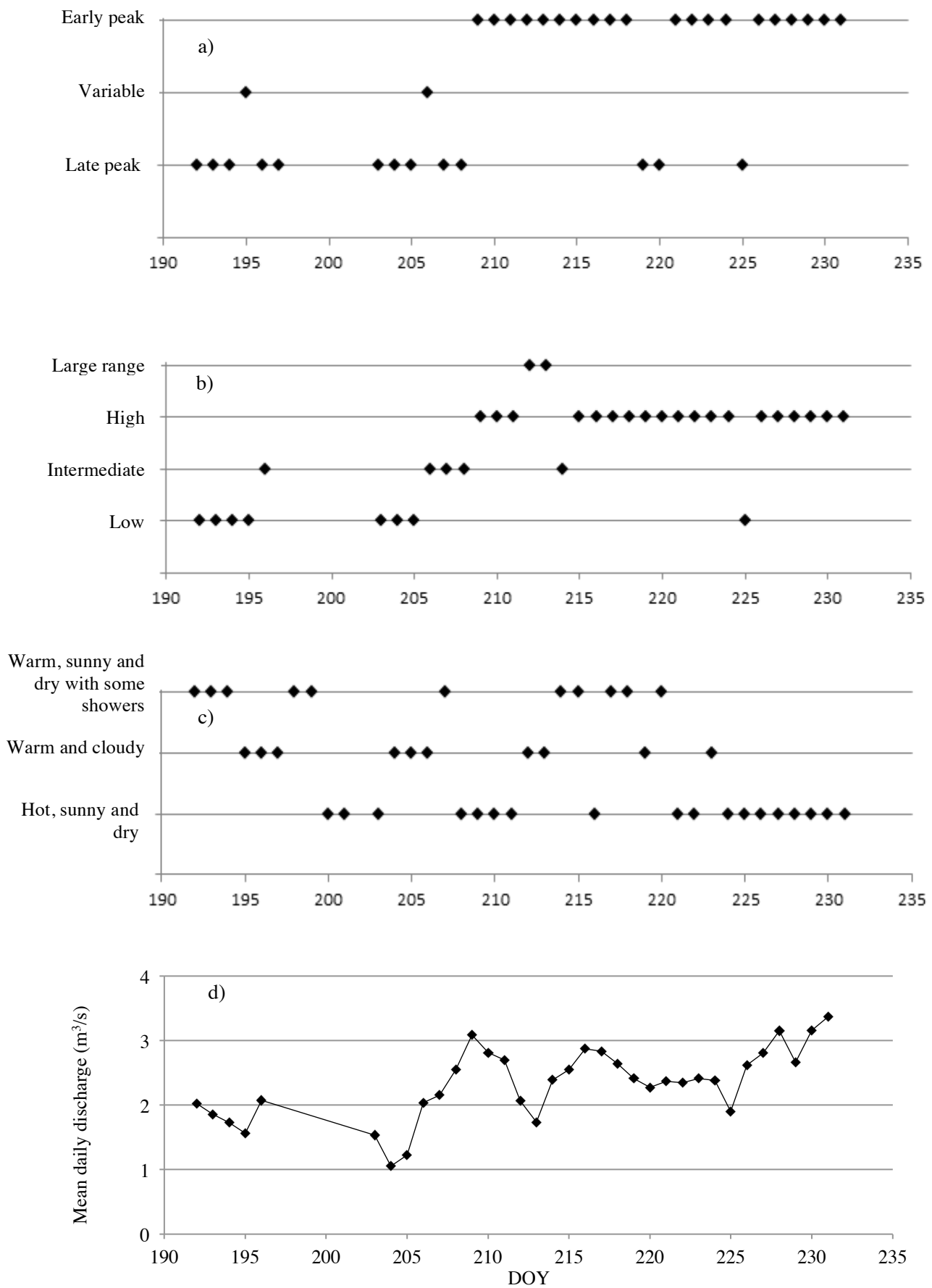


Figure 5.6: Plots of temporal patterns in hydrograph shape (a) and magnitude (b) indicating a seasonal transition around DOY 209. Temporal patterns in meteorological periods identified by HCA (c) with mean daily proglacial discharge by HCA (d).

To further examine the potential controls on hydrograph shape and magnitude, cluster analysis was performed on the meteorological data series. HCA of the meteorological indices identified four distinct meteorological periods for the ablation season which are summarised by their statistics in Table 5.4.

Table 5.4: Summary statistics for the four meteorological periods identified by the cluster analysis

<i>Magnitude Cluster</i>	<i>T_{mean}</i> (°C)	<i>T_{max}</i> (°C)	<i>T_{min}</i> (°C)	<i>T_{range}</i> (°C)	<i>Mean Rainfall Daily Total</i> (mm)	<i>Mean Total Daily Global Radiation</i> (MW)	<i>N</i>
1	15.54	22.52	9.78	12.74	2.91	20.26	23
2	9.14	13.1	6.3	6.8	45.5	3.65	1
3	11.89	17.05	7.8	9.23	2.41	15.5	15
4	10.94	17.94	4.89	13.05	1.15	23.63	13

These four distinct meteorological periods for the ablation season were interpreted from their summary statistics as follows:

- Cluster 1: Hot and sunny with some showers.
- Cluster 2: Intense storm and rainfall event on DOY 184.
- Cluster 3: Warm and cloudy with some showers.
- Cluster 4: Warm, dry and sunny.

The seasonal distribution of these clusters are shown in Figure 5.6 and the proglacial discharge patterns for the four meteorological periods were calculated based on their indices (Table 5.5).

Table 5.5: Summary statistics for proglacial discharge for the four meteorological periods identified by the cluster analysis. The statistics for Cluster 2, which represents the storm event on DOY184, are based on an incomplete data record as the sensors were out of measurable range for approximately 76 minutes coinciding with peak rainfall and discharge.

<i>Meteorological Cluster</i>	Q_{mean} ($m^3 s^{-1}$)	Q_{range} ($m^3 s^{-1}$)	SQR ($m^3 s^{-1}$)	Q_{std} ($m^3 s^{-1}$)	Q_b ($m^3 s^{-1}$)	N
1	2.6	2.7	2.1	0.8	1.4	16
2	3.2	3.2	1.9	0.9	1.7	1
3	1.8	2.7	5.1	0.8	0.72	9
4	2.3	2.5	2.4	0.76	1.16	9

The temporal pattern of hydrograph classes according to their shape and magnitude, along with the temporal pattern in meteorological conditions and mean daily discharges, is presented in Figure 5.6. The magnitude classifications revealed that the primary distinction between classes was mean discharge and the range of discharge values and shape classifications revealed the dominance of diurnal hydrographs, with differences in the time to peak implying a glacier hydrological system that is able to efficiently transmit meltwater. There is a clear seasonal transition of hydrograph classes evident, whereby late peaking hydrographs dominate until DOY 208 and early peaking hydrographs dominate from DOY 209. A concurrent trend is apparent in the classifications of discharge magnitude. Low and intermediate magnitude classifications are dominant until DOY 208 with high magnitude days dominant from DOY 209, along with two days classed as experiencing a large diurnal range in discharge. The observed trends in hydrograph classifications suggests a seasonal increase in the efficiency of the transfer of meltwater to the proglacial zone, which has been interpreted in other studies to be indicative of the increase in surface transit times of meltwater due to the removal of the surface snowpack, the decrease in surface albedo due to the removal of the surface snowpack, and a seasonal increase in the subglacial drainage network efficiency (e.g. Swift *et al.*, 2005a). Here, the dominance of the peaked hydrograph form suggests

that efficient subglacial drainage occurred throughout the study period and the shortening time to peak may suggest that the efficiency of the network may have increased from around DOY 208, due to the enlargement of subglacial conduits or the up-glacier expansion of subglacial conduits. However, the finding that the transition between late peaking to early peaking hydrographs on DOY 209 coincided with the transition between low and intermediate discharge magnitudes to high discharge magnitudes suggests that increased ablation did not precede the increase in drainage network capacity. In addition, the timing of the transitions closely coincided with the reduction in lag times between discharge and air temperature (Section 5.3.1), which were typically correlated without a time-lag from DOY 205, suggesting highly efficient meltwater transfer. This suggests that either the subglacial drainage system is characterised by a conduit-dominated system that experiences typically low water pressures and, as such, has the ability to rapidly transport high volumes of meltwater. This interpretation would suggest that the rates of input of surface ablation are more significant in controlling the proglacial hydrograph rather than the configuration and competence of the subglacial drainage network. In order to further examine controls on the proglacial hydrograph form and the nature of the glacial hydrological system, a glacier runoff model was constructed and is described and discussed in the following chapter.

5.5.2 SSC curve Classification Method

The aim of applying SSC curve classification techniques was to assess the nature and range of potential driving forces responsible for determining SSC patterns and magnitudes within the Feegletscher Nord catchment. Differences in SSC curve shape and magnitude can be used to identify and characterise proglacial controls on sediment transfer patterns (Orwin & Smart, 2004a; Leggat *et al.*, 2015). Here, SSC records from the three proglacial monitoring stations were utilised to explore the throughput of

suspended sediment within the catchment during 2012. The analytical approach adopted here follows that for the hydrograph classification described in Section 5.5.1 with the following amendments: to classify daily suspended sediment magnitude, the classification was based on the indices suggested for SSC by Orwin and Smart (2004a). These comprised: mean daily SSC, daily SSC range, daily SSC standard deviation, daily minimum and maximum and total suspended sediment load. The SSC indices were standardised as z -scores, whereby mean = 0 and standard deviation = 1. HCA was performed on n columns comprising the standardised daily indices for N rows of days in the series. The coefficients in the agglomeration schedule of possible clusters, in addition to visual examination of the cluster dendrogram, were used to select the appropriate number of clusters.

5.5.2.1 SSC curve Classification Results

PCA undertaken on the SSC time-series revealed between three and five components at the three proglacial gauging stations (Table 5.6), highlighting the varying degree of complexity in the controls on proglacial suspended sediment transfer within the proglacial zone. The component score plots at each station (Figure 5.7) show differences in the time to peak of suspended sediment concentration, in addition to more irregular response patterns at the three locations.

Four components were retained for Station B that cumulatively explained 94% of observed variance in the data series. PC1 and PC2 display a clear diurnal signal, with differing times to peak in SSC. PC3 and PC4 display a more irregular pattern, with PC4 showing discrete multiple peaks. The nature and number of the retained components at this location draw similarities to the components retained from the discharge PCA in

Section 5.5.1. Cluster analysis on the four retained component loadings identified three clusters which were interpreted as follows:

- Cluster 1: The SSC curves in this cluster displayed a strong diurnal peak (n = 20).
- Cluster 2: The SSC curves in this cluster showed earlier diurnal peaks than cluster 1, often with a more attenuated shape and receding limb (n = 8).
- Cluster 3: The sole member of this cluster displayed an irregular pattern with multiple peaks.

Five components were retained for Station C that cumulatively explained 91% of observed variance in the data series. PC1 and PC3 display a discrete diurnal signal, whilst PCs 2, 4 and 5 are more irregular, with multiple peaks and a noisier SSC signal. This may suggest there are potentially more diverse controls on SSC operating at this location compared to the other stations. Cluster analysis on the five retained components identified 3 clusters, which were interpreted as follows:

- Cluster 1: The SSC curves in this cluster displayed irregular shaped curves with multiple peaks in SSC (n = 8).
- Cluster 2: The SSC curves in this cluster generally showed a strong diurnal signal with some scatter or multiple peaks (n = 13).
- Cluster 3: The SSC curves in this cluster displayed a strong diurnal signal with generally earlier peaks in SSC than clusters 1 and 2 and some scatter or multiple peaks (n = 8).

Three components were retained for Station D that cumulatively explained 91% of observed variance in the data series. All PCs show a discrete diurnal signal, with differing times to peak that may reflect the discontinuous data record that was obtained

at this location. Cluster analysis on the three retained components identified four clusters, which were interpreted as follows:

- Cluster 1: The SSC curves in this cluster displayed a strong discrete diurnal signal (n = 6).
- Cluster 2: The members of this cluster displayed a double peak in SSC (n = 3).
- Cluster 3: The members of this cluster displayed a strong diurnal signal in SSC, which generally peaks earlier than those in cluster 1 (n = 5).
- Cluster 4: The members of this cluster displayed a strong diurnal signal with a more attenuated curve and falling limb (n = 11).

Table 5.6: Summary of the PCA performed on the proglacial SSC time-series.

	<i>Station B</i>	<i>Station C</i>	<i>Station D</i>
<i>Principle Components</i>	<i>Variance (%) explained</i>	<i>Variance (%) explained</i>	<i>Variance (%) explained</i>
PC1	47.9	39.4	41
PC2	35.1	21.8	33.8
PC3	6.9	15.3	15.7
PC4	4.4	10.5	-
PC5	-	6.2	-

The results of the PCA analysis on the SSC time-series suggest that, as with discharge, diurnal forcing dominates sediment transfer patterns. Upon examination of the retained components, differences in the number of retained components were apparent with four retained at station B (representing 94% of the variance in the data), 5 retained at station C (representing 93% of the variance in the data), and 3 retained at station D (representing 91% of the variance in the data). The number of components retained at station B showed the strongest similarities with the components retained for discharge at this location, whereby PC1 and PC2 exhibited strong diurnal signatures that together account for 83% of the variance in the data), whereas PC3 and PC4 were more

irregular. Station C is notable for the number of components retained with an Eigenvalue > 1 ($n = 5$), which is greater than the three components retained by both Orwin and Smart (2004a) and Leggats *et al.* (2015). Of these, PC1 was the sole components with a strong diurnal signature, with PC2 and PC3 displaying double-peaked patterns and PC4 and PC5 showing an irregular response that was apparently independent of discharge, which suggests that Station C appears to experience additional SSC forcing, with irregular and high-frequency patterns superimposed on the diurnal signal. Together, PC1 and PC2 accounted for 61% of the variance in the data at Station C, which is similar the equivalent components retained by Orwin and Smart (2004a) and Leggats *et al.* (2015), which represented an average of 57% of the variance in both of those studies. However, the variance explained by the first and second principal components at Stations B and D was larger at 83% and 75%, respectively. The interpretation of the components retained for Station D is more problematic owing to the sporadic data record obtained at this location. However, the strong diurnal shape of the components and an absence of additional variability could reflect a downstream decrease in variability in SSC transfer and a stronger discharge-driven regime. This may result from the lower proglacial lake upstream of Station D acting as a filter to episodic or stochastic upstream inputs of SSC, or may reflect the downstream increase in the armouring of proglacial surfaces, the effect of which would be in reducing extra-channel or channel-marginal sediment mobilisation due to surface stabilisation (Orwin & Smart, 2004a). When the results for Station C are viewed in light of the similarity between the SSC and discharge components retained at Station B and the more distinct diurnal components at Station D, it is suggested that the processes controlling proglacial SSC are spatially dependent. This finding draws a comparison to studies that have identified spatially variable sediment transfer patterns within recently deglaciated forefields that have been attributed to processes of sediment storage and release within

the proglacial zone (Orwin & Smart, 2004a; Leggat *et al.*, 2015). The results in this research suggest that spatial variability at the Feegletscher Nord proglacial zone is characterised by readily mobilised sediment stores at Station C, which results in increased SSC variability at this location. This is in contrast to limited sediment storage and release processes at stations B and D, as interpreted from more discrete SSC patterns with a stronger association with discharge.

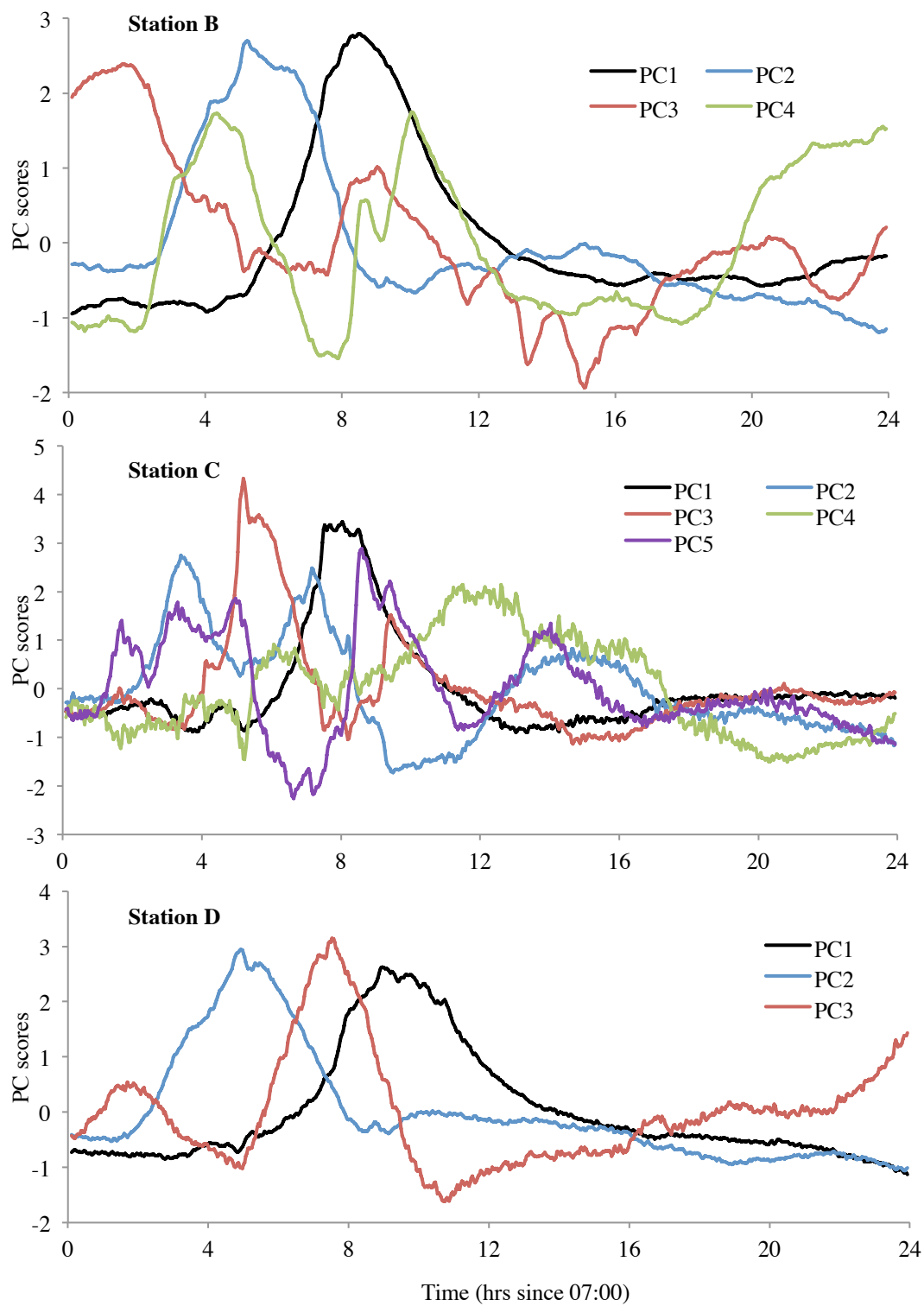


Figure 5.7: Plot of PC scores at the three proglacial suspended sediment gauging Stations.

Cluster analysis was performed on the daily suspended sediment concentration indices for each station. Between three and four clusters were revealed for each station and were interpreted from their summary statistics (Table 5.7) as follows:

Station B:

- Cluster 1: Very low magnitude. The 3 days in this cluster experienced the lowest average S_{mean} , S_{max} , S_{min} , S_{range} , S_{std} and S_{load} .
- Cluster 2: Low magnitude. The 18 days in this cluster experienced higher indices than cluster 1 but lower than both cluster 3 and 4.
- Cluster 3: Very high magnitude. The single member of this cluster (DOY 209) experienced the highest S_{mean} , S_{max} , S_{range} , S_{std} and S_{load} .
- Cluster 4: High magnitude. The 7 members of this cluster experience the highest S_{min} whilst the remaining indices were between those for clusters 2 and 3.

Station C:

- Cluster 1: Low magnitude. The 21 days in this cluster experienced the lowest average S_{mean} , S_{max} , S_{min} , S_{range} , S_{std} and S_{load} .
- Cluster 2: High magnitude: The sole member of this cluster (DOY 209) experienced the highest S_{mean} , S_{min} , S_{std} and S_{load} . S_{max} and S_{range} were below those for cluster 3.
- Cluster 3: High magnitude: The sole member of this cluster (DOY 214) experienced the highest average S_{max} and S_{range} with average S_{mean} , S_{min} , and S_{std} below those for cluster 2. Average S_{load} was below that for cluster 4.
- Cluster 4: Intermediate magnitude: The 6 members of this cluster experienced average indices higher than cluster 1, but below those in clusters 2 or 3, with the exception of S_{load} which was higher than cluster 3.

Station D:

- Cluster 1: Low magnitude. The 16 days in this cluster experienced the lowest S_{mean} , S_{min} , S_{std} and S_{load} and occurred early in the ablation season.
- Cluster 2: Storm event. The single member of this cluster (DOY 184) represents sediment transfer during a significant storm event. All indices show very high sediment concentrations and loads with a significant range. The sensors were out of measurable range for approximately 76 minutes during peak rainfall and discharge.
- Cluster 3: High magnitude. The 7 days in this cluster experienced higher average S_{mean} , S_{min} , S_{std} and S_{load} than for cluster 1 and occurred towards the end of the ablation season.

Table 5.7: Summary statistics of the magnitude clusters for each station identified from the cluster analysis.

Station	Magnitude Cluster	Average	Average	Average	Average	Average	<i>N</i>	
		S_{mean} ($g\ l^{-1}$)	S_{max} ($g\ l^{-1}$)	S_{min} ($g\ l^{-1}$)	S_{range} ($g\ l^{-1}$)	S_{STD} ($g\ l^{-1}$)		S_{Load} ($kg\ per\ day$)
B	1	0.1	0.16	0.07	0.08	0.02	3720	3
	2	0.2	0.36	0.13	0.23	0.06	11331	18
	3	0.37	1.1	0.14	0.91	0.24	28199	1
	4	0.33	0.83	0.17	0.66	0.17	21817	7
C	1	0.21	0.5	0.12	0.38	0.08	20586	21
	2	0.71	3.36	0.17	3.19	0.78	102210	1
	3	0.52	4.72	0.15	4.57	0.54	60165	1
	4	0.42	2.33	0.14	2.2	0.46	65287	6
D	1	0.07	0.61	0.05	0.55	0.03	10520	16
	2	0.66	9.94	0.05	9.89	1.47	153353	1
	3	0.20	0.41	0.13	0.28	0.08	14950	7

The cluster analysis revealed that, with the exception of the significant storm event, the magnitude of suspended sediment response can generally be grouped into high and low magnitude classes at each gauging station (Table 5.8). Low magnitude classes comprised 72% of the suspended sediment response at stations B and C and 67% at Station D. The remaining days were classed as either high magnitude or as an extreme event, as in DOY 184 at Station D. The results for Station D are not directly comparable to those for stations B and C, as much of the record for Station D was obtained early in the ablation season. However, the results from this station suggest that there is a seasonal increase in suspended sediment load, in addition to a downstream decrease in sediment load. This may result from the lower proglacial lake acting as a

sediment trap as sediment is transferred downstream from streams B and C via the proglacial lake to D. The higher mean suspended sediment concentrations and loads at Station C compared to Station B appear to reflect the higher discharges in this stream and also suggest greater sediment availability in the proglacial stream where Station C is located. The similar average S_{mean} and S_{min} values for stations B and C for low classes suggest that both streams experience similar controls on SSC magnitude during these periods and this may suggest an underlying baseload component to SSC. However, high average S_{load} , S_{max} and S_{range} indices at Station C for low classes compared to B further suggest that this stream experiences greater variability in SSC magnitudes due to in-channel or channel-marginal sediment mobilisation. The indices for high classes at Station C show average S_{load} , S_{max} and S_{range} to be significantly higher than at Station B whilst average S_{min} is similar. This suggests that increases in discharge at Station C resulted in considerably higher SSCs compared to Station B under otherwise comparable discharges.

Table 5.8: Average suspended sediment indices for high and low magnitude classes for each gauging station. Data from the storm event on DOY 184 was excluded.

Station	Magnitude Cluster	Average		Average		Average		N
		S_{mean} ($g\ l^{-1}$)	S_{max} ($g\ l^{-1}$)	S_{min} ($g\ l^{-1}$)	S_{range} ($g\ l^{-1}$)	S_{STD} ($g\ l^{-1}$)	S_{Load} ($kg\ per\ day$)	
B	Low	0.19	0.33	0.12	0.21	0.06	10244	21
	High	0.34	0.86	0.17	0.69	0.18	22615	8
C	Low	0.21	0.50	0.12	0.38	0.08	20586	21
	High	0.47	2.76	0.14	2.62	0.51	69262	8
D	Low	0.07	0.58	0.05	0.52	0.03	10584	16
	High	0.20	0.41	0.13	0.28	0.08	37992	7

SSC curve shape and magnitude classifications were cross-tabulated by dividing the shape classes by the magnitude classes at each station. The resulting composite SSC curve classification comprised 4 or 5 main curve types that exhibit strong diurnal signals (Figures 5.8, 5.9 & 5.10). The composite classes highlight more subtle changes in the pattern of SSC, similar to the results of the hydrograph composite classes. The time to peak is one aspect of the variation, with slight reductions in the time to peak over the monitoring period. This draws a comparison to the findings in this research of a reduction in time to peak discharge over the season, which supports the interpretation that the Feegletscher Nord experiences a slight seasonal increase in the efficiency of the glacial hydrological system (e.g. Nienow *et al.*, 1998). In addition, the time to peak may also be influenced by a seasonal exhaustion of sediment supply (Collins, 1979), due to transport capacity of the subglacial streams exceeding sediment supply. However, this latter point has not been apparent from the cross-correlation analysis. The composite SSC curves also highlight irregular SSC patterns, potentially influenced by rainfall or stochastic inputs of sediments to the streams.

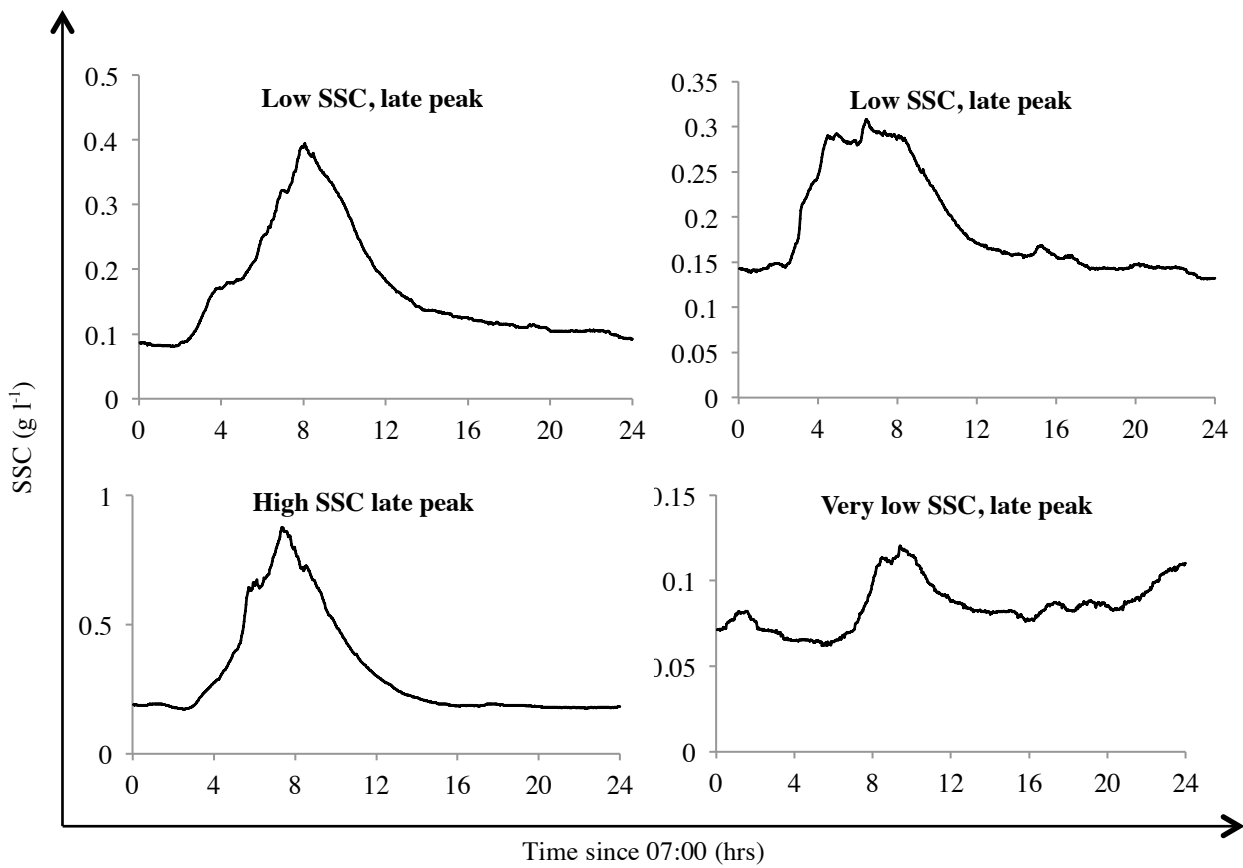


Figure 5.8: Composite SSC curve classification classes for Station B highlighting subtle changes in the diurnal pattern of SSC. Days with very high SSC and an irregular pattern occurred on only two occasions and, as such, were not considered distinct curve classes. Days with high SSC were not associated with early peak patterns.

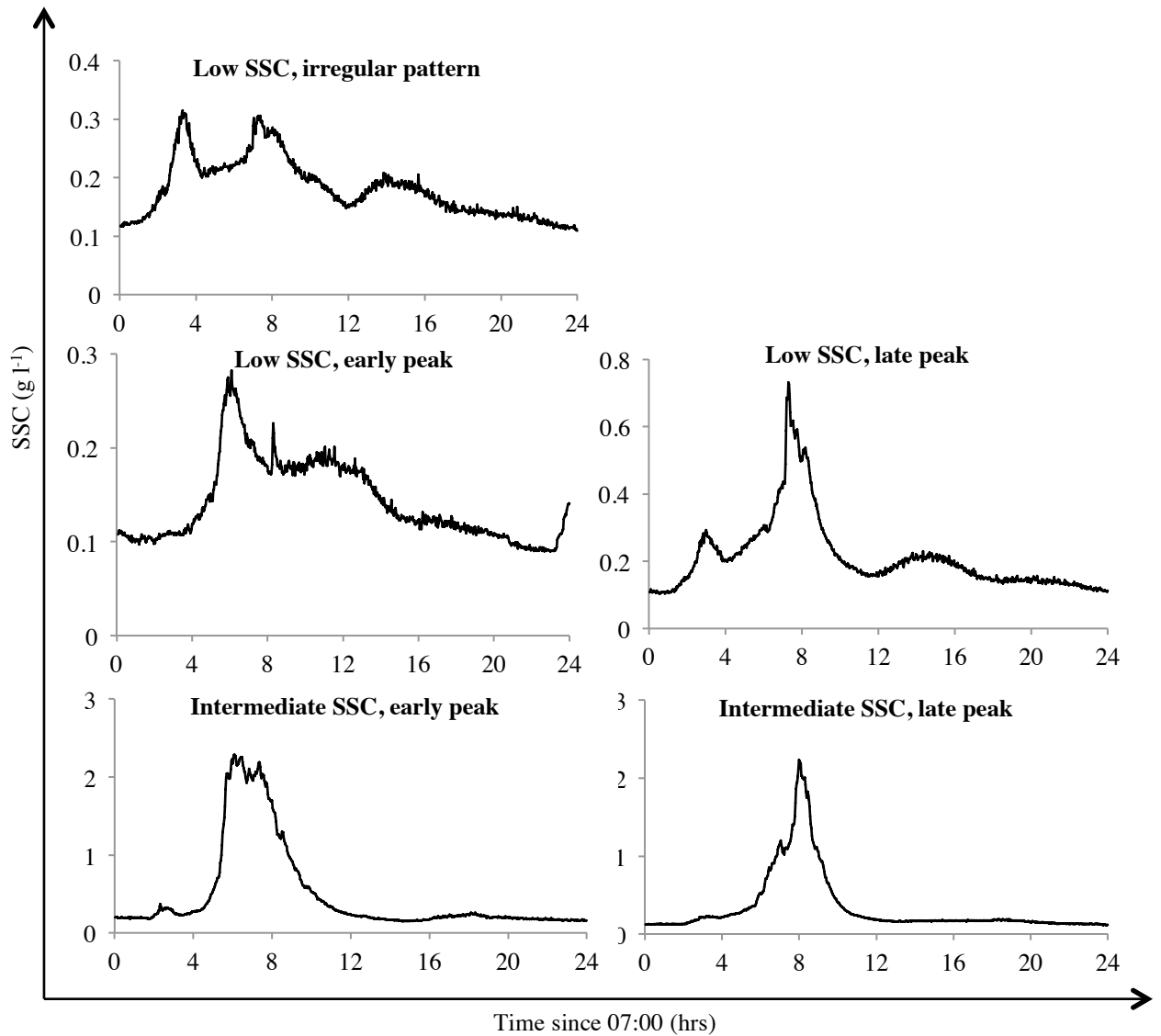


Figure 5.9: Composite SSC curve classification classes for Station C highlighting subtle changes in the diurnal pattern of SSC. Days with high SSC occurred on two occasions and, as such, were not considered distinct curve classes.

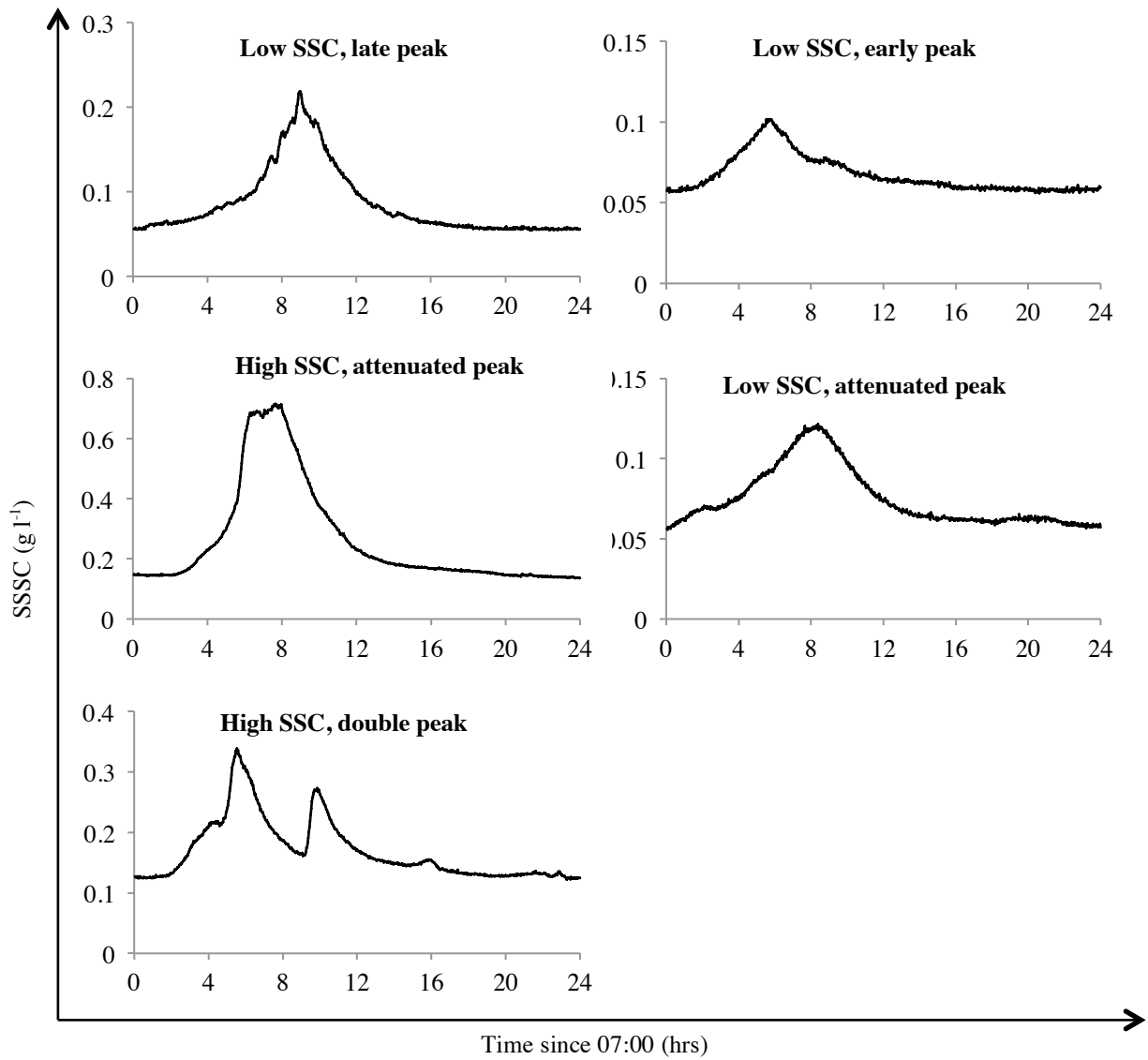


Figure 5.10: Composite SSC curve classification classes for Station D highlighting subtle changes in the diurnal pattern of SSC.

Proglacial suspended sediment patterns for the four meteorological periods identified by cluster analysis (Table 5.4, Section 5.5.1) were calculated based on their indices (Table 5.9). High suspended sediment concentrations and loads are associated with meteorological clusters 1 and 4, which represent warm conditions with high amounts of global radiation and infrequent and minor rainfall events. This suggests that both high average air temperature and cloud-free conditions are good predictors for high suspended sediment loads. The physical basis for this would be that high discharges resulting from high amounts of glacier ablation (as suggested from the analysis of discharge patterns during the same meteorological clusters) facilitate subglacial sediment evacuation either by increasing the rate of fluvial evacuation or increasing the availability of subglacial sediment. This raises questions as to the origin of any increases in sediment availability. Sediment availability may be increased due to enhanced glacier erosion associated with increased motion due to high subglacial water pressure variations (e.g. Hallet *et al.*, 1996; Swift *et al.*, 2005b) or the evacuation of debris from the ice-bed interface (e.g. Swift *et al.*, 2002). Additionally, it may increase due to the flushing of fine sediments located adjacent to subglacial channels as a result of diurnal fluctuations in water pressures (e.g. Hubbard *et al.*, 2005). Furthermore, the proglacial zone may be a source of high sediment availability due to the potential for high discharges to result in the mobilisation of in-channel or channel-marginal proglacial sediments (e.g. Warburton, 1990; Leggat *et al.*, 2015).

Table 5.9: Suspended sediment indices during the four meteorological periods identified by cluster analysis in Section 5.5.1: Cluster 1 was hot, sunny with some showers. Cluster 2 was the storm event on DOY 184. Cluster 3 was warm and cloudy with some showers. Cluster 4 was warm, dry and sunny.

Station	Met Magnitude Cluster	Average		Average		Average		Average	
		S_{mean} ($g\ l^{-1}$)	S_{max} ($g\ l^{-1}$)	S_{min} ($g\ l^{-1}$)	S_{range} ($g\ l^{-1}$)	S_{STD} ($g\ l^{-1}$)	S_{Load} ($kg\ per\ day$)		N
B	1	0.24	0.52	0.15	0.37	0.1	15076	16	
	2								
	3	0.17	0.32	0.12	0.2	0.06	8974	7	
	4	0.25	0.56	0.13	0.43	0.1	15332	6	
C	1	0.3	1.19	0.13	1.06	0.23	41128	16	
	2								
	3	0.2	0.47	0.11	0.36	0.07	16108	7	
	4	0.31	1.72	0.13	1.59	0.24	35931	6	
D	1	0.14	1.76	0.08	1.67	0.12	29987	5	
	2	0.66	9.94	0.05	9.89	1.47	153352	1	
	3	0.08	0.13	0.06	0.06	0.01	10898	9	
	4	0.13	0.25	0.09	0.16	0.04	21984	9	

The SSC shape and magnitude clusters were then cross-tabulated with discharge and meteorological clusters to determine whether differences in catchment hydrological and meteorological conditions resulted in distinctive patterns in sediment response at each station. Comparison of the cluster membership suggests that magnitude responses at stations B and C experience similar controls owing to the similar cluster memberships. However, there are significant differences in the magnitudes observed at each station, with Station C showing higher SSCs and SSLs compared to B, suggesting an increased availability of sediment associated with this stream. A lack of overlapping time-series at Station D prevents this record being included in the comparison. Comparisons of shape responses at Station B and C reveal similarities between shape classes of discharge and SSC at Station B, but no clear associations between sediment

response and the other variables at Station C, suggesting other factors may be responsible for determining shape responses at this location.

To further elucidate the controls on suspended sediment response at the stations, visual comparisons between hydrology, meteorology and sediment transfer were made by producing composite plots of sediment shape and magnitude responses with daily mean air temperature and discharge and total daily SSL and rainfall (Figures 5.11, 5.12 and 5.13). The composite plots revealed rainfall to be a driver of irregular shape responses at all stations. Irregular shape responses at Station C appear strongly dependent on either discharge or rainfall, whereas responses at Station B are more typically diurnal, with a lack of irregular patterns. The composite plots for stations C and D reveal that the association between mean daily discharge and total daily SSL is strongest late in the ablation season. After around DOY 217 the trends of SSL and mean daily discharge follow a similar pattern, whereas prior to this point, there is wider variation between the daily patterns of SSL and Q. It is suggested that DOY 217 represents a change point in the ablation season, whereby prior to DOY 217 there is a more diverse range of controls on proglacial SSC and possibly greater sediment availability. After DOY 217, a more discrete range of controls on proglacial SSC is apparent, due to the stronger relationship between Q and SSC along with potentially more limited sediment availability. Such potential sub-seasonal changes in the fluvial and proglacial controls on the observed patterns of SSC are further considered in Chapter 7.

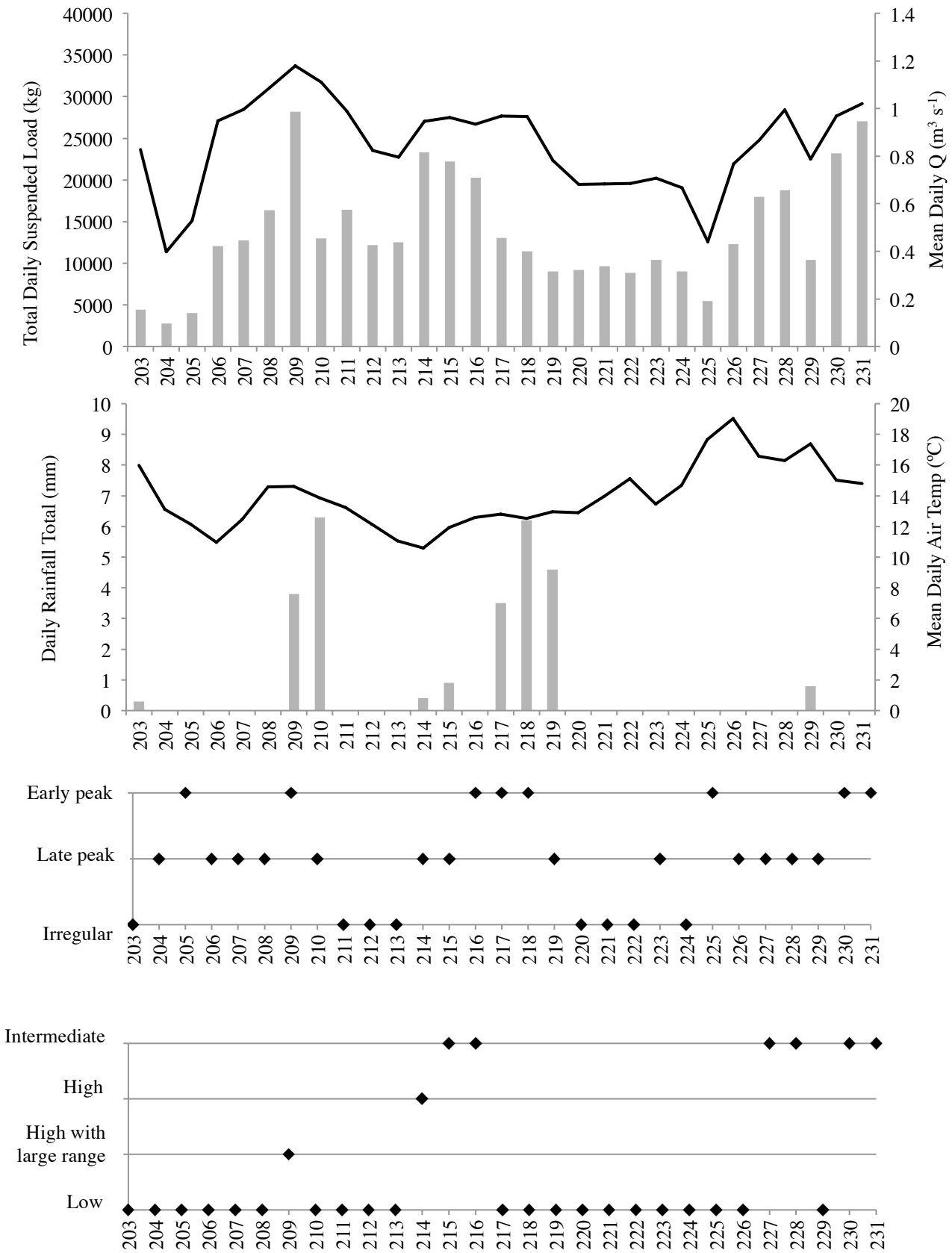


Figure 5.11: Composite plots of mean daily discharge and total daily suspended sediment load, daily rainfall total and mean daily air temperature with SSC shape and magnitude classifications at station B.

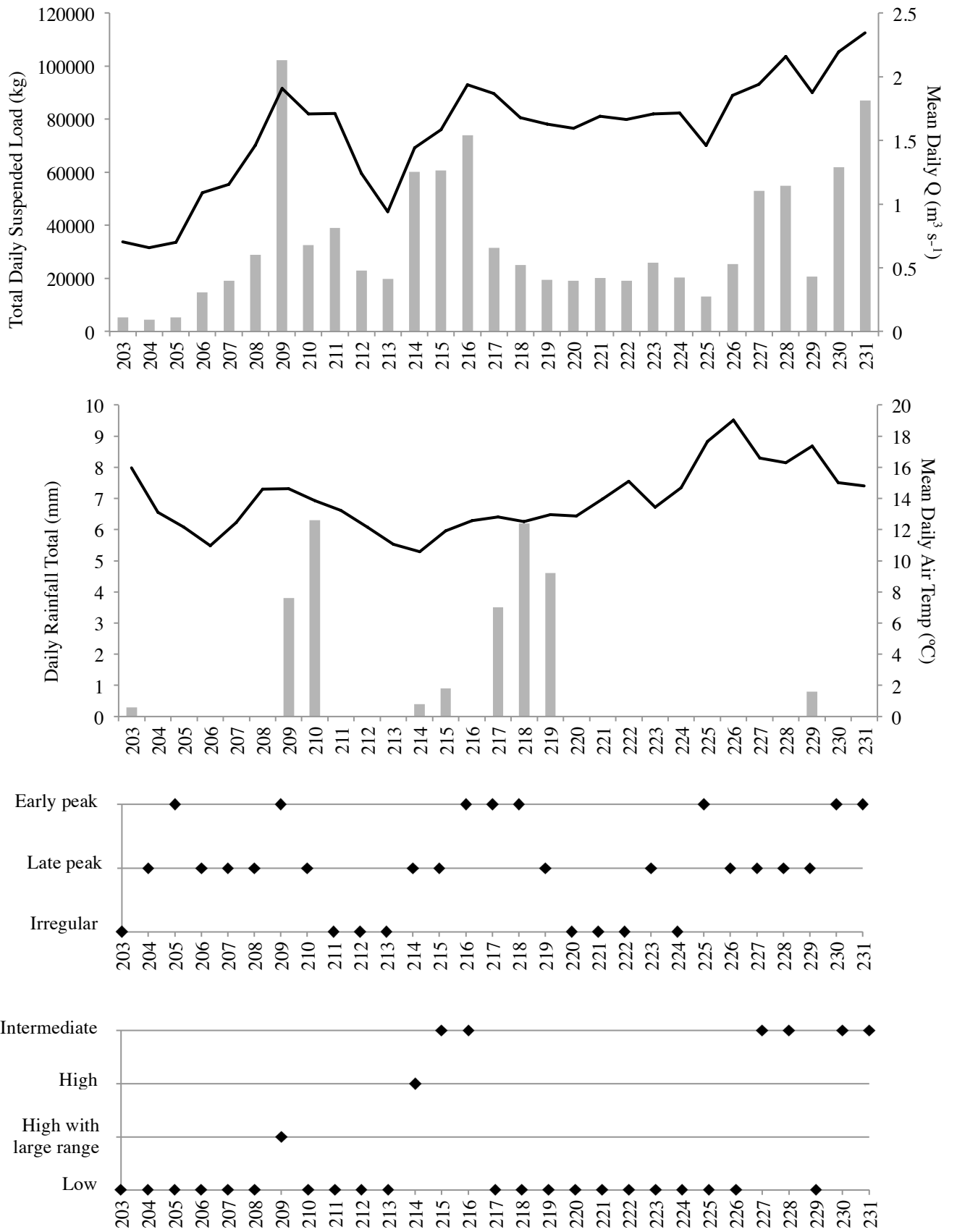


Figure 5.12: Composite plots of mean daily discharge and total daily suspended sediment load, daily rainfall total and mean daily air temperature with SSC shape and magnitude classifications at Station C.

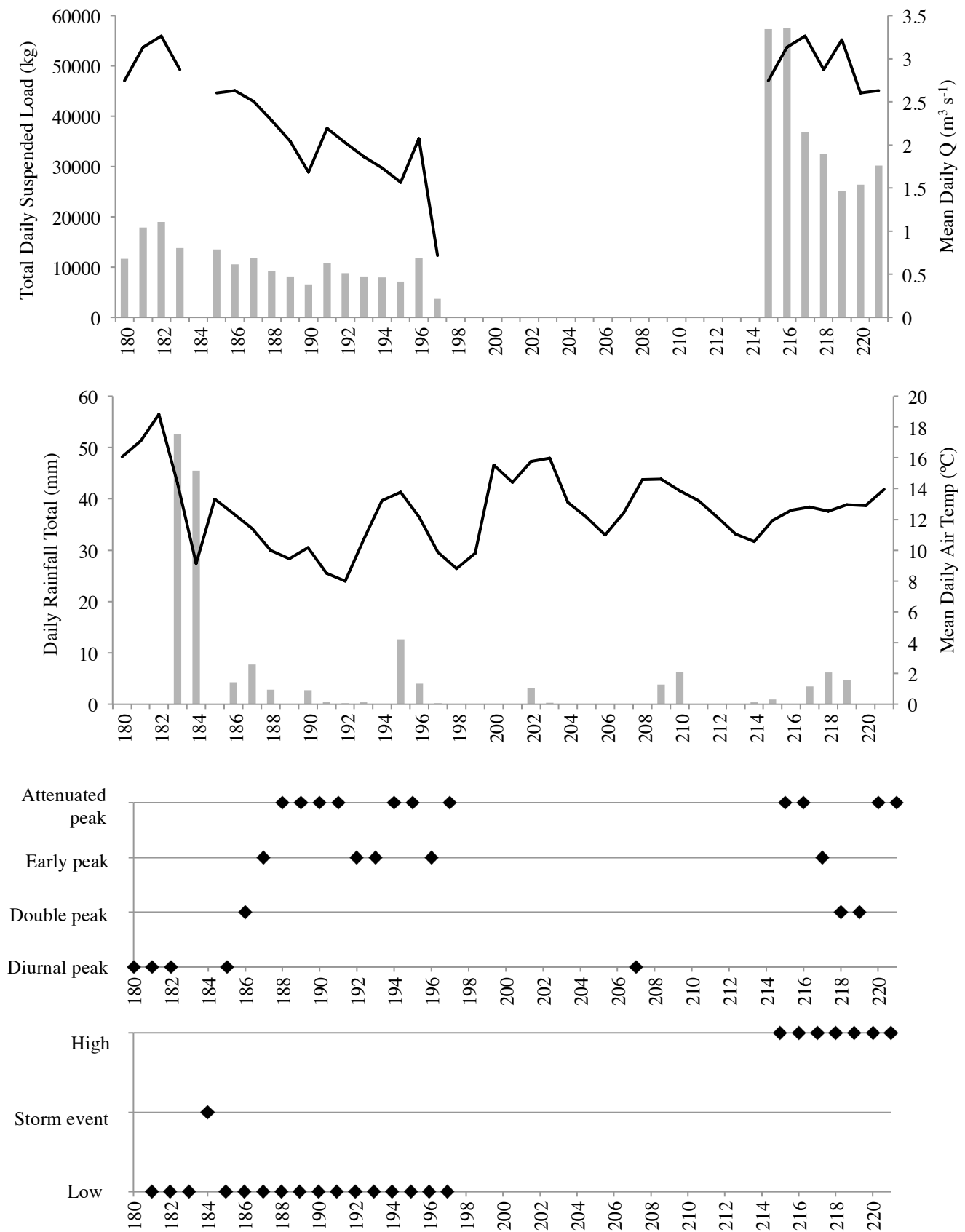


Figure 5.13: Composite plots of mean daily discharge and total daily suspended sediment load, daily rainfall total and mean daily air temperature with SSC shape and magnitude classifications at Station D.

This chapter has presented the analysis of hydrological and suspended sediment data series from the Feegletscher Nord catchment. The key findings of this analysis are summarised here:

- A total of 37 diurnal hydrographs spanning DOY 180–241 were quantitatively analysed revealing that very short time-lags (mean = 40 minutes) characterise the diurnal relationship between air temperature and discharge. These time-lags display a declining trend over the ablation season, suggesting an increase in the efficiency of meltwater throughput. Analysis of SSC and discharge time-lags revealed diurnal sediment exhaustion and an unusual lack of seasonal trends in time-lags.
- Time-lags between peaks in air temperature and discharge were generally much lower than time-lags between the minimum values of air temperature and discharge, suggesting that ablation may not be the main driver of discharge around the time of the hydrograph minima and that storage processes may be significant in driving overnight discharges.
- Analysis of hydrograph recession curves indicated that most meltwater storage occurs as short-term storage ($K < 45$ hours).
- Classification of hydrograph shapes revealed a seasonal transition in the time-to-peak, indicating an increase in the efficiency of meltwater throughput. Classification of hydrograph magnitude showed a seasonal transition from low and intermediate discharges early in the monitoring period, to high magnitude discharges from DOY 208.
- Classification of SSC curves revealed the strong dependence of SSC on discharge forcing along with a seasonal increase and downstream decrease in suspended sediment loads.

- Suspended sediment loads were found to be strongly determined by ablation-driven meltwater discharge. However, the controls on SSC patterns are spatially variable, as shown by additional irregularity at Station C (likely resulting from the mobilisation of proglacial sediment sources).

In summary, it is apparent that proglacial discharge is strongly dependent on ablation. However, questions remain regarding the nature of meltwater storage processes and their physical basis. The analysis presented here has revealed that proglacial SSC is strongly dependent on discharge at all locations in the proglacial zone. However, there are clear spatial differences in both the magnitude and patterns of SSC response depending on the gauging location. The results of the analysis presented in this chapter raise the possibility that surfaces or streams within the proglacial zone may be acting as both a source and sink of glacial sediment over a range of timescales, with distinct patterns and controls suggested between Stations B and C. However, these analytical approaches have been unable to provide detailed insights into the physical processes controlling SSC transfer. This is partly because such approaches tend to smother detailed changes in glacial and proglacial processes by neglecting short-term patterns in the data. In light of this, there is a compelling need to establish, in detail, the processes controlling proglacial SSC at a range of timescales. In particular, further analysis is required to explain proglacial SSC controls during the sub-periods characterised by magnitude, pattern and meteorological conditions, in addition to the individual days highlighted as experiencing high magnitude or irregular SSC curve shapes. To achieve this, Chapter 7 undertakes a range of multivariate analysis to establish the glacio-fluvial controls on SSC with a view to applying the relationship between discharge and SSC in a forward model. In light of the strong relationship between discharge and air temperature identified in this chapter, in addition to the rapid

meltwater routing and short-term storage processes, the following chapter presents the development of a glacier runoff model at the Feegletscher Nord.

6 Modelling Glacier Ablation and Runoff

6.1 Introduction

The preceding chapter explored proglacial hydrographs from the Feegletscher Nord in order to characterise the nature of, and controls on, proglacial discharge. It is apparent that an efficient subglacial drainage system characterises the Feegletscher Nord and air temperature is strongly associated with discharge. However, the preceding chapter raised questions as to the extent to which proglacial hydrographs are modified by the glacier drainage system. The proglacial hydrograph is a product of subglacial drainage system competency and changes in the rate of delivery of surface meltwater (Flowers, 2008; Gulley *et al.*, 2012b). Therefore, the ability to correctly interpret the hydrological processes determining the proglacial hydrograph is dependent on detailed knowledge of supraglacial ablation processes in addition to glacier drainage system characteristics. As discussed in Section 2.3, the extent to which supraglacial meltwater has access to the glacier bed is a fundamental determinant of subglacial suspended sediment transfer (Alley *et al.*, 1997). In light of the aim of understanding the controls on suspended sediment transfer within the Feegletscher Nord catchment, the aim of this chapter is to develop a glacier runoff model of the Feegletscher Nord in order to estimate glacier ablation and the resultant inputs to the glacier hydrological system which form the principle medium for suspended sediment entrainment and evacuation at temperate glaciers. The ability to successfully simulate runoff from glaciated catchments is essential if future response of glacier runoff and associated glacio-fluvial sediment transfer to climate change is to be understood (Syvitski, 2002; Bliss *et al.*, 2014; Huss *et al.*, 2014). However, there is a paucity of research into the development of runoff modelling approaches, in particular, for temperature-index approaches that can

account for diurnal melt and discharge cycles whilst retaining physically justified parameters (Hock, 2003).

Specifically, this chapter details the basis, development and performance of a temperature-index runoff model of the Feegletscher Nord for subsequent application in exploring possible future changes in meltwater and associated suspended sediment runoff in the following chapters. The theoretical meltwater discharge estimated by this runoff model is compared to observed discharges for the ablation season in 2012 to assess the model performance and implications for hydrological processes and dynamics in operation at the Feegletscher Nord. The basis for glacier runoff modelling is outlined in Section 6.2 with sections 6.3 and 6.4 exploring the merits of the two approaches to modelling: Energy balance models (EBMs) and temperature-index models (TIMs) respectively. The development of a Feegletscher Nord runoff model is detailed in Section 6.5 and the performance of this model is detailed and summarised in Section 6.6.

6.2 Outline to runoff modelling

If discharge is to be successfully predicted in a glaciated catchment, the processes responsible for the ablation of snow and ice must be accurately quantified. This is a complex undertaking, as it involves quantifying and subsequently predicting variables and processes, which can vary significantly in space and time. The melting of snow and ice will be determined by the interaction between the glacier surface and the atmosphere and the ice-bed interface. The net energy balance at the glacier-atmosphere interface is the principal determinant of the amount of snow and ice melt, although subglacial melt processes may also be significant, particularly at temperate glaciers. This energy balance is controlled by the meteorological conditions above the glacier as well as the physical properties of the glacier such as surface albedo. These interactions are

complex, because whilst the atmosphere supplies the energy which generates melt, the atmospheric conditions are modified by the presence of snow, ice and surface debris and are subject to high temporal and spatial variability. Comprehensive reviews of the complexity of the interactions between glacier surfaces and the energy balance have been made (e.g. Hock, 2005). Therefore, this chapter introduces the methods of modelling glacier ablation with the aim of determining meltwater runoff in a glaciated alpine catchment.

Glacier melt models aim to assess the energy flux to and from the surface of a glacier and compute the volume of melt produced. Energy balance models (EBMs) provide the physical basis for such modelling attempts as, at a surface temperature of 0°C, they assume that any surplus energy at the glacier-atmosphere interface is used immediately and wholly for melting (e.g. Braithwaite & Olesen, 1990). The physical basis of EBMs and their application is briefly discussed in Section 6.3. Difficulties in the accurate quantification and extrapolation of energy balance components throughout basins has led to attempts to empirically relate the melting of snow and ice to air temperature (Ohmura, 2001). Changes in air temperature are largely responses to differences in the surface energy balance and, as such, temperature index models (TIMs) are capable of using a temperature index to predict meltwater generation through the use of a degree-day factor to convert °C above a threshold, to mm of surface melt (Ferguson, 1999). The physical basis and applications of TIMs are examined in Section 6.3, and Section 6.4 expands upon this to explain the development of a TIM for the Feegletscher Nord catchment.

6.3 Energy Balance Models

Attempts to model the amount of surface melting of snow and ice have been based on assessments of the flux of energy to and from the surface whereby, at a surface temperature of 0°C, it is assumed that any surplus of energy at the surface immediately generates melt (e.g. Braithwaite & Olesen, 1990). The balance of energy received at the surface of the glacier controls the melting of surface snow and ice and can be described by its components:

$$Q_S + Q_L + Q_H + Q_E + Q_C + Q_P = Q_M \quad (6.1)$$

where Q_S is net short-wave radiation, Q_L is long wave radiation, Q_H and Q_E are turbulent heat fluxes of sensible heat and latent heat, respectively, Q_C is the heat through conduction, required to raise the temperature of snow or ice at the surface before melting can occur, Q_P is the heat supplied by rain, and Q_M is the net energy available to melt ice and snow. The physical principles of these components have been reviewed in detail by Hock (2005) and are summarised and presented in Table 6.1. If the net energy is positive this indicates an energy gain at the surface and if negative represents an energy loss. When there is a positive net energy (Q_M) in the balance equation (6.1), this heat will either raise the temperature of the snow or ice or generate melt if the surface is already at 0°C. The meltwater generated may be retained in the snowpack until a storage capacity is reached, but will ultimately flow into, and become part of, the glacier's hydrological system. The effect of snowpack storage and retention of meltwater, which usually occurs early in the melt season, must be integrated into attempts to model meltwater runoff from glaciers through parameters representing the storage capacity of the snowpack in addition to any refreezing taking place overnight (Jansson *et al.*, 2003).

The assessment of the energy balance components described in equation 6.1 results in energy balance models providing a comprehensive assessment of the net energy available to melt. Such models have generally been the basis for the most accurate glacier runoff models and are either applied as point studies (e.g. Konya *et al.*, 2004) or distributed models (e.g. Arnold *et al.*, 1996; Hock & Noetzli, 1997). Despite the strong physical basis and associated accuracy of energy balance modelling, the extensive data collection required coupled with expensive and highly specialised monitoring equipment has resulted in many studies adopting either simple temperature-index or hybrid approaches, so-called enhanced temperature-index models (e.g. Hock, 1999). The physical basis for such models is that many energy balance components can be strongly correlated (or calculated) from meteorological variables such as air temperature. The following Section explains the most straightforward of such approaches, the temperature-index model, and subsequent enhancements to this approach in the form of enhanced temperature-index models.

Table 6.1: Components of the energy balance equation and their physical principles adapted from Hock (2003).

Energy balance component	Physical principles
Shortwave radiation (Q_S)	<p>Shortwave radiation refers to the wavelength range of approximately 0.15 - 4 μm and mainly originates directly from the sun. This radiation can be approximated using date, time and location information to account for the variation in fluxes as a result of slope, aspect and effective horizon which can reduce the incoming radiation by obstruction of the sky, particularly in mountainous environments.</p> <p>In addition, shortwave radiation is subject to energy losses as a result of atmospheric scattering and absorption by aerosols. The amount of shortwave radiation delivered to the glacier surface requires adjustment for the glacier surface slope angle.</p>
Longwave radiation (Q_L)	<p>Longwave radiation refers to the wavelength range of 4 - 120 μm and is predominantly thermal radiation of terrestrial and atmospheric origin. Water vapour, carbon dioxide and ozone are the main atmospheric sources of longwave radiation. Changes in the amount of incoming radiation are due to the amount of cloud cover and amount and temperature of water vapour which leads to irradiance decreasing with altitude. This results in greater amounts of radiation originating from the lowest levels of the atmosphere. Modelling of longwave radiation in EBMs is usually based on the empirical relationship between longwave irradiance and air temperature and vapour pressure which can be measured by standard meteorological methods. Complexities in the quantification of longwave irradiance in EBMs can arise due to the variations in emissivity of the atmosphere to take into account cloud cover and the properties of clouds.</p>
Turbulent fluxes (Q_H and Q_E)	<p>Turbulent fluxes of sensible and latent heat are small compared to the fluxes of short and longwave radiation. These fluxes originate from the gradients created between air and the surface which are driven by temperature and moisture, in addition to turbulence generated in the lower atmosphere by vertical heat exchange. The transfer of sensible heat may be an important component in the energy balance during periods of cloudy or rainy weather and increase with wind speed. It can, in some cases, be the dominant term when snow or ice cover is patchy, whereby heat is advected from warmer ice-free surfaces. Turbulent heat fluxes are not usually integrated to EBMs due to the sophisticated instrumentation required to monitor them. However, latent heat flux can be a major driver of short-term melt generation for temperate glaciers in maritime environments.</p>
Conduction and Precipitation (Q_C and Q_P)	<p>Heat transferred by conduction is responsible for raising the near-surface ice and snow to the melting point. Temperate glacier ice usually experiences zero heat flux except when nocturnal refreezing occurs, whereas the surface ice of cold-based glaciers may require portions of the total net energy to raise the surface layer to the melting point.</p> <p>Rain has the capacity to generate surface melt through the advection of sensible heat (and friction). Rainfall events may constitute a significant short-term heat source if the rainfall is prolonged, heavy and warm. However, weather systems associated with precipitation may result in lower air temperatures and reduced short-wave radiation due to cloud cover.</p>

6.4 Temperature-Index Models

6.4.1 Introduction

The use of energy balance models for runoff modelling is challenging due to the combination of difficult and comprehensive data collection, in addition to extrapolation inaccuracies, particularly for large or topographically complex catchments (Hock, 2005). This has led to the development of simplified models based on an empirical relationship between observations of melt and surface air temperature (Braithwaite & Olesen, 1989; Ohmura, 2001). These temperature-index models assume that when air temperature reaches a threshold, typically 0°C, melt will occur. The physical justification of the temperature-index methodology is that net all-wave radiation is predominantly responsible for melt, as measurements of the energy fluxes of surfaces have shown net radiation to usually be the main heat source (Ohmura, 2001). Incoming longwave radiation comprises between 60 to 80% of net all-wave radiation. The largest portion of longwave radiation originates from the low atmosphere, the temperature and water vapour content of which is strongly influenced by the surface temperature (being in close proximity to the surface).

The correlation between positive air temperatures and surface ablation allows for the development of glacier runoff models which benefit from moderate data collection needs (with surface temperature being the principle input) and calibration through straightforward approaches to measure surface ablation and resultant runoff. Consequently, the TIM approach has become widespread for studies attempting to simulate glacier ablation or runoff (e.g. Braithwaite & Olesen, 1989; Braithwaite, 1995; Braithwaite & Zhang, 1999; Hock, 1999; Schneeberger *et al.*, 2003; Verbunt *et al.*, 2003; Pellicciotti *et al.*, 2005; Huss *et al.*, 2008; Koboltschnig *et al.*, 2008; Stahl *et al.*,

2008; Carezzo *et al.*, 2009; Huss *et al.*, 2010; Farinotti *et al.*, 2011; Magnusson *et al.*, 2011; Bliss *et al.*, 2014; Irvine-Fynn *et al.*, 2014; Riedel *et al.*, 2015; Sun *et al.*, 2015).

In light of the aim of this research to develop a Feegletscher Nord runoff model capable of simulating potential runoff, the following Section discusses the physical basis and relative merits of the temperature-index approach.

6.4.2 Degree-day models

An empirical relationship between air temperature and surface melt forms the basis for degree-day models. Air temperature forms the input to TIM models, which is then extrapolated across the elevation range of glacier surface. Melt is then calculated as a function of this temperature at different points at the glacier surface which is then integrated over the whole surface area of the glacier to calculate the total volume of melt generated at each time step. This approach can be expressed as follows:

$$\sum_{i=1}^n M = DDF \sum_{i=1}^n T^{+ve} \Delta t \quad (6.2)$$

whereby the amount of snow or ice melt, M (mm), which occurs during n time intervals, Δt , is a function of the sum of positive air temperatures of each time interval, T^{+ve} ($^{\circ}\text{C}$), with the factor of proportionality being the degree-day factor of either snow or ice, DDF , ($\text{mm d}^{-1} \text{ }^{\circ}\text{C}^{-1}$) (Braithwaite & Olesen, 1989): Degree-day factors are determined from field measurements of ablation and require *in situ* determination due to their generally poor transferability between glaciers (MacDougall *et al.*, 2011). Due to the differing densities of snow and ice, separate degree-day factors are normally calculated for each surface type and applied according to the spatial variability of the transient snow line (e.g. Hock, 1999; Anderson *et al.*, 2006). Table 6.2 highlights the significant variability in degree-day factors in studies simulating ablation. Degree-day factors will

decrease with increasing elevation, increasing direct solar radiation, and with decreasing albedo, and under otherwise similar conditions will vary according to differences in the relative significance of the energy balance components (Table 6.1). These variations will largely arise from the energy balance components that are most strongly associated with changes in air temperature. At diurnal time-scales, degree-day factors have been shown to approximately follow the diurnal variation in incoming shortwave radiation (Singh & Kumar, 1996), whereas seasonal variation in degree-day factors is typically associated with variations in surface albedo and incoming solar radiation (Hock, 2003). Degree-day factors may also be reduced when low air humidity results in sublimation, which may be significant on the lee-side of mountains (Zhang *et al.*, 2006). The use of constant degree-day factors in degree-day models will result in uniform estimations of melt rates across the glacier surface. In reality, due to the aforementioned controls on melt rates, there is strong spatial variability in melt rates as a result of topographic effects (MacDougall *et al.*, 2011) which, similarly, has been observed in studies of the spatial variation in mass balance (e.g. Anderson *et al.*, 2006). However, the degree-day factor will generally provide a good index of the average melt rates across the glacier (Hock, 1999; Ohmura, 2001; Hock, 2003).

The temporal and spatial variability of degree-day factors associated with glacier surface characteristics and the surface energy balance has led to the use of variable melt and degree-days factors which scale seasonally or vary according to meteorological characteristics. Hock (2003) suggested that the use of a melt factor instead of degree-day factor is capable of improving model performance, as it can account for melt occurring at or below 0°C. Melt factors have been scaled across the ablation season as a function of albedo and monthly mean air temperature (Arendt & Sharp, 1999) or

according to meteorological condition, which can impact albedo or components of the surface energy balance (e.g. Brinkhaus, 2003).

Table 6.2: Overview of degree-day factors at various locations and glaciers. Adapted from Braithwaite and Zhang (2000) and Singh *et al.* (2000).

<i>Location</i>	<i>DDF ice</i> ($\text{mm } ^\circ\text{C}^{-1} \text{ day}^{-1}$)	<i>DDF snow</i> ($\text{mm } ^\circ\text{C}^{-1} \text{ day}^{-1}$)	<i>Reference</i>
Various, Switzerland	5.0 - 7.0		Kasser (1959)
		4.0 - 8.0	Yoshida (1962)
Spitsbergen	13.8		Schytt (1964)
St. Supphellebreen, Norway	6.3		Orheim (1970)
	8.0	3.0 - 5.0	Borovikova <i>et al.</i> (1972)
		1.3 - 3.7	Anderson (1973)
Aletschgletscher, Switzerland		5.4	Lang <i>et al.</i> (1977)
Various, Norway	5.5 ± 2.3		Braithwaite (1977)
	8.0	5.0	Abal'yan <i>et al.</i> (1980)
Canada	6.3 ± 1.0		Braithwaite (1981)
Aletschgletscher, Switzerland	11.7	5.3	Lang (1986)
	7.2	2.5	Braithwaite and Olesen (1988)
Franz Josef Glacier, New Zealand	6.0	3.0	Woo and Fitzharris (1992)
Sátujökull, Iceland	7.7	5.7	Jóhannesson <i>et al.</i> (1995)
Nigardsbreen, Norway	6.4	4.4	Jóhannesson <i>et al.</i> (1995)
Ålftobreen, Norway	6.0	4.5	Laumann and Reeh (1993)
Nigardsbreen, Norway	5.5	4.0	Laumann and Reeh (1993)
Hellstugubreen, Norway	5.5	3.5	Laumann and Reeh (1993)
Nordbogletscher, W. Greenland	8.1	2.9	Braithwaite (1995)
Qamanârssûp sermia, W. Greenland	8.3	3.7	Braithwaite (1995)
Storglaciären	4.4	6.3	Hock (1999)
Griesgletscher, Switzerland	8.3 - 9.4		Braithwaite and Zhang (2000)
Franz Josef Glacier, NZ	7.2	4.6	Anderson <i>et al.</i> (2006)

The temporal resolution of degree-day models has been commonly based on daily or weekly air temperature records, whereby the sum of positive degree-days is assumed to be proportional to the total melt during a given time period. This temporal resolution fails to capture the pronounced variability in runoff, which is associated with strong diurnal variations in melt rates. As such, peak diurnal discharges will not be captured by such a modelling approach. However, such temporal resolutions can be well-suited to simulate discharge over longer time periods such as at seasonal timescales for purposes of mass balance monitoring (Hock, 2005). Temperature-index based melt models have been successfully developed for purposes of flood forecasting and hydrological modelling through the use of hourly temporal resolutions (e.g. Hock, 1999; Koboltschnig *et al.*, 2008; Carenzo *et al.*, 2009; Pellicciotti *et al.*, 2008), however, there is a need to further develop temperature-index models capable of simulating diurnal melt and discharge cycles (Hock, 2003). In addition, many such approaches have attempted to overcome some of the drawbacks of the classical degree-day approach through the incorporation of energy balance components, representing a transition from empirically based melt models to those which are more physically based. This is often achieved through the incorporation of potential incident solar radiation into the temperature-index approach (e.g. Hock, 1999; Pellicciotti *et al.*, 2008; MacDougall *et al.*, 2011; Irvine-Fynn *et al.*, 2014). However, it is generally accepted that for studies seeking to estimate runoff, the robust approximation of melt provided through the TIM approach is appropriate despite the potential for improvements to the physical basis of such models.

6.5 Development and Application of the Feegletscher Temperature-Index Model (FTIM)

The development of a temperature-index model was undertaken for the Feegletscher Nord in order to simulate the temporal variability in ablation and surface recharge to the glacial hydrological system and facilitate modelling of the subsequent throughput and output of this meltwater within the catchment. With the aim of simulating potential meltwater for runoff, a simple temperature-index approach was utilised which required only air temperature and precipitation as inputs. Degree-day factors were calculated from observed ablation at four ablation stakes. The model was spatially distributed to account for variations in ablation associated with changes in elevation and albedo. The model was run at an hourly resolution. Section 6.5.1 sets out the basis for the model along with the required components and their calibration.

6.5.1 Model Outline

The strong correlation between ablation and positive air temperatures at the Feegletscher Nord (Section 6.3.1) suggested a temperature-index approach was justified in order to simulate glacier runoff. The TIM developed here is based on the classical degree-day method:

$$M = \begin{cases} \frac{1}{n} \text{DDF} & T : T > 0 \\ 0 & : T \geq 0 \end{cases} \quad (6.3)$$

where M is the melt rate (mm h^{-1}), DDF is the degree-day factor ($\text{mm d}^{-1} \text{ } ^\circ\text{C}^{-1}$), T is air temperature and n is the number of time steps per day (here $n = 24$ as an hourly time step is adopted). Variables of temperature and precipitation were required as inputs for the Feegletscher TIM (FTIM) which were obtained during the 2012 study period. Measurements of ablation obtained from the four stakes described in Section 4.3 were used to calculate degree-day factors. The model was optimised with the use of discharge

measured at automated gauging stations in the proglacial zone which have been described in Section 4.4.4. The following sections outline the components of FTIM.

6.5.1.1 Temperature Component

The data recorded at the Saas Fee weather Station were used as the primary input of air temperature data. In applying distributed models, researchers have typically extrapolated temperature across glacier surfaces through the use of constant, linear lapse rates as derived from the difference between concurrent air temperatures recorded at temperature sensors of varying altitude (e.g. Hock, 1999; Huss *et al.*, 2008; Farinotti, 2010). Studies utilising linear lapse rates in the European Alps have reported values of -0.0056 °C/m (Farinotti, 2010), -0.00567 °C/m (Huss *et al.*, 2008), and -0.009 °C/m (Turpin *et al.*, 1997); compared to a mean lapse rate in mountainous terrain of around -0.0065 °C/m (Barry, 1992). It is widely recognised that the climatology of mountain regions can lead to significant errors in models utilising constant linear lapse rates, particularly due to high short-term variability in synoptic conditions (Ferguson, 1999). This is particularly acute in studies considering alpine areas with large elevation ranges and has resulted in the adoption of either lapse rates which vary over time to account for seasonality or synoptic conditions (e.g. Ferguson, 1999) or non-linear lapse rates based on a logarithmic function of altitude (e.g. Irvine-Fynn *et al.*, 2014).

In rationalising the approaches to lapse rate investigation for the Feegletscher Nord TIM, there are two points for consideration. Firstly, the principal meteorological dataset was obtained 1.8 km downvalley of the glacier terminus, supplemented by a further station adjacent to the glacier snout and two on-ice stations for which short records were obtained. The lack of long-term, continuous on-ice records prevented a robust relationship for a temporally varying lapse rate over the study period to be defined. In addition, the relatively small study area under investigation, and a robust

programme of data collection at a wide elevation range ameliorated the potential errors associated with utilising constant, linear lapse rates over large areas. This reasonably justified the adoption of a constant, linear lapse rate that was calculated by deriving the average differences in air temperature from the suite of temperature sensors ranging from 1796 m asl in the proglacial zone to 3000 m asl and 3450 m asl at the glacier surface for the available data periods. This approach yielded a lapse rate of -0.0054 °C/m and is detailed in Section 4.2.2.

6.5.1.2 *Threshold Temperature Component*

The temperature-index model proposed by Hock (1999) adopts a threshold temperature of 0 °C to define the air temperature at which ablation occurs. However, as air temperature is a product of the energy balance, a threshold of 0 °C may not be physically based with regards to the commencement of melt. Consequently, a wide range of positive and negative threshold temperatures have been utilised in modelling attempts (e.g. Kane *et al.*, 1997; Carenzo *et al.*, 2009; Irvine-Fynn *et al.*, 2014). For example, Kane *et al.* (1997) justified the use of a negative threshold temperature obtained through model optimisation because of the generation of melt through radiative heating. In contrast, Irvine-Fynn *et al.* (2014) adopted a positive threshold temperature derived from regressing ablation data against cumulative air temperature above a series of thresholds to ascertain the optimum threshold that best accounts for ablation, which was justified as it aligned with the threshold temperature for the equal probability of precipitation falling as snow or rain at the study site in question.

These approaches leave the use of a particular threshold temperature open to optimisation, provided it can be justified for the physical or environmental characteristics of the study site. To select an appropriate threshold temperature for FTIM, ablation data at each stake was regressed against cumulative positive air

temperatures above a series of thresholds (e.g. Irvine-Fynn *et al.*, 2014) from -5 °C to +3 °C at intervals of 1 °C (Figure 6.1). The results indicated strong variation in the optimum thresholds between individual stakes in addition to only marginal improvements in the correlation coefficients when compared to a threshold of 0 °C. As such, a threshold temperature of 0 °C was utilised and subsequently confirmed as suitable through optimising threshold coefficients in the runoff model as per Kane *et al.* (1997).

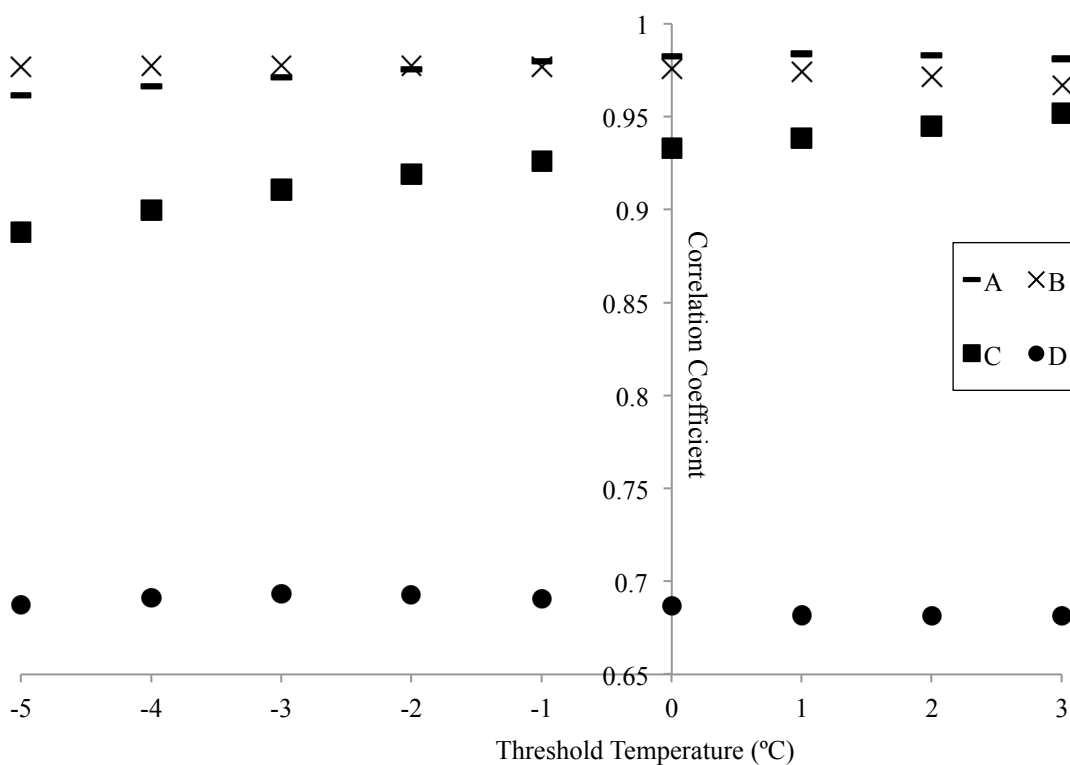


Figure 6.1: Correlations between threshold temperatures for melt and observed ablation at each ablation stake highlighting variations between optimum threshold temperatures between stakes and minor improvements to correlation coefficients. All relationships were significant at $p \leq 0.05$.

6.5.1.3 Precipitation Component

With the exception of two significant storm events, field observations and the low intensity and frequency of rainfall events suggested precipitation was not a significant process of ablation. As such, precipitation was accounted for in the model as per Hock (1999). To account for the spatial distribution of precipitation and the type, the threshold air temperature was used to define the type of precipitation falling on each elevation band. Liquid precipitation was accounted for whereby measured precipitation is added to the total water equivalent transferring at each time step from every elevation zone.

6.5.1.4 Spatial Distribution

A high resolution digital elevation model of the Feegletscher (swissALTI3D) with a grid size of 2 m² was utilised to account for the spatial variability in ablation due to changes in air temperature and melt rates with elevation. The glacier extent was principally defined through geocorrection of Spot-5 satellite imagery (5 m resolution) obtained in 2007 by SwissTopo (Federal Office of Topography, Switzerland) with a reported 3-dimensional average error of 1 – 3 m for elevations above 2000 m asl. A minimum of six ground control points were used in the geocorrection of each image and field photographs were used to further delineate the glacier extent to account for retreat since 2007. The resultant glacier extent was in good agreement with the Feegletscher Nord outline determined in the GLIMS Glacier Database (Raup *et al.*, 2007; Kargel *et al.*, 2014) and of considerably more detailed delineation due to the additional use of field observations and photographs. The elevation range of the glacier was divided into 10 elevation bands using Jenks (1977) classification method that minimises the variance within each elevation band while maximising the variation between bands (Table 6.3). The dependence of air temperature on altitude was accounted for by applying the lapse

rate determined in Section 5.2.2 to the difference in elevation between the Saas Fee meteorological station and the mid-point of each elevation band.

Table 6.3: Elevation zones of the Feegletscher Nord in FTIM

<i>Zone</i>	<i>Elevation Range (m asl)</i>	<i>Zone interval (m)</i>	<i>Area (10⁵ m²)</i>	<i>Area %</i>
1	2161 - 2425	263	1.3	1.9
2	2425 - 2688	263	2.4	3.5
3	2688 - 2872	183	4.1	6.0
4	2872 - 3040	167	8.1	11.9
5	3040 - 3199	159	11.1	16.1
6	3199 - 3367	167	11.1	16.2
7	3367 - 3535	167	11.7	16.0
8	3535 - 3718	183	9.6	14.0
9	3718 - 3942	223	5.8	8.5
10	3942 - 4197	255	3.3	4.9

6.5.1.5 Degree-Day Factors

Degree-day factors were first established by applying a linear regression between observed cumulative ablation and air temperature at each stake. These degree-day factors (Table 6.4) show some variation, but are in broad agreement with values reported elsewhere in the European Alps (Table 6.2). Differences between degree-day factors for snow and ice are apparent (Table 6.5) with a mean degree-day factor for snow and ice of 5.4 and 9.4 mm d⁻¹ °C⁻¹, respectively.

Table 6.4: Average degree-day factors (DDF) over the 2012 ablation season. Relationships were significant at $p \leq 0.1$ except at Stake D which was not significant.

<i>Stake</i>	<i>Elevation (m asl)</i>	<i>Time-range (days)</i>	<i>DDF (mm d⁻¹ °C⁻¹)</i>	<i>r²</i>
A	3000	70	8.4	0.98
B	3010	70	7.0	0.99
C	3448	64	6.0	0.9
D	3450	64	5.5	0.73

Examination of the degree-day factors for individual stakes highlights a lower degree-day factor attributed to stake B compared to stake A despite similar elevations. This variation is likely to be a result of increased topographic shading, as stake B was located *c.* 20 m from a bedrock ridge to the north and a steep ice fall located a similar distance to the west that likely resulted in the observed delayed removal of the snowpack at this location compared to stake A. The lower coefficient of determination for stake D was likely to result from the susceptibility of the location to snow drifting, as it was located upon an exposed, north-facing ridge. In addition, the presence of supraglacial debris close to stake D that was revealed after the removal of the snowpack may have also contributed to variability in melt rates.

Table 6.5: Degree-day factors (mm d⁻¹ °C⁻¹) for snow and ice at each ablation stake.

	<i>Stake A</i>	<i>Stake B</i>	<i>Stake C</i>	<i>Stake D</i>
Snow	7.3	6.7	5.1	2.4
Ice	10.6	8.6	9.8	8.6

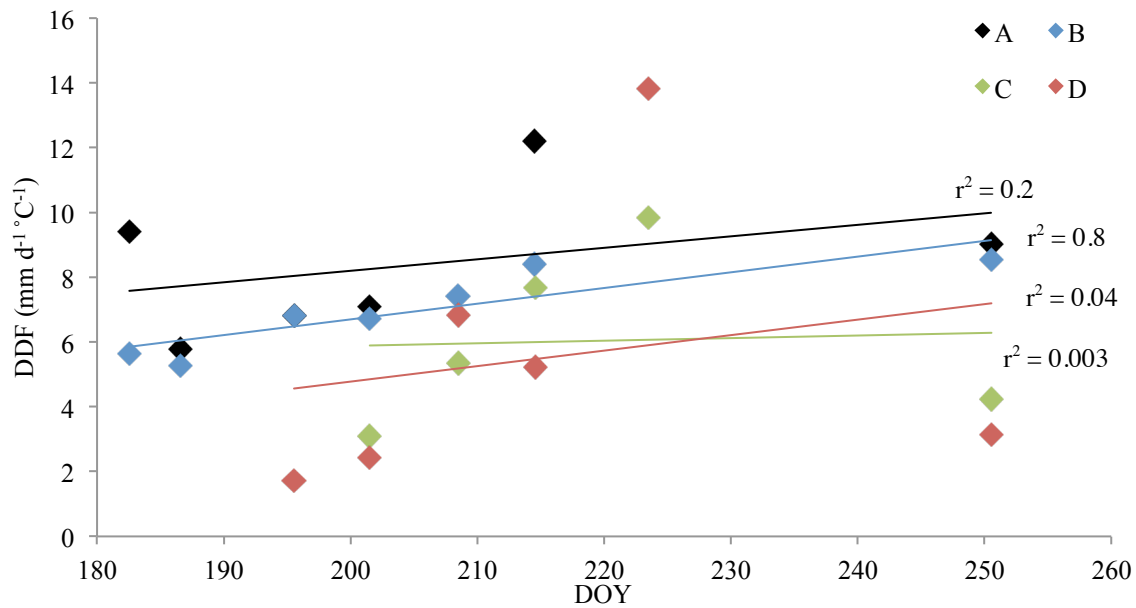


Figure 6.2: Trends in degree-day factors (DDF) at the four ablation stakes over the 2012 monitoring period indicating increasing trends at all stakes. Relationships were not significant at $p \leq 0.1$ except Stake B which was significant at $p \leq 0.05$.

The determination of degree-day factors for use in the runoff model from only four ablation stakes could result in the introduction of error into the model. Therefore, further optimisation of degree-day factors was achieved through the development of the runoff model. Fixed degree-day factors are not generally considered representative of the spatial and temporal variability in ablation rates (e.g. Hock, 1999; Huss *et al.*, 2008) (see Section 6.4.2). In order for the model to accurately simulate ablation whilst remaining physically based, it was necessary to account for changes in degree-day factors over the ablation season associated with changes in surface albedo due to the removal of surface snow cover. Figure 6.2 illustrates these changes as degree-day factors at stakes A and B (c. 3000 m asl) showed a moderate increasing trend over time (as a likely result of the rapid removal of the surface snowpack) whilst degree-day factors at stakes C and D (c. 3450 m asl) showed a weak increasing trend (as a likely result of the occasional replenishment and delayed removal of the snowpack at higher elevations). This variation is most often accounted for in runoff modelling through the

application of separate degree-day factors for snow and ice (Table 6.2) according to the location of the transient snowline. However, the determination of the snowline at the Feegletscher Nord was challenging owing to the complex topography and hypsometry, the inaccessibility of the glacier surface, infrequent snowfall at higher elevations, and the necessity to obtain field measurements of ablation from the Feegletscher Sud.

In order to develop a robust and physically based model capable of simulating runoff from the Feegletscher Nord, a range of degree-day factors were applied in light of the aforementioned observed values and temporal trends in degree-day factors. A range of degree-day factors were applied to calculate ablation in comparison to observed ablation (Table 6.6). These covered a range of possible values in addition to average observed values. In addition, in light of the rising trends in degree-day factors over the monitoring period and the uncertainty in snowline elevations, two sets of scaling degree-day factors were applied. These factors scaled linearly over time for the monitoring period, starting with the lowermost degree-day factor and increased at a constant rate over time. This approach is novel within the context of runoff modelling and follows the suggestion by Hock (2003) that varying model parameters as a function of time can reflect temporal trends in melt rates over the ablation season, as was observed at the Feegletscher Nord. The first set of scaling degree-day factors were determined from the observed linear trends in degree day factors at all stakes and ranged from 6.1 on day 180 to 7.7 mm d⁻¹ °C⁻¹ on day 251. The second set were determined from the observed trends at the elevations of the ablation stakes (3000 m asl and 3500 m asl) and ranged from 6.6 mm d⁻¹ °C⁻¹ on day 180 to 9.5 mm d⁻¹ °C⁻¹ on day 251 at 3000 m asl, and from 4.6 to 6.8 mm d⁻¹ °C⁻¹ at 3500 m asl over the same time period. The results suggested that fixed degree-day factors are unsuitable owing to the wide range of deviations at the individual stakes between predicted and observed

ablation. As expected, fixed degree-day factors based on averages from each stake produced the closest agreement, however, such an approach is not compatible with application in a spatially distributed runoff model. The degree-day factors that scaled over time produced broadly agreeable calculations of ablation despite some under and over-prediction at individual stakes and an overall over estimation of ablation. In light of the apparent capability of the scaling degree-day factors to simulate ablation and their enhanced physical basis compared to fixed factors in the absence of precise snowline locations, the ability and appropriateness of the degree-day factors was further explored through their application into a temperature-index runoff model (Table 6.7). Comparisons of daily modelled runoff and measured runoff revealed the scaling degree-day factors were able to simulate runoff with only slight over predictions. Therefore, further optimisation of the scaling degree-day factors was undertaken to establish the range of values that produced optimal simulations of ablation.

Table 6.6: Percentage of simulated ablation compared to measured ablation at each of the four ablation stakes for a range of degree-day factors (DDF). Relationships were significant at $p \leq 0.01$.

<i>DDF</i> ($mm\ d^{-1}$ $^{\circ}C^{-1}$)	4	5	6	7	8	9	<i>Individual</i> <i>Stake</i> <i>Average</i>	<i>All</i> <i>Stake</i> <i>Average</i>	<i>Scaling by</i> <i>elevation</i>	<i>Scaling</i>
A (%)	-55.8	-44.7	-33.7	-22.6	-11.5	-0.5	-7.4	-25.1	-6	-21.3
B (%)	-48.4	-35.5	-22.6	-9.7	3.2	16.1	-10.1	-12.7	9.4	-8.4
C (%)	-24.7	-5.8	13	31.8	50.7	35.5	13.7	27.5	16.1	35.5
D (%)	-20.2	-0.3	19.7	39.6	59.6	79.5	10.2	35	22.6	43.2
Σ (%)	-149.1	-86.3	-23.6	39.1	102	130.6	6.4	24.7	42.1	49
r^2	0.8	0.8	0.8	0.8	0.8	0.8	0.86	0.79	0.89	0.8

Table 6.7: Percentage of total daily modelled runoff compared to measured runoff (n = 45) for a range of degree-day factors (DDF). Note the stake mean DDFs (Table 6.6) cannot be applied in a spatially distributed model. Relationships were significant at $p \leq 0.001$.

<i>DDF</i>	4	5	6	7	8	9	<i>All stake Average</i>	<i>Scaling by elevation</i>	<i>Scaling</i>
Runoff (%)	-40.7	-25.8	-11	3.8	18.7	33.5	0.4	4.6	3.1
r^2	0.58	0.57	0.57	0.56	0.55	0.55	0.56	0.57	0.58
η^2	-1.9	-0.53	-0.05	-0.43	-1.7	-3.8	-0.26	-0.32	-0.28

The scaling degree-day factors were applied by elevation, with the first set of scaling degree-day factors applied at lower elevations of 2161 to 3200 m asl and the second to upper elevations of 3200 m asl to 4198 m asl. Degree-day factor values were varied close to the observed values and the performance of the factors was assessed through examination of their agreement with observed ablation and runoff, in addition to a range of summary statistics. Variance between the simulated and observed values was assessed through an F-test. Agreement with observed discharges was assessed through goodness-of-fit criteria including the coefficient of determination (r^2), and the Nash-Sutcliffe Efficiency criteria (η) (e.g. Legates & McCabe, 1999; Krause *et al.*, 2005) given as:

$$\eta^2 = 1 - \frac{\sum(Q_{calc} - Q_{obs})^2}{\sum(\bar{Q}_{obs} - Q_{obs})^2} \quad (6.4)$$

where Q_{calc} represents simulated discharge and Q_{obs} represents observed discharge. η^2 ranges from $-\infty$ to one. The advantage of the criteria is its ability to indicate whether the model performs better than the observed mean, determined by a value of zero (Legates & McCabe, 1999).

Table 6.8 indicates all variations of the scaling degree-day factors produced reasonable simulations of melt, particularly in comparison to the use of fixed degree-day factors, with daily runoff simulated to within $\pm 5\%$ of observed and coefficient of determinations were 0.57 or 0.58 (significant at $p \leq 0.001$). Upon further examination of the performance of the range of scaling degree-day factors, four sets of scaling degree-day factors were identified from their heightened accuracy, low variance and root mean square errors, and high Nash-Sutcliffe criteria that were further explored through their application in a runoff model at an hourly resolution (Table 6.9).

Table 6.8: Comparative summary of ablation and runoff simulation with a range of scaling degree-day factors applied according to glacier elevation. Lower elevations (L) were from 2161 m asl to 3200 m asl (39% glacier area). Higher elevations (H) were from 3200 m asl to 4198 m asl (61% glacier area). Percentage of ablation simulated at each stake (A – D) is indicated along with percentage of daily runoff and a range of summary statistics. Relationships were significant at $p \geq 0.001$.

Stake	L: 6.6-9.5 H: 4.6-6.8	L: 7-10 H: 4-6	L: 7-9 H: 4-6	L: 7-9 H: 3.5-6	L: 7.5-8.5 H: 3.5-6	L: 7.5-8.5 H: 3-6	L: 7.5-8.5 H: 4-6	L: 7.5-9 H: 3-6	L: 7-9 H: 3-6
A	-21.3	-0.8	-8.1	-8.1	-9.8	-9.8	-9.8	-6.2	-8.1
B	-8.4	15.4	7.1	7.1	5.1	5.1	5.1	9.3	7.1
C	35.5	2	2	-0.8	-0.9	-3.5	2	-3.5	-3.5
D	43.2	7.7	7.7	4.7	4.7	1.6	7.7	1.6	1.6
% runoff simulated	4.6	4.1	0.3	-1.5	-1	-2.8	0.8	-0.9	-3.2
F value	2.9	2.7	2.5	2.4	2.3	2.3	2.4	2.4	2.4
r ²	0.57	0.57	0.58	0.58	0.58	0.58	0.58	0.58	0.58
RMSE (% mean)	28.3	27.5	25.6	25.2	24.8	24.4	25.3	25	24.9
η^2	-0.33	-0.25	-0.086	-0.051	-0.019	0.01	-0.065	-0.04	-0.032

Table 6.9: Comparative summary of ablation and runoff simulation at hourly time-steps with the four sets of scaling degree-day factors identified in Table 6.8 applied similarly according to glacier elevation. Relationships were significant at $p \leq 0.001$.

	<i>L: 7-9</i> <i>H: 4-6</i>	<i>L: 7.5-8.5</i> <i>H: 3.5-6</i>	<i>L: 7.5-8.5</i> <i>H: 4-6</i>	<i>L: 7.5-9</i> <i>H: 3-6</i>
% hourly runoff	2.84	0.98	2.4	1.87
F value	3.2	3.04	3.1	3.08
r^2	0.68	0.679	0.677	0.681
RMSE (% mean)	45.2	43.5	44.7	43.9
η^2	-0.25	-0.17	-0.22	-0.18

Table 6.9 indicates the four identified sets of scaling degree-day factors were able to simulate hourly runoff to an accuracy ranging from 0.98 to 2.84% of observed which is high, particularly in the absence of runoff routing parameters (such as linear or dynamic reservoirs). Variance and root mean square errors increased significantly in comparison to the daily simulations in Table 6.8 which is unsurprising given the simple temperature-index approach (see Hock, 1999). Similarly, the values of the Nash-Sutcliffe criteria decreased, however, coefficients of determination increased compared to the daily simulations suggesting the suitability of the approach for high-resolution runoff simulation, despite some appreciable uncertainty in the range of simulated values. In light of the aforementioned results in Table 6.9, it is apparent that scaling degree-day factors of $7.5 - 8.5 \text{ mm d}^{-1} \text{ }^\circ\text{C}^{-1}$ at lower elevations and $3.5 - 6 \text{ mm d}^{-1} \text{ }^\circ\text{C}^{-1}$ at higher elevations (second column, Table 6.9) produced the most accurate and robust set of degree-day factors to simulate melt at hourly resolutions. Furthermore, despite some scatter, the identified scaling degree-day factors were able to account for the variance in observed ablation with a coefficient of determination of 0.9 (significant at $p \leq 0.001$) (Figure 6.3).

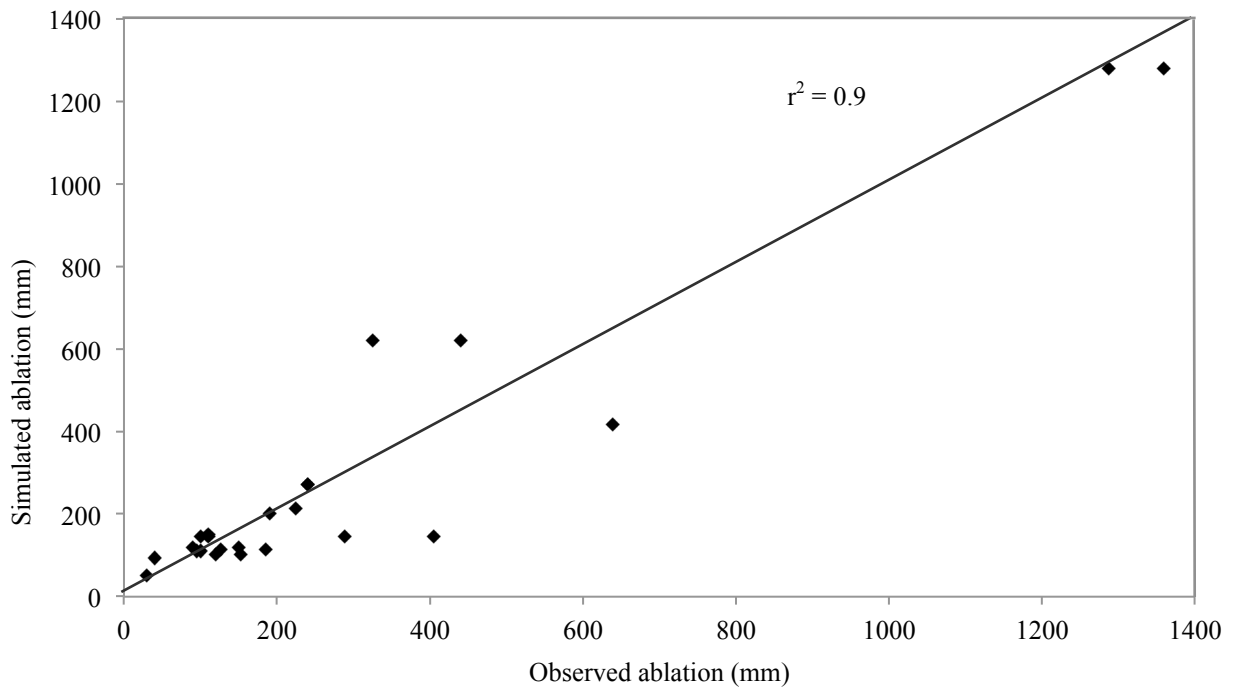


Figure 6.3: Plot of observed ablation and simulated ablation using optimised scaling degree-day factors. The 1:1 line is shown for clarity along with the regression coefficient. Relationship was significant at $p \leq 0.001$.

6.5.2 Modelled Runoff from the Feegletscher Nord

With the application of the optimised scaling degree-day factor into a spatially distributed temperature-index runoff model at an hourly resolution, the time-series of potential water available for runoff at the Feegletscher Nord is presented in Figure 6.4. The total proglacial discharge record is also included for comparison with the model performance. Qualitatively, the general trends in discharge are replicated well by the model and, despite the simple nature of the TIM approach, the diurnal variability in discharge is replicated, confirming that ablation processes are the dominant control on the patterns of discharge. However, whilst the patterns of discharge are replicated successfully, the magnitudes of modelled and predicted discharge show wider diurnal variability, despite being approximately centred upon similar average values suggesting broad agreement in the magnitudes of simulated and measured discharges. Glacial hydrological processes are a possible cause of the variability as modelled runoff will not immediately transfer to the portal and will instead be transferred through the glacier

hydrological system and associated storage reservoirs. The storage of water at a range of timescales within the glacier, as explored in Section 5.4, will generate delayed runoff responses to ablation. This is apparent from Figure 6.4 whereby predicted ablation is zero due to low overnight air temperatures and *c.* 0.9 cumec of runoff occurs. In addition, precipitation events are a possible cause of some of the observed variances, however, precipitation was generally light and infrequent and such a relationship is unsupported from the time-series of observed discharges (Figures 6.4 and 6.5).

When the time-series of simulated and measured runoff were explored further, a paired t-test showed no significant difference in the means of predicted and observed runoff ($p < 0.05$, $t = 0.18$). An F-test showed a significant difference between the variance of predicted and observed runoff ($F = 3.2$, $p < 0.01$) which is unsurprising given the qualitatively apparent variances between modelled and observed runoff. Furthermore, as W represents potential water available for runoff without consideration of travel time within and through the glacial hydrological system, this variance may be expected prior to the introduction of routing parameters within the runoff model. To establish meltwater transit times, cross-correlation undertaken in the previous chapter (Section 5.3) revealed Q follows W with an average lag of 1 hour over the ablation season. Examination of the lags of peak observed Q for individual days revealed a declining trend in lag time over the study period, suggesting an increase in the efficiency of the glacial hydrological system towards the end of the ablation season.

This diurnal variability was further explored by correlating the observed discharge and air temperature indices. Pearson correlations were undertaken between observed discharge and meteorological indices (Table 6.10). Minimum daily air temperature was found to correlate poorly to minimum or mean discharge, suggesting that factors other

than air temperature are responsible for driving discharge overnight. Interestingly, the total amount of global radiation during the preceding day was also found to correlate poorly to minimum discharge (in addition to mean and maximum discharges) suggesting that thermal energy storage in areas of exposed bedrock or from the surrounding slopes is not a significant driver of ablation. In light of the potential influence of precipitation on both runoff and ablation processes, examination of the regression residuals (Figure 6.5) displayed no strong association between higher magnitude residuals and rainfall events, however, the patterns in the residuals show strong variability.

Table 6.10: Pearson correlation coefficients between discharge and air temperature indices. Results that were not significant at $P < 0.1$ are shaded grey.

	<i>Q_{min}</i>	<i>Q_{mean}</i>	<i>Q_{max}</i>
<i>T_{min}</i>	0.225	0.221	0.269
<i>T_{max}</i>	0.541	0.506	0.449
<i>T_{mean}</i>	0.445	0.396	0.375
<i>TotGLR</i>	0.163	0.131	-0.002

When the total daily runoff volumes are considered (Figure 6.6.a) it is apparent that the model successfully predicts the longer-term trends in water volumes over the ablation season. However, the higher frequency of daily under-predictions is balanced by fewer larger magnitude over-predictions suggesting shorter-term sub-seasonal trends. This is clearer on Figure 6.6.c which shows the glacier water budget and indicates release from storage occurring early during the ablation season (DOY 196-205) which then becomes balanced by DOY 209 and is followed by a second period of water storage release which eventually balances by DOY 233. The implications of these results supports the findings of the hydrograph analysis undertaken in Section 5.4 and further suggests that significant storage is likely to be taking place within the Feegletscher at a range of temporal scales that requires consideration within the runoff model.

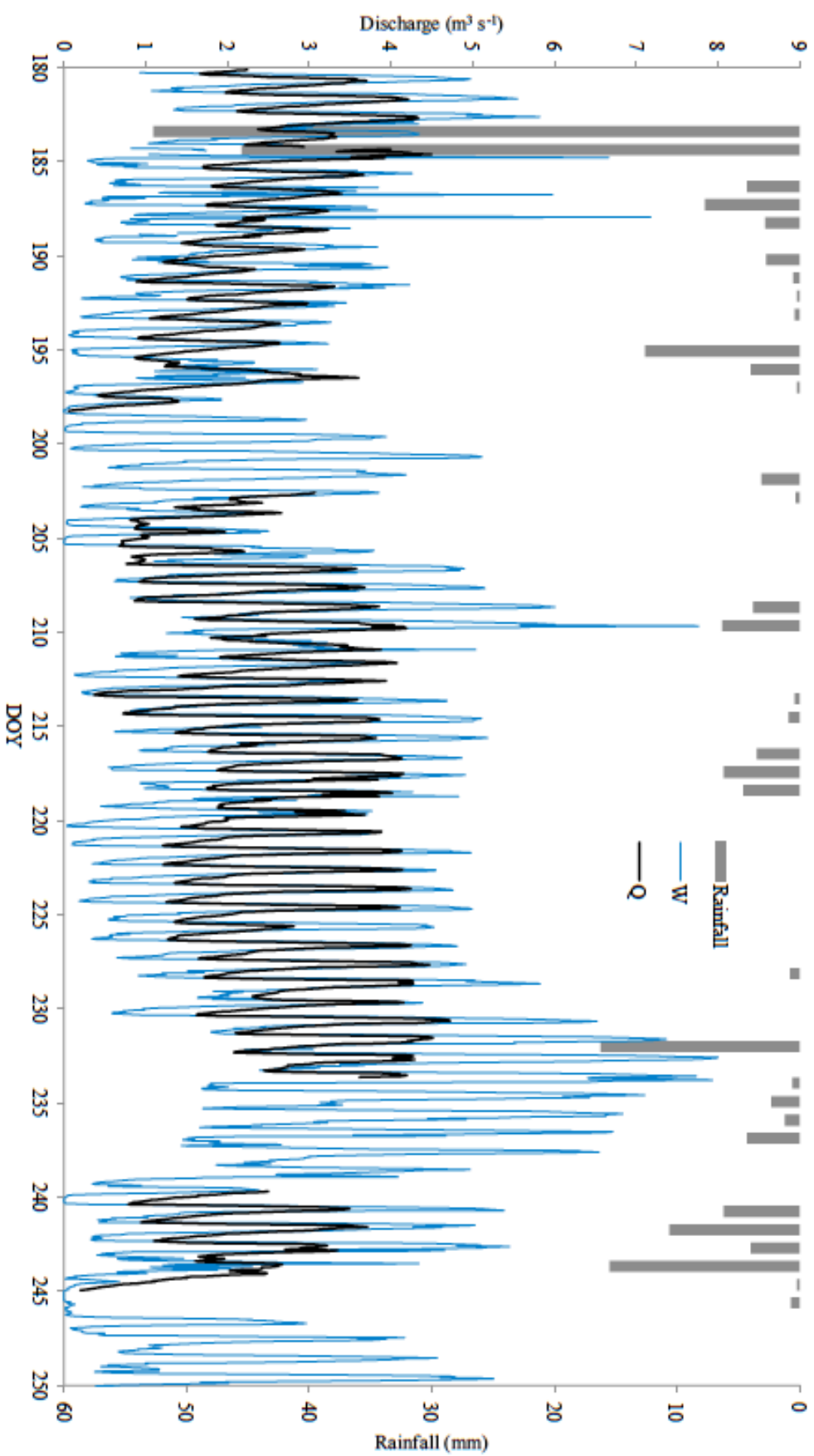


Figure 6.4: Time-series of hourly measured discharge (Q) and predicted potential runoff (W). The potential error in Q was $\pm 29.7\%$ and the uncertainty for W was $\pm 37.7\%$. Whilst the general pattern of W follows that of Q in the longer term, the diurnal amplitude for W remains much greater than Q . A significant precipitation event on DOY 184 has been removed from the discharge time-series for clarity.

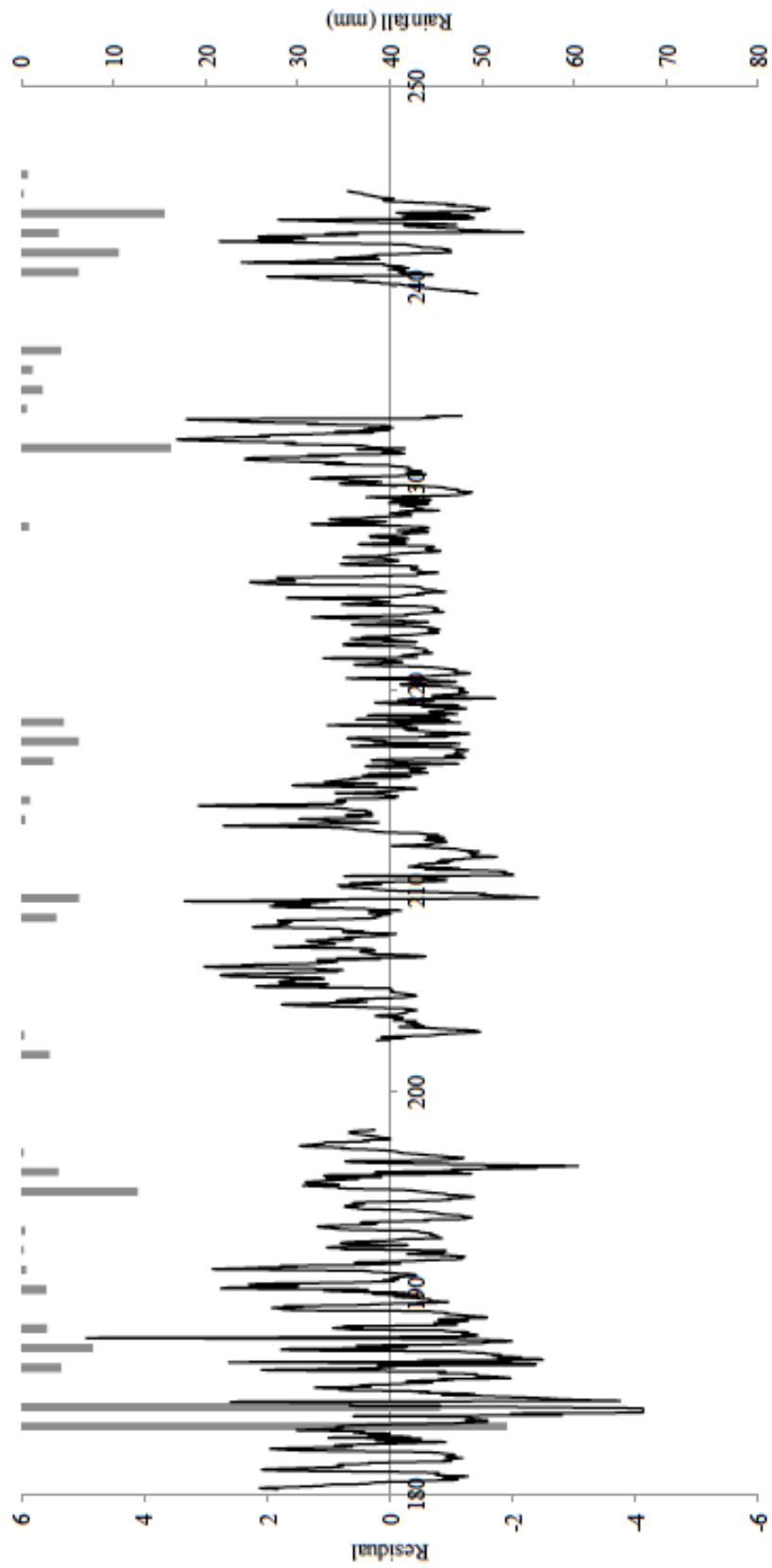


Figure 6.5: Plot of residuals in the OLS regression of measured runoff, simulated ablation and rainfall highlighting a lack of clear association between larger residuals and rainfall events although the trends are highly scattered.

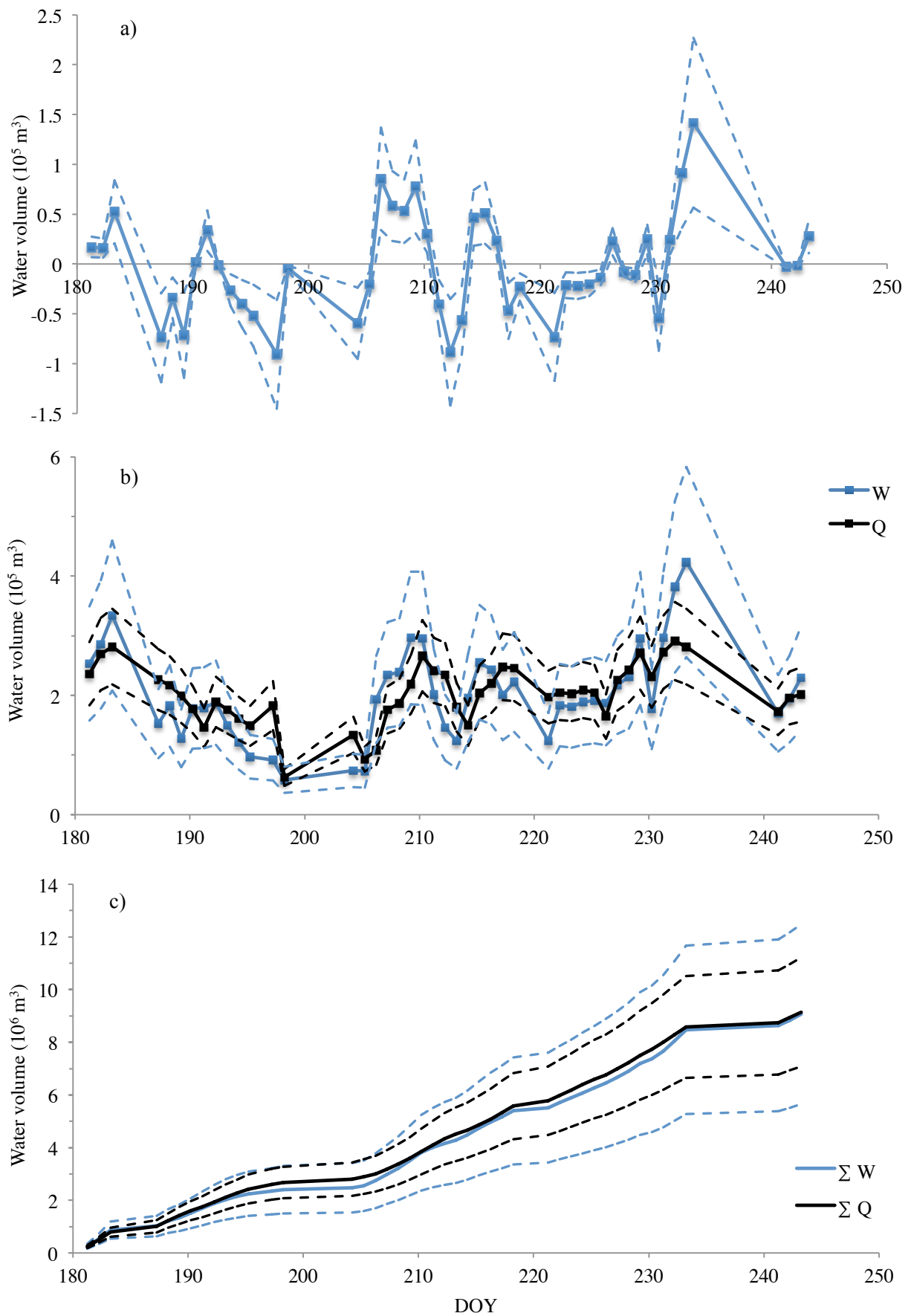


Figure 6.6: Time-series plots of a) daily water budget calculated as difference between calculated ablation and measured runoff, b) daily total discharge (Q) and simulated potential runoff (W), and c) the cumulative daily total discharge and simulated runoff. Dashed lines represent the maximum uncertainty limits for their respective series.

6.5.3 Meltwater Routing

The results of the initial modelling attempts indicated that the storage and release of meltwater is likely to be occurring within the Feegletscher Nord hydrological system and this water storage requires consideration within the modelling approach if discharge is to be successfully simulated. The discrepancies in the amplitudes of simulated and observed discharges (Figure 6.4) suggest the occurrence of diurnal storage and release processes whereby water becomes stored during periods of increased ablation and this water is subsequently released during melt minima. Such storage processes are likely to be a significant contributory factor in the weak Nash-Sutcliffe coefficient for the initial model output of potential runoff. In addition, longer term processes of storage and release are suggested from Figure 6.6c with two periods of model under-prediction occurring early and late in the ablation season. However, it should be noted that long-term agreement over the 2012 fieldwork period (DOY 180–250) between total simulated and observed discharge was a criteria used to assess the performance of the Feegletscher TIM during model optimisation (Section 6.5) and zero net water storage at DOY 180 is unlikely to be an accurate assumption.

It is well established that meltwater becomes stored within glaciers at a range of timescales during the ablation season (Richards *et al.*, 1996; Hubbard & Nienow, 1997; Fountain & Walder, 1998; Jansson *et al.*, 2003). This storage of water has been interpreted from hydrographs through the concept of storage reservoirs (e.g. Gurnell, 1993; Hannah & Gurnell, 2001) which has been undertaken in Section 5.4. Knowledge and understanding of storage reservoirs has subsequently been applied in glacier hydrological modelling to predict runoff by defining the storage and routing that occurs within the glacier between meltwater generation at the surface and discharge processes at the portal (Hannah & Gurnell, 2001). Storage reservoirs have been conceptualised and applied as a number of flow reservoirs (often one to four), analogous to physical

reservoirs of differing residence time (e.g. firn, snow, ice and groundwater) or to represent efficient or inefficient subglacial drainage competencies (e.g. Hock & Noetzli, 1997; Hock, 1999; Hannah & Gurnell, 2001; Farinotti *et al.*, 2011). This is most often achieved similar to Hock and Noetzli (1997) and Klok *et al.* (2001) whereby a discharge model is coupled with a melt model by to enable runoff to be determined according to the varying hydrological dynamics of the reservoirs, as defined by their storage coefficients (k -values), rates of recharge and throughflow velocities.

At the Feegletscher Nord, the observed differences in the water balance of Figure 6.6a and the results of the hydrograph recession analysis in Chapter 5 indicate the occurrence and dominance of short-term storage processes that result in the significant quantities of meltwater becoming stored within a range of possible reservoirs of relatively short residence time. Specifically, water appeared to be being stored in between two and three reservoirs with average storage coefficients of 19 to 27 hours. This storage appeared analogous to short term water storage and release within ice reservoirs or as part of a distributed drainage network. In light of this, it is suggested that the physical basis for a routing model of the Feegletscher Nord comprised of multiple discrete reservoirs that were analogous to storage in discrete reservoirs such as snow, firn and ice may be challenging to define and subsequently parameterise, due to the majority of storage occurring as relatively short-term storage (i.e. within the diurnal cycle), and therefore, coupled with ablation processes. In addition, the determination of the precise nature and characteristics of such reservoirs is challenging owing to the high degree of scatter in the observed storage coefficients along with inconclusive seasonal trends. This is exacerbated by the need to accurately simulate discharge within the diurnal cycle at a high temporal resolution in comparison with other modelling studies. In light of this, it is suggested that the physical basis for a routing model of the Feegletscher Nord comprised of multiple discrete reservoirs may not be well justified,

and instead, routing components that are a function of ablation may be better suited to account for what could be characterised as dynamic short-term storage processes.

Therefore, in order to account for short-term storage processes within the model, a simple aggregated reservoir routing model in the Feegletscher TIM was developed according to elevation whereby, potential runoff in each elevation band was assigned a k -value determining the proportions of direct or indirect runoff, which could be interpreted as runoff through either efficient or inefficient drainage systems, or runoff delayed to a degree due to storage in a range of reservoirs. These runoff proportions were then assigned lag times to represent the throughflow velocities, recharge rates and capacities of storage within the hydrological system of the glacier. As such, the approach possesses the ability to simulate the range of storage and runoff processes in a discharge model as determined from synthesis of the aggregated results from the hydrological analysis in Chapter 5 and the results of the potential runoff time-series whilst avoiding the determination of specific hydrological configurations and storage reservoirs that may not be well justified without support from further *in situ* evidence. Such an approach also significantly constrains the shortcomings of determining routing parameters through model optimisation alone, which would further lack physical justification.

The procedure for the determination of optimal reservoir characteristics was as follows: A fixed portion of potential runoff in the ten elevation bands was assigned as direct runoff or indirect runoff flow and a range of transit times were applied according to elevation (Table 6.11). Initial values were set arbitrarily at 70% direct runoff and 30% indirect runoff for all elevation bands. This was determined from the average difference between simulated runoff and observed discharge. Time-lags were varied from a lag of zero (the minimum dominant time-lag identified from cross-correlation

analysis in Section 5.3) to 23 hours (identified from hydrograph recession analysis results in Section 5.4). Permutations of quick and slow flow portions and time-lags for the reservoirs was varied and optimal combinations were determined systematically through examination of efficiency criteria (coefficient of determination and the Nash-Sutcliffe Efficiency criteria as per Section 6.5.1) with the constraints that both higher amounts of indirect flow occurred, and longer lag times exist at higher elevations.

Table 6.11 presents the resultant optimisation that assigned 90% of flow from elevation bands one through five as direct runoff which was transferred immediately through the drainage system, whilst elevation bands six to ten scaled from 60 to 40% direct runoff with corresponding time lags of one to five hours, representing delayed flow possibly as a result of the competence of the subglacial drainage network or increased storage within short-term reservoirs as suggested from the recession curve analysis in Section 5.4. The corresponding slow flows were assigned time lags of between six and 15 hours from the lowest to highest elevations, analogous to storage and release from possible ice and snow reservoirs of relatively short-term duration, as suggested from Section 5.4.

Table 6.11: Optimised routing parameters utilised in FTIM according to elevation bands within the model.

<i>Elevation Band</i>	<i>Elevation Range (m asl)</i>	<i>Glacier Area (%)</i>	<i>Direct Runoff (%)</i>	<i>Direct Runoff Time-lag (hours)</i>	<i>Delayed Runoff (%)</i>	<i>Delayed Runoff Time-lag (hours)</i>
1	2161-2425	1.9	90	0	10	6
2	2425-2688	3.5	90	0	10	7
3	2688-2872	6.0	90	0	10	8
4	2872-3040	11.9	90	0	10	9
5	3040-3199	16.1	90	0	10	10
6	3199-3367	16.2	60	1	40	11
7	3367-3535	17.0	60	2	40	12
8	3535-3718	14.0	50	3	50	13
9	3718-3942	8.5	50	4	50	14
10	3942-4197	4.9	40	5	60	15

The application of these routing parameters significantly improved the goodness of fit for the hourly time-series of simulated and observed runoff with the Nash-Sutcliffe coefficient increasing from -0.17 to 0.48. In contrast to the simulated potential runoff series, an F-test showed no significant variance between the new simulated and observed series ($F = 0.69$, $p < 0.01$) and a Pearson's t-test indicated no significant difference in the means of the two series ($p < 0.05$) further suggesting the suitability of the routing parameters. In addition, the effectiveness of the routing parameters was examined through comparison of the new routed runoff time-series to a one of derived from a linear regression between net storage (i.e. simulated potential runoff minus observed discharge) and simulated potential runoff (Figure 6.7), the physical basis for which is the increased subglacial storage of water as high water pressures from increased surface meltwater inputs force water into subglacial sediments adjacent to conduit margins and pore spaces at the ice-bedrock interface that is subsequently released as return flow when water pressures fall in response to reductions in ablation. The resultant regression enabled net water storage at each time-step to be simulated as a function of potential runoff and added or subtracted to the potential runoff time-series. Despite some disagreement around the hydrograph minima due to the regression equation intercept ($c = -1.28$), the simulated runoff series incorporating predicted net storage performed slightly better than the routed runoff series with a Nash-Sutcliffe coefficient of 0.68 compared to 0.48. When compared to simulated runoff with the routing parameters, this time-series demonstrates the suitability of the optimised routing parameters in generating a good agreement with observed discharge (Figure 6.8) with the routing coefficients resulting in a runoff model capable of simulating discharge to a high accuracy ($r^2 = 0.64$, $p \leq 0.001$). It is also apparent that the new simulated time-series with routing parameters successfully dampened the diurnal signal resulting in a qualitatively improved agreement with observed discharge, highlighting the importance

of short-term storage and runoff processes at the Feegletscher Nord. However, it must be noted that routing coefficients determined through model optimisation and the inverse approaches to hydrological investigations in Chapter 5 can only be cautiously interpreted in terms of the possible configuration and competence of the glacial hydrological network or in order to infer the physical basis for storage reservoirs.

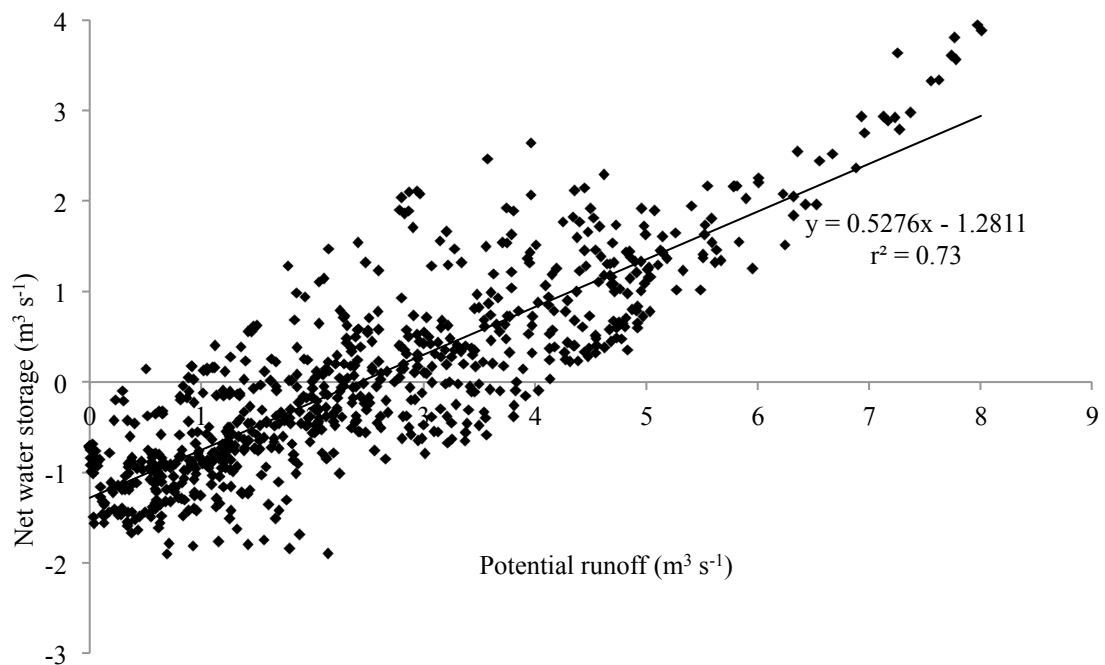


Figure 6.7: Plot of simulated potential runoff and net storage (simulated potential runoff minus discharge) indicating a strong relationship between water storage processes and ablation. Relationship was significant at $p \leq 0.001$.

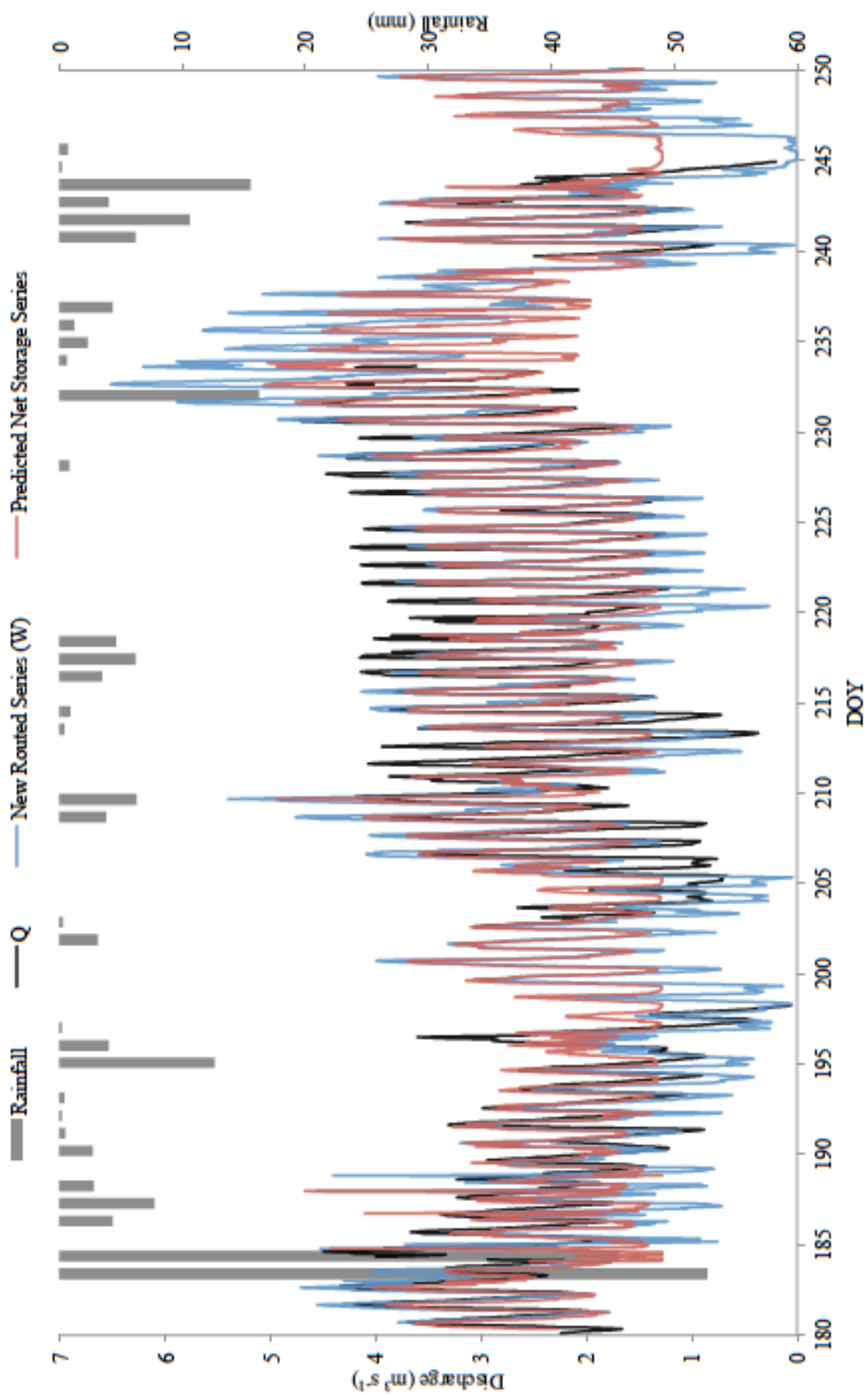


Figure 6.8: Time-series of optimised modelling runoff incorporating routing parameters (blue line) along with discharge time-series (black line) and a time-series of simulated runoff incorporating predicted net storage (red line) along with precipitation.

This chapter has presented the development of a temperature-index runoff model for the Feegletscher Nord capable of simulating runoff at an hourly resolution with modest data inputs, comprising temperature and precipitation. The model was calibrated against field data obtained during the 2012 ablation season and this field data, along with hydrological data analysis undertaken in the previous chapters, has shown the calibrated model parameters to be valid and realistic. The application of the model with 2012 field data demonstrated robust performance, with around 90% of the variance in ablation simulated and around 64% of the variance in hourly discharge accounted for. In addition, the model simulated total runoff over the 2012 field season to within < 3 %. Furthermore, the variance and averages of the simulated runoff time-series were shown to be indifferent to those of the measured time-series with > 95% confidence. However, it is acknowledged that total potential errors in the simulated time-series were modest. These were principally associated with field data collection. For example, it is apparent that moderate errors were introduced through the determination of degree-day factors from the use of only four ablation stakes at two elevations. However, in light of the aim of this research to develop a robust and physically-based runoff model, known errors associated with parameters determined from *in situ* field data are preferable to those associated with parameters optimised against goodness-of-fit criteria during model development, or those associated with the use of *ex situ* values. In addition, some evidence was found that associated poor model performance with rainfall events, which would be unsurprising given the complex interactions between precipitation, ablation and runoff, particularly at a steep and topographically varied glacier.

The model represents an advancement in temperature-index modelling attempts, in particular, through the capability of the model in simulating the diurnal cycles in melt

and runoff without the need for additional model parameters such as radiation components (e.g. Hock, 1999). In addition, the application of spatially distributed degree-day factors that scale over the ablation season was found to significantly improve the model performance whilst overcoming the drawbacks of fixed degree-day factors that were shown to be unsuitable for application at the Feegletscher Nord due to wide spatial and temporal variability. This approach ameliorated the need for precise snowline elevations and this is likely to be an advancement for ablation modelling of glaciers with complex topography and surface conditions associated with deglaciation.

The use of a two-component runoff routing model to simulate quantities and throughflow times of meltwater as quick or delayed flow was found to be effective in accounting for diurnal meltwater storage and throughflow. This was based on the synthesis of a range of hydrological analyses. However, this routing method did not account for storage that occurred at longer timescales, this was due to the lack of consistent identification of longer-term storage processes, despite hydrograph recession analysis in the previous chapter and the comparisons of simulated and measured runoff presented here. Further work to explore the relative merits of this approach in comparison to the use of linear reservoir approaches is advocated for future research.

7 Glacio-Fluvial Suspended Sediment Transfer and Deglaciation

7.1 Introduction

In Chapter 5, the controls on, and nature of, suspended sediment transfer patterns and magnitudes at the Feegletscher Nord were explored through detailed examination of discharge and suspended sediment concentration records in addition to meteorological influences. A strong dependence of proglacial SSC on discharge forcing was found with a seasonal increase and downstream decrease in suspended sediment loads. These findings are comparable to the range of empirical observations and theoretical expectations of processes of glacio-fluvial sediment transfer processes at temperate Alpine glaciers (e.g. Hallet *et al.*, 1996; Alley *et al.*, 1997; Swift *et al.*, 2005a). However, observations of seasonal increases in sediment availability are unusual as sediment availability is typically either constant or experiences short-duration increases (Gurnell, 1995; Clifford *et al.*, 1995; Hodson *et al.*, 1998; Hodgkins *et al.*, 2003; Swift *et al.*, 2005b), which raises questions as to the possible causes of such an unusual increase. In addition, spatial variability between the SSC patterns observed at the monitoring stations was found, suggesting proglacial modification of SSC patterns, particularly at Station C. Such findings draw interesting comparisons to studies that have demonstrated proglacial controls on suspended sediment transfer in relation to surface age (Orwin & Smart, 2004b), however, differences in the nature of the proglacial controls at the Feegletscher Nord were found at proglacial locations that are assumed to have been deglaciated for similar amounts of time, which raises questions as to the forefield processes and characteristics that resulted in these sediment transfer patterns. These observations from the Feegletscher Nord forefield were hypothesised to be related to in-channel and channel-marginal sediment availability. In deglaciating environments these in-channel and channel-marginal influences are expected to be

controlled by the rate of paraglacial sedimentation, operating over the ‘paraglacial period’ (Church & Ryder, 1972) with resultant impacts on suspended sediment yields. However, the notion of a ‘paraglacial period’ has proven difficult to define and demonstrate due to a range of apparently complex links between suspended sediment yield and sediment transfer processes within deglaciated environments (e.g. Orwin & Smart, 2004a; Etienne *et al.*, 2008; Porter *et al.*, 2010). In particular, it is the processes controlling the storage and release of sediments in forefields by glacio-fluvial reworking and redistribution (e.g. Warburton, 1990; Hodson *et al.*, 1998; Hodgkins *et al.*, 2003; Orwin & Smart, 2004a; Geilhausen *et al.*, 2013; Leggat *et al.*, 2015) that are unclear and require attention if suspended sediment yields and the downstream impacts of deglaciation are to be understood (e.g. Murray *et al.*, 1993; Hay, 1998; Syvitski, 2002; Raiswell *et al.*, 2006; Sugden *et al.*, 2009; Bhatia *et al.*, 2013; Hood *et al.*, 2015). Given the possible reworking of sediments in the proglacial zone at the Feegletscher Nord by glacio-fluvial processes (Curry *et al.*, 2009; Hampel, 2009; Cook *et al.*, 2013), there is a compelling need to explore and characterise these sediment transfer processes in light of recent and future deglaciation and the potential resultant geomorphological, glacial and hydrological activity.

In this chapter, a range of multivariate techniques are applied to field data obtained from a network of spatially distributed discharge and suspended sediment gauging stations installed at the Feegletscher Nord proglacial zone during 2012 with the overarching aim of exploring and characterising processes of sediment mobilisation, transfer and storage that determine proglacial suspended sediment concentrations. Specifically, the development of multivariate regression models are presented in section 7.2 and discussed. The basis for this approach is outlined in section 7.2 with the results presented in sections 7.3 and 7.4. This is followed in section 7.5 by the development

and application of an exploratory forward SSC modelling approach, which builds upon the development of a temperature-index runoff model for the Feegletscher Nord in Chapter 7. Future potential changes in suspended sediment concentrations and loads driven by the characterised glacio-fluvial sediment transfer processes are explored according to future meltwater runoff regimes associated with predicted meteorological and glacier changes through the 21st Century.

7.2 Outline to approach

Section 2.3 illustrated how the transfer of sediments in suspension through glaciated catchments is strongly dependent on the transfer of meltwater through a subglacial drainage system, which has access to the glacier bed. However, as discussed in section 2.3.4, the proglacial zone is a potential source of significant variability in the temporal and spatial patterns of sediment transfer. Environments that have recently become ice-free have the potential to experience a range of enhanced geomorphological activity associated with deglaciation. This enhanced and glacially-conditioned activity has been termed ‘paraglacial’ (Church & Ryder, 1972; Ballantyne, 2002a). Furthermore, processes of sediment production and storage in proglacial channels have been documented to occur at a range of timescales with implications for suspended sediment yields (e.g. Gurnell, 1982; Warburton, 1990; Gurnell *et al.*, 1994; Willis *et al.*, 1996; Hodson & Ferguson, 1999; Hodgkins *et al.*, 2003; Richards & Moore, 2003; Orwin & Smart, 2004a; Baewert & Morche, 2014; Marren & Toomath, 2014; Leggat *et al.*, 2015). In light of the principal aim of this research to accurately assess the controls on proglacial SSC, there is a need to examine the nature of SSC transfer and the controls exerted on SSC by discharge with an integrated approach that accounts for potential glacio-fluvial-slope linkages, which have the potential to modify the SSC-Q relationship. Analytical approaches to the investigation of SSC transfer are typically inverse, owing to the inaccessibility of the subglacial environment. Therefore, in section

7.3, the potential controls by discharge on proglacial SSC at a range of timescales are investigated through the use of multivariate regression models constructed with discharge-based predictor variables (e.g. Willis *et al.*, 1996; Hodgkins, 1999; Hodson & Ferguson, 1999; Richards & Moore, 2003; Irvine-Fynn *et al.*, 2005a). Such studies have demonstrated that changes in sediment supply and availability can be incorporated into regression models of proglacial SSC through the use of hydrological predictor variables including:

- Instantaneous discharge Q , can be used to account for instantaneous forcing of SSC (e.g. Hodson & Ferguson, 1999).
- The rate of change of discharge ΔQ can be used to account for short-term (diurnal) sediment supply variability. This is obtained by subtracting previous discharge values from current values (e.g. Willis *et al.*, 1996).
- Q^2 can be used to account for non-linearity between SSC and Q , whereby small increases in Q result in large changes in SSC due to the rapid entrainment of available sediment (e.g. Irvine-Fynn *et al.*, 2005a). This can result from in channel entrainment and mobilisation when high sediment availability exists, or may be a result of channel bank erosion and mobilisation associated with increases in hydraulic radius and turbulent flow.
- Medium-term variability can be accounted for by calculating the time since discharge was last equalled or exceeded ($hQ!$), to account for the entrainment of previously sequestered sediment during high flows (e.g. Hodgkins, 1999).
- Cumulative discharge ΣQ during the study period was used as a surrogate for seasonal sediment supply variations to account for the exhaustion of sediment supplies by fluvial evacuation over the ablation season (e.g. Richards & Moore, 2003).

Furthermore, the use of multivariate regression models can enable the identification of non-fluvial or -glacial controls on suspended sediment concentrations through examination of the model residual time-series. For example, thaw-related extra-glacial sediment mobilisation processes (e.g. Irvine-Fynn *et al.*, 2005a; Porter *et al.*, 2010) may be suggested from associations between high model residuals and air temperature. Also, the mobilisation of fine extra-channel sediments by rainfall (e.g. Richards, 1984; Orwin & Smart, 2004b; Liermann *et al.*, 2012; Diodato *et al.*, 2013) can be revealed through residual associations with precipitation, in addition to hysteresis relationships.

7.3 Suspended Sediment and Discharge Relationships

Despite the strong association between discharge and suspended sediment concentrations, the relationship between SSC and Q at Stations B, C and D is scattered over the 2012 monitoring season. In particular, the records for Stations B and C demonstrate strong non-linear relationships at higher discharges. To account for this heteroscedasticity, a logarithmic transformation (\log_{10}) was applied to the raw discharge and SSC series prior to further analysis (e.g. Richards, 1984; Gurnell, 1987; Hodgkins, 1999; Hodson & Ferguson, 1999; Irvine-Fynn *et al.*, 2005a; Haritashya *et al.*, 2010). This was considered to be an appropriate transformation as it significantly improved the normality of the ordinary least squares (OLS) regression residuals. Simple linear regression models were applied to the transformed SSC and Q time-series for the selected sub-periods highlighted by the PCA and CA procedures (Table 7.1). These periods comprised:

- DOY 203 – 231 at Stations B and C to examine the longer-term controls on proglacial SSC during the ablation season and their spatial variation within the proglacial zone;

- DOY 203 – 216 at Stations B and C to examine controls during the first subseason identified by the PCA and CA, abbreviated as S1;
- DOY 217 – 231 at Stations B and C to examine the second subseason, S2;
- DOY 215 to 221 at Stations B, C and D to examine spatial variations in the range of controls on proglacial SSC operating throughout the proglacial zone;
- DOY 185 – 197 at Station D to examine early ablation season controls on proglacial SSC;
- DOY 209 at Stations B and C to identify and examine the range of controls on SSC during this high SSL magnitude event identified by the PCA and CA procedures;
- DOY 214 at Stations B and C to identify and examine the range of controls on SSC during this high SSL magnitude event identified by the PCA and CA;
- DOY 219 at Stations B and C to examine the possible controls on SSC resulting in an irregular SSC curve shape at Station B.

The linear regression models revealed that changes in SSC are moderately associated with discharge variability at a range of timescales, with the exception of DOY 219 at Station B where the relationship was not significant, likely due to rainfall (Table 7.1). Discharge accounted for 36% and 23% of the seasonal variance in SSC over the monitoring period at Stations B and C respectively. The period DOY 185-197 at Station D experienced the weakest relationship between $\log Q$ and $\log SSC$. The presence of autocorrelation was tested using the Durbin-Watson statistic, which tests the correlation in the residuals, and suggested autocorrelation was present in the residuals of these simple regression models. This is a common problem in the use of simple linear regression models of SSC and Q (Fenn *et al.*, 1985; Fenn, 1989; Hodgkins, 1999). To further examine the controls on proglacial SSC and the spatial variability, these simple

regression models were supplemented with additional discharge-based predictor variables.

The simple linear regression relationships in Table 7.1 indicate that discharge is unlikely to be the sole driver of the observed variance in SSC. This is supported by the results of Chapter 5 that suggested the variability in the SSC data series is not an instantaneous response to discharge. As discussed in section 7.2, multivariate regression models (MRMs) constructed with discharge-based predictors can be used to explore changes in sediment supply and availability within subglacial and proglacial channels. Sub-periods for MRM analysis were selected based on the findings of the principle components analysis (PCA) and cluster analysis (CA) presented in Chapter 5. It was necessary to attain linearity in the data-sets to reduce heteroscedasticity which was achieved by a logarithmic (\log_{10}) transformation of the raw SSC and Q data. In addition, the discharge-based variables were shifted to match the lag or lead between SSC and Q identified by cross-correlation analysis for the individual time-periods under consideration. Unexplained variance in SSC has been explored through the use of autoregressive techniques (e.g. Gurnell & Fenn, 1984; Willis *et al.*, 1996; Hodgkins, 1999), lagged SSC predictor variables (e.g. Hodson & Ferguson, 1999; Swift *et al.*, 2005b), and examination of model residuals (e.g. Clifford *et al.*, 1995; Swift *et al.*, 2005b). In rationalising the approaches for accounting for autoregressive and stochastic SSC behaviour, models that were easily physically interpretable were required in order to assess the potential range of sediment transfer processes in operation and their possible causes through examination of the residual time-series (e.g. Swift *et al.*, 2005b). In addition, the use of lagged SSC values as predictors was an approach considered incompatible with the subsequent use of these regression relationships in simulating potential future suspended sediment concentrations and loads later in this chapter. However, it is acknowledged that, despite the use of lagged discharge data,

autocorrelation remained present in the residual series, the presence of which was confirmed through the incorporation of a time-series of previous 10-min SSC values, which found that previous high SSC values result in high SSC at short time-scales. Best-subsets regression was used to identify the predictors included in each model (e.g. Hodson & Ferguson, 1999), as this technique assesses all possible combinations of predictors along with their summary statistics (coefficients of determination and p -values).

Table 7.1: Simple regression models of proglacial SSC. Table shows the number of observation (n), regression coefficients of determination and $\log Q$ predictor coefficients for each station for the selected sub-periods in addition to the regression constant k . The Durbin-Watson ($D-W$) statistic is shown for each regression. Italic entries highlight non-significant variables at $p \leq 0.05$.

Location	Period	n	r^2	k	$\log Q$	$D-W$
B	203-231	22331	0.36	-0.98	0.34	0.0019
	S1	9663	0.36	-1.1	0.42	0.0023
	S2	11012	0.31	-0.63	0.3	8.2×10^{-4}
	209	720	0.35	-0.67	2.3	0.0035
	214	720	0.57	0.44	0.61	0.0023
	219	720	0	-0.75	<i>-0.0064</i>	0.0015
	215-221	5040	0.19	-0.63	0.31	4.8×10^{-4}
C	203-231	22331	0.23	-0.72	0.46	0.0035
	S1	9663	0.36	-0.63	0.52	0.0069
	S2	11012	0.51	-0.99	1.2	0.0035
	209	720	0.44	-0.68	1.4	0.0029
	214	720	0.42	-0.46	0.71	0.004
	219	720	0.67	-0.77	0.19	0.0081
	215-221	5040	0.28	-0.83	0.87	0.0018
D	185-197	9151	0.11	-1.2	0.17	0.009
	215-221	5040	0.57	-1.1	0.86	7.6×10^{-4}

All periods show a significant improvement in the coefficients of determination in the multivariate regression models, in addition to a decrease in the presence of autocorrelation indicated by the Durbin-Watson statistics, however, positive serial autocorrelation remains present (Table 7.2).

Table 7.2: Multivariate regression models of proglacial SSC constructed with discharge-based predictor variables. Table shows MRM coefficients of determination and predictor coefficients for each station along with their t-statistics (t-stat) for the selected sub-periods in addition to the regression constant *k*. Bold entries show the most significant predictor in each MRM. Blank entries indicate non-significant variables at $p \leq 0.05$. The Durbin-Watson (*D-W*) statistic is shown for each regression. Number of observations is the same as in Table 7.1.

Location	Period	R ²	k	log Q	t-stat	ΔQ	t-stat	Q ²	t-stat	hQ!	t-stat	ΣQ	t-stat	D-W
B	203-231	0.57	-1.1	-0.092	-15			0.27	93.6	-0.00021	-2.6	1.3E-07	84.7	0.0073
	S1	0.72	-1.3	-0.22	-17.7			0.29	64	-0.00057	-2.1	4.6E-07	106.6	0.0093
	S2	0.69	-1.2	-0.13	-24.8	0.28	4.3	0.27	98.2	0.00026	4.5	1.7E-07	55.5	0.0054
	209	0.5	1.6	5.8	9.2			-0.61	-5.5	-0.0028	-2.1	-3.5E-06	-14.6	0.011
	214	0.86	-2.7	-0.098	-3.9	5	5.7	0.034	33.3	0.0027	3.4	0.000022	14.5	0.076
	219	0.75	0.12	-0.87	-43.4	-1.7	-2.7	0.38	45.2	0.00089	2	-9.9E-07	-9.4	0.024
215-221	0.45	-0.47	-0.32	-19.8			0.29	39.4	-0.0014	-7.3	-4E-07	-29.2	0.0047	
C	203-231	0.51	-0.79	0.073	10	-0.08	-2.1	0.077	97	-0.0018	-11.1	-7E-08	-51.7	0.013
	S1	0.66	-0.94	0.052	6.5			0.078	62.3	-0.0023	-8.4	2.2E-07	52.3	0.013
	S2	0.66	-0.88	-1.4	-35.5			0.14	70	-0.001	-7.5			0.016
	209	0.6	-0.47	-0.78	-4.9			0.15	13.9	-0.0096	-3.7	-4.7E-07	-2.7	0.033
	214	0.56	-3	-0.67	-6.9	7.1	4.5	0.14	14.7			0.000002	0.2	0.03
	219	0.58	0.65	-2.2	-24.9	-1.5	-3.6	0.15	26.4	0.0014	3	-7.1E-07	15.1	0.042
215-221	0.52	-0.27	-0.5	-7.5			0.082	21	-0.0012	-6.9	-3E-07	-38.9	0.014	
D	185-197	0.57	-1.3	-0.27	-34.1			0.037	79.5	-0.00081	-15.5	6E-08	57.3	0.05
	215-221	0.84	-0.54	-1.2	-53.9			0.061	94.5			-6E-08	-29.9	0.0039

The seasonal and subseasonal trends revealed by the MRMs highlight the positive coefficients and dominance of Q^2 as a strong predictor of SSC (Table 7.2). This indicates that small increases in discharge result in a larger and non-linear increase in SSC. This is interpreted to indicate high sediment availability while the lack of spatial variability in the strength and nature of this predictor suggests this availability can be (at least partly) attributed to the presence of a single source of sediment which was readily mobilised without significant depletion over the monitoring period. In addition, as small increases in discharge result in increases in the hydraulic radius, this may result in greater-than-linear increases in SSC which is mobilised in-channel at the banks due to the turbulent flow (e.g. Irvine-Fynn *et al.*, 2005a). The general failure and weakness of ΔQ as a predictor in the MRMs suggests a lack of diurnal hysteresis. This result was surprising given the strong diurnal variation observed in the raw data series and may arise from best-matching the SSC time series to discharge through cross-correlation analysis. This possibility makes the interpretation of diurnal sediment supply variability from the MRMs challenging. However, it is noteworthy that such a finding is unusual due to the temperate thermal regime of the Feegletscher and is similar to findings in Arctic basins (e.g. Hodgkins, 1999; Hodson & Ferguson, 1999; Irvine-Fynn *et al.*, 2005a) whereby weak, negative or insignificant coefficients for ΔQ have been reported for glaciers with non-temperate thermal structures and interpreted as reflecting complex SSC responses to discharge. The presence of non-glacial sediment transfer processes in the proglacial zone may be a possible cause of the apparent complex SSC response to discharge. A possible mechanism may be the stochastic delivery of sediments to the channel through channel-bank collapse which has been observed to occur in the streams in the vicinity of Station C (Hampel, 2009). A subseasonal trend in SSC variability in the MRMs is apparent, whereby coefficients of ΣQ are generally positive earlier in the ablation season and negative later in the season indicating an early season increase in

SSC followed by exhaustion. However, spatial variability exists in these trends with Station B generally experiencing an unusual seasonal increase in SSC, whilst Station C shows a seasonal decrease in SSC. The positive coefficient for $\log Q$ at Station C indicates SSC sediment mobilisation and transfer results from discharge forcing and suggests the presence of in-channel or channel marginal sediment sources which are readily entrained by high discharges, suggesting increases in discharge are associated with increases in the suspended sediment load and total sediment yield (e.g. Swift *et al.*, 2005b). A possible mechanism for this is in-channel sediment entrainment due to bank collapse which has been observed at this location (Hampel, 2009). In addition, this was directly observed during the two storm events during the 2012 ablation season whereby evidence of significant undercutting and collapse of channel banks was observed at Station C with sediment deposition downstream of Station C in the vicinity of the lower proglacial lake. Conversely, there was no discernible change in channel morphology or surfaces in the stream at Station B from these two events. The negative coefficients for $\log Q$ experienced at Stations B and D suggest that a more complex response where sediment mobilisation did not occur as an instantaneous response to discharge and may suggest the reduced availability of easily mobilised sediments. Similar findings have been interpreted by others as a dilution effect indicative of limited or easily exhausted sediment sources (e.g. Irvine-Fynn *et al.*, 2005a). The synthesis of these results suggests that spatial differences in sediment availability exist within the proglacial zone. The possible causes for the results from Stations B and D include the rapid exhaustion of in-channel or channel-marginal sediments in the streams, increased surface armouring at these locations, or a paucity of easily entrainable fine material. However, whilst the results suggest high sediment availability and in-channel or channel-marginal sediment transfer processes at Station C, it is clear from the MRMs that a complex range of controls on sediment transfer were in operation at this location, particularly later in the

ablation season. To further elucidate the controls on proglacial sediment transfer, results from the MRMs for selected subperiods are interpreted and discussed.

For the period DOY 215-221, the significant predictors at both stations B and C (in order of significance) were Q^2 , ΣQ , $\log Q$, and hQ' . The strong positive coefficient for Q^2 suggests either effective in-channel and channel-marginal sediment mobilisation or high subglacial sediment mobilisation and evacuation as high flows tap stored sediments. The negative coefficients for $\log Q$, and hQ' indicate neither high flows nor the length of time since a comparable discharge were responsible for increases in SSCs. The failure of ΔQ as a predictor indicates a lack of diurnal hysteresis and limited diurnal sediment supply variability. These results suggest limited in-channel sediment availability in the proglacial zone, possibly as a result of exhaustion. For the same period, the significant predictors at stations D (in order of significance) were Q^2 , $\log Q$, and ΣQ implying a simpler range of controls on downstream SSC. Interestingly, the strong negative coefficient for $\log Q$ suggests a dilution effect may be more pronounced further downstream in the proglacial zone or may be the result of sediment accumulation and storage within the proglacial zone. This may arise from the lower proglacial lake acting a store between Station D and Stations B and C. When this is compared to the early season MRM from DOY 185-197 at Station D, the significant predictors (in order of significance) were Q^2 , ΣQ , $\log Q$, and hQ' highlighting a strong seasonal decrease in SSC suggesting high sediment availability early in the ablation season.

DOY 209 was analysed due to high suspended sediment loads on this day. At Station B, the significant predictors (in order of significance) were $\log Q$, ΣQ , Q^2 , and hQ' . The strong positive coefficient for $\log Q$ indicates that SSC was primarily the result

of instantaneous forcing by discharge. For the same period at Station C, Q^2 was found to be the main driver of SSC indicating that SSC responded non-linearly to increases in discharge which, in light of the dominance of discharge at Station B, may suggest that SSC at stream C experienced high availability of in-channel or channel-marginal sediments which resulted in a greater-than-linear increase in SSC at this location compared to Station B.

DOY 214 was analysed to ascertain the controls and processes resulting in high SSL. At Station B, the significant predictors (in order of significance) were Q^2 , ΣQ , ΔQ , $\log Q$, and hQ' . The strong positive coefficients for Q^2 , ΔQ , and hQ' indicate that increases in discharge during the rising hydrograph limb resulted in greater-than-linear increases in SSC which likely resulted from exceptionally high sediment availability from glacial sources (as suggested by the positive coefficient for ΣQ) and in-channel sources (as suggested by ΔQ). Similarly, at Station C, the dominance of Q^2 and the strong positive coefficient for ΔQ suggests the high availability of sediment which was mobilised during rising discharges resulted in the high SSL observed.

Day 219 was analysed to explore the possible causes of irregular SSC curve shapes, particularly at Station B, and the influence of rainfall on the controls on SSC. Both stations B and C were dominated by a positive coefficient for Q^2 suggesting rapid entrainment of readily-mobile sediments. However, the negative coefficient for $\log Q$ suggests that high discharges did not necessarily result in high SSCs and this may point to the influence of rainfall mobilising extra-channel sediment sources. Furthermore, the coefficient for $\log Q$ is significantly greater at Station C than B suggesting this effect may be more pronounced at Station C.

In summary, it is apparent from the MRMs for the seasonal and selected periods that Station B experienced higher coefficients of determination compared to Station C. This suggests that the controls on SSC at Station B are better accounted for by the discharge-based predictor variables than at Station C whereby a more complex response exists that may result from the presence of sediment transfer processes that are not discharge dependent, such as those associated with input from channel-margins and adjacent surfaces. Q^2 was found to be a strong positive predictor for SSC at both stations suggesting that small increases in discharge resulted in a greater non-linear increase in SSC. The comparisons between models of different time scales did not reveal significant differences in the range of controls, however, DOY 209 at Station B showed an unusually strong SSC response to $\log Q$.

In light of the general similarities in the seasonal controls on proglacial SSC at Stations B and C and the aim of developing an exploratory forward model for SSC from the Feegletscher Nord, observations of SSC and Stations B and C were pooled in order to create a single multivariate model of total proglacial SSC. Total suspended sediment load and runoff at Stations B and C were calculated from the observations for DOY 203 – 231 which were then summed at each time-step in order to create a time-series of total proglacial SSC and discharge. Best subsets regression was undertaken to identify the significant discharge-based predictor variables. The multivariate regressions models of total proglacial SSC for the season (DOY 203-231) are shown in Table 7.3. The results echo those for the individual stations, with a dominance of Q^2 as a predictor in all models, suggesting a non-linear relationship between SSC and discharge, and the failure of ΔQ as a significant predictor, suggesting a lack of diurnal hysteresis. $\log Q$ loaded negatively suggesting a possible dilution effect and the weak negative coefficient for $hQ!$ suggested that the length of time since a comparable discharge did not result in

higher SSCs. Seasonal sediment exhaustion was significant although loaded weakly in the model. Overall, the total proglacial SSC regression model accounted for around 58 % of the observed variance in SSC, representing a slight improvement compared to the seasonal MRMs of the individual stations and its performance in simulating discharge is shown in Figure 7.1, which shows a number of days with large model residuals due to high magnitude SSC events.

Table 7.3: Multivariate regression model of proglacial SSC constructed with pooled observations from Stations B and C from DOY 203-231 ($n = 22331$). Table shows MRM coefficients of determination and predictor coefficients for each station for the season in addition to the regression constant k . The Durbin-Watson ($D-W$) statistic is shown. Bold entries show the most significant predictor in the MRM. ΔQ was not a significant predictor at $p \leq 0.05$.

Period	R^2	k	$\log Q$	Q^2	$hQ!$	ΣQ	$D-W$
203-231	0.58	-0.9	-0.052	0.036	-0.00081	-5.4×10^{-09}	0.012

Upon examination of the model residuals, no consistent relationship between residual SSC and temperature is apparent (Figure 7.2), however, Figure 7.3 demonstrates that SSC around the peak diurnal air temperature cycle is generally associated with positive model residuals until DOY 217 (the end of sub-season S1), indicating an under prediction in SSC, whereas during S2 this association is inverse, with lower SSCs than expected suggesting sediment exhaustion during the latter part of the ablation season. A weak positive correlation between air temperature and residual SSC exists with $r = 0.11$. However, when the time-series is examined according to the two sub-seasons (S1 & S2) a stronger positive association exists during S1 ($r = 0.27$) and a moderate negative correlation exists during S2 ($r = -0.38$). This reinforces the finding that the MRM under predicts SSC during S1 and over predicts during S2. A time-series of air temperature recorded at the Saas Fee weather Station was included into the MRM as a predictor variable but this improved model performance by $<1\%$

and resulted in the failure of $\log Q$ as a significant predictor (at 95% confidence) suggesting an absence of thaw-related sediment mobilisation (e.g. Irvine-Fynn *et al.*, 2005). With regards to precipitation, Figure 7.2 indicates a complex association between precipitation and residual SSC. Rainfall on DOY 209-211 generated both positive and negative residuals and rainfall on DOY 217-219 generated negative residuals. A very weak negative correlation between precipitation and residual SSC exists, with $r = -0.08$ (not significant at 95% confidence). Upon examination of the days with rainfall, a weak negative association exists for DOY 209-211 ($r = -0.08$, not significant at 95% confidence), a moderate negative association exists for DOY 217-219 ($r = -0.36$, not significant at 95% confidence), and a very weak positive association exists on DOY 229 ($r = 0.07$, not significant at 95% confidence). Excluding the latter result due to its weakness, the inverse association with precipitation indicates the over prediction of SSC, which is unusual as rainfall is associated with the mobilisation of fine channel-marginal and extra-channel sediments. Such an inverse relationship may instead represent a dilution effect whereby, despite sediment mobilisation, increased discharges due to rainfall result in less rapid increases in SSC than would otherwise be predicted from the MRMs. However, this is not well supported by the discharge time-series, which was not strongly influenced by precipitation inputs. These effects may relate to ablation processes, whereby melt is suppressed due to the reduction in incoming solar radiation and air temperatures during precipitation-bearing weather systems. This effect is weakly supported by the results of the cluster analysis on meteorological indices in Chapter 5, whereby several of the precipitation events examined here were included in the clusters with cooler and wet days. To investigate this further, a time-series of precipitation was included in the MRM as a predictor variable but failed to be a significant predictor of SSC at $p \leq 0.05$, which is unsurprising given the aforementioned complexity in the SSC response to precipitation. In light of

these results, the relationship between rainfall and SSC was further explored through hysteresis analysis.

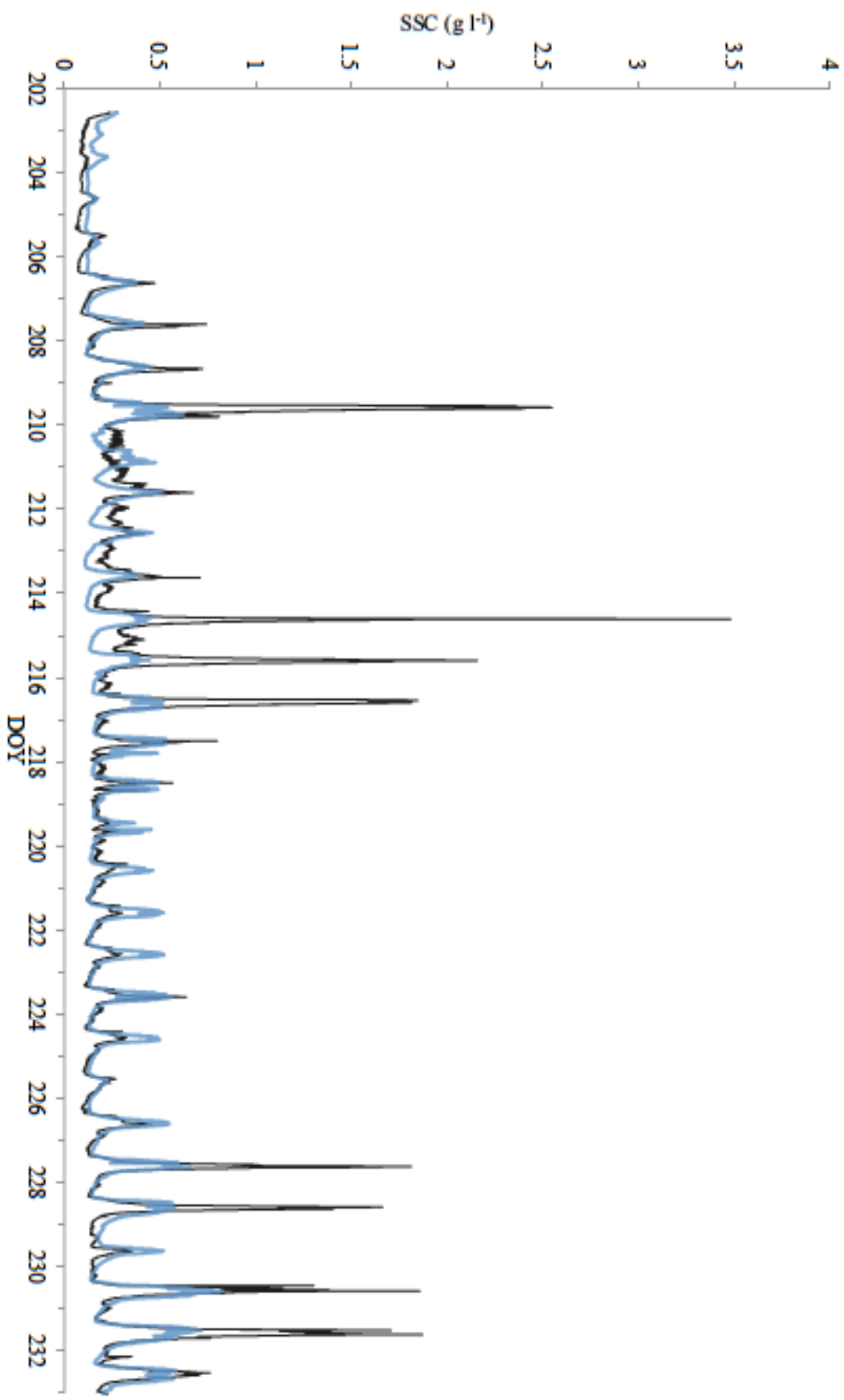


Figure 7.1: Plot of measured total proglacial SSC for DOY 202–232 (Black line) and predicted proglacial SSC (Blue line) from the multivariate regression model highlighting a number of days with large model residuals.

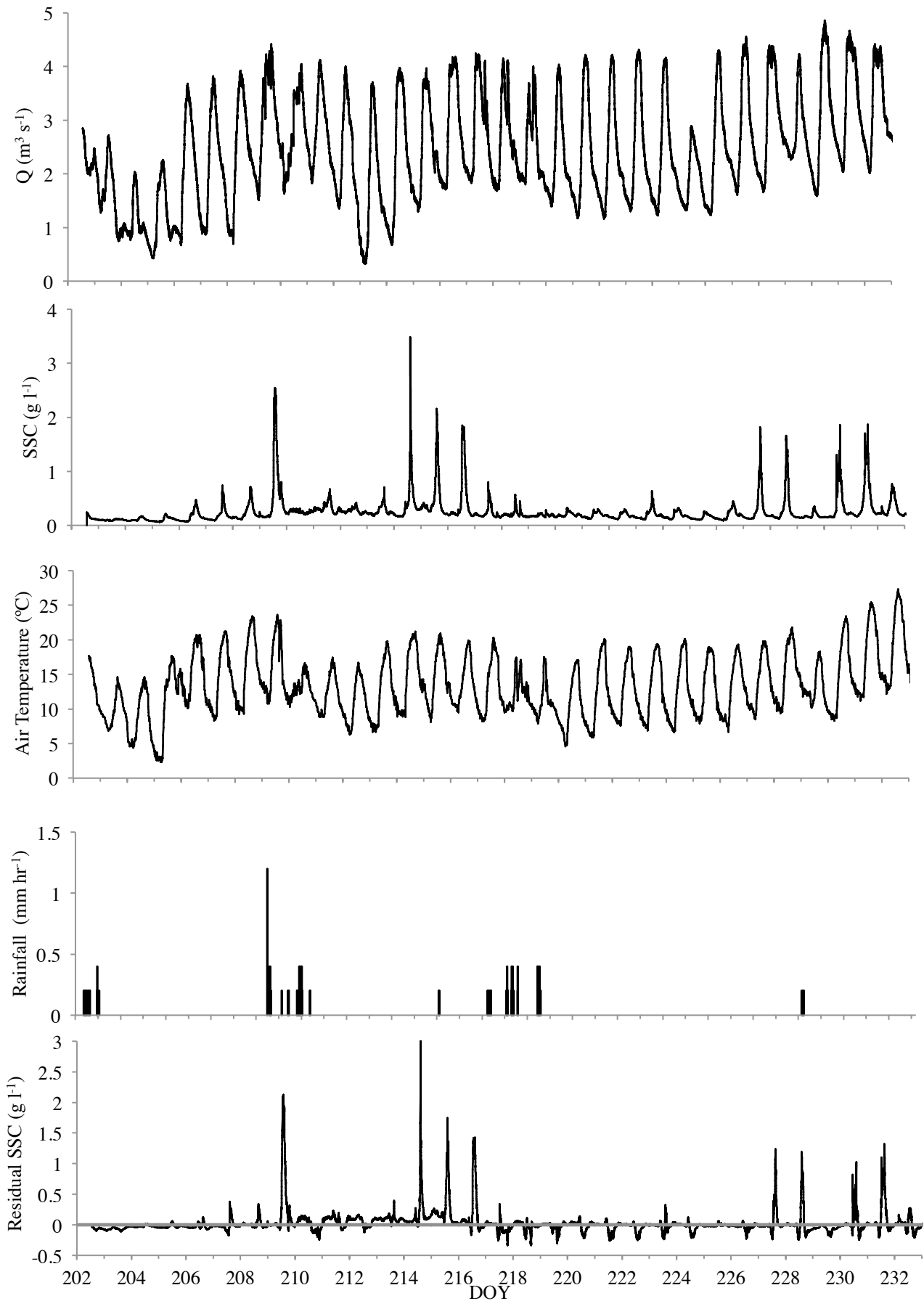


Figure 7.2: Plots of 2-minute total proglacial discharge and SSC along with hourly air temperature and precipitation recorded at the Saas Fee weather station and residual SSC from the pooled MRM of total proglacial SSC presented in table 8.3.

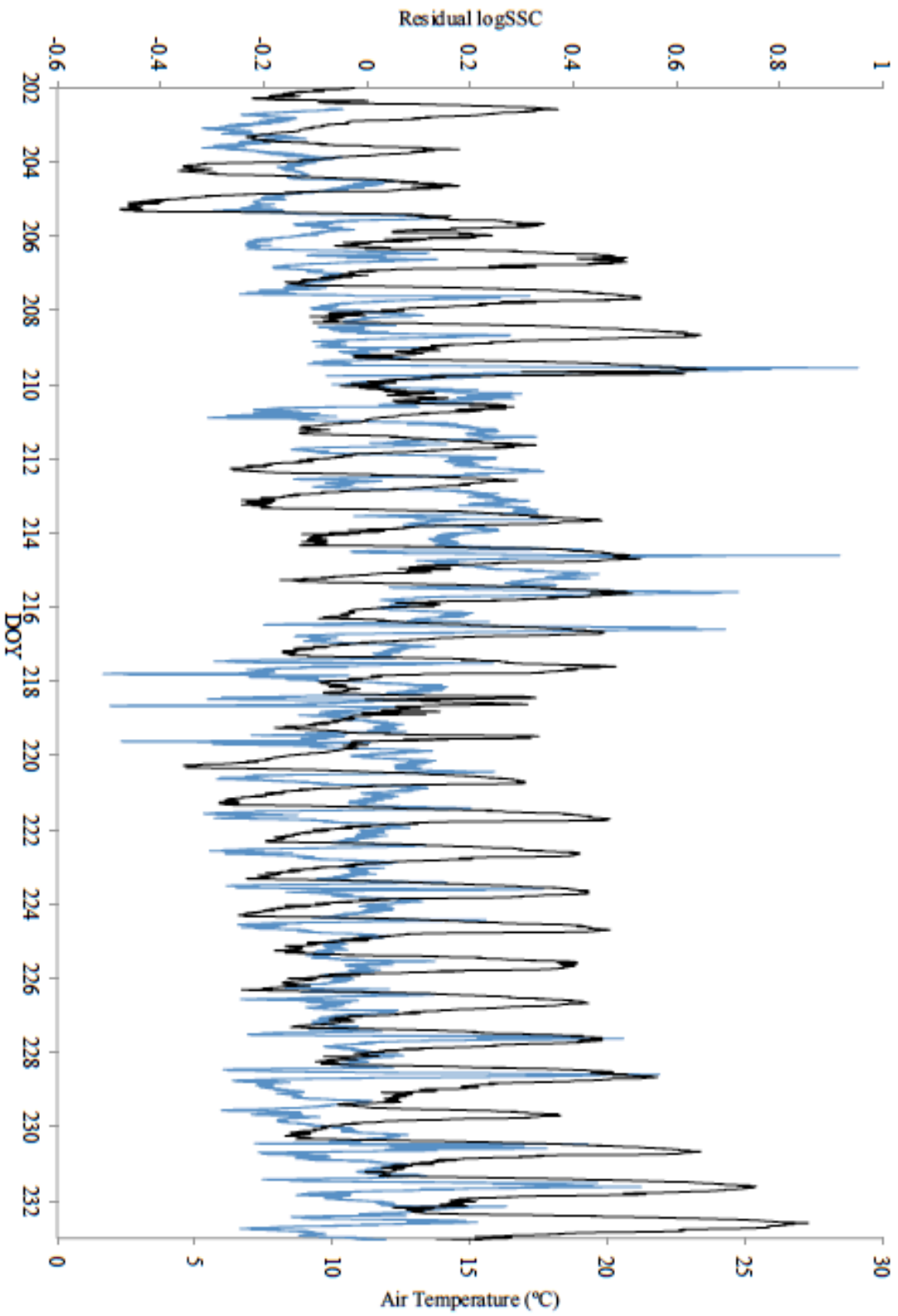


Figure 7.3: Plot of residual log SSC and Air Temperature for DOY 203–231 with vertical dotted line separating S1 and S2 at DOY 217. During S2 higher temperatures are generally associated with negative residuals indicating an over prediction in SSC.

The influence of rainfall on patterns and loads of SSC were assessed through examination of the proglacial SSC, discharge and meteorological time-series. Data were analysed to identify the SSC response at each gauging location to two general classifications of precipitation types: Significant precipitation events (e.g. storms) which occurred twice during the monitoring period were scrutinised and; the response of SSC to more general (and less extreme) precipitation was examined. Minor rainfall events which did not generate a discernible SSC response were excluded from the analysis. The rainfall events were scrutinised to infer the relationship between rainfall duration and intensity and sediment mobilisation from in-channel and extra-channel surfaces, while the SSC response was used to gauge the degree of sediment availability of in-channel and extra-channel sources. In addition, the nature and patterns of hysteresis between SSC and discharge was used to infer potential sediment sources during a rainfall event (e.g. Richards, 1984; Fenn & Gomez, 1989; Williams, 1989; Clifford *et al.*, 1995; Lenzi & Marchi, 2000; Jansson, 2002; Orwin & Smart, 2004b; Seeger *et al.*, 2004; Megnounif *et al.*, 2013). Such studies have demonstrated that clockwise hysteresis during rainfall events is generally associated with the mobilisation and subsequent rapid exhaustion of near or in-channel sources of sediment. For example, clockwise hysteresis can indicate the washout or erosion of fine material from channel banks and proximal extra-channel surfaces where there is a short-travel time. Anticlockwise hysteresis is generally associated with SSC peaking after discharge, either due to the mobilisation of more distant sediment sources or the erosion of less readily-mobile sediments (Richards, 1984). For example, this may occur as material at the channel bed is mobilised at the highest discharges or due to high intensity rainfall or pluvial flows scouring armoured extra-channel surfaces to expose and mobilise sub-surface sediments. For flood events, anticlockwise patterns have also been found to be

caused by the difference between the travel time of the flood wave and the sediment peak, as sediment in suspension tends to travel at velocities close to mean flow velocity which is below the velocity of the flood wave (Williams, 1989). More complex hysteresis patterns comprising multiple loops and figure eights have been associated with high soil erodibility combined with prolonged erosion (Williams, 1989), soil saturation leading to Hortonian overland flow and significant erosion (Seeger *et al.*, 2004; Megnounif *et al.*, 2013) and multiple cycles of erosion and deposition during the event (Fenn & Gomez, 1989). However, complex hysteresis patterns may also result from the pattern of precipitation, for example, when there is irregular precipitation delivery during the day which episodically flushes extra-channel sediments into streams.

Six rainfall events were included for analysis:

- Rainfall on DOY 184 totalled 71.7 mm and occurred between 0200 and 1900 h, peaking between 0500 and 0700 h with a secondary peak around 1100 h (Figure 7.4). However, data for this event is limited due to the sensor measurement ranges being exceeded at Station D and the gauging station and sensors at Station C being destroyed by the resultant flood.
- Rainfall on DOY 210 totalled 10.6 mm and was dispersed throughout the day with additional heavy bursts between 2000 and 0000 h (Figure 7.5).
- Rainfall on DOY 217 totalled 4.6 mm and occurred later in the day between 1800 and 2200 h followed by 1 mm around 0400 h overnight (Figure 7.6).
- Rainfall on DOY 218 totalled 8.6 mm and occurred between 1100 and 0000 h. There was initial rainfall of 3 mm at around 1100 h followed by another event of 4 mm at around 1600 h with three minor rainfall events later in the evening of very short durations and small volumes (Figure 7.7).

- Rainfall on DOY 219 totalled 5.4 mm and occurred between 1400 and 1700 h (Figure 7.8).
- Rainfall on DOY 233 totalled 11.8 mm and occurred between 1500 and 2200 h (Figure 7.9). However, data for this event is limited to Station B as the resultant flood destroyed the gauging station structure at Station C.

The storm event on DOY 184 was recorded at Station D as Station B was yet to be installed and Station C was destroyed by the resulting flood. Due to the high magnitude of the event there is a data gap spanning approximately 76 minutes when both stage and turbidity sensors were outside their measurable ranges. This occurred during the first peak in SSC and Q as a result of the most intense rainfall between 0500 and 0700 h. The limited data suggests a clockwise hysteresis response for the first peak which was followed by a significant reduction in rainfall intensity until around 1100 h when a secondary peak in rainfall generated a further peak in SSC and discharge with an anticlockwise hysteresis pattern (Figure 7.4). The timing of the third peak coincides with the typical diurnal pattern in SSC and discharge and the direction of hysteresis is clockwise. These patterns are interpreted to reflect significant entrainment from in-channel and channel marginal sources during the first peak event as this would be the likely cause of clockwise hysteresis. This is followed by the transport of weakened or freshly exposed sediments from channel beds and extra-channel surfaces during the second peak which is suggested from the anticlockwise hysteresis and minor secondary peak in SSC. The final peak is interpreted as reflecting glacial sources owing to the clockwise hysteresis (e.g. Richards & Moore, 2003) and rapidly exhausted SSC signal which exhibits a rapidly receding falling limb suggesting rapid exhaustion of sources and/or limited sediment availability following the preceding two flood peaks.

The event on DOY 210 was captured at Stations B and C. Anticlockwise hysteresis patterns between discharge and SSC were evident although at least two minor clockwise loops occur at each station (Figure 7.5). The interpretation of these hysteresis patterns in identifying sediment transfer processes and sources is challenging for this event due to the sporadic patterns of precipitation which resulted in an unusual pattern of discharge and SSC, particularly at Station C where, discharge rose rapidly and plateaued and SSC decreased and then increased rapidly during the falling hydrograph limb. This echoes the similarly challenging interpretation of diurnal controls on sediment transfer in the multivariate regression models due to the general failure of ΔQ as a predictor of SSC. However, it is apparent that SSC responded differently to the rainfall event at each station. Station C experienced the highest variability characterised by rapid fluctuations in SSC coinciding with bursts in rainfall. This may indicate that sediment transfer occurred rapidly as sediment was mobilised by rainfall from sources close to the channel suggesting high availability of readily-mobile sediments close to Station C which would be supported by field observations of the sedimentary settings of these surfaces as comprising glacial-fluvial deposits and reworked paraglacial debris (Cook *et al.*, 2013). This is in contrast to Station B which showed an SSC response to rainfall that more-closely followed the pattern of discharge. This may suggest a more limited availability of readily-mobile sediments in the channels and streams close to Station B, or the effects of pronounced sediment exhaustion. The two peaks in SSC which appear to occur as a result of two short bursts of rainfall between DOY 210.8 and 211, and the absence of similar discrete peaks in prior rainfall, suggest that a mobilisation threshold exists that requires a certain intensity or volume of rainfall to mobilise sediments at or close to Station B which is interpreted to result from surface armouring or the necessity for armouring capacity to be exceeded. The surfaces in the vicinity of Station B are characterised by hummocky moraine formed of consolidated glacio-fluvial deposits,

and paraglacial rock avalanche deposits (Cook *et al.*, 2013), suggesting the lack of fine and unconsolidated material may be significant in both limiting fine sediment availability and providing surface armouring.

The rainfall event on DOY 217 occurred after the diurnal peak in SSC and discharge. A clockwise hysteresis pattern between discharge and SSC is evident at both stations with a narrow loop at Station C (Figure 7.6). This pattern most likely reflects the diurnal variability in ablation-driven discharge acting as the dominant control on SSC, as the rainfall occurred after the diurnal peaks. At Station B, SSC responded to the rainfall with a double-peak which closely followed the corresponding discharge response. At Station B there was a significant discharge response which exhibited a double peak. However, SSC showed a single peaked response with an attenuated falling limb. This suggests that the SSC response to rainfall at Station B was likely driven by increases in transport capacity or the entrainment of in-channel sediments as the hydraulic radius of the channel increased. The response at Station C also appears to have been driven by discharge but there appears to be more pronounced sediment source exhaustion and lower sediment availability which would account for the lack of a secondary peak coinciding with discharge. This is supported by the rapid falling SSC limb at Station C on the diurnal signal around DOY 217.5 compared to the more typical attenuated limb observed at Station B and suggests low sediment availability potentially due to the exhaustion of sediment sources.

Rainfall on DOY 218 occurred in a number of short events over a period of 13 hours. The infrequent nature of the rainfall and the resultant patterns of SSC and discharge generated complex hysteresis without a dominant direction and a number of clockwise and anticlockwise loops at both Stations B and C (Figure 7.7). The first event occurred during the rising hydrograph limb and there was negligible impact on SSC or

discharge. The second rainfall event generated a significant SSC response at both stations, with the response at Station C most pronounced and comprising discrete single peaks suggesting high near or in-channel sediment availability and a short travel time. However, Station B exhibited a double peaked response as seen on the rainfall event of DOY 217 suggesting that, in addition to an instantaneous response from nearby sources, sediment was mobilised from more distant sources or from those which experience increased armouring. The minor rainfall which occurred after DOY 218.7 generated a small response in SSC and discharge at Station C but no appreciable response at Station B, further supporting the possibility that streams and surfaces close to Station B experience greater surface armouring or have limited availability of readily-mobilised sediments with the lack of response to the later rainfall events indicative of supply exhaustion. However, the complex responses of SSC to rainfall at the two locations suggest there is unlikely to be a single reason for the observed patterns.

Rainfall on DOY 219 occurred in one event lasting between 2 and 3 hours and after the diurnal peak in SSC and discharge (Figure 7.8). Station B experienced broadly clockwise although complex hysteresis with additional clockwise and anticlockwise loops. Station C experienced a more complex hysteresis pattern that was dominated by a large anticlockwise loop and also experienced several switches between anticlockwise and clockwise behaviour. The observed patterns at Station B suggest high sediment availability as SSC followed the discharge response to rainfall exhibiting a double peak. This may indicate that rainfall on the preceding two days (DOY 217 and 218) mobilised or weakened armoured sediments that were subsequently able to be mobilised as the transport capacity and erosive potential in the streams increased with discharge. This raises the possibility that surface armouring is significant in determining sediment transfer patterns at this location. Furthermore, there is an unusual increase in SSC from around DOY 220 as discharge decreased, the cause of which is unresolved owing to an

apparent absence of coincident patterns in the meteorological or discharge time-series. The response of SSC to rainfall at Station C draws comparisons to DOY 217, whereby there is a strong instantaneous response to rainfall generating a peak in SSC, which is followed by rapid exhaustion, as SSC patterns are then uncorrelated to the second peak in discharge. A further peak in SSC that is uncorrelated with discharge then occurs approximately four hours later around DOY 219.9 raising the possibility that rainfall mobilised more distant sediment sources in the catchment or weakened in-channel or channel-marginal sediments to be entrained by discharge possible due to channel-bank collapse.

The event on DOY 233 was the second significant storm event of the ablation season and approximately coincided with the diurnal peak in SSC and discharge (Figure 7.9). The data record at Station C is largely incomplete for this event due to high discharges damaging the gauging Station structure and sensors. For Station B, patterns of hysteresis between SSC and discharge show a dominant anticlockwise pattern with a number of rotations and loops. Following the initial peak, SSC experiences a second peak, whilst discharge falls. This may suggest the mobilisation of more distant or more armoured sediment sources following the initial response of SSC to rainfall. Rapid and pronounced exhaustion is then experienced as subsequent rainfall has no discernible impact on SSC.

The proglacial SSC response to rainfall events in the Feegletscher Nord forefield showed variable patterns of sediment transfer that differed according to the location of the monitoring stations. The transfer of fine sediment generally showed an instantaneous response to rainfall at all locations suggesting the availability of fine sediments for removal. However, significant differences in these transfer patterns occur. Surfaces at Station B appear to experience a mobilisation threshold that requires a

certain duration and intensity of rainfall to be achieved, the determination of which were not definable from the data here. The presence of a mobilisation threshold suggests surface armouring exists in this location combined with a lack of available sediments relative to Station C, which would be supported by the geomorphology in the vicinity of Station B as comprising paraglacial rock avalanche debris and hummocky moraine (Cook *et al.*, 2013). In contrast, surfaces at Station C appear to experience the rapid mobilisation and removal of fine sediments with subsequent rapid exhaustion, which suggests a lack of surface armouring combined with increased sediment availability relative to Station B. This may reflect the susceptibility of the in-channel and channel-marginal sediments in the stream at Station C to bank collapse, which would be supported by field observations during 2012 and in other research (Hampel, 2009; Porter, *pers comms*). These suggested links between surface characteristics and sediment transfer processes draw comparisons to other research (e.g. Orwin & Smart, 2004b) whereby the rapid removal of fine sediments was associated with young (most recently deglaciated) surfaces and conversely, more mature (older) surfaces were associated with a limited SSC response to rainfall events, as a result of surface armouring. However, the notable difference in this research is that the results are obtained principally from two gauging stations (B & C) which, by their locations as described in Chapter 3, are assumed to experience similar surface ages (i.e. they were deglaciated at similar times). This would appear to suggest that factors other than surface age and maturity are responsible for the observed spatially distinct patterns of fine sediment transfer within the Feegletscher Nord proglacial zone. Here, it is suggested that factors such as the availability of fine sediments, the degree of surface armouring, the extent of sediment consolidation, and the susceptibility of channel banks to collapse, are all likely to be factors with potential to control sediment transfer by glacio-fluvial processes. These suggested factors can broadly be attributed to

sedimentary and geomorphological characteristics of areas of the proglacial zone as deduced from field observations and previous research (e.g. Curry *et al.*, 2009; Hampel, 2009; Cook *et al.*, 2013). Surfaces in the vicinity of Station C comprised glacio-fluvial deposits with channel banks that were prone to collapse, possibly triggered by fluvial undercutting. This would likely result in enhanced sediment availability for mobilisation and a strong and rapid association between precipitation and SSC. In contrast, surfaces in the vicinity of Station B were comprised of consolidated paraglacial rock avalanche debris and a lack of exposed and unconsolidated glacio-fluvial deposits and, in particular, fine material. This would likely result in a weaker association between precipitation and rainfall due to a lack of fine material available for mobilisation and the requirement for greater duration or intensity of rainfall to exceed the surface armouring. However, in light of the complex relationships between SSC and rainfall found in these results, it is likely that a combination of these factors is in operation and responsible for the observed patterns in, and relationships between, SSC, rainfall and discharge, and the elucidation of specific sediment transfer processes and their controls is challenging.

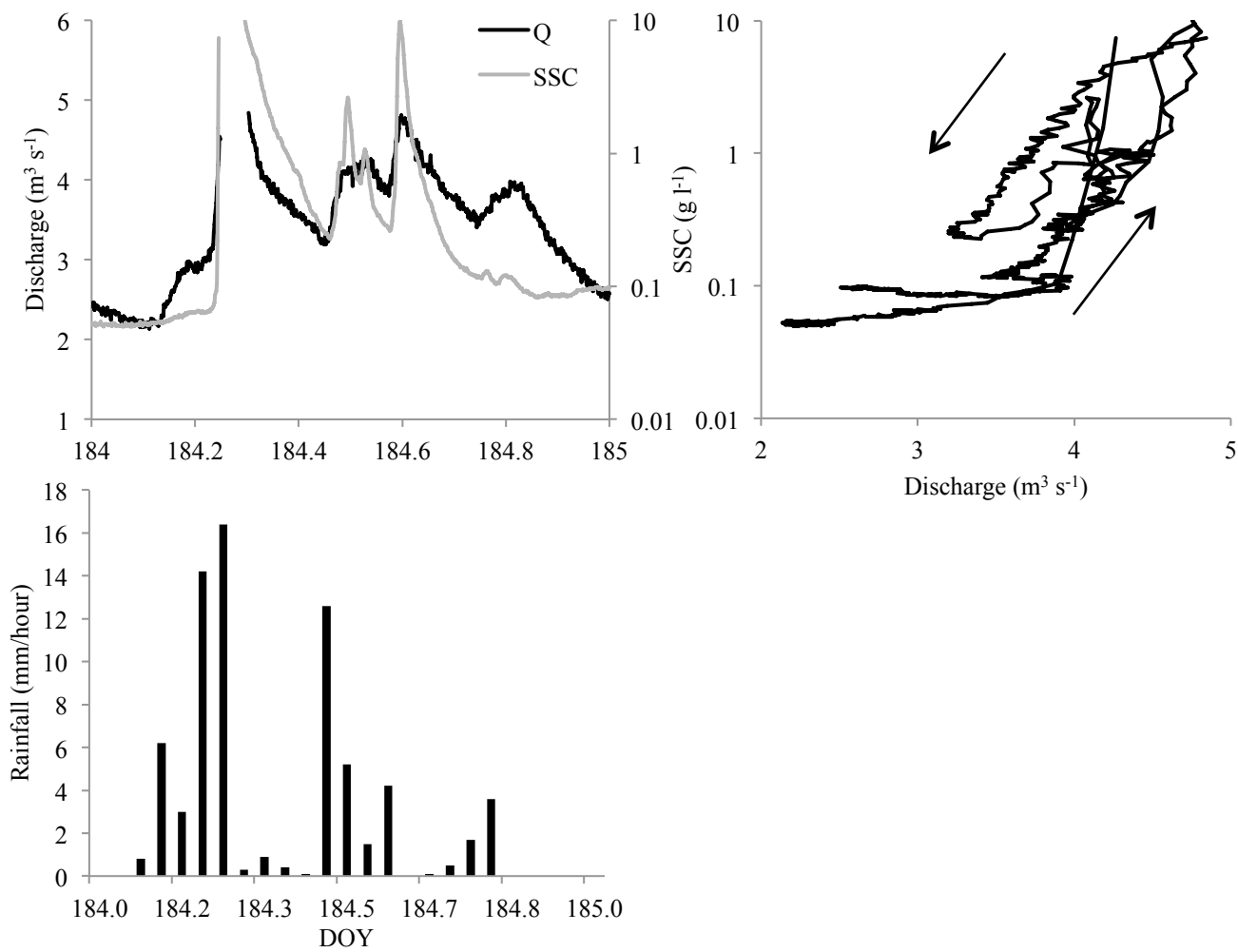


Figure 7.4: Left column shows proglacial SSC and discharge (Q) response at Station D to the DOY 184 rainfall event. Right column shows SSC-Q hysteresis plot with dominant hysteresis direction indicated by arrows. SSC is plotted on a logarithmic scale for clarity.

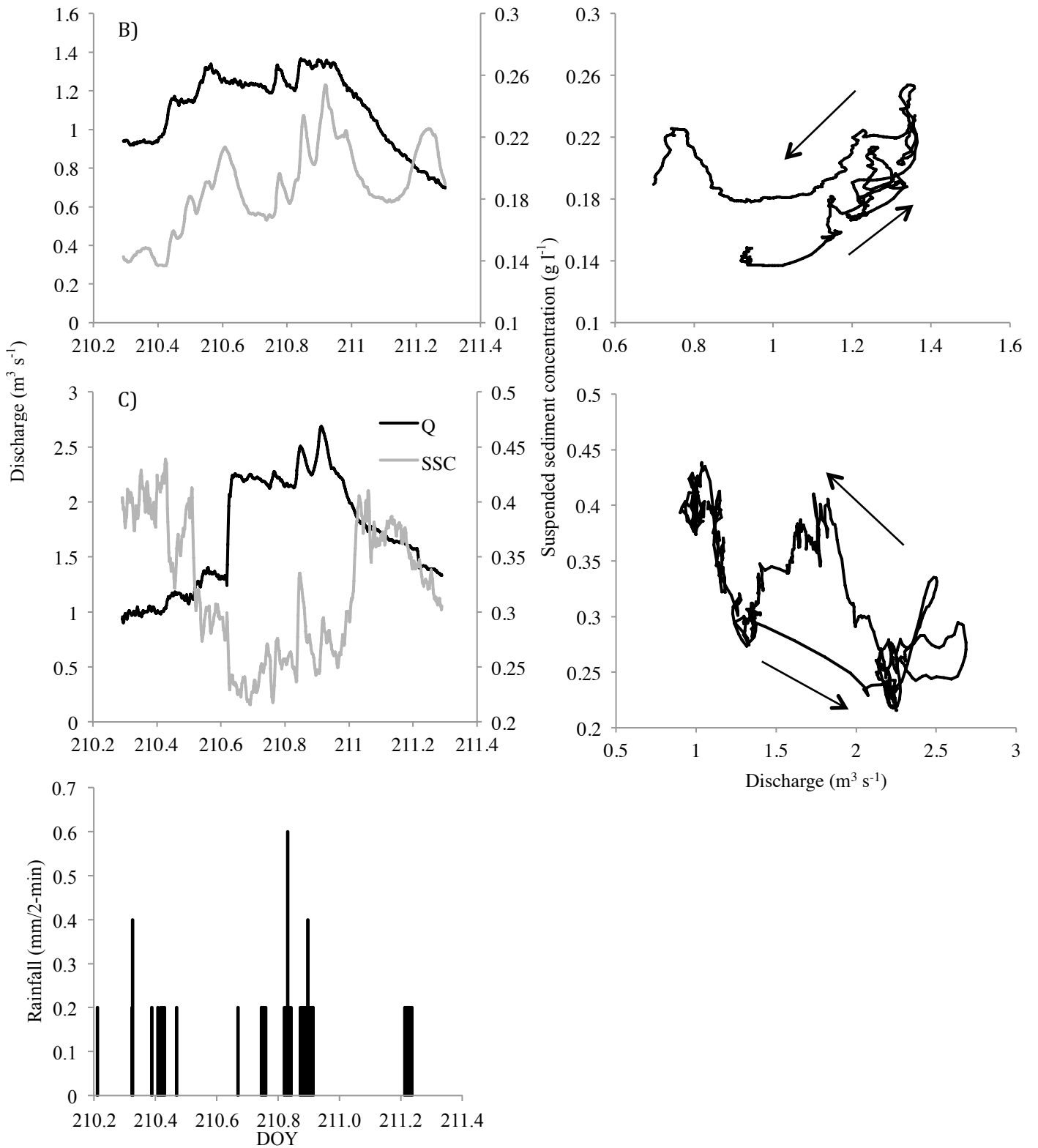


Figure 7.5: Left column shows proglacial SSC and discharge (Q) at Stations B and C response to the DOY 210 rainfall event. Right column shows SSC-Q hysteresis plots with dominant hysteresis direction indicated by arrows.

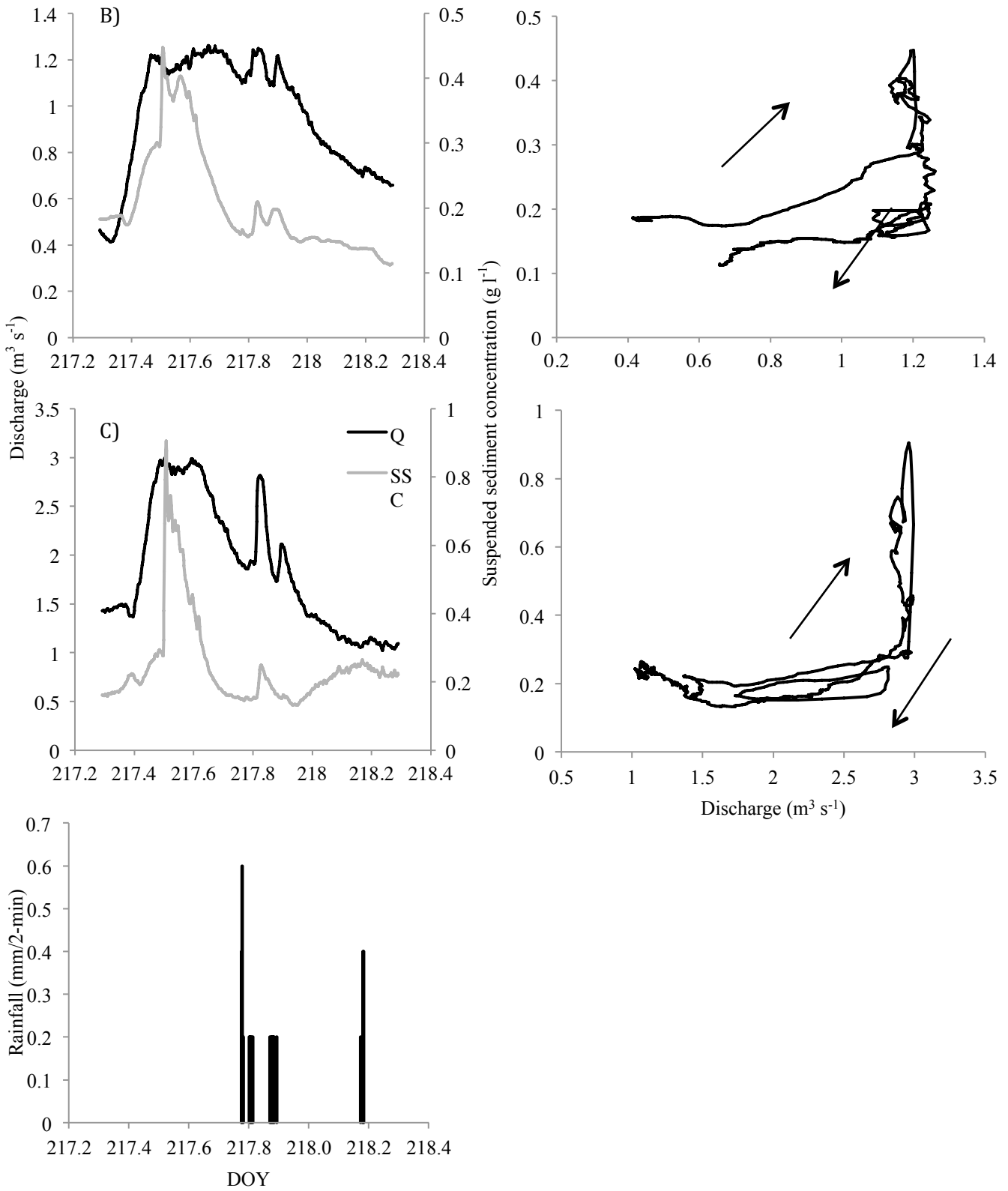


Figure 7.6: Left column shows proglacial SSC and discharge (Q) at stations B and C response to the DOY 217 rainfall event. Right column shows SSC-Q hysteresis plots with dominant hysteresis direction indicated by arrows.

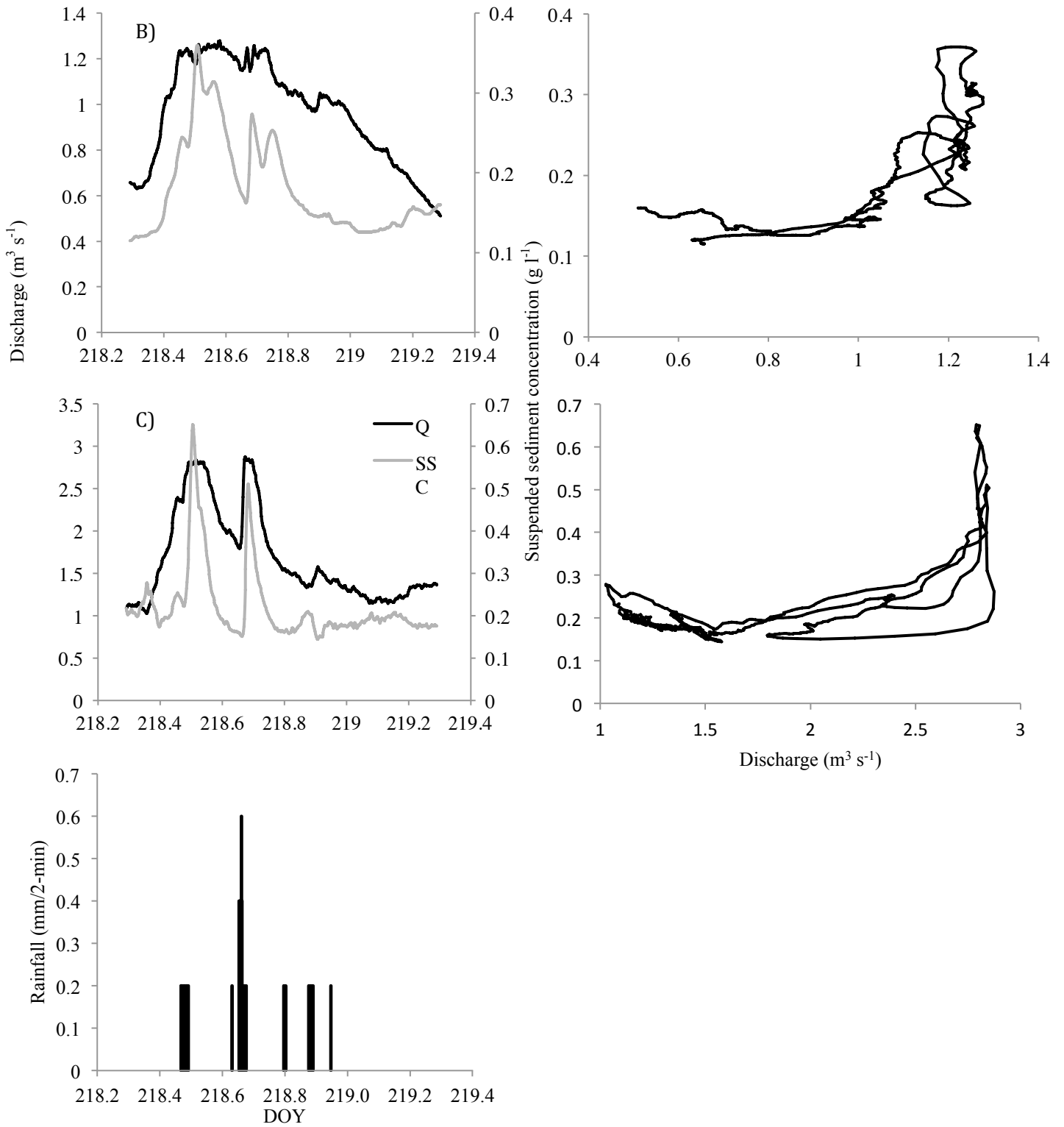


Figure 7.7: Left column shows proglacial SSC and discharge (Q) at stations B and C response to the DOY 218 rainfall event. Right column shows SSC-Q hysteresis plots. However, no dominant pattern of hysteresis could be determined.

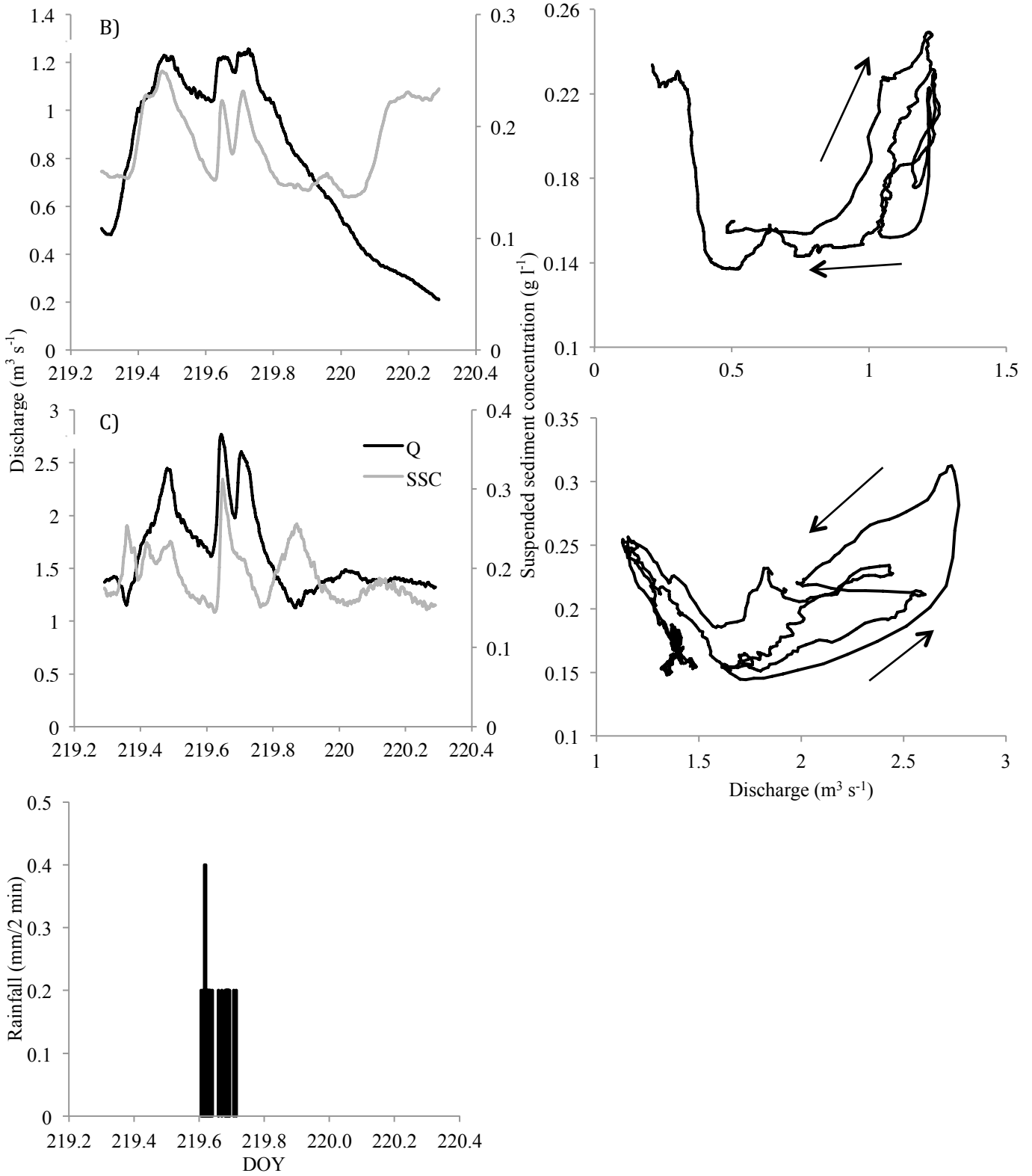


Figure 7.8: Left column shows proglacial SSC and discharge (Q) at stations B and C response to the DOY 219 rainfall event. Right column shows SSC-Q hysteresis plots with dominant hysteresis direction indicated by arrows.

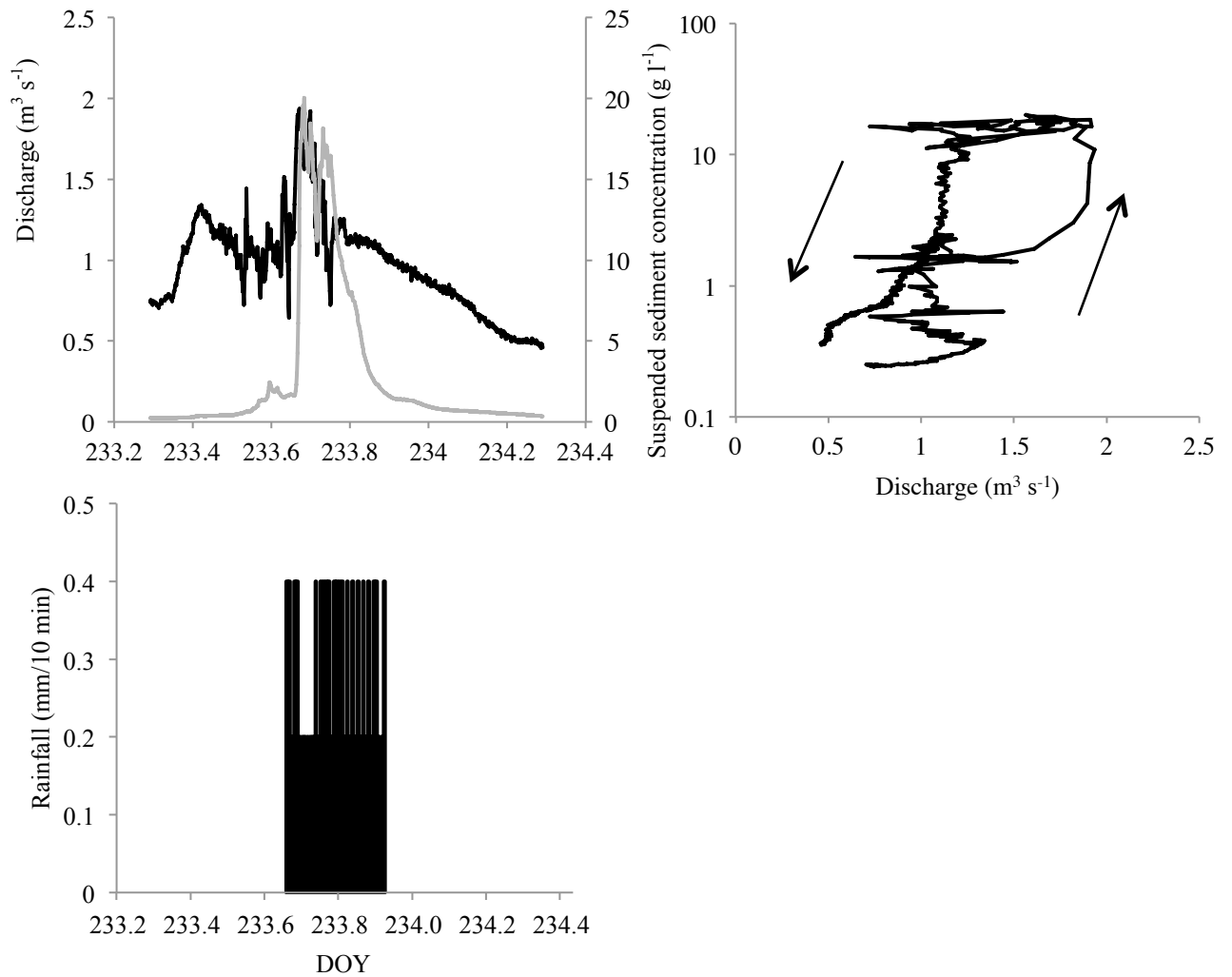


Figure 7.9: Left column shows proglacial SSC and discharge (Q) at Station B to the DOY 233 rainfall event. Right column shows SSC-Q hysteresis plots with dominant hysteresis direction indicated by arrows.

7.5 Forward Modelling of Sediment Transfer

An exploratory forward model was developed in order to project possible future changes in summer meltwater runoff and associated glacio-fluvial suspended sediment loads from the Feegletscher Nord under projected future climate changes associated with anthropogenic greenhouse gas emission scenarios. Despite several decades of glacier retreat, there is a paucity of data into long-term changes in the sediment loads of rivers draining glaciated catchments with unknown future trends (Warburton *et al.*, 2007; Diodato *et al.*, 2013). The dependence of geomorphological processes on climate, particularly in glaciated regions and catchments (Syvitski, 2002), provides one

opportunity to explore the consequences of climate change through the modelling of *in situ* sediment transfer processes under the current climate (Morehead *et al.*, 2003; Stott & Mount, 2007; Warburton, 2007; Warburton *et al.*, 2007; Diodato *et al.*, 2013; Pralong *et al.*, 2015). Improved understanding of how glacio-fluvial processes and sediment loads may respond to deglaciation is needed in order to aid predictions of landscape evolution and the interpretation of sedimentary records (e.g. Hambrey *et al.*, 2001; Lønne & Lysa, 2005; Lukas *et al.*, 2005; Knight & Harrison, 2009), particularly due to the role of glacio-fluvial processes in reworking and redistributing glacial sediments (e.g. Warburton, 1990; Hodson *et al.*, 1998; Ballantyne, 2002; Hodgkins *et al.*, 2003; Orwin & Smart, 2004; Barnard *et al.*, 2006; Leggat *et al.*, 2015).

A number of attempts at forecasting future glacier changes and their resultant glacio-hydrological impacts have been made (e.g. Huss *et al.*, 2008; Stahl *et al.*, 2008; Huss *et al.*, 2010; Farinotti *et al.*, 2012; Bliss *et al.*, 2014; Huss *et al.*, 2014; Pralong *et al.*, 2015). The approaches of Huss *et al.* (2010) and Bliss *et al.* (2014) utilise temperature-index melt model approaches to predict 21st Century glacier mass balance and runoff, whereby input parameters, such as temperature, are derived from *in situ* data sets that are shifted for future time periods according to climate changes derived from regional and global climate models under specific emissions scenarios. These approaches also account for glacier shrinkage through changes derived from mass balance models and regional estimates of mass loss. However, establishing the response of glaciers to future climate is complicated by the heterogeneous responses of individual glaciers to changes in climate, influenced by factors such as glacier size, topographic setting, local climate, and mass balance.

In light of the development of the Feegletscher temperature-index runoff model (FTIM) in Chapter 6, which accounted for around 64% of the variance in observed hourly runoff during the 2012 monitoring period and predicted total runoff to within < 3 % of observed, the approach here used a temperature-index approach to generate future predictions of runoff at the Feegletscher Nord. FTIM was then coupled to the discharge-based multivariate regression model for predicting SSC described in Section 7.3 and outlined in Table 7.3 with the capability to account for around 58% of the variance in observed suspended sediment concentrations and predicted total suspended sediment load to within 10% of observed. The following section outlines the basis and development of the forward model and the model outputs are presented in Section 7.5.2.

7.5.1 Forward Modelling Approach

FTIM requires input data of hourly temperature and precipitation to predict glacier runoff. The Swiss Climate Change Scenarios CH2011 project (CH2011, 2011) provides a regional assessment of possible 21st Century climate changes according to future global greenhouse gas emissions pathways. The assessment utilises two non-intervention emission scenarios (A2 and A1B) and a climate stabilisation scenario (RCP3PD) (Table 7.4) to project changes in temperature and precipitation for three future time periods: 2020-2049, 2045-2074, and 2070-2099, based on a reference period of 1980-2009. This output is derived from coupled Global Climate Model (GCM) and Regional Climate Model (RCM) chains used in the EU ENSEMBLES climate change prediction project for Europe (van de Linden & Mitchell, 2009). The project used eight GCMs and 14 RCMs with 20 simulations in total with a grid spacing of 25 km that mostly cover the period 1950-2100. In summary, the project forecasts mean temperature increases for all areas of Switzerland, with more pronounced summer increases. Precipitation is expected to decrease in summer, with Southern Switzerland

experiencing winter increases, although winter changes in other regions are uncertain. The output of CH2011 (2011) provides regionally averaged daily additive temperature and multiplicative precipitation changes are predicted for three regions of Switzerland (West, North-East and South). CH2011 (2011) does not make specific predictions for the Alpine region due to the complex topography and highly localised climatic processes. However, the aggregated results of the predictions for Switzerland represent the most current and localised predictions for the general region in light of the available future climate change predictions. Therefore, the results of the CH2011 (2011) project were selected for this forward modelling approach, as they provide robust data on possible climate changes localised to Switzerland with high-resolution output that was conducive to the data requirements of FTIM.

Table 7.4: Descriptions of the three climate change emission scenarios used in the generation of regional projections for Switzerland in the Swiss Climate Scenarios CH2011 project (CH2011, 2011, p.16). The emission scenarios are among those prepared in the Special Report on Emissions Scenarios (IPCC, 2000) and the Representative Concentration Pathway (RCP3-PD) scenario presented by IPCC (2007).

Scenario	Description
<i>A1B</i>	The A1B emission scenario is a non-intervention scenario characterised by a balance across fossil-intensive and no fossil energy sources. It belongs to the A1 scenario family describing a future world of very rapid economic growth, global population that peaks in mid-century and declines thereafter, and the rapid introduction of new and more efficient technologies.
<i>A2</i>	The A2 emission scenario is a non-intervention scenario that describes a very heterogeneous world. Fertility patterns across regions converge very slowly, which results in continuously increasing population. Economic development is regionally oriented and per capita economic growth and technological change are more fragmented and slower than in other emission scenarios.
<i>RCP3-PD</i>	The RCP3-PD scenario illustrates an emission scenario that stabilises the atmospheric CO ₂ equivalent concentration near 450 ppm by the end of the century. It supposes that emissions are reduced by around 50% by 2050 relative to 1990. The RCP3-PD scenario likely prevents global warming of more than two degrees Celsius since the pre-industrial period (van Vuuren <i>et al.</i> , 2007); a goal to which countries have agreed to as decided by the Conference of the Parties of the United Nations Framework Convention on Climate Change in Cancun, Mexico, 2010. The scenario implies strong reductions in greenhouse gas emissions in the next decades and assumes strong mitigation measures are adopted.

However, the data predictions made in CH2011 (2011) utilise two future climate change scenarios presented in the Special Report on Emissions Scenarios (SRES) (IPCC, 2000) that have subsequently been replaced by the current Representative Concentration Pathways (RCPs) in the Fifth Assessment Report (AR5) and presented in Moss *et al.* (2008). Consequently, it is necessary to quantitatively contextualise the two SRES scenarios (A1B and A2) with the updated and current RCPs, so as to enable the identification of the extent to which the predictions made here may be considered similar or different to predictions made in the wider literature. Rogelj *et al.* (2012) provided comparisons of the global temperature increases projected by both SRES scenarios and RCPs (Table 7.5) according to a single modelling approach of the climate system and carbon-cycle that is constrained by observed historical warming. These predictions demonstrate the strong similarity between SRES scenario B2 and RCP6, whilst scenario A1B lies between the estimates generated for RCP6 and RCP8.5.

Table 7.5: Comparison of probabilistic temperature increase estimates in 2100 above pre-industrial levels for SRES scenarios and RCPs by Rogelj *et al.* (2012). The 66% range series represents the likely range of predictions as defined by IPCC (2000) as having a greater than 66% probability of occurring.

Scenario	Median (°C)	66% range (°C)
<i>A1B</i>	3.5	2.9-4.4
<i>B2</i>	3.0	2.6-3.7
<i>RCP3PD</i>	1.5	1.3-1.9
<i>RCP4.5</i>	2.4	2.0-3.0
<i>RCP6</i>	3.0	2.6-3.7
<i>RCP8.5</i>	4.9	4.0-6.1

Mean daily additive changes in temperature and multiplicative changes in precipitation were derived from the CH2011 (2011) predictions for the three regions for each day of the modelling period (DOY 180-251) based on the medium value in the

probability distribution of the predicted change (Table 7.5). As these changes were with reference to 1980-2009, it was necessary to ascertain the difference in the precipitation and temperature time-series from 2012 to the reference period in order to construct a 1980-2009 reference period time-series of temperature and precipitation. Data on temperature and precipitation for 2012 was obtained from the Saas Fee weather Station operated by MeteoSwiss. Data from this weather station were not available for the majority of the reference period, therefore, the nearby MeteoSwiss station situated 11 km away at Grächen and at a similar altitude (1605 m asl compared to 1790 m asl at Saas Fee) was used to ascertain the differences between 2012 and the reference period. In order to ascertain the suitability of the meteorological data from the Grächen meteorological station for the reference period, correlations between the 2012 data at Saas Fee and Grächen were undertaken. Comparisons of longer timescales were not possible owing to the aforementioned gaps in the data available for the Saas Fee Station. Correlations were undertaken after the air temperature time-series at Saas Fee had been adjusted for altitude by applying the environmental lapse rate in Chapter 4. Correlations between the Saas Fee and Grächen stations revealed air temperature to be highly correlated with $r = 0.9$ and precipitation was correlated with $r = 0.5$. A t-test demonstrated there was no significant difference in the means of the two air temperature series at the 95% significance level (t -value = 5.4). However, differences in the precipitation records were apparent (at the 95% significance level, t -value = 0.5) and likely relate to the two significant storm events. The mean difference in daily temperature between the reference period and 2012 calculated for DOY 180-251 was +1.2°C, indicating 2012 was warmer than the reference period. Average daily precipitation was 1.96 mm for 1980-2009 compared to 3.17 mm day⁻¹ for 2012, highlighting the influence of the two storm events. These mean additive temperature and multiplicative precipitation differences were applied to the 2012 Saas Fee time-

series of precipitation and temperature in order to create a time-series that represented the reference period, 1980-2009. The mean additive temperature and multiplicative precipitation changes from the CH2011 (2011) projections in Table 7.5 were applied to this reference time-series to create the input data for FTIM in order to simulate glacier runoff (e.g. Huss *et al.*, 2008), which are summarised in Table 7.6.

Table 7.6: Mean additive temperature (T, °C) and multiplicative precipitation (P) changes for the three emissions scenarios for DOY 180-251 for the future projection periods from CH2011 (2011) data.

Time period	A2		A1B		RCP3PD	
	T	P	T	P	T	P
2020-2049	1.24	0.98	1.39	0.97	1.31	0.97
2045-2074	2.68	0.87	2.74	0.86	1.64	0.92
2070-2099	4.61	0.73	3.95	0.77	1.69	0.9

Table 7.7: Mean average air temperature and total precipitation for DOY 180–251 in the shifted time-series of temperature and precipitation for the three future time periods and emissions scenarios according to the changes in Table 7.5. For reference, mean air temperature for DOY 180-251 in 1980-09 was 12 °C and mean total precipitation was 99.3 mm

Time period	A2		A1B		RCP3PD	
	T (°C)	P (mm)	T (°C)	P (mm)	T (°C)	P (mm)
2020-2049	13.2	96.9	13.3	96.6	13.3	96.7
2045-2074	14.6	86	14.7	85.8	13.6	91.2
2070-2099	16.6	72.3	15.9	76.1	13.6	89.4

It is well established that the recent loss of snow and ice in the Swiss alps has been pronounced (e.g. Haeberli *et al.*, 2007) with negative changes since 1980 in the volume of glaciers across all elevations, amounting to approximately $-0.59 \text{ m w.e. yr}^{-1}$ in the Valais, Switzerland, with the largest losses at lower elevations (Fischer *et al.*, 2014). In modelling future glacier shrinkage in the Alps, Huss (2011) calculated glacier area changes in the European Alps for 50 glaciers of sizes ranging from 0.08-80 km² for 1970-2008 with glaciers of 6-10 km² experiencing a 11.9 % decline in area. Between 3

and 10 digital elevation models of each glacier in the sample were used to characterise past changes in glacier extent and volume by Bauder *et al.* (2007) which were calibrated with point mass balance measurements collated by Huss *et al.* (2010). These data were used to calibrate accumulation and temperature-index melt models for each glacier by Huss (2011), driven by daily temperature and precipitation at a range of meteorological stations. Glacier storage changes were then simulated by Huss (2011) for 1908-2008 and these changes were then extrapolated from the 2008 extents to 2100 at a monthly time-step according to the median of 16 RCMs provided in the PRUDENCE project, which simulated regional climate changes at seasonal resolution (Christensen & Christensen, 2007). The projections of which are most similar to the A1B scenario in this research with the A2 and RCP3PD scenarios similar to the extreme changes. For glaciers of the size class of the Feegletscher Nord, median future area reductions of 5 % by 2035, 50 % by 2060 and 75 % by 2085 (corresponding to the mid-point years of the three future time periods) were predicted by Huss (2011) which are in good agreement with other mass loss forecasts (e.g. Haeberli *et al.*, 2007; Huss *et al.*, 2008; Bliss *et al.*, 2014; Fischer *et al.*, 2014). In light of the lack of ice volume data for the Feegletscher, and the complex response of glacial systems to climate forcing, these median area reductions by Huss (2011) are adopted in this forward model as possible changes rather than those likely to occur. Therefore, they function as indicative scenarios for changes in glacier runoff and sediment transfer associated with future glacier extents that are aligned to the median predictions of possible future climates. In applying these future glacier extents, area changes were weighted to lower elevations in order to retain the hypsometric area distribution of the Feegletscher, as mass loss will be more pronounced at lower elevations (Figure 7.10).

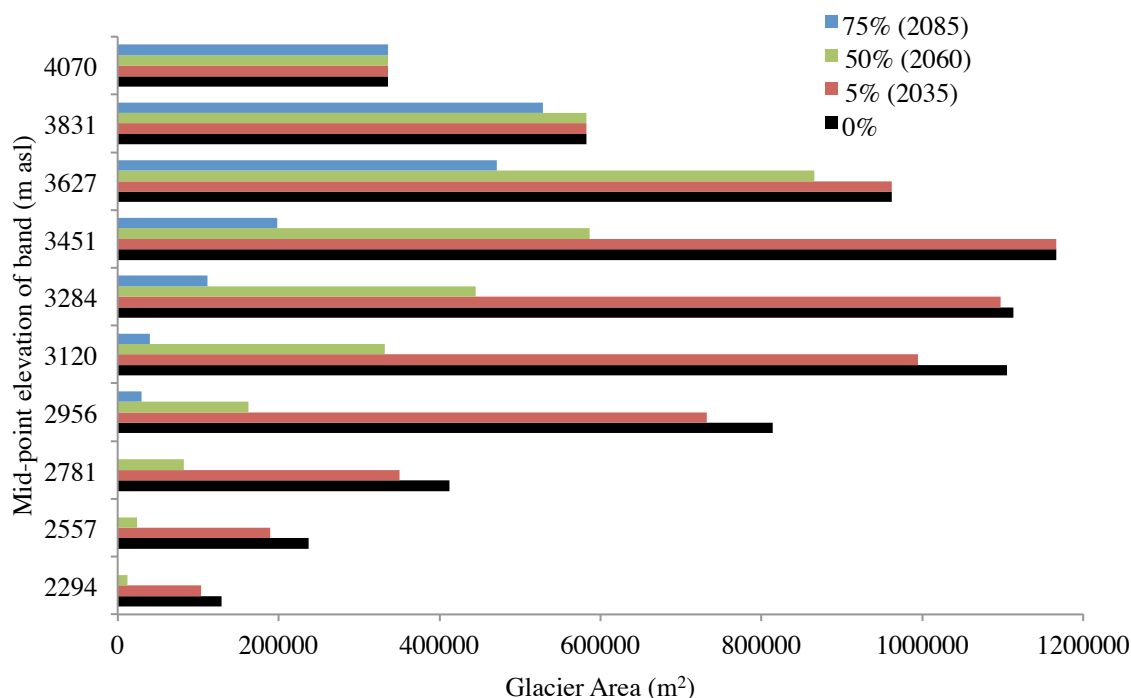


Figure 7.10: Hypsometric curve of Feegletscher Nord glacier area and the possible future area changes as applied to the model of 5% reduction by 2035, 50% by 2060 and 75% by 2085 as in Huss (2011).

As discussed in Chapter 6, the empirical relationship between snow and ice melt and air temperature is used to calculate glacier ablation through the use of degree-day factors, whereby melt is calculated as the amount of snow or ice melt which occurs during n time intervals, as a function of the sum of positive air temperatures of each time interval, with the factor of proportionality being the degree-day factor. Future changes in degree-day factors are also possible owing to their sensitivity to temperature changes (Pellicciotti *et al.*, 2005; Huss *et al.*, 2009) and variations in global radiation and turbulent heat fluxes (Braithwaite, 1995; Ohmura, 2001). In addition, there are a range of dynamics associated with deglaciation that may cause variations in degree-day factors due to changing albedos. These factors include increasing amounts of debris cover (Oerlemans *et al.*, 2009; Juen *et al.*, 2014) or changes in the ice, snow and firn proportions (Braithwaite, 2008). However, the specific relationships resulting in long-term variations in degree-day factors are not well established (Huss *et al.*, 2008; Huss *et al.*, 2014). In light of this uncertainty, the forward model adopted degree-day factors derived from the 2012 field data, described in Section 6.5.1. However, as longer-term

changes are possible and their resultant impacts undetermined, the influence of changes in degree-day factors was also explored by varying degree-day factors by 25% of the values utilised in FTIM (Section 6.5.1) for one climate scenario (A1B) in order to explore the influence of possible changes in ablation processes on future runoff and associated suspended sediment transfer.

Hourly runoff ($\text{m}^3 \text{ s}^{-1}$) was then simulated using FTIM (Chapter 6) for DOY180-251 for the range of time-periods and scenarios. FTIM routing components remained as described in Chapter 6 owing to the unknown impacts of climate change and glacier extent reductions on the hydrological drainage network configuration. The associated hourly SSC (g l^{-1}) was calculated using the multivariate regression equation derived from the model presented in Table 7.3:

$$\log SSC = -0.052 \log Q + 0.036 Q^2 - 8.1 \times 10^{-4} hQ! - 5.4 \times 10^{-9} \Sigma Q \quad (7.1)$$

whereby the predictor variables $\log Q$ (\log_{10} simulated discharge), Q^2 (square of simulated discharge), $hQ!$ (hours since discharge was last equalled or exceeded, initiated at DOY 180), and ΣQ (cumulative discharge, initiated at DOY 180) were recalculated for each simulation.

7.5.2 Future Perspectives for Glacier Runoff and Suspended Sediment Transfer

The model runs for the 21st Century indicate increases in glacier runoff of between 11.4 and 13.8 % for the period 2020-2049 relative to 1980-2009 that are then followed by rapid declines of between 78 and 86.2 % towards the end of the century, depending on the emission scenario (Table 7.7). These predictions are broadly in line with similar forecasts of runoff increases in the coming decades followed by significant reductions in summer discharges by the end of the century (e.g Huss *et al.*, 2010; Khadka *et al.*,

2014). This indicates that the additional runoff generated from water stored as snow and ice at the Feegletscher Nord due to a warmer climate will be offset by reductions in glacier extent by around mid-century, suggesting that the effect of the so-called ‘deglaciation discharge dividend’ (e.g. Kaser *et al.*, 2003; Collins, 2008) will be most pronounced in the coming decades. The results of future changes in suspended sediment loads are more pronounced, with increases of between 11 and 16.4 % for the period 2020-2049 relative to 1980-2009 followed by rapid decreases of between 91.9 and 95% towards the end of the century (Table 7.7). Mean SSC decreases by only around 50% towards the end of the century relative to the reference period, despite decreases of around 80% in mean discharge, emphasising the non-linear relationship between SSC and discharge. Somewhat counterintuitively, the decreases in suspended sediment loads towards the end of the century are largest for the RCP3PD scenario due to it predicting the smallest increases in air temperature resulting in reduced meltwater generation compared to the other scenarios. However, the assumption of identical mass losses as applied here for each of the scenarios is likely to be unrealistic and does not lend itself to comparability between scenarios as glacier extent reductions were applied prescriptively and not according to changes in air temperature, owing to uncertainties in both the mass balance of the Feegletscher Nord and how future glacier extents will be associated with changes in air temperature. Despite this, however, the use of a range of indicative possible scenarios of future glacier extent is a fruitful avenue for exploring possible changes in sediment transfer and associated glacio-fluvial sediment loads, for which there is a paucity of data from *in situ* derived data-series (Warburton *et al.*, 2007; Pralong *et al.*, 2015). Table 7.8 indicates only minor deviations from these reductions in SSL and runoff with changes of $\pm 25\%$ in degree-day factors, with SSL differing by $\pm 2\%$ and runoff by $\pm 5\%$ for 2070-2099 compared to 1980-2009. The most pronounced predicted impact with variations in degree-day factors is for the period 2020-2049,

when the deglaciation discharge dividend is greatest, owing to the minor (5%) simulated reductions in glacier extent. For this period, SSL is predicted to increase by 209% relative to 1980-2009 for a 25% increase in degree-day factors, whilst a 25% reduction in degree-day factors results in a 43% decrease in SSL relative to 1980-2009.

Figure 7.11 highlights the pronounced declines in seasonal suspended sediment loads and demonstrates the significance of reductions in glacier extent in determining these loads, despite the increased air temperatures and precipitation reductions predicted in each of the scenarios. The results of all three scenarios predict rapid and pronounced decreases in runoff and suspended sediment loads following relatively minor increases in the coming decades compared to the reference period. The effect of glacier extent reductions (50% relative to 2012) is responsible for much of the large decline in the seasonal suspended sediment load between 2020-2049 and 2045-2074 (Figure 7.11), which is also influenced by the reductions in glacier area being weighted to lower elevations where meltwater generation is greatest. The predictions also suggest that contemporary water and sediment loads may be around their peak for this century, if the assumed glacier extent reductions are realised. However, the aggregated predictions demonstrate the dominance of variations in meltwater production in the determination of future suspended sediment yields from glaciated catchments (Pralong *et al.*, 2015) and highlight the uncertainties in these predictions in the absence of more detailed forecasts of future glacier extents. For example, the area of the glacier in contact with the ice-bedrock interface is a strong determinant of glacial erosion, therefore, reductions in glacier area may decrease suspended sediment yields due to reduced sediment production (Hallet *et al.*, 1996). Sediment availability may also increase due to reductions in glacier extent as the proglacial area is extended, which may increase the number of sediment sources within the catchment. In addition, the development of proglacial lakes

that form as a response to glacier shrinkage can impact upon downstream sediment fluxes due to their capacity to act as both sediment sources and sinks (Smith, 1981; Carrivick & Tweed, 2013; Bogen *et al.*, 2015). Knowledge of these changes, in addition to further understanding of processes of ablation and sediment transfer during deglaciation, will be needed in order to refine forecasts of proglacial suspended sediment loads. Furthermore, despite the decline in glacio-fluvial suspended sediment loads predicted here, questions are raised as to the extent to which the increase of sediment availability associated with deglaciation over the paraglacial period will offset this decline, as sediment availability was assumed to remain high in these simulations, which was suggested to be experienced at the Feegletscher Nord due to the dominance of Q^2 in the results of the multivariate regression models in Section 7.3. This may be an unrealistic assumption as sediment yield is expected to be highest immediately following the commencement of deglaciation (Church & Ryder, 1972), however, in the absence of data on the rates of paraglacial sedimentation and the impacts of ice loss on glacial erosion and the replenishment of forefield sediment stores, it is problematic to reliably characterise and forecast future changes in sediment availability (e.g. Orwin & Smart, 2004a). In addition, the influence of changing precipitation patterns was not able to be separately determined in these predictions, which is important as precipitation will form an increasingly greater portion of runoff as glacier extent reduces (Collins, 2008), despite predictions of summer reductions in precipitation (CH2011, 2011). The CH2011 (2011) predictions of reduced summer precipitation may possibly lead to a decline in sediment yields due to reductions in slope wash and sediment redistribution. However, the assessment of the influence of precipitation on proglacial SSC in Sections 7.3 and 7.4 suggested a complex relationship between rainfall and SSC that was associated with proglacial geomorphology and forefield sediment availability.

Table 7.8: Summary statistics of modelled changes in suspended sediment transport and meltwater runoff (Q) for DOY 180-251 according to predicted 21st Century climate changes under three emissions scenarios (A2, A1B and RCP3PD) and compared to 1980-2009 reference period and simulated time-series for 2012 based on FTIM (n = 1687). μ is mean average, σ is standard deviation and μ_Q is discharge-weighted mean average. Glacier extent was changed in these simulations according to the mid-year of each future time period: a 5% area reduction by 2035, 50% reduction by 2060, and 75% reduction by 2085.

SSC	1980 - 09	2012	2020 - 2049			2045 - 2074			2070 - 2099		
		(simulated)	A2	A1B	RCP3PD	A2	A1B	RCP3PD	A2	A1B	RCP3PD
μ (g t ⁻¹)	0.2	0.24	0.22	0.22	0.22	0.12	0.12	0.12	0.11	0.11	0.1
σ (g t ⁻¹)	0.21	0.32	0.2	0.21	0.2	0.02	0.02	0.02	0.01	0.01	0.02
Average SSL (kg h ⁻¹)	2104	2854	2335	2450	2393	469	474	390	171	156	106
μ_Q	0.1	0.11	0.1	0.1	0.1	0.12	0.12	0.13	0.24	0.26	0.37
Σ SSL (tonnes)	3550	4777	3939	4133	4037	792	780	657	289	263	179
SSL change to 1980-09 (%)	-	34.6	11	16.4	13.7	-77.7	-78	-81.5	-91.9	-92.6	-95
Q	1980 - 09	2012	2020 - 2049			2045 - 2074			2070 - 2099		
		(simulated)	A2	A1B	RCP3PD	A2	A1B	RCP3PD	A2	A1B	RCP3PD
μ (m ³ s ⁻¹)	2.02	2.26	2.25	2.3	2.28	1.03	1.04	0.88	0.44	0.4	0.28
σ (m ³ s ⁻¹)	1.21	1.24	1.21	1.21	1.21	0.49	0.49	0.47	0.21	0.2	0.17
Average hourly runoff (m ³ h ⁻¹)	7261	8077	8108	8282	8197	3701	3729	3171	1583	1449	1010
Σ Runoff (10 ⁶ m ³)	12.3	13.7	13.7	14	13.9	6.3	6.3	5.4	2.7	2.5	1.7
Runoff change to 1980-09 (%)	-	11.4	11.4	13.8	13	-48.8	-48.8	-56.1	-78.0	-79.7	-86.2

Table 7.9: Summary statistics of modelled changes in suspended sediment transport and meltwater runoff (Q) for DOY 180-251 with $\pm 25\%$ variations in degree-day factors (DDFs) according to scenario A1B and compared to 1980-2009 reference period and simulated time-series for 2012 (n = 1687). μ is mean average, σ is standard deviation and μ_Q is discharge-weighted mean average. Simulated future time periods are denoted by the mid-year of the time period.

SSC	1980-09	2012 (simulated)	DDF + 25 %			DDF - 25 %		
			2035	2060	2085	2035	2060	2085
μ (g l ⁻¹)	0.2	0.24	0.39	0.13	0.11	0.16	0.12	0.1
σ (g l ⁻¹)	0.21	0.32	0.85	0.03	0.01	0.09	0.02	0.01
Mean SSL (kg h ⁻¹)	2104	2854	6501	639	197	1201	338	117
μ_Q	0.1	0.11	0.14	0.1	0.22	0.09	0.15	0.34
Σ SSL (tonnes)	3550	4777	10967	1078	331	2026	571	198
SSL change to 1980-09 (%)	-	34.6	208.9	-69.6	-90.7	-42.9	-83.9	94.4
Q	1980-09	2012 (simulated)	DDF + 25 %			DDF - 25 %		
			2035	2060	2085	2035	2060	2085
μ (m ³ s ⁻¹)	2.02	2.26	2.85	1.28	0.5	1.75	0.79	0.31
σ (m ³ s ⁻¹)	1.21	1.24	1.49	0.6	0.24	0.95	0.39	0.16
Average hourly runoff (m ³ h ⁻¹)	7261	8077	10256	4614	1790	6307	2843	1109
Σ Runoff (10 ⁶ m ³)	12.3	13.7	17.3	7.8	3.0	10.7	4.8	1.9
Runoff change to 1980-09 (%)	-	11.4	40.7	-36.6	-75.6	-13	-61	84.6



Figure 7.11: Modelled total suspended sediment loads for DOY 180-251 from the reference period 1980-09 and 2012 to the end of the 21st Century given by the mid-year of each future time-period (2020-2049, 2045-2074, 2070-2099) according to the three emissions scenarios (A2, A1B, RCP3PD).

7.6 Summary

This chapter has presented the analysis of relationships between suspended sediment concentrations and discharge along with an examination of factors, such as precipitation, that can influence these relationships. An exploratory model was developed in order to explore possible future changes in sediment transfer under possible future climate change scenarios. The key findings of these analyses are summarised here:

- Simple linear regression relationships between discharge and SSC were unsuitable for simulating suspended sediment transfer as they accounted < 36

% of the variance in SSC for the monitoring period. This was unsurprising given the complexities in sediment transfer processes suggested in Chapter Six.

- Multivariate regression models constructed with discharge-based predictor variables were able to account 58% of the variance in total proglacial SSC and not less than 50 % of the variance at individual gauging stations.
- There was a dominance of Q^2 as a predictor in all models, suggesting a non-linear relationship between SSC and discharge that was interpreted as reflecting high sediment availability. However, other sediment transfer processes were revealed to be complex in nature, with spatial and temporal variability in the nature and strength of the other predictor variables of different models.
- The results reinforced previous findings of spatially variable proglacial sediment transfer processes (e.g. Orwin & Smart, 2004a; Leggat *et al.*, 2015). The results for Station C suggested the presence of readily-mobilised in-channel or channel marginal sediment sources that experienced exhaustion over the ablation season, whereas results for Stations B and D suggest that sediment stores experience rapid exhaustion, increased surface armouring or a paucity of fine material. Station B experienced an unusual seasonal increase in sediment availability whilst Station C experienced seasonal exhaustion.
- It is likely that proglacial surface characteristics are important in controlling the nature of proglacial sediment availability and accessibility, as Station B was located in an area of reworked paraglacial rock avalanche debris and consolidated hummocky moraine and glacio-fluvial deposits were adjacent to Station C.
- Examination of the model residuals revealed no clear and consistent relationships with rainfall. Rainfall typically coincided with over predictions of SSC, suggesting a lack of extra-channel sediment mobilisation, a dilution

effect, or the suppression of ablation due to the associated precipitation-bearing weather systems. Hysteresis relationships suggested a link between SSC response to rainfall and extra-channel sediment availability.

- Associations between air temperature and residual SSC were characterised by under-predictions of SSC in the first part of the ablation season followed by over-predictions from DOY 217, indicating diurnal and seasonal sediment exhaustion.
- The coupling of the MRM for total proglacial SSC and the temperature-index runoff model for the Feegletscher Nord predicted rapid and pronounced decreases in runoff ($> 78\%$) and suspended sediment loads ($> 90\%$) towards the end of the century under all three emissions scenarios. The predictions also suggest that contemporary water and sediment loads may be around their peak for this century.
- Despite the possible future temperature, precipitation and albedo changes, the predictions demonstrate the dominance of reduced glacier extent and associated reductions in meltwater runoff in determining suspended sediment loads. The assumptions and uncertainties in future mass loss need to be addressed if these projections are to be refined. The results also raise questions as to the extent to which the increase in sediment availability associated with deglaciation over any 'paraglacial period' will offset this decline.

In summary, it is apparent that sediment transfer at the Feegletscher Nord is strongly associated with hydrological process of meltwater runoff and the catchment generally experiences very high sediment availability. Echoing the findings of Chapter 5, important spatial differences were found in sediment transfer processes and sediment sources, particularly obvious at Stations B and C. However, a paucity of field data from

other locations (Stations A and D) precluded further insights from other proglacial locations. This chapter has built on the previous findings to suggest that these differences appear to relate more to sediment source characteristics rather than distinct glacio-fluvial sediment transfer processes. This finding is significant, as Stations B and C are assumed to have experienced the same time since deglaciation, a factor which has been previously linked to spatial differences in proglacial sediment transfer patterns (e.g. Orwin & Smart, 2004a). This emphasises the potential complexities and uncertainties in utilising proglacial records of SSC for studies seeking to understand glacier dynamics as glacio-fluvial transfer relationships can be modified within recently deglaciated forefields.

The exploration of future suspended sediment loads suggests rapid decline until the end of the century associated with a decrease in runoff due to reductions in glacier extent which draws comparisons to other hydrological and sediment transfer forecasts of forthcoming declines in water and sediment loads (e.g. Huss *et al.*, 2010; Pralong *et al.*, 2015). However, the extent to which these declines may be offset by enhanced sediment availability due to the exposure of previously ice-covered areas is unknown and is identified, along with the refinement of mass loss estimates, as a future research priority for understanding glacio-fluvial sediment transfer during enhanced deglaciation.

8 Synthesis and Conclusion

8.1 Introduction

The overall aim of this thesis was to examine the controls on suspended sediment transfer at the Feegletscher Nord in light of the range of possible glacial, fluvial and proglacial controls on fluvial sediment loads and the extent to which these processes may be associated with processes of, and responses to, deglaciation. A changing climate is predicted to continue the already pronounced deglaciation that is occurring in the cryosphere (e.g. Ramillien *et al.*, 2006; Rignot *et al.*, 2008; Farinotti *et al.*, 2009; van den Broeke *et al.*, 2009), leading to uncertainties as to the impact of deglaciation and changes in air temperature and precipitation upon glacier runoff (Collins & Crescent, 2007; Huss *et al.*, 2014). Consequently, these changes are likely to have resultant impacts upon glacio-fluvial sediment transfer due to the significance of meltwater runoff in mobilising and transporting sediments in glaciated catchments (Diodato *et al.*, 2013). The availability of sediment in glaciated catchments is an important control on the rates of sediment transfer (Hallett *et al.*, 1996; Alley *et al.*, 1997; Swift *et al.*, 2005b), particularly those transiently stored in the proglacial zone, the mobilisation of which has been found to impact upon sediment transfer patterns and form substantial components of total glacio-fluvial sediment loads (e.g. Gurnell, 1982; Warburton, 1990; Hodgkins *et al.*, 2003; Richards & Moore, 2003). However, the controls on proglacial sediment availability are poorly constrained due to apparently complex processes of sediment storage and mobilisation within the proglacial zone, which can occur at a range of timescales (e.g. Hodgkins *et al.*, 2003; Orwin & Smart, 2004a). Elevated sediment yields are expected to occur during deglaciation due to the progressive exposure and downstream cascade of unstable glacial sediments (Church & Ryder, 1972; Ballantyne, 2002a). However, processes of sediment transfer and controls on

sediment availability in deglaciated forefields appear complex (e.g. Orwin & Smart, 2004a; Leggat et al., 2015), resulting in spatial and temporal variability in sediment fluxes within proglacial zones (e.g. Hodgkins *et al.*, 2003; Orwin & Smart, 2004a). Enhanced geomorphological activity during deglaciation is also likely to impact upon patterns of sediment transfer, resulting in complex slope-glacio-fluvio linkages (e.g. Curry *et al.*, 2009; Porter *et al.*, 2010; Carrivick *et al.*, 2013; Cook *et al.*, 2013). The potential for this activity to enhance rates of sediment transfer raises questions as to what constitutes typical sediment yields during the ‘paraglacial period’, a notion that has proved hard to interpret in light of the influence of paraglacial controls in determining the availability of glacial sediment for subsequent entrainment and evacuation by fluvial processes (e.g. Orwin & Smart, 2004a). This suggests that the quantification of contemporary sediment transfer patterns and yields during deglaciation requires careful consideration and interpretation in light of the range of potential hydrological and geomorphological responses to deglaciation. However, the understanding of linkages between meltwater runoff, sediment transfer and deglaciation dynamics are limited and require investigation, particularly if the impacts upon rates of sediment transfer are to be quantified and subsequently used for the forecasting of suspended sediment yields, the interpretation of sedimentary records and landforms, reconstructions of erosional history, and the prediction of landscape response to deglaciation (Lønne & Lyså, 2005; Lukas *et al.*, 2005; Warburton, 2007).

Therefore, this programme of research was undertaken with a view to characterising those controls and applying them in an exploratory model to predict possible future changes in sediment loads with progressive deglaciation, associated with a changing climate. An integrated approach was taken for this work, combining field data collection methods and analytical techniques adapted and developed from a wide range

of studies on glacier hydrology and glacio-fluvial sediment transfer (e.g. Richards *et al.*, 1996; Hodson & Ferguson, 1999; Hannah *et al.*, 2000; Hannah & Gurnell, 2001; Hodgkins *et al.*, 2003; Orwin & Smart, 2004a; Irvine-Fynn *et al.*, 2005a; Swift *et al.*, 2005b; Leggat *et al.*, 2015). These findings are discussed in this chapter in order to address the overall aim of this research with particular consideration to the implications of these findings for understanding the sedimentary system in glaciated catchments during deglaciation.

It is useful here to reiterate the objectives of this programme of research at the Feegletscher Nord:

- To scrutinise proglacial stream discharge hydrographs and suspended sediment records to establish the dominant controls on suspended sediment entrainment and transport and the nature of spatial and temporal variability in these records.
- To investigate water and suspended sediment transfer through the proglacial environment in order to identify the controls on proglacial discharge and suspended sediment concentrations.
- To simulate glacier runoff through the creation of a glacier melt model in order to establish the controls on meltwater production and routing and subsequently, predict meltwater generation under a range of climate change scenarios.
- To compare the simulated runoff time-series to measured proglacial discharge in order to elucidate the functioning of the glacier hydrological system, with consideration of the implications for sediment entrainment and evacuation by meltwater.
- To combine the characterisation of glacio-fluvial suspended sediment transfer processes with the glacier runoff model in order to explore potential future changes in proglacial sediment loads under future climate change scenarios.

Section 8.2 presents a discussion of the findings of this research programme, where the significant findings with respect to glacier hydrology are outlined and discussed in Section 8.2.1. In Section 8.2.2 these findings are discussed with respect to glacio-fluvial sediment transfer, while the consequent implications for the understanding of sediment transfer dynamics in deglaciating catchments are discussed in Section 8.2.3. The synthesis of these findings is presented in Section 8.3 in order to address the aim of the programme of research in this thesis, which was to advance understanding of the glacio-fluvial sedimentary system during enhanced deglaciation. Section 8.3.3 identifies potential avenues for future research and Section 8.4 summarises and concludes the key findings of this research.

8.2 Research Synthesis

8.2.1 Hydrology of the Feegletscher Nord

Characterisation of the hydrology of the Feegletscher Nord was undertaken due to the coupling of discharge and the glacio-fluvial sedimentary system, whereby suspended sediment concentrations and loads were found to be strongly associated with meltwater runoff. Detailed understanding of the drivers of ablation and the controls on the resultant proglacial hydrograph characteristics was needed in order to establish the relationships between meteorological forcing, ablation and runoff allowing the development of a model capable of simulating glacier runoff and, subsequently, proglacial SSC. The variety of research methods employed in this research revealed a number of key findings with respect to glacier hydrology:

- Firstly, an efficient hydrological system appeared in operation at the Feegletscher Nord with limited seasonal changes in competency.

- Secondly, the storage of meltwater within the glacier was apparently dominated by short-term storage, the release of which appeared to drive overnight discharges around hydrograph minima.
- Thirdly, a temperature-index approach was effective in simulating glacier ablation, however, complex findings with respect to storage processes limited the effectiveness of the model in simulating hourly runoff and required derivation of a two-component routing model to arbitrarily account for quick-flow and delayed-flow.
- Finally, glacier ablation was simulated more accurately when the degree-day factors increased with time over the ablation season.

These key findings are discussed in greater depth in the following sub-sections in order to infer their consequences for the understanding of temperate glacier hydrology and the potential hydrological response of glaciers to progressive deglaciation and mass loss.

8.2.1.1 Hydrological System

The findings of pronounced diurnal runoff cycles and very short time-lags between air temperature and proglacial discharge in Section 5.3.1 (mean = 40 minutes for DOY 180–241) indicate rapid throughput of meltwater from the glacier surface and through the hydrological system to the proglacial zone. Whilst in part this may represent the high gravitational potential of meltwater as a result of the steep setting of the glacier, it suggests both the significance of meteorological drivers of ablation and a dominance of an efficient subglacial drainage network, drawing comparisons to proglacial hydrographs recorded at other Alpine glaciers that have shown strong diurnal variations associated with meteorological variables and rapid meltwater throughput during the mid

to late ablation season when predominantly efficient subglacial drainage systems were in operation (e.g. Nienow *et al.*, 1998; Swift *et al.*, 2005a). This is a general interpretation supported by the high suspended sediment concentrations in the proglacial streams observed in this study, suggesting the likelihood of processes of sediment entrainment by meltwater at the ice-bed interface, in addition to potential proglacial sediment entrainment, which is discussed later in this Chapter. However, the characterisation of hydrograph shapes and magnitudes in Section 5.5.1 revealed only minor changes in the shape of the diurnal hydrographs throughout the monitoring period with a slight decrease in the time-to-peak from around DOY 209 which coincided with an increase in mean daily discharge. Therefore, the results also suggest an efficient drainage system was already established and well developed by the commencement of monitoring at DOY 180, which would support the findings of Collins (1979) that conduits at the Feegletscher adjust rapidly to early ablation season inputs, and suggests the Feegletscher Nord is likely to be similar to other temperate Alpine glaciers in this respect, where the up-glacier extension of conduits has been associated with inputs of surface melt in the early ablation season (e.g. Nienow *et al.*, 1998).

However, the hydrograph form is controlled not only by drainage system competency but also by changes in the rate and quantity of melt delivery from the glacier surface (Flowers, 2008; Swift *et al.*, 2005; Covington *et al.*, 2012; Gulley *et al.*, 2012a). The limited transition in hydrograph form from DOY 180 suggests a lack of further drainage system evolution or the limited effects of snowline retreat and associated decreases in albedo. The latter two points were difficult to ascertain from field observations and the measurements of ablation, which displayed increased degree-day factors over the monitoring period. This raises the possibility that limited drainage network evolution due to up-glacier conduit extension occurred after DOY 180, which

is surprising considering that the progressive extension of conduits was detected to occur throughout the ablation season until late summer at other Alpine glaciers such as Haut Glacier d'Arolla, although this extension of conduits was found to occur at a reduced rate later in the ablation season compared to early summer by Nienow *et al.* (1998). Consequently, uncertainties are apparent regarding the hydrological system dynamics at the Feegletscher Nord.

Possible causes of the observed seasonal drainage system dynamics include the steep topographic setting of the Feegletscher Nord. Steep glacier beds create conditions favourable to conduit development due to meltwater possessing higher gravitational potential that results in increased potential energy available for melt. Consequently, such glaciers would be expected to exhibit earlier transitions from distributed to conduit-based hydrological systems compared to those with shallower or adverse bed slopes (Flowers, 2008). A further consideration is the heavily crevassed ice structure over much of the Feegletscher Nord, suggesting a permeable ice structure that would allow for the throughput of meltwater over a wider area in comparison to glaciers where inputs of meltwater are confined to discrete supraglacial drainage features such as moulins (Fountain & Walder, 1998; Flowers & Clarke, 2002). This observation draws comparisons to so-called 'fracture flow' that has been noted to permit the transfer of meltwater where sub-surface fractures or crevasses create pathways for meltwater (e.g. Boon & Sharp, 2003; Fountain *et al.*, 2005; Irvine-Fynn *et al.*, 2005b; van der Veen, 2007). Such features have been found to link supraglacial, englacial and hydrological systems and result in rapid meltwater input to the base of glaciers (van der Veen, 2007). Glaciers with numerous crevasses or fractures have been hypothesised to experience drainage systems comprised of 'fracture networks' (Fountain *et al.*, 2005; Irvine-Fynn *et al.*, 2005b) due to the significance of such hydrological features upon glacier

hydrology, whereby fractures can exert controls on the locations of subglacial drainage features and drainage system dynamics (e.g. Boon & Sharp, 2003; Irvine-Fynn *et al.*, 2005b). If the crevassed structure of the Feegletscher Nord permits rapid throughput of melt to a subglacial drainage network, as the short lag-times between meteorological and discharge variables show, such a ‘fracture network’ may have also dampened the temporal changes in lag-times over the season due to a lack of conduit extension upglacier where the crevassing is most extensive. However, this hypothesis was unable to be tested owing to an absence of *in-situ* observations of crevasse depth and hydrological connectivity due, in part, to the lack of surface accessibility for tracer studies.

A final possible cause of the observed seasonal dynamics in meltwater throughput and the apparently rapid development of a ‘fast’ drainage system could include the inter-annual preservation of conduits. It has been suggested that it is possible for conduits to survive over winter when they would typically be expected to close due to the processes of creep closure (Nienow *et al.*, 1998). It was determined that conduits at Haut Glacier d’Arolla extending a short-distance (700 m) upglacier from the snout could survive the winter due to the low ice-thicknesses (of < 90 m) in this region that would minimise creep closure rates due to low ice overburden pressures. This conduit preservation was hypothesised to promote drainage system evolution in early summer. Ice thicknesses beneath the Feegletscher Nord are unknown, however, ground penetrating radar surveys of the Feegletscher Sud have found maximum ice thicknesses of between 67-73 m at elevations ranging from *c.* 2900 to 3460 m asl (Urbini, 2012, *pers comms*; Urbini & Baskaradas, 2010), suggesting ice thicknesses may be low at similar elevations of the Feegletscher Nord, which comprise around 60% of the glacier extent. This raises the possibility that ice overburden pressures create conditions conducive to

the preservation of conduits at the Feegletscher Nord, as determined by Nienow *et al.* (1998) at Haut Glacier d'Arolla. Such a hypothesis may have important implications for the understanding of glacier hydrology, as it suggests a link can be drawn between hydrological system characteristics and deglaciation. If progressive ice-thickness reductions during deglaciation reduces rates of conduit closure, then the presence of perennial drainage features at temperate Alpine glaciers has important implications for meltwater throughput. Perennial subglacial conduits would permit rapid meltwater throughput over the ablation season, with similarly efficient rates of glacio-fluvial sediment transfer. However, the possible presence of long-lived drainage features raises questions as to the resultant impacts upon subglacial sediment availability, which is strongly determined by the morphology and dynamics of the glacier drainage system (e.g. Swift *et al.*, 2005a). Therefore, it is uncertain as to whether high subglacial sediment availability could be sustained with progressive deglaciation, due to the possible exhaustion of stores of basal sediment within and adjacent to perennial conduits, a possibility which has been discussed from observations at other temperate Alpine glaciers (e.g. Swift *et al.*, 2002).

8.2.1.2 Meltwater Storage

The interpretation of hydrograph recessions presented in Section 5.4.1 revealed a dominance of short-term meltwater storage within the glacier that was interpreted as reflecting storage in ice reservoirs such as crevasses, the supraglacial active layer, subglacial sediments or within the hydrological system. This was supported by the findings that overnight discharges around the hydrograph minima were poorly associated with meteorological forcing variables and, instead, drainage from these storage reservoirs was hypothesised to be the significant driver of discharge during these periods. A smaller number of reservoirs were attributed to storage in snow reservoirs and these displayed a weak declining trend in storage coefficients, which is

likely to be attributed to snowpack decline and removal. Ice reservoir coefficients displayed a lack of seasonal trend indicating that the characteristics and nature of the storage reservoirs may not significantly change over the ablation season, suggesting they may be a perennial physical characteristic of the glacier. Therefore, these short-term storage mechanisms could be conceptualised as a distributed hydrological system, whereby meltwater becomes stored during the diurnal cycle in reservoirs, such as crevasses or sediments, due to limited flow capacity and competency (e.g. Hubbard *et al.*, 1995). The evidence from the results in this thesis might suggest the Feegletscher Nord drainage system is comparable to other glaciers in the Alps, and could, therefore, be characterised as comprising discrete conduits that are surrounded by a distributed system of limited efficiency, whereby meltwater is transferred into conduits from the surrounding reservoirs, with the rate of transfer driven, in part, by variations in subglacial water pressures in the conduits (e.g. Hubbard *et al.*, 1995; Fountain & Walder, 1998; Nienow *et al.*, 1998; Swift *et al.*, 2002). This interpretation would account for the lack of association between air temperature and discharge during the minima in the diurnal cycle, as discharge during these periods was instead being predominantly forced by the release of stored meltwater as inferred from water pressure variations in boreholes at Haut Glacier d'Arolla by Hubbard *et al.* (1995). In light of the hypothesis that the highly crevassed surface at the Feegletscher Nord may be a significant pathway in the routing of supraglacial melt to the subglacial hydrological system (e.g. Fountain *et al.*, 2005), this may offer a potential explanation that is physically based that accounts for the observed short-term storage of meltwater, whereby meltwater becomes stored in crevasses during the day which is then drained into conduits overnight, and hence, becomes a significant component of drainage during low discharges, as suggested from the hydrograph records.

The implications of such a hydrological configuration for sediment transfer would be that meltwater would be able to readily-access subglacial sediments and transport them efficiently through the conduit system (Hubbard *et al.*, 1995; Alley *et al.*, 1997; Swift *et al.*, 2002). This is apparently supported by the findings of a strong dependence of SSC on discharge, the generally high suspended sediment loads from the Feegletscher Nord, and the results of the multivariate regression modelling of SSC which are further discussed in Section 8.2.2. Consequently, this characterisation of the hydrology of the Feegletscher Nord largely conforms to our understanding of the hydrology of temperate and Alpine glaciers, whereby meltwater is routed through a ‘fast’ drainage system that has access to the ice-bed where stores of sediments can become entrained by meltwater and transported downstream (e.g. Richards *et al.*, 1996; Hubbard & Nienow, 1997; Fountain & Walder, 1998; Nienow *et al.*, 1998; Swift *et al.*, 2005a). These subglacial stores of sediment would be expected to experience exhaustion at a range of timescales as meltwater evacuates available sediment (e.g. Swift *et al.*, 2005b), particularly if a central conduit is the dominant meltwater pathway. It is, however, important to note that the lack of dynamics within the storage coefficients for ice reservoirs is unusual, as these have been found to typically decline over the ablation season due to increased hydraulic connectivity in the drainage system (e.g. Richards *et al.*, 1996; Hannah & Gurnell, 2001; Jobard & Dzikowski, 2006). However, the results in this research show some similarity to the pattern of results observed at a small ‘remnant glacier’, Taillon Glacier, France, where limited seasonal changes in ‘fast’ meltwater routing components were observed which was attributed to a lack of subglacial drainage system evolution over the ablation season, and instead, highlighted the role of snowline retreat in the determination of the resultant hydrograph (Hannah & Gurnell, 2001). Therefore, further questions are raised regarding the seasonal dynamics of the subglacial drainage system and the resultant controls on the

proglacial hydrograph at the Feegletscher Nord. Specifically, uncertainties are highlighted regarding the timing and extent to which seasonal evolution and rationalisation of the subglacial drainage system occurs. The potential comparisons between the observations at the Feegletscher Nord and small or non-temperate glaciers raise important questions as to the extent to which these hydrological characteristics may be associated with deglaciation dynamics, specifically regarding the role of reduced ice-thickness in controlling meltwater routing and storage, the investigation of which has been limited to a small number of studies (e.g. Hooke, 1984; Nienow *et al.*, 1998; Flowers, 2008). Furthermore, it is apparent that the processes of, and controls on, meltwater storage within glaciers are poorly constrained (Jansson *et al.*, 2003), due, in part, to limited access to the englacial and subglacial environment and a consequent reliance on inverse approaches. Therefore, it is clear that there are uncertainties in the ability to forecast future runoff from glaciers and glaciated basins in the absence of improved understanding of the influence of glacier shrinkage upon glacier hydrological systems (e.g. Huss *et al.*, 2014). Consequently, this constitutes a potential avenue for future research due to the forecasts of future changes in climate and mass loss from glaciers (e.g. Zemp *et al.*, 2006; CH2011, 2011), which is elaborated upon later in this Chapter.

8.2.1.3 *Simulation of Glacier Ablation and Runoff*

The Feegletscher temperature-index runoff model (FTIM) performed well in accounting for processes of ablation and simulating runoff along with the subsequent application of the model in simulating future potential changes in proglacial suspended sediment concentrations and loads, which are discussed later in this chapter. In particular, FTIM represents an advance in the development of temperature-index approaches through the ability of the model to account for diurnal cycles in runoff with only modest data requirements and physically-based parameters obtained from field

data. The high temporal resolution of the output addresses Hock's (1999) call for models capable of simulating diurnal melt cycles, whilst retaining modest data requirements and physically-justified parameters. Despite inputs of only air temperature and precipitation, FTIM produced good agreement between simulated and observed runoff, with around 64% of the variance in hourly runoff simulated and total runoff for the monitoring period was predicted to within < 3 %. A number of factors are hypothesised to be responsible for the unaccounted variance in the hourly time-series. Short-term routing or storage processes are suggested to be an important factor due to the greater accuracy of FTIM in predicting total runoff compared to hourly runoff, suggesting the processes responsible are likely to be operating over short-timescales. However, as the monitoring period fails to capture the full hydrological year, it is acknowledged that the assumption of zero net water storage within the glacier or catchment at the commencement and termination of the field season is unverifiable and also likely unrealistic.

Focussing upon short-term dynamics, examination of the simulated and measured runoff time-series revealed that model residuals were most pronounced during the peaks and troughs of the diurnal hydrograph. This suggests that much of the error in the model is likely to be attributed to the assumptions of constant storage volumes within the delayed-flow reservoir, as these are likely to vary with the volume of discharge and over time (e.g. Gurnell, 1993; Hock, 1999; Hannah & Gurnell, 2001; Jansson *et al.*, 2003), characteristics which were found in this research to be problematic to identify and subsequently parameterise into routing components (e.g. Gurnell, 1993). This was reinforced from the examination of the water balance between predicted and observed daily runoff in Section 6.5.3 that suggested the presence of storage processes occurring over time-scales of several days or more. These variations in net water storage appeared

as alternating periods of positive and negative water budgets that were of between two and seven days in duration, and, as such, not accounted for in the model's routing parameters. The parameters derived in FTIM accounted for processes of delayed or quick flow that occurred over periods of 1 to 15 hours (i.e. at similar temporal resolutions to the model). Due to the lack of data supporting the identification of these medium-term storage processes and the calibration of FTIM using total runoff as a criterion of model performance, the overall nature of the water budget of the Feegletscher Nord was not identified and Collin's (1979) hypothesis that the drainage of englacial or subglacial stored water occurred late in the ablation season was unverified. However, it cannot be discounted as a cause of the unexplained variance in simulated hourly runoff. In addition, despite generally strong associations between air temperature and ablation, complex relationships between glacier surface characteristics and ablation at short timescales are highlighted as a further possible cause of the unaccounted for variance in the hourly time-series of predicted runoff. For example, the Feegletscher Nord is characterised by a heavily crevassed surface, which has the potential to enhance melt rates due to the increased surface area of crevassed regions and the penetration of air and meltwater below the glacier surface, consequently raising the temperature of the ice and enhancing rates of ablation (Weertman, 1973; Alexander *et al.*, 2011; Fleischer, 2014).

A further characteristic of the Feegletscher Nord with the potential to influence ablation processes is the largely debris-covered lowermost portion of the glacier (extending *c.* 1.2 km upglacier from the terminus). Ablation processes can be strongly influenced by the presence of debris-covered snow and ice as first demonstrated by Østrem (1959). However, the characteristics of local climate and debris lithology can result in complex ablation processes due to the capacity for debris cover to influence

surface albedo and act as both a source and sink of heat energy (e.g. Kirkbride & Warren, 1999; Kayastha *et al.*, 2000; Singh *et al.*, 2000; Takeuchi *et al.*, 2000; Mihalcea *et al.*, 2006; Nicholson & Benn, 2006; Hagg *et al.*, 2008; Huss *et al.*, 2008; Scherler *et al.*, 2011; Benn *et al.*, 2012). Furthermore, enhanced rates of supraglacial debris accumulation from ice-marginal sources has been observed with progressive deglaciation, resulting in transformations from ‘clean’ glaciers to those with substantial portions of debris-cover, particularly in the lowermost portions, which are likely to eventually become stagnant ice masses (Kellerer-Pirklbauer, 2008; Oerlemans *et al.*, 2009) and experience enhanced supraglacial water storage (e.g. Benn *et al.*, 2012). This suggests that slope-glacier linkages have the capacity to introduce complexity into processes of ablation and runoff, and therefore, understanding of the paraglacial response to deglaciation within a catchment is necessary for processes of ablation and runoff to be characterised. However, such linkages are poorly constrained, in part, due to limited observations of non-glacial sediment reworking and redistribution (e.g. Etzelmüller *et al.*, 2000; Etienne *et al.*, 2008; Oerleman *et al.*, 2009; Porter *et al.*, 2010). Consequently, uncertainties in ablation and runoff modelling attempts are likely to persist, particularly as *in situ* observations at a particular glacier or catchment will be needed to constrain model parameters that address the potential effects of deglaciation, such as increasing amount of debris cover, on ablation and resultant runoff (e.g. Kayastha *et al.*, 2000; Reid & Brock, 2010; Huss *et al.*, 2014).

The development of FTIM revealed simulations of glacier ablation and runoff to be improved with the application of temporally scaling degree-day factors, as opposed to those which are fixed and typically vary according to the location of the transient snowline or are indirectly varied through the incorporation of energy balance components into models (e.g. Hock, 1999; Braithwaite & Zhang, 2000; Pellicciotti *et*

al., 2005; Huintjes *et al.*, 2010; Irvine-Fynn *et al.*, 2014). The determination of degree-day factors from field measurements of ablation in Section 6.5.1 indicated increasing trends in degree-day factors over the monitoring period. This was supported by field observations from the Feegletscher, whereby increasing debris cover exposure as snow and surface ice was removed suggested surface albedo was likely to decrease over the ablation season, and draws comparisons to observations of seasonal declines in albedo (e.g. Brock *et al.*, 2000), which has been associated with changes in glacier surface properties such as snowpack depletion, debris cover, and the presence of organic matter (e.g. Takeuchi *et al.*, 2001; Dumont *et al.*, 2014; Edwards *et al.*, 2014; Lutz *et al.*, 2014). Such factors may be associated with enhanced deglaciation (e.g. Oerlemans *et al.*, 2009), raising the possibility of progressively complex runoff responses to meteorological forcing as glaciers shrink. A further consideration in the development of degree-day factors in FTIM was the topographic complexity of the Feegletscher Nord, which was not favourable to allow detailed identification of the spatial extent of the snowpack and the timing of the retreat of the transient snowline. As such, the application of temporally scaling degree-day factors in FTIM may be considered as a potential mechanism to account for seasonal changes in albedo in high resolution ablation models for glaciers with seasonal changes in surface conditions, or where complex surface conditions can introduce errors in spatially lumped melt models. This development is similar to alternative approaches where albedo is accounted for indirectly through the variation in radiation components over time (e.g. Pellicciotti *et al.*, 2005; Irvine-Fynn *et al.*, 2014) to account for the dependence of albedo on temperature (due to variations in snow cover) and the decline in albedo over time (associated with seasonal snowpack depletion). However, the determination of the physical basis of the mechanisms responsible was beyond the scope of this study and represents potential future research, which may have significant implications for the

modelling of runoff and associated glacio-fluvial sediment transfer at receding glaciers or those exhibiting topographic complexity.

8.2.2 Glacio-Fluvial Sediment Transfer

Assessment of glacio-fluvial sediment transfer at the Feegletscher Nord was undertaken in order to investigate the processes of, and controls on, proglacial suspended sediment concentrations. Proglacial SSC in the streams draining the Feegletscher Nord was hypothesised to be influenced by a range of glacial, proglacial and nonglacial processes, owing to the diverse range of controls on proglacial suspended sediment concentrations observed in proglacial zones (e.g. Gurnell, 1982; Warburton, 1990; Hodgkins *et al.*, 2003; Richards & Moore, 2003; Orwin & Smart, 2004a; Leggat *et al.*, 2015) and the potential for deglaciation to result in elevated rates of sediment transfer (Church & Ryder, 1972; Ballantyne, 2002). However, observations from recently deglaciated forefields have highlighted uncertainties regarding the controls on rates of paraglacial sedimentation, raising questions as to the ‘normal’ rates of sediment transfer to be expected in these environments (Orwin & Smart, 2004b). Typically, exploration of these processes through suspended sediment monitoring considers sediment transfer within a catchment as a black box and, consequently, will fail to capture the spatial and temporal variability of that activity within the catchment, consequently, hindering the identification and quantification of sediment sources, transfer processes and fluxes (Warburton 1990; Carrivick *et al.*, 2013). Therefore, sampling of proglacial SSC was undertaken through a number of spatially distributed sampling stations in the Feegletscher Nord forefield, and the subsequent analysis of the SSC and discharge time-series in Chapters 5 and 7 revealed a number of key findings with respect to glacio-fluvial sediment transfer:

- Firstly, proglacial SSC is strongly forced by processes of discharge, however, spatial variability between proglacial gauging stations exists in SSC transfer patterns and trends.
- Secondly, spatial variability in forefield sediment availability appears to be a strong/principal determinant of proglacial SSC and is hypothesised as one cause of the observed spatial variability in sediment transfer patterns.
- Thirdly, the Feegletscher Nord catchment appears to experience generally high sediment availability with a lack of seasonal dynamics in availability during the observation period.
- Finally, these findings of variability in sediment transfer patterns within the forefield suggest complex sediment transfer processes can exist and operate even within the same basin, which has important implications for the interpretation of SSC time-series and the development of models to predict SSC.

These key findings are discussed in the following sub-sections in order to better understand the processes responsible for the observed suspended sediment patterns and infer their consequences for the characterisation of sediment transfer processes and their rates in deglaciating environments.

8.2.2.1 Patterns and Trends in Proglacial SSC

The time-series of proglacial SSC recorded at the Feegletscher Nord demonstrated strong diurnal forcing of proglacial SSC at all stations. Such patterns likely reflect the dominance of sediment entrainment and evacuation by meltwater that has access to a subglacial drainage network (e.g. Gurnell, 1987; Collins, 1990; Hallet *et al.*, 1996; Alley *et al.*, 1997; Swift *et al.*, 2002), however, the results of the Principal Components

Analysis and Cluster Analysis in Chapter 5 suggested sediment transfer patterns were modified in the proglacial zone. The high number of principal components ($n = 5$) retained at Station C was unusual in comparison to other studies (e.g. Orwin & Smart, 2004; Leggat *et al.*, 2015) and suggest particularly diverse controls on SSC at this location. Furthermore, only the first principal component displayed a discrete diurnal signature, suggesting considerable variability was introduced into the SSC time-series at this location. This was in contrast to Stations B and D, where fewer principal components were retained and, those which were, displayed stronger diurnal signals, which was interpreted as reflecting sediment transfer patterns that were more strongly associated with discharge forcing. Suspended sediment magnitude classifications indicated that Station C experienced higher mean SSC and SSL compared to Stations B and D. These were interpreted as indicating greater sediment availability at Station C compared to Stations B and D. Interestingly, the cross-tabulation of the shape and magnitude classes with discharge and meteorological data indicated a lack of clear association between high SSC or SSL and high discharges over the monitoring period, with no strong associations between irregular shape classes and meteorological variables, a link which has previously been found in similar studies (e.g. Orwin & Smart, 2004a). However, this analysis did suggest sub-seasonal variations in sediment availability may occur, whereby qualitatively stronger associations between SSL and mean daily discharge at Stations C and D were apparent after DOY 217, suggesting sediment availability may be higher at these locations in the early ablation season, as well as possibly more complex sediment transfer mechanisms due to the mobilisation of in-channel and channel-marginal sediments. Therefore, it is apparent that the sediment transfer patterns differed between the three monitoring stations, and in particular, the processes at Station C were different from those at Stations B and D. These results suggest the presence of both spatial and temporal variability in the input of easily

mobilised in-channel or channel-marginal sediments, and consequently, sediment flux within the Feegletscher Nord catchment has the capacity to vary in space and time. Observations of such spatial and temporal variability in proglacial environments are not unusual (e.g. Richards, 1984; Warburton, 1990; Orwin & Smart, 2004a; Leggat *et al.*, 2015), and hence, reinforces the challenges of characterising processes of glacio-fluvial sediment in deglaciating forefields and the need for representative (i.e. spatially distributed) monitoring strategies and long-term (i.e. inter-annual) data collection (e.g. Orwin *et al.*, 2010). The presence of variability in SSC transfer patterns, within even small a catchment such as the Feegletscher Nord and collected during a short-term and spatially distributed monitoring programme, suggest that extrapolating sediment transfer relationships and sediment fluxes to explore possible future changes will be challenging, due to apparently inherently complex drivers of SSC and a paucity of contemporary data sets that can reliably characterise sediment transfer processes and resultant sediment fluxes in deglaciating environments. Consequently, this research reinforces the notion that the ability to infer rates of sediment transfer and predict future changes in suspended sediment yields and resultant landscape modification from proglacial discharge and suspended sediment concentration time-series appears challenging.

8.2.2.2 *Controls on Proglacial SSC*

Insights into the physical processes and dynamics responsible for the observed spatial and temporal variability in proglacial suspended sediment concentrations were gained through multivariate regression modelling of SSC as discussed in Chapter 7. The regression models revealed a number of interesting findings, particularly regarding the complexity of controls on SSC in space and time. The models revealed the dominance of Q^2 as a strong predictor of SSC at all proglacial gauging stations, demonstrating a non-linear response of proglacial SSC to discharge that was interpreted as reflecting

generally high sediment availability in the catchment. There was also significant complexity in the nature and significance of the other predictor variables both in space and time. Examples of this complexity include the seasonal changes in sediment availability indicated by the ΣQ predictor. Station B was found to experience a seasonal increase in sediment availability, whilst Station C experienced a seasonal decrease, suggesting that, despite generally high sediment availability in the catchment, the seasonal availability of sediment was both spatially and temporally dynamic within the forefield. This finding corresponds to the results of studies that have found temporal changes in sediment availability within Arctic proglacial zones, controlled by runoff regimes (Hodgkins *et al.*, 2003), raising similar possibilities that the observed changes in sediment availability may represent within-catchment changes in sediment aggradation or degradation as a sediment budget equilibrium is sought. However, links between proglacial sediment storage or release and runoff regimes were not forthcoming in this research, likely owing to the lack of inter-annual data for comparison and data collection during only part of the 2012 ablation season.

Spatial and temporal variability in forefield sediment availability has been attributed to paraglacial sedimentation (e.g. Warburton, 1990; Orwin & Smart, 2004b), raising questions as to the extent which sediment availability in the Feegletscher Nord forefield is controlled by paraglacial sedimentation or fluvial processes of sediment redistribution and reworking. In addition, variations in SSC response to rainfall at the Feegletscher Nord were used to gauge forefield sediment availability, as such approaches have enabled links to be drawn between proglacial surface age and the extent of paraglacial sedimentation (e.g. Orwin & Smart, 2004b). Examination of the associations between SSC and rainfall in this research indicated SSC response to rainfall was found to be variable between locations and through time. Hysteresis relationships suggested that this

variability was likely associated with the amount of extra-channel fine sediment available to be mobilised at the different sampling locations, with Station C experiencing rapid mobilisation and exhaustion of sediments, compared to Station B where there was a limited SSC response to rainfall. This finding is noteworthy, as rainfall has generally been documented to result in the mobilisation and input of fine extra-channel sediments into proglacial streams (e.g. Richards, 1984; Richards & Moore, 2003; Leggat *et al.*, 2015), and has been used as a predictor in attempts to model sediment transport (e.g. Richards & Moore, 2003; Pralong *et al.*, 2015). The finding of distinct responses to rainfall between surfaces of assumed similar ages at the Feegletscher Nord suggests that, despite generally high sediment availability in the catchment, links between suspended sediment response and paraglacial sedimentation may be complicated by sediment characteristics within forefields, possibly as a result of perturbations such as paraglacial rock avalanches or the rejuvenation of sediment sources due to significant sediment redistribution and reworking by large floods. Consequently, it appears that links between sediment transfer patterns, sediment availability and paraglacial sedimentation in proglacial zones are not straightforward and the results of this research may constitute one example of sediment availability being controlled by geomorphological activity associated with deglaciation.

Furthermore, the generally high sediment availability in the Feegletscher Nord catchment and the apparent variability in forefield sediment availability is perhaps unsurprising given the presence of a number of potentially abundant sediment stores in the catchment, likely comprising stores of subglacial sediment (e.g. Alley *et al.*, 1997), the recently sedimented former proglacial lake located upstream of the gauging stations (e.g. Carrivick & Tweed, 2013; Bogen *et al.*, 2015), the sediments in the forefield that have been deposited and exposed due to the shrinkage of the Feegletscher Nord (e.g.

Church & Ryder, 1972; Ballantyne, 2002), and the debris from a large rock avalanche in 1954 (Cook *et al.*, 2013). Recently deglaciated forefields are expected to be characterised by a range of exposed and unstable surfaces that can be subject to reworking and remobilisation by fluvial processes and rainfall (e.g. Richards, 1984; Orwin & Smart, 2004), consequently, rates of sediment transfer at the Feegletscher Nord may be enhanced by the presence of forefield deposits associated with deglaciation. The availability of sediment within forefields due to the presence of sediment sources in the proglacial zone is expected to result in high sediment yields during, and soon after, deglaciation (Church & Ryder 1972; Maizels, 1979; Warburton, 1990), which would then decline due to paraglacial sedimentation as sediment availability reduces and surfaces stabilise and become resistant to mobilisation (Church & Slaymaker, 1989; Orwin & Smart, 2004a; 2004b). The apparently high sediment availability found at the Feegletscher Nord may suggest that deglaciation has resulted in the elevation of suspended sediment concentrations beyond their 'norm'. However, the diverse range of potential sediment sources in the Feegletscher Nord catchment raises questions as to what constitutes 'normal' suspended sediment yields during deglaciation. In addition, the nature and diversity of the range of potential sources in the Feegletscher Nord catchment suggests that the range of potential forefield sediment sources that can be mobilised by glacio-fluvial processes may be especially diverse in nature, even within a small forefield, resulting in distinct SSC responses to discharge and rainfall depending on the location of the gauging stations. For example, the sedimentation of the upper proglacial lake at the Feegletscher Nord, that appeared to occur within 10 years of its formation, is likely to have resulted in a switch from the lake acting a sediment sink to a source, drawing similarities to inter-annual variations in sediment production and storage that can occur in forefields (e.g. Hodgkins *et al.*, 2003). This raises the possibility that sediment availability in deglaciated forefields may

not necessarily scale with time since deglaciation, and instead, proglacial fluvial suspended sediment yields may predominantly reflect interactions between geomorphology and a range of glacial, fluvial and nonglacial sediment transfer processes. This would have significant implications for the understanding of rates of paraglacial sedimentation in deglaciating environments, as the controls on sediment availability may be especially diverse in nature and variable in space and time. This echoes Orwin and Smart's (2004a) finding that forefield sediment storage and release processes may hinder the identification of any 'paraglacial period'. Consequently, it is apparent from the Feegletscher Nord that knowledge of catchment sediment sources and their controls is likely to be needed before any assessment of 'normal' sediment transfer patterns, rates or yields can be made, without which, uncertainties are likely to arise in the interpretation of glacio-fluvial suspended sediment records in deglaciating catchments.

Other than the aforementioned findings with respect to sediment availability, there was a lack of consistency in the remaining insights offered by the MRMs. Unexplained variance in the models of SSC remained modest, as models at the seasonal and sub-seasonal scales accounted for an average of around 64% of the variance in SSC, suggesting complex SSC responses to discharge and the possible presence of stochastic sediment transfer mechanisms. A notable finding from the analysis in Chapter 7 was the lack of diurnal hysteresis as indicated by the general failure of ΔQ as a predictor. This is unusual for glaciers that have strong diurnal variations in discharge and SSC (e.g. Hodgkins, 1999; Hodson & Ferguson, 1999; Irvine-Fynn *et al.*, 2005a), whereby SSC would be expected to be higher during rising discharges than falling discharges due to the entrainment of in-channel sediments during rising discharges. It was hypothesised that this result may be an artefact of shifting the time-series of discharge predictors to

match SSC in order to ameliorate autocorrelation, or that it reflects stochastic sediment mobilisation. Furthermore, the regression coefficients for $\log Q$ and hQ' in the MRMs suggested complex SSC responses to discharge, whereby sediment mobilisation was not necessarily associated with higher discharges. For example, Station C demonstrated sub-seasonal trends in SSC forcing by discharge, whereby $\log Q$ was positive during the first part of the season and negative during the second part, suggesting that fluvial entrainment of in-channel or channel-marginal sediments was significant at this location early in the season. However, in the second part of the ablation season, $\log Q$ was negative, suggesting there was either a lack of mobilisation or the presence of a dilution effect at higher discharges. This is possibly a further indication of reduced sediment availability at this location later in the ablation season, which would be a result of the exhaustion of in-channel or channel-marginal sediment supplies. In addition, the lack of clear association between high discharges and high SSCs may also point to the stochastic delivery of sediments to the channel through processes of in-channel and channel-marginal sediment release, such as channel-bank collapse, which has been observed to occur in the stream at Station C (Hempel, 2009) and has been documented as a cause of stochastic SSC behaviour (e.g. Fenn, 1989; Clifford *et al.*, 1995; Hodson & Ferguson, 1999; Stott & Grove, 2001; Richards & Moore, 2003). Stochastic sediment supply processes that are unrelated to discharge have been commonly observed in SSC or turbidity records in proglacial zones, due to the presence of unstable and readily-mobilised glacial sediments through mechanisms such as channel-bank collapse (e.g. Hammer & Smith, 1983; Gurnell & Warburton, 1990; Hodson *et al.*, 1998; Orwin & Smart, 2004a). Evidence of such processes being coupled to paraglacial activity in Arctic basins (e.g. Porter *et al.*, 2010) has raised the possibility that such sediment mobilisation processes are likely to become more common with progressive deglaciation, due to an increased propensity in these environments for

geomorphological ‘paraglacial’ activity and an increased availability of sediment (Mercier, 2000). Therefore, if stochastic processes are indeed responsible for the observed suspended sediment concentrations at the Feegletscher Nord, these findings suggest that stochastic sediment transfer may constitute a characteristic of sediment transfer in deglaciating environments, with consequent uncertainties for the ability to characterise and simulate sediment transfer processes.

To attempt to summarise the findings with respect to the controls on proglacial suspended sediment transfer, it is apparent that the controls on proglacial SSC at the Feegletscher Nord exhibited spatial and temporal variability and were complex in nature. The insights into the sediment transfer processes in operation revealed a generally strong association between SSC and discharge, whereby increases in discharge resulted in greater increases in SSC, however, there were differences in the strength and of this relationship between the monitoring stations. The results here suggest that the mechanisms responsible for the unexplained variance in SSC may be stochastic, whereby sediment is input into streams due to mechanisms, such as channel bank collapse, at locations in the forefield where fine in-channel and channel-marginal sediments are available. Therefore, it appears that forefield fine sediment availability appears to be a strong control on the observed spatial and temporal variability in proglacial SSC, and is likely to be a dominant control on the modification of SSC patterns and magnitudes in deglaciating forefields. This reinforces findings that suspended sediment concentrations are, in part, controlled by complex interactions between sediment supply and glacio-fluvial processes of sediment transfer (e.g. Warburton, 1990; Harbor & Warburton, 1993; Hodgkins *et al.*, 2003; Richards & Moore, 2003; Orwin & Smart, 2004a), and importantly, the location of proglacial

channels and the extent to which they have access to sediment stores will exert controls upon the observed patterns and magnitudes of suspended sediment transfer.

The apparently marked spatial variability in sediment supply within the proglacial zone at the Feegletscher Nord, which is notable for the small area of the forefield (< 1 km²) and as recorded between short distances (*c.* 80m between Stations B & C), highlights the localisation in these controls on observed suspended sediment patterns within the forefield. This has important implications for the understanding of sediment transfer processes in deglaciating environments as it is hypothesised that these differences in sediment availability can be broadly linked to the sedimentology and abundance of forefield sediment deposits. Surfaces in the vicinity of the stream at Station C were characterised by glacial-fluvial deposits and reworked paraglacial debris (Curry *et al.*, 2009; Cook *et al.*, 2013) with field observations of weakly consolidated channel banks, resulting in both high sediment supply and processes of glacio-fluvial sediment transfer with resultant elevated rates of sediment transfer in this part of the proglacial zone. In contrast, surfaces adjacent to the stream at Station B comprised hummocky moraines formed of consolidated glacio-fluvial deposits and paraglacial rock avalanche deposits (Schnyder, 2012, *pers comms*; Cook *et al.*, 2013), resulting in limited in-channel and channel-marginal sediment availability. Therefore, these findings raises questions as to what constitutes 'typical' glacier forefield landsystems and associated processes of glacio-fluvial sediment transfer expected to operate in these environments.

The geomorphological and hydrological characteristics at the Feegletscher Nord proglacial zone could be described as an uncommon example of a recently deglaciating forefield, likely as a result of the glacier's somewhat complex responses to deglaciation,

characterised by multiple advances and retreats since the Little Ice Age. In addition, the impacts of the rock avalanche in 1954 that resulted in landforms and sediment assemblages that are strongly conditioned by this paraglacial debris (Cook *et al.*, 2013) constitutes a further example of processes of sediment transfer being potentially conditioned by paraglacial activity. Finally, the lack of significant areas of valley sandur or outwash plain within the Feegletscher Nord proglacial zone, as commonly seen to characterise deglaciated forefields, particularly in Arctic environments (e.g. Fenn & Gurnell, 1987; Hodson *et al.*, 1998; Hodgkins *et al.*, 2003; Marren, 2002), is notable due to the potential for these sandurs to act as sources or sinks of sediment, processes which can be controlled by glacio-fluvial sediment transfer (e.g. Warburton, 1990; Hodson *et al.*, 1998; Hodgkins *et al.*, 2003; Marren, 2002; 2005). Therefore, this research is presented as an example of how a range of deglaciation dynamics can influence proglacial suspended sediment transfer, contributing to the limited body of evidence on the possible impacts of such examples of geomorphological responses to deglaciation upon forefield sediment characteristics and resultant sediment transfer.

However, a number of important questions are raised from this research. Given the variability in sediment transfer patterns and their apparent controls at the Feegletscher Nord, questions are raised regarding the extent to which the modification of suspended sediment patterns in proglacial zones is likely to increase downstream due to an increase in the contributing area (e.g. Slaymaker, 1987; Warburton, 1999), as the availability of sediments may not necessarily scale with time since deglaciation (Church & Ryder, 1972). Similar conclusions were drawn from the results obtained at Small River Glacier, Canada, where the storage and release of sediments within proglacial channels suggested a reduced role of paraglacial sedimentation in the determination of fluvial suspended sediment yields (Orwin & Smart, 2004a). Furthermore, it is apparent from

the results at the Feegletscher Nord that establishing links between paraglacial sedimentation and fluvial suspended sediment yields is challenging, and models of landscape response to deglaciation may be difficult to apply to individual forefields, due to the variability in forefield characteristics that can potentially control rates of sediment transfer, which can arise from the geomorphological responses to deglaciation exhibited at the study site under examination. This is likely to be further complicated by the presence of sequestered glacial sediments from previous glaciations that can be remobilised by fluvial processes (Church & Slaymaker, 1989). Consequently, this reinforces the need to investigate forefield sediment storage processes in light of forefield geomorphology in order to establish rates of sediment transfer and resultant suspended sediment yields (e.g. Orwin & Smart, 2004a). However, this research has demonstrated that identifying sediment transfer processes and their controls, even within a small catchment, is challenging especially in the absence of the quantification of glacio-fluvial suspended sediment fluxes and budgets. Without such knowledge, the usefulness of sediment transfer relationships for predictive purposes or establishing rates of denudation is likely to be limited. Consequently, the potential for variations in sediment availability and the resultant supply of this sediment to proglacial channels within forefields must be acknowledged for studies utilising proglacial gauging stations, as records of SSC and SSC-discharge relationships obtained from forefields will be influenced by the choice of location for monitoring due to the possible presence of paraglacial activity and complex geomorphological histories. These findings add to the growing body of evidence from Arctic and Alpine systems that deglaciation results in variations in catchment and forefield sediment supply and influences processes of sediment reworking and redistribution which, in turn, can control suspended sediment transfer (e.g. Ballantyne, 2002a; Orwin & Smart, 2004a; Hubbard *et al.*, 2005; Lukas *et al.*, 2005; Korup & Tweed, 2007; Porter *et al.*, 2010; Carrivick & Tweed, 2013;

Carrivick *et al.*, 2013; Cook *et al.*, 2013; Diodato *et al.*, 2013; Leggat *et al.*, 2015). Consequently, in order to fully understand sediment transfer processes, three key facets of deglaciating catchments need to be understood:

1. The characterisation and understanding of the role of meltwater in transferring, reworking and redistributing sediments;
2. Understanding of the *in situ* geomorphological characteristics and processes that can transfer sediments and control sediment availability within glaciated catchments, particularly within the forefield, and;
3. An assessment of forefield fluvial sediment budgets and suspended sediment fluxes.

8.2.3 Glacio-Fluvial Sediment Transfer: Future Perspectives

Modelling of future proglacial suspended sediment loads in Chapter 7 predicted rapid and pronounced decreases in proglacial SSC and suspended sediment loads, owing to the impact of reductions in glacier extent on meltwater runoff volumes. Similar links between patterns of runoff and sediment loads have been noted in other studies (e.g. Stott & Mount, 2007; Pralong *et al.*, 2015), and the results of Chapter 7 suggest that any increases in runoff and suspended sediment loads due to a deglaciation discharge dividend will be minor and short-lived in comparison to the declines of > 90% that are forecast to occur by the end of the century, compared to 1980-2009. Runoff is predicted to increase by between *c.* 11 and 14% for the period 2020-2049, due to increased air temperatures of between 1.2 and 1.3 °C, relative to 1980-2009. This excess meltwater discharge due to release from the long-term stores of ice is predicted to be responsible for enhanced volumes of sediment transport during the coming decades, with uncertain implications as to the impact of this enhanced downstream cascade of sediment on catchment sediment availability. The extent to which these enhanced quantities of

sediment transport will become stored within the forefield or evacuated downstream from the catchment is unknown and the possibility is raised that sediment exhaustion will occur and result in a decline in sediment availability in the catchment unless significant quantities of these sediments become stored within the forefield. Consequently, the ability to forecast future changes in suspended sediment loads is limited, due to poorly constrained forefield sediment storage processes at the Feegletscher Nord. It is established that the proglacial flux of sediment in glaciated catchments is strongly determined by the nature and magnitude of meltwater runoff (e.g. Maizels, 1979; Warburton, 1990; Hodgkins *et al.*, 2003; Orwin & Smart, 2004a), however, the future forecasts raise questions as to the impact of future changes to runoff regimes on long-term forefield sediment fluxes. A range of hydrological responses to climate change can be expected to impact upon runoff and associated sediment transfer (e.g. CH2011, 2011), which will introduce uncertainty into attempts to forecast future rates of sediment transfer and suspended sediment yields, particularly as forecasts are typically undertaken by extrapolating contemporary rates of sediment transfer (as in this research). Examples of the mechanisms responsible for this uncertainty include the possible future lengthening of the ablation season due to climatic warming, which may result in enhanced sediment transport, whilst reductions in the magnitudes of proglacial discharge due to glacier shrinkage may limit rates of sediment transfer. In addition, field observations of high amounts of sediment transfer and redistribution as a result of two significant storm events at the Feegletscher Nord reinforced the importance of high magnitude discharge events in the downstream cascade of sediments (e.g. Church & Ryder, 1972; Richards, 1984), events that have been forecast to occur more frequently with climate change (CH2011, 2011). Therefore, uncertainties in these future forecasts of suspended sediment loads at the Feegletscher Nord arise from the unknown impacts of lengthened ablation seasons due to the possibilities for increased downstream

evacuation of subglacial and proglacial sediments coupled with the possibility that such sediment sources may become exhausted more rapidly. In addition, the role of precipitation as a sediment transfer mechanism is likely to become increasingly important due to the increasing proportion of precipitation in total runoff as the stores of snow and ice deplete (Collins, 2008) and the increased likelihood of precipitation delivery occurring in episodic storm events (CH2011, 2011). Consequently, the increasingly important role of precipitation in mobilising forefield, supraglacial and ice-marginal sediments requires particular attention, as it is likely that sediment will be increasingly mobilised and transported by rainfall runoff in episodic patterns, suggesting an increasingly irregular step-wise downstream cascade of sediment with progressive deglaciation. However, the previous section of this Chapter highlighted the importance and likely dominance of forefield sediment availability in the determination of suspended sediment concentration responses to rainfall and meltwater discharge, as found in a number of similar studies (e.g. Richards 1984; Richards & Moore, 2003; Orwin & Smart, 2004b). Sediment availability in glaciated catchments is expected to exponentially decline following deglaciation (Ballantyne, 2002a), with fluvial sediment yields peaking shortly-after deglaciation during the ‘paraglacial period’ (Church & Ryder, 1972). Paraglacial adjustment of exposed forefield sediments is expected to occur as fine sediments become exhausted and armoured over time (Ballantyne, 2002a; Orwin & Smart, 2004b), the effect of which is a reduction in sediment availability, as these sediments become stabilised or are cascaded downstream, predominantly by fluvial processes in a step-wise manner (Lønne & Lyså, 2005; Lukas *et al.*, 2005; Lukas *et al.*, 2007). However, the results from the Feegletscher Nord suggest that time since deglaciation may be a poor indicator of sediment availability for mobilisation, which suggests that the application of the ‘paraglacial period’ to catchments where complex geomorphological responses to deglaciation have taken place is challenging. In this

research, the effect of proglacial lakes as transient sediment sources and sinks, the presence of areas of paraglacial rock avalanche debris that appeared to limit the availability of fine sediment for mobilisation, and the presence of deposits of loosely consolidated glacio-fluvial material, were all suggested as possible factors in controlling forefield sediment availability. These observations, and the findings of spatial trends in erosion and deposition within other deglaciating forefields (e.g. Carrivick *et al.*, 2013), reinforce that observed patterns of suspended sediment transfer are likely to reflect the competing controls of sediment supply and glacio-fluvial processes of sediment transfer. This has important implications for studies, such as this programme of research, that seek to examine the controls on sediment transfer at short timescales and make predictions into the near future, as it is suggested that processes of proglacial sediment transfer can be conditioned by the responses to deglaciation in particular catchments (e.g. Orwin & Smart, 2004a; Porter *et al.*, 2010; Carrivick *et al.*, 2013; Cook *et al.*, 2013) and, consequently, the characterisation of processes of sediment transfer are not transferable between catchments. A major uncertainty therefore arises in the interpretation of future trends in suspended sediment loads due to the capacity for deglaciation dynamics to enhance or limit the ability for sediments to be mobilised by fluvial processes.

The switch from systems dominated by glacial processes to those dominated by paraglacial activity has been hypothesised to result in enhanced sediment yields (Ballantyne, 2002a; Porter *et al.*, 2010). The findings of this research suggest that enhanced rates of glacio-fluvial sediment transfer and suspended sediment yields cannot be assumed to be a consequence of deglaciation due to the spatial variability in sediment transfer patterns observed in the Feegletscher Nord forefield, that appeared conditioned by variations in the availability of sediment for mobilisation by fluvial

processes. If sediment availability is limited in one area of a proglacial zone, whilst enhanced in another, the concept of any 'paraglacial period' is challenging, if not impossible, to define and may be of limited use for establishing contemporary rates of sediment transfer in order to predict future sediment loads. This echoes the conclusions of similar studies that have raised questions as to what constitutes typical fluvial suspended sediment yield during deglaciation (Orwin & Smart, 2004a). Therefore, it appears that if an understanding of the nature of proglacial sediment storage is required, then gauging proglacial suspended sediment fluxes by SSC monitoring at proximal and distal ends of the proglacial area will be sufficient (e.g. Hodgkins *et al.*, 2003; Leggat *et al.*, 2015). However, the significant variability in suspended sediment transfer patterns observed within the relatively small forefield of the Feegletscher Nord suggests that significant uncertainty may be introduced into attempts to establish contemporary rates of sediment transfer with the use of single proglacial gauging stations. Consequently, this finding has important implications for understanding landscape responses to deglaciation. The dominance of meltwater in the modification of landforms has been observed in Arctic basins (e.g. Lønne & Lyså, 2005; Lukas *et al.*, 2005), suggesting that constraining the rates of this glacio-fluvial sediment transfer during deglaciation is an important priority for future research if rates of landscape adjustment and the resultant landscape evolution is to be understood. This research suggests that the spatial variability of sediment availability within proglacial zones, and the extent to which meltwater can access these stores, are two important factors in understanding the geomorphological consequences of deglaciation.

8.3 Future Research Priorities

Important questions and uncertainties have been raised in this research that provide potential avenues for future research. This section provides an overview of these

potential areas for future research in the field of glacio-fluvial sediment transfer that build upon the results obtained from the Feegletscher Nord in order to address these uncertainties and to enhance understanding of the influence and consequences of deglaciation upon glacier hydrological and sedimentary systems.

With regards to glacier hydrology, the research presented in this thesis demonstrated complexity as to the controls that dictate proglacial hydrograph characteristics. Specifically, two areas have been identified as fruitful avenues for future research. Firstly, further exploration of meltwater storage processes is required in order to characterise the nature and physical basis of storage reservoirs, and to investigate the causes of the apparent lack of seasonal changes in storage coefficients. As discussed in the previous section, the lack of seasonal dynamics in reservoir coefficients was unusual. The k -values determined through hydrograph recession analysis revealed the dominance of short-term storage of meltwater, which was hypothesised to occur within ice-reservoirs comprising fracture, crevasses or components of a 'slow' drainage system. The uncertainty in these interpretations reflects the challenges associated with characterising the internal hydrology of glaciers through direct, *in situ* observation and the associated degree of interpretation necessary to deduce the physical basis for observations derived from proglacial discharge records (e.g. Gurnell, 1993). Consequently, knowledge of transient meltwater storage processes and drivers remains incomplete in both Arctic and Alpine contexts, as reflected by recent research that highlights the importance of englacial hydrological connectivity (e.g. Benn *et al.*, 2009; Gulley *et al.*, 2009; Colgan *et al.*, 2011) and supraglacial meltwater routing and storage processes (e.g. Benn *et al.*, 2001; Shea *et al.*, 2005; Scott Munro, 2011; Singh *et al.*, 2011) in determining the resultant meltwater runoff and proglacial hydrograph, both of which are likely to be influenced by a changing climate due to increased surface melt

production and the resultant transfer of meltwater through glaciers. Despite knowledge of the subglacial hydrology of temperate Alpine glacier, this suggests that there is scope to enhance the understanding of the characteristics and significance of englacial and supraglacial glacier hydrology, which has been noted for Arctic and polythermal contexts (e.g. Irvine-Fynn *et al.*, 2011). This characterisation of meltwater storage and release processes within glacier hydrological systems is needed due to the importance of meltwater throughput in the determination of subglacial sediment availability, entrainment and evacuation (Hubbard *et al.*, 1995; Alley *et al.*, 1997; Swift *et al.*, 2002), and the need to characterise these storage processes for glacier runoff modelling attempts (Jansson *et al.*, 2003). Therefore, field observations of water storage processes are needed to constrain the physical basis and dynamics of meltwater storage at glaciers, particularly in light of enhanced rates of ablation during deglaciation and the capacity for enhanced meltwater storage and throughput due to deglaciation dynamics such as increased debris cover (e.g. Benn *et al.*, 2001), reduced ice-thicknesses (e.g. Flowers, 2008) and the increasing potential for ice-marginal meltwater routing and storage (e.g. Hodgkins *et al.*, 2013b). However, the investigation of these processes is limited by the lack of accessibility to the englacial and subglacial environment, except for a small number of notable exceptions where direct observations have been possible (e.g. Rea & Whalley, 1994; Gulley *et al.*, 2012). Consequently, tracer studies (e.g. Nienow *et al.*, 1998), proglacial stream gauging (e.g. Hannah *et al.*, 2000; Hannah & Gurnell, 2001), and the monitoring of water pressures with the installation of pressure transducers in boreholes and crevasses (e.g. Hubbard *et al.*, 1995; Swift *et al.*, 2005a) are the most widely used approaches to the study of meltwater storage and release processes. In addition, it is apparent that ground-penetrating radar has shown the capability to yield information on the water content of, and hydrological features within, glaciers (e.g. Murray *et al.*, 2000; Pettersson *et al.*, 2004; Irvine-Fynn *et al.*, 2006; Urbini &

Baskaradas, 2010), particularly for water that may be retained and transferred within the active layer of ice and, consequently, is likely a useful approach for determining the volumes of water involved and seasonal or inter-annual storage changes. Therefore, integrated approaches to the study of water storage processes and dynamics are clearly a fruitful research direction for the characterisation of these processes, the main contribution of which will be in aiding the determination of appropriate parameters for storage and meltwater transit in glacier runoff modelling, as these are commonly determined through a combination of hydrograph recession analysis and routing parameter optimisation during runoff model development (e.g. Hock & Noetzli, 1997; Hock, 1999; Huss *et al.*, 2008). Furthermore, glacier retreat and thinning was hypothesised influence the hydrology of glaciers through reduced rates of conduit closure and lower subglacial water pressures (e.g. Flowers, 2008). Therefore, it is clear that the potential exists for thinning ice masses to result in a dominance of perennial drainage features. Consequently, combining studies on glacier structure and geometry with field observations of hydrological characteristics represents a potentially useful approach to advance understanding of glacier hydrology and hydrological processes during deglaciation.

It has been shown in Section 6.5 that scaling degree-day factors were effective in simulating glacier ablation. However, despite this relative success there is still a compelling need to validate this parameterisation of the degree-day factor in FTIM through improved observations of the variability in glacier ablation in space and time, particularly as the processes responsible for any temporal changes in albedo were undetermined in this research. More widely in the literature, a paucity of observations in changes in albedo due to factors other than snowline retreat is apparent (e.g. Paul *et al.*, 2005), suggesting that scope exists to explore the mechanisms responsible for any

temporal or spatial changes in surface albedo, which can be postulated to relate to a range of factors associated with deglaciation, due to observations at glaciers and ice-sheets of processes such as snowpack depletion, increases in debris cover, and ‘biological darkening’ (e.g. Takeuchi *et al.*, 2001; Oerlemans *et al.*, 2009; Irvine-Fynn *et al.*, 2012; Dumont *et al.*, 2014; Edwards *et al.*, 2014; Irvine-Fynn & Edwards, 2014; Lutz *et al.*, 2014). In addition, there is paucity of data that links observations of these changes with processes of ablation for the purposes of simulating glacier melt and resultant runoff (Hock, 2005). Consequently, characterisation of potential processes responsible for albedo variability and the determination of any link between albedo variations and processes of ablation may provide a potential method for accounting for temporal and variability in melt parameters in glacier melt models, which is an area of melt modelling that has been highlighted as requiring particular attention (e.g. Hock, 2003; 2005), in order to improve both the accuracy and physical basis of melt and mass balance models.

Several questions relating to the controls on proglacial SSC were raised. Importantly, research into the causes of the unexplained variance in the relationship between SSC and discharge is required to elucidate the physical processes responsible for the apparently stochastic SSC behaviour observed here in this research. Field observations and the findings of previous studies at the Feegletscher Nord forefield (e.g. Curry *et al.*, 2009; Cook *et al.*, 2013) enabled a range of forefield processes to be suggested as possible causes of the unexplained SSC variance, however, their physical basis was not satisfactorily determined in this research, in part due to the failure to determine proglacial suspended sediment fluxes as a result of equipment loss and/or failure due to storms and technical problems at the gauging stations located at the distal and proximal ends of the forefield. Therefore, questions remain regarding the extent and

nature of processes of in-channel and channel-marginal sediment mobilisation. The influence of these forefield processes on SSC has been challenging to determine in short-term or high temporal resolution proglacial gauging studies (e.g. Fenn, 1989; Clifford *et al.*, 1995; Hodson & Ferguson, 1999; Stott & Grove, 2001; Richards & Moore, 2003), but has been more adequately characterised in studies which adopted sediment budget approaches (e.g. Maizels, 1979; Warburton, 1990; Hodgkins *et al.*, 2003; Orwin & Smart, 2004a; Leggat *et al.*, 2015). Consequently, programmes of research in deglaciating catchments that adopt sediment budget approaches, combined with the whole-catchment hydro-meteorological approach presented in this study, would appear to provide the most comprehensive approach to research design in order to address such questions, resulting in approaches that yield high resolution data on a range of variables that possess the capability to influence processes of glacio-fluvial suspended sediment transfer. Furthermore, the findings of this research have suggested that significant uncertainties will persist in attempts to forecast SSC due to complex relationships between proglacial SSC and discharge, even with data obtained at multiple gauging locations. Therefore, there is considerable scope to improve upon the forward modelling approach developed in this research in light of the short-term variability in SSC. The introduction of parameters describing such variability into modelling attempts (e.g. Morehead *et al.*, 2003; Mount & Stott, 2008) seem a potentially worthwhile avenue if future changes in suspended sediment loads from glaciated catchments are to be accurately forecast, and contribute to improvements in understanding of rates of downstream sediment transfer and landscape modification during contemporary deglaciation.

In addition, questions were raised regarding the extent to which forefield geomorphology and geomorphic activity exerts a control on sediment transfer processes

due their hypothesised influence on fine sediment availability. It is clear that exploration of the interactions between forefield geomorphological activity, sediment sources and fluvial sediment fluxes is needed due to a paucity of data on these processes and their interrelationships (Carrivick *et al.*, 2013). This is likely to be particularly important in catchments where paraglacial reworking and redistribution of sediments may result in complex slope-fluvio-glacial linkages (Curry *et al.*, 2009; Porter *et al.*, 2010; Cook *et al.*, 2013). Determination of a link between geomorphic changes in the proglacial zone and rates of suspended sediment transfer provides a potential route for exploring the controls on paraglacial sedimentation, the study of which has predominantly been restricted to hydrological gauging of glacio-fluvial suspended sediment transfer to infer the availability and stability of forefield sediments (e.g. Church & Ryder, 1972; Orwin & Smart, 2004a), which is likely to fail to capture all geomorphological activity within a forefield. Consequently, the apparent potential for terrestrial laser scanning to examine geomorphological changes within a proglacial zone (e.g. Carrivick *et al.*, 2013) combined with the gauging of fluvial sediment loads and fluxes through a network of spatially distributed gauging stations (e.g. Hodgkins *et al.*, 2003; Orwin & Smart, 2004; Leggat *et al.*, 2015) would seem a promising avenue for research in order to identify the impact of geomorphological activity upon sediment sources and the resultant fluvial suspended sediment loads. Such an approach has the potential to yield valuable understanding on processes and rates of landscape adjustment, and furthermore, would help to resolve uncertainties regarding the significance and dominance of continuous processes of sediment redistribution versus episodic processes, such as storm events, in determining proglacial sediment storage and fluxes. Furthermore, the long-term monitoring of these processes requires attention due to a lack of long-term data on rates of sediment transfer in deglaciating environments, and would make significant

contributions to the understanding of rates of glacio-fluvial sediment transfer and the resultant impacts on proglacial geomorphology and landscape adjustment.

8.4 Thesis Summary Conclusion

This thesis has presented an investigation into glacio-fluvial sediment transfer at the Feegletscher Nord, Switzerland, utilising a catchment-based approach to explore the controls on, and processes of, proglacial suspended sediment transfer. Differences were revealed in suspended sediment transfer patterns and the observed patterns were dependent on the location of the gauging station, which reinforced the importance of forefield sediment availability in determining proglacial SSC. Importantly, the findings of differing patterns of sediment transfer between stations located at similar distances from the glacier terminus suggested that factors other than terrain age can influence the availability of fine sediments for mobilisation. Field observations and other studies undertaken in the catchment suggested a range of geomorphological responses to deglaciation was likely to exert a control on this variability in sediment availability, which are likely to be an example of slope-fluvio-glacio linkages that require further research. The development of multivariate regression models to simulate proglacial SSC were coupled to a temperature-index runoff model of the Feegletscher Nord that was developed in order to explore the effects of future climate changes, reductions in glacier extent, and variations in degree-day factors on proglacial runoff and suspended sediment transfer. These simulations highlighted the dominance of variations in glacier extent upon suspended sediment loads due to meltwater production and associated glacio-fluvial sediment transfer. The simulations suggested that contemporary fluvial suspended sediment loads could be around their peak for this century and may decline exponentially to < 90 % compared to 1980-2009 by the end of the century. Consequently, it appears that the expected declines in suspended sediment yields during deglaciation are likely to occur rapidly. The simulations also raised questions regarding

the possible effects of changes in sediment availability with progressive deglaciation. Increases in paraglacial activity in deglaciating environments may result in enhanced sediment yields, whilst reductions in glacier erosion due to reductions in glacier extent and the progressive stabilisation and evacuation of glacial sediments from these catchments may deplete sediment stores. Therefore, a whole catchment approach to exploring glacio-fluvial sediment transfer is advocated for characterising sediment transfer processes and their control in light of a range of potentially complex hydrological and geomorphological responses to deglaciation that may exist in these environments.

Bibliography

- Alcamo, J., Flörke, M., & Märker, M. (2007). Future long-term changes in global water resources driven by socio-economic and climatic changes. *Hydrological Sciences Journal*, 52(2), 247-275.
- Alexander, D., Shulmeister, J., & Davies, T. (2011). High basal melting rates within high-precipitation temperate glaciers. *Journal of Glaciology*, 57(205), 789-795.
- Alley, R. B. (1992). How can low-pressure channels and deforming tills coexist subglacially?. *Journal of Glaciology*, 38(128).
- Alley, R. B., Cuffey, K. M., Evenson, E. B., Strasser, J. C., Lawson, D. E., & Larson, G. J. (1997). How glaciers entrain and transport basal sediment: physical constraints. *Quaternary Science Reviews*, 16(9), 1017-1038.
- Anderson, S. P., Fernald, K. T., Anderson, R. L., & Humphrey, N. F. (1999). Physical and chemical characterization of a spring flood event, Bench Glacier, Alaska, USA: evidence for water storage. *Journal of Glaciology*, 45(150), 177-189.
- Anderson, B., Lawson, W., Owens, I., & Goodsell, B. (2006). Past and future mass balance of 'Ka Roimata o Hine Hukatere' Franz Josef Glacier, New Zealand. *Journal of Glaciology*, 52(179), 597-607.
- Arendt, A., & Sharp, M. (1999). Energy balance measurements on a Canadian high arctic glacier and their implications for mass balance modelling. *IAHS Publication*, 165-172.
- Arnold, N. S., Willis, I. C., Sharp, M. J., Richards, K. S., & Lawson, W. J. (1996). A distributed surface energy-balance model for a small valley glacier. I. Development and testing for Haut Glacier d'Arolla, Valais, Switzerland. *Journal of Glaciology*, 42(140), 77-89.
- Ashmore, P. (1993). Contemporary erosion of the Canadian landscape. *Progress in Physical Geography*, 17(2), 190-204.
- Baewert, H., & Morche, D. (2014). Coarse sediment dynamics in a proglacial fluvial system (Fagge River, Tyrol). *Geomorphology*, 218, 88-97.
- Ballantyne, C. K. (2002a). A general model of paraglacial landscape response. *The Holocene*, 12(3), 371-376.
- Ballantyne, C. K. (2002b). Paraglacial geomorphology. *Quaternary Science Reviews*, 21(18), 1935-2017.
- Barnard, P. L., Owen, L. A., Finkel, R. C., & Asahi, K. (2006). Landscape response to deglaciation in a high relief, monsoon-influenced alpine environment, Langtang Himal, Nepal. *Quaternary Science Reviews*, 25(17), 2162-2176.
- Barry, R. G. (1992). *Mountain weather and climate*. Psychology Press.

- Bauder, A., Funk, M., & Huss, M. (2007). Ice-volume changes of selected glaciers in the Swiss Alps since the end of the 19th century. *Annals of Glaciology*, 46(1), 145-149.
- Beniston, M., Rebetez, M., Giorgi, F., & Marinucci, M. R. (1994). An analysis of regional climate change in Switzerland. *Theoretical and applied climatology*, 49(3), 135-159.
- Benn, D., & Evans, D. J. (2014). *Glaciers and glaciation*. Routledge.
- Benn, D. I., Wiseman, S., & Hands, K. A. (2001). Growth and drainage of supraglacial lakes on debris-mantled Ngozumpa Glacier, Khumbu Himal, Nepal. *Journal of Glaciology*, 47(159), 626-638.
- Benn, D., Gulley, J., Luckman, A., Adamek, A., & Glowacki, P. S. (2009). Englacial drainage systems formed by hydrologically driven crevasse propagation. *Journal of Glaciology*, 55(191), 513-523.
- Benn, D. I., Bolch, T., Hands, K., Gulley, J., Luckman, A., Nicholson, L. I., ... & Wiseman, S. (2012). Response of debris-covered glaciers in the Mount Everest region to recent warming, and implications for outburst flood hazards. *Earth-Science Reviews*, 114(1), 156-174.
- Bezinge, A. (1987). Glacial meltwater streams, hydrology and sediment transport: the case of the Grande Dixence hydroelectricity scheme. *Glacio-Fluvial Sediment Transfer: An Alpine Perspective*. John Wiley and Sons, New York New York. 1987. p 473-498.
- Bhatia, M. P., Kujawinski, E. B., Das, S. B., Breier, C. F., Henderson, P. B., & Charette, M. A. (2013). Greenland meltwater as a significant and potentially bioavailable source of iron to the ocean. *Nature Geoscience*, 6(4), 274-278.
- Bircher, W. (1982). *Zur Gletscher-und Klimageschichte des Saastales: glazialmorphologische und dendroklimatologische Untersuchungen*. Doctoral thesis, Universität Zürich.
- Björnsson, H., Pálsson, F., Sigurðsson, O., & Flowers, G. E. (2003). Surges of glaciers in Iceland. *Annals of Glaciology*, 36(1), 82-90.
- Bliss, A., Hock, R., & Radić, V. (2014). Global response of glacier runoff to twenty-first century climate change. *Journal of Geophysical Research: Earth Surface*, 119(4), 717-730.
- Bogen, J. (1989). Glacial sediment production and development of hydro-electric power in glacierized areas. *Annals of Glaciology*, 13, 6-11.
- Bogen, J. (1995). Sediment transport and deposition in mountain rivers. *Sediment and water quality in river catchments*, edited by I. D. L. Foster, A. M. Gurnell and B. W. Webb. John Wiley & Sons, Chichester, 437-451.

- Bogen, J., & Bønsnes, T. E. (2003). Erosion and sediment transport in High Arctic rivers, Svalbard. *Polar Research*, 22(2), 175-189.
- Bogen, J., Xu, M., & Kennie, P. (2015). The impact of pro-glacial lakes on downstream sediment delivery in Norway. *Earth Surface Processes and Landforms*, 40, 942-952.
- Boon, S., & Sharp, M. (2003). The role of hydrologically-driven ice fracture in drainage system evolution on an Arctic glacier. *Geophysical Research Letters*, 30(18).
- Boulton, G. S. (1978). Boulder shapes and grain-size distributions of debris as indicators of transport paths through a glacier and till genesis. *Sedimentology*, 25(6), 773-799.
- Boulton, G. S. (1979). Processes of glacier erosion on different substrata. *Journal of glaciology*, 23, 15-38.
- Boulton, G. S. (1982). *Processes and patterns of glacial erosion*. Springer Netherlands.
- Boulton, G. S., & Hindmarsh, R. C. A. (1987). Sediment deformation beneath glaciers: rheology and geological consequences. *Journal of Geophysical Research: Solid Earth (1978–2012)*, 92(B9), 9059-9082.
- Bousquet, R., Goffé, B., Vidal, O., Oberhänsli, R., & Patriat, M. (2002). The tectono-metamorphic history of the Valaisan domain from the Western to the Central Alps: New constraints on the evolution of the Alps. *Geological Society of America Bulletin*, 114(2), 207-225.
- Braithwaite, R. J. (1981). On glacier energy balance, ablation, and air temperature. *Journal of Glaciology*, 27, 381-391.
- Braithwaite, R. J., & Olesen, O. B. (1989). *Calculation of glacier ablation from air temperature, West Greenland* (pp. 219-233). Springer Netherlands.
- Braithwaite, R. J. (1995). Positive degree-day factors for ablation on the Greenland ice sheet studied by energy-balance modelling. *Journal of Glaciology*, 41(137), 153-160.
- Braithwaite, R. J., & Zhang, Y. (2000). Sensitivity of mass balance of five Swiss glaciers to temperature changes assessed by tuning a degree-day model. *Journal of Glaciology*, 46(152), 7-14.
- Braithwaite, R. J. (2008). Temperature and precipitation climate at the equilibrium-line altitude of glaciers expressed by the degree-day factor for melting snow. *Journal of Glaciology*, 54(186), 437-444.
- Braun, L. N., Weber, M., & Schulz, M. (2000). Consequences of climate change for runoff from Alpine regions. *Annals of glaciology*, 31(1), 19-25.
- Brinkhaus, M. (2003). *Modelling melt and runoff on a High Arctic glacier: Midre Lovénbreen, Svalbard*. Unpublished MSc thesis, Ruhr University Bochum.

- Brock, B. W., Willis, I. C., & Sharp, M. J. (2000). Measurement and parameterization of albedo variations at Haut Glacier d'Arolla, Switzerland. *Journal of Glaciology*, 46(155), 675-688.
- Carenzo, M., Pellicciotti, F., Rimkus, S., & Burlando, P. (2009). Assessing the transferability and robustness of an enhanced temperature-index glacier-melt model. *Journal of Glaciology*, 55(190), 258-274.
- Carrivick, J. L., & Rushmer, E. L. (2009). Inter-and intra-catchment variations in proglacial geomorphology: an example from Franz Josef Glacier and Fox Glacier, New Zealand. *Arctic, Antarctic, and Alpine Research*, 41(1), 18-36.
- Carrivick, J. L., Geilhausen, M., Warburton, J., Dickson, N. E., Carver, S. J., Evans, A. J., & Brown, L. E. (2013). Contemporary geomorphological activity throughout the proglacial area of an alpine catchment. *Geomorphology*, 188, 83-95.
- Carrivick, J. L., & Tweed, F. S. (2013). Proglacial lakes: character, behaviour and geological importance. *Quaternary Science Reviews*, 78, 34-52.
- CH2011: Swiss Climate Change Scenarios. (2011). C2SM. *MeteoSwiss, ETH, NCCR Climate, OcCC, Zurich*.
- Church, M., & Ryder, J. M. (1972). Paraglacial sedimentation: a consideration of fluvial processes conditioned by glaciation. *Geological Society of America Bulletin*, 83(10), 3059-3072.
- Church, M., & Slaymaker, O. (1989). Disequilibrium of Holocene sediment yield in glaciated British Columbia. *Nature*, 337(6206), 452-454.
- Christensen, J. H., & Christensen, O. B. (2007). A summary of the PRUDENCE model projections of changes in European climate by the end of this century. *Climatic change*, 81(1), 7-30.
- Clarke, G. K. (1987). Subglacial till: a physical framework for its properties and processes. *Journal of Geophysical Research: Solid Earth (1978–2012)*, 92(B9), 9023-9036.
- Clifford, N. J., Richards, K. S., Brown, R. A., & Lane, S. N. (1995). Scales of variation of suspended sediment concentration and turbidity in a glacial meltwater stream. *Geografiska Annaler. Series A. Physical Geography*, 45-65.
- Colgan, W., Steffen, K., McLamb, W. S., Abdalati, W., Rajaram, H., Motyka, R., ... & Anderson, R. (2011). An increase in crevasse extent, West Greenland: Hydrologic implications. *Geophysical Research Letters*, 38(18).
- Collins, D. N. (1979). *Meltwater characteristics as indicators of the hydrology of Alpine glaciers*. Doctoral thesis, University of Nottingham, Nottingham.
- Collins, D. N. (1979). Hydrochemistry of meltwaters draining from an alpine glacier. *Arctic and Alpine Research*, 307-324.

- Collins, D. N. (1979). Sediment concentration in melt waters as an indicator of erosion processes beneath an Alpine glacier. *Journal of Glaciology*, 23, 247-257.
- Collins, D. N. (1979). Quantitative determination of the subglacial hydrology of two Alpine glaciers. *Journal of Glaciology*, 23, 347-362.
- Collins, D. N. (1989). Hydrometeorological conditions, mass balance and runoff from alpine glaciers. In *Glacier fluctuations and climatic change* (pp. 235-260). Springer Netherlands.
- Collins, D. N. (1981). Seasonal variation of solute concentration in melt waters draining from an alpine glacier. *Annals of Glaciology*, 2(1), 11-16.
- Collins, D. N. (1990). Seasonal and annual variations of suspended sediment transport in meltwaters draining from an Alpine glacier. *Hydrology in Mountainous Regions I: Hydrological Measurements; the Water Cycle*, 439-446.
- Collins, D. N. (1998). Suspended sediment flux in meltwaters draining from Batura glacier as an indicator of the rate of glacial erosion in the Karakoram mountains. *Journal of Quaternary Science*, 13(6), 1-10.
- Collins, D. N. (2008). Climatic warming, glacier recession and runoff from Alpine basins after the Little Ice Age maximum. *Annals of Glaciology*, 48(1), 119-124.
- Collins D. N., & Crescent, S. (2007). Climatic variation, glacier recession and runoff from Alpine basins. *climate & water*, 103.
- Cook, S. J., Porter, P. R., & Bendall, C. A. (2013). Geomorphological consequences of a glacier advance across a paraglacial rock avalanche deposit. *Geomorphology*, 189, 109-120.
- Cook, S. J., & Swift, D. A. (2012). Subglacial basins: Their origin and importance in glacial systems and landscapes. *Earth-Science Reviews*, 115(4), 332-372.
- Cossart, E., Braucher, R., Fort, M., Bourlès, D. L., & Carcaillet, J. (2008). Slope instability in relation to glacial debuitressing in alpine areas (Upper Durance catchment, southeastern France): evidence from field data and 10 Be cosmic ray exposure ages. *Geomorphology*, 95(1), 3-26.
- Covington, M. D., Banwell, A. F., Gulley, J., Saar, M. O., Willis, I., & Wicks, C. M. (2012). Quantifying the effects of glacier conduit geometry and recharge on proglacial hydrograph form. *Journal of Hydrology*, 414, 59-71.
- Curry, A. M., Cleasby, V., & Zukowskyj, P. (2006). Paraglacial response of steep, sediment-mantled slopes to post 'Little Ice Age' glacier recession in the central Swiss Alps. *Journal of Quaternary Science*, 21(3), 211-225.
- Curry, A. M., Sands, T. B., & Porter, P. R. (2009). Geotechnical controls on a steep lateral moraine undergoing paraglacial slope adjustment. *Geological Society, London, Special Publications*, 320(1), 181-197.

- de Woul, M., Hock, R., Braun, M., Thorsteinsson, T., Jóhannesson, T., & Halldorsdottir, S. (2006). Firn layer impact on glacial runoff: a case study at Hofsjökull, Iceland. *Hydrological Processes*, 20(10), 2171-2185.
- Diodato, N., Støren, E. W., Bellocchi, G., & Nesje, A. (2013). Modelling sediment load in a glacial meltwater stream in western Norway. *Journal of Hydrology*, 486, 343-350.
- Dowdeswell, J. A., Hambrey, M. J., & Wu, R. (1985). A comparison of clast fabric and shape in Late Precambrian and modern glacial sediments. *Journal of Sedimentary Research*, 55(5).
- Dumont, M., Brun, E., Picard, G., Michou, M., Libois, Q., Petit, J. R., ... & Josse, B. (2014). Contribution of light-absorbing impurities in snow to Greenland's darkening since 2009. *Nature Geoscience*.
- Eberhardt, E., Stead, D., & Coggan, J. S. (2004). Numerical analysis of initiation and progressive failure in natural rock slopes - the 1991 Randa rockslide. *International Journal of Rock Mechanics and Mining Sciences*, 41(1), 69-87.
- Edwards, A., Mur, L. A., Girdwood, S. E., Anesio, A. M., Stibal, M., Rassner, S. M., ... & Sattler, B. (2014). Coupled cryoconite ecosystem structure–function relationships are revealed by comparing bacterial communities in alpine and Arctic glaciers. *FEMS microbiology ecology*, 89(2), 222-237.
- Eisen, O., Harrison, W. D., Raymond, C. F., Echelmeyer, K. A., Bender, G. A., & Gorda, J. L. (2005). Variegated Glacier, Alaska, USA: a century of surges. *Journal of Glaciology*, 51(174), 399-406.
- Elliston, G. R. (1973). Water movement through the Gornergletscher. In *Symposium on the Hydrology of Glaciers*, 95, 79-84.
- Etienne, S., Mercier, D., & Voldoire, O. (2008). Temporal scales and deglaciation rhythms in a polar glacier margin, Baronbreen, Svalbard. *Norsk Geografisk Tidsskrift-Norwegian Journal of Geography*, 62(2), 102-114.
- Etzelmüller, B., Ødegård, R. S., Vatne, G., Mysterud, R. S., Tønning, T., & Sollid, J. L. (2000). Glacier characteristics and sediment transfer system of Longyearbreen and Larsbreen, western Spitsbergen. *Norsk Geografisk Tidsskrift*, 54(4), 157-168.
- Evans, M. (1997). Temporal and spatial representativeness of alpine sediment yields: Cascade Mountains, British Columbia. *Earth Surface Processes and Landforms*, 22(3), 287-295.
- Evans, D. J. A., Phillips, E. R., Hiemstra, J. F., & Auton, C. A. (2006). Subglacial till: formation, sedimentary characteristics and classification. *Earth-Science Reviews*, 78(1), 115-176.
- Farinotti, D., Huss, M., Bauder, A., & Funk, M. (2009). An estimate of the glacier ice volume in the Swiss Alps. *Global and Planetary Change*, 68(3), 225-231.

- Farinotti, D. (2010). *Simple methods for inferring glacier ice-thickness and snow-accumulation distribution*. Doctoral thesis, Eidgenössische Technische Hochschule (ETH) Zürich.
- Farinotti, D., Usselman, S., Huss, M., Bauder, A., & Funk, M. (2012). Runoff evolution in the Swiss Alps: projections for selected high-alpine catchments based on ENSEMBLES scenarios. *Hydrological Processes*, 26(13), 1909-1924.
- Fenn, C. R. (1987). Sediment transfer processes in Alpine glacier basins. *Glacio-Fluvial Sediment Transfer: An Alpine Perspective*. John Wiley and Sons, New York. 1987. p 59-85.
- Fenn, C. R. (1989). Quantifying the errors involved in transferring suspended sediment rating equations across ablation seasons. *Annals of Glaciology*, 13, 64-68.
- Fenn, C. R., Gurnell, A. M., & Beecroft, I. R. (1985). An evaluation of the use of suspended sediment rating curves for the prediction of suspended sediment concentration in a proglacial stream. *Geografiska Annaler. Series A. Physical Geography*, 71-82.
- Fenn, C. R., & Gomez, B. (1989). Particle size analysis of the sediment suspended in a proglacial stream: Glacier de Tsidjiore Nouve, Switzerland. *Hydrological Processes*, 3(2), 123-135.
- Fischer, M., Huss, M., & Hoelzle, M. (2014). Surface elevation and mass changes of all Swiss glaciers 1980–2010. *The Cryosphere Discussion*, 8, 4581-4617.
- Fleisher, P. J. (2014). Surface depressions (Lacunas) on Bering Glacier, Alaska: a product of downwasting through differential ablation. *The Cryosphere Discussions*, 8(3), 2403-2424.
- Flowers, G. E., & Clarke, G. K. (2002). A multicomponent coupled model of glacier hydrology 2. Application to Trapridge Glacier, Yukon, Canada. *Journal of Geophysical Research: Solid Earth (1978–2012)*, 107(B11), ECV-10.
- Flowers, G. E. (2008). Subglacial modulation of the hydrograph from glacierized basins. *Hydrological Processes*, 22(19), 3903-3918.
- Fountain, A. G., Jacobel, R. W., Schlichting, R., & Jansson, P. (2005). Fractures as the main pathways of water flow in temperate glaciers. *Nature*, 433(7026), 618-621.
- Fountain, A. G., & Vecchia, A. (1999). How many stakes are required to measure the mass balance of a glacier?. *Geografiska Annaler: Series A, Physical Geography*, 81(4), 563-573.
- Fountain, A. G. & Walder, J. S. (1998). Water flow through temperate glaciers. *Reviews of Geophysics* 36.3: 299-328.
- Geilhausen, M., Morche, D., Otto, J. C., & Schrott, L. (2013). Sediment discharge from the proglacial zone of a retreating Alpine glacier. *Zeitschrift für Geomorphologie, Supplementary Issues*, 57(2), 29-53.

- Gomez, B., & Church, M. (1989). An assessment of bed load sediment transport formulae for gravel bed rivers. *Water Resources Research*, 25(6), 1161-1186.
- Gregory, K. J. (1987). Hydrogeomorphology of Alpine Proglacial Areas. *Glacio-Fluvial Sediment Transfer: An Alpine Perspective*. John Wiley and Sons, New York. 87-107.
- Grove, J. M. (1997). The spatial and temporal variations of glaciers during the Holocene in the Alps, Pyrenees, Tatra and Caucasus. *Glacier Fluctuations During the Holocene: Stuttgart, Fischer*, 95-103.
- Gulley, J. D., Walthard, P., Martin, J., Banwell, A. F., Benn, D. I., & Catania, G. (2012a). Conduit roughness and dye-trace breakthrough curves: why slow velocity and high dispersivity may not reflect flow in distributed systems. *Journal of Glaciology*, 58(211), 915-925.
- Gulley, J. D., Grabiec, M., Martin, J. B., Jania, J., Catania, G., & Glowacki, P. (2012b). The effect of discrete recharge by moulins and heterogeneity in flow-path efficiency at glacier beds on subglacial hydrology. *Journal of Glaciology*, 58(211), 926-940.
- Gurnell, A. M. (1982). The dynamics of suspended sediment concentration in an Alpine pro-glacial stream network. *Hydrological Aspects of Alpine and High Mountain Areas*, 319-330.
- Gurnell, A. M., & Fenn, C. R. (1984). Box-Jenkins transfer function models applied to suspended sediment concentration-discharge relationships in a proglacial stream. *Arctic and Alpine Research*, 93-106.
- Gurnell, A. M. (1987). Suspended sediment. *Glacio-Fluvial Sediment Transfer: An Alpine Perspective*. John Wiley and Sons, New York. p 305-354.
- Gurnell, A. M., & Warburton, J. (1990). The significance of suspended sediment pulses for estimating suspended sediment load and identifying suspended sediment sources in Alpine glacier basins. *Hydrology of Mountainous Regions*, 1, 463-470.
- Gurnell, A. M., Clark, M. J., Hill, C. T., Greenhalgh, J., Bogen, J., Walling, D. E., & Day, T. (1992). Reliability and representativeness of a suspended sediment concentration monitoring programme for a remote alpine proglacial river. In *Erosion and Sediment Transport Monitoring in River Basins, Proceedings of the Oslo Symposium* (Vol. 24, p. 28). Wallingford, Oxfordshire, UK: IAHS Press.
- Gurnell, A. M. (1993). How many reservoirs? An analysis of flow recessions from a glacier basin. *Journal of Glaciology*, 39(132), 409-414.
- Gurnell, A. M. (1995). Sediment yield from alpine glacier basins. *Sediment and Water quality in River Catchments*, Chichester: Wiley, 407-435.
- Haeberli, W., & Beniston, M. (1998). Climate change and its impacts on glaciers and permafrost in the Alps. *Ambio*, 258-265.

- Haerberli, W., Hoelzle, M., Paul, F., & Zemp, M. (2007). Integrated monitoring of mountain glaciers as key indicators of global climate change: the European Alps. *Annals of Glaciology*, 46(1), 150-160.
- Hagg, W., Mayer, C., Lambrecht, A., & Helm, A. (2008). Sub-debris melt rates on southern Inylchek Glacier, central Tian Shan. *Geografiska Annaler: Series A, Physical Geography*, 90(1), 55-63.
- Haldorsen, S. (1981). Grain-size distribution of subglacial till and its relation to glacial crushing and abrasion. *Boreas*, 10(1), 91-105.
- Hallet, B., Hunter, L., & Bogen, J. (1996). Rates of erosion and sediment evacuation by glaciers: A review of field data and their implications. *Global and Planetary Change*, 12(1), 213-235.
- Hambrey, M. J., Huddart, D., Bennett, M. R., & Glasser, N. F. (1997). Genesis of 'hummocky moraines' by thrusting in glacier ice: evidence from Svalbard and Britain. *Journal of the Geological Society*, 154(4), 623-632.
- Hambrey, M. J., Bennett, M. R., Dowdeswell, J. A., Glasser, N. F., & Huddart, D. (1999). Debris entrainment and transfer in polythermal valley glaciers. *Journal of Glaciology*, 45(149), 69-86.
- Hambrey, M. J., Davies, J. R., Glasser, N. F., Waters, R. A., Dowdeswell, J. A., Wilby, P. R., ... & Etienne, J. L. (2001). Devensian glacial sedimentation and landscape evolution in the Cardigan area of southwest Wales. *Journal of Quaternary Science*, 16(5), 455-482.
- Hammer, K. M., & Smith, N. D. (1983). Sediment production and transport in a proglacial stream: Hilda Glacier, Alberta, Canada. *Boreas*, 12(2), 91-106.
- Hampel, N. (2009). *Proglacial controls on short-term suspended sediment concentration variability in a melt water stream*. Unpublished undergraduate dissertation: University of Hertfordshire.
- Hannah, D. M., Smith, B. P., Gurnell, A. M., & McGregor, G. R. (2000). An approach to hydrograph classification. *Hydrological processes*, 14(2), 317-338.
- Hannah, D. M., & Gurnell, A. M. (2001). A conceptual, linear reservoir runoff model to investigate melt season changes in cirque glacier hydrology. *Journal of Hydrology*, 246(1), 123-141.
- Hannah, D. M., Kansakar, S. R., Gerrard, A. J., & Rees, G. (2005). Flow regimes of Himalayan rivers of Nepal: nature and spatial patterns. *Journal of Hydrology*, 308(1), 18-32.
- Harbor, J., & Warburton, J. (1993). Relative rates of glacial and nonglacial erosion in alpine environments. *Arctic and Alpine Research*, 1-7.
- Haritashya, U. K., Singh, P., Kumar, N., & Gupta, R. P. (2006). Suspended sediment from the Gangotri Glacier: Quantification, variability and associations with discharge and air temperature. *Journal of Hydrology*, 321(1), 116-130.

- Haritashya, U. K., Kumar, A., & Singh, P. (2010). Particle size characteristics of suspended sediment transported in meltwater from the Gangotri Glacier, central Himalaya—An indicator of subglacial sediment evacuation. *Geomorphology*, *122*(1), 140-152.
- Harper, J. T., & Humphrey, N. F. (1995). Borehole video analysis of a temperate glacier's englacial and subglacial structure: Implications for glacier flow models. *Geology*, *23*(10), 901-904.
- Harris, N. M., Gurnell, A. M., Hannah, D. M., & Petts, G. E. (2000). Classification of river regimes: a context for hydroecology. *Hydrological Processes*, *14*(16-17), 2831-2848.
- Harrison, S., Glasser, N., Winchester, V., Haresign, E., Warren, C., & Jansson, K. (2006). A glacial lake outburst flood associated with recent mountain glacier retreat, Patagonian Andes. *The Holocene*, *16*(4), 611-620.
- Hasholt, B., Walling, D. E., & Owens, P. N. (2000). Sedimentation in arctic proglacial lakes: Mittivakkat Glacier, south-east Greenland. *Hydrological Processes*, *14*(4), 679-699.
- Hasnain, S. I. (1996). Factors controlling suspended sediment transport in Himalayan glacier meltwaters. *Journal of hydrology*, *181*(1), 49-62.
- Hay, W. W. (1998). Detrital sediment fluxes from continents to oceans. *Chemical geology*, *145*(3), 287-323.
- Hicks, D. M., McSaveney, M. J., & Chinn, T. J. H. (1990). Sedimentation in proglacial Ivory Lake, Southern Alps, New Zealand. *Arctic and Alpine Research*, 26-42.
- Hock, R., & Noetzi, C. (1997). Areal melt and discharge modelling of Storglaciären, Sweden. *Annals of Glaciology*, *24*, 211-216.
- Hock, R. (1998). *Modelling of glacier melt and discharge*. Doctoral thesis, Eidgenössische Technische Hochschule (ETH) Zürich.
- Hock, R. (1999). A distributed temperature-index ice-and snowmelt model including potential direct solar radiation. *Journal of Glaciology*, *45*(149), 101-111.
- Hock, R. (2003). Temperature index melt modelling in mountain areas. *Journal of Hydrology*, *282*(1), 104-115.
- Hock, R., & Jansson, P. (2005). Modeling glacier hydrology. Wiley: *Encyclopedia of hydrological sciences*.
- Hodgkins, R. (1999). Controls on suspended-sediment transfer at a High-Arctic glacier, determined from statistical modelling. *Earth Surface Processes and Landforms*, *24*(1), 1-21.

- Hodgkins, R., Cooper, R., Wadham, J., & Tranter, M. (2003). Suspended sediment fluxes in a high-Arctic glacierised catchment: implications for fluvial sediment storage. *Sedimentary Geology*, 162(1), 105-117.
- Hodgkins, R., Carr, S., Pálsson, F., Guðmundsson, S., & Björnsson, H. (2013a). Modelling variable glacier lapse rates using ERA-Interim reanalysis climatology: an evaluation at Vestari-Hagafellsjökull, Langjökull, Iceland. *International Journal of Climatology*, 33(2), 410-421.
- Hodgkins, R., Cooper, R., Tranter, M., & Wadham, J. (2013b). Drainage-system development in consecutive melt seasons at a polythermal, Arctic glacier, evaluated by flow-recession analysis and linear-reservoir simulation. *Water resources research*, 49(7), 4230-4243.
- Hodson, A., Gurnell, A., Tranter, M., Bogen, J., Hagen, J. O., & Clark, M. (1998). Suspended sediment yield and transfer processes in a small High-Arctic glacier basin, Svalbard. *Hydrological Processes*, 12(1), 73-86.
- Hodson, A. J., & Ferguson, R. I. (1999). Fluvial suspended sediment transport from cold and warm-based glaciers in Svalbard. *Earth Surface Processes and Landforms*, 24(11), 957-974.
- Holmlund, P., Burman, H., & Rost, T. (1996). Sediment-mass exchange between turbid meltwater streams and proglacial deposits of Storglaciären, northern Sweden. *Annals of Glaciology*, 22, 63-67.
- Hood, E., Battin, T. J., Fellman, J., O'Neel, S., & Spencer, R. G. (2015). Storage and release of organic carbon from glaciers and ice sheets. *Nature Geoscience*, 8(2), 91-96.
- Hooke, R. L. (1984). On the role of mechanical energy in maintaining subglacial water conduits at atmospheric pressure. *Journal of Glaciology*, 30(105), 180-187.
- Hooke, R. L., Wold, B., & Hagen, J. O. (1985). Subglacial hydrology and sediment transport at Bondhusbreen, southwest Norway. *Geological Society of America Bulletin*, 96(3), 388-397.
- Hooke, R. L., & Iverson, N. R. (1995). Grain-size distribution in deforming subglacial tills: role of grain fracture. *Geology*, 23(1), 57-60.
- Hubbard, B., & Glasser, N. F. (2005). *Field techniques in glaciology and glacial geomorphology*. John Wiley & Sons.
- Hubbard, B. P., Sharp, M. J., Willis, I. C., Nielsen, M. T., & Smart, C. C. (1995). Borehole water-level variations and the structure of the subglacial hydrological system of Haut Glacier d'Arolla, Valais, Switzerland. *Journal of Glaciology*, 41(139), 572-583.
- Hubbard, B., & Nienow, P. (1997). Alpine subglacial hydrology. *Quaternary Science Reviews*, 16(9), 939-955.

- Hubbard, B., & Glasser, N. F. (2005). *Field techniques in glaciology and glacial geomorphology*. John Wiley & Sons.
- Hubbard, B., Heald, A., Reynolds, J. M., Quincey, D., Richardson, S. D., Luyo, M. Z., ... & Hambrey, M. J. (2005). Impact of a rock avalanche on a moraine-dammed proglacial lake: Laguna Safuna Alta, Cordillera Blanca, Peru. *Earth Surface Processes and Landforms*, 30(10), 1251-1264.
- Huintjes, E., Li, H., Sauter, T., Li, Z., & Schneider, C. (2010). Degree-day modelling of the surface mass balance of Urumqi Glacier No. 1, Tian Shan, China. *The Cryosphere Discussions*, 4(1), 207-232.
- Humphrey, N., Raymond, C., & Harrison, W. (1986). Discharges of turbid water during mini-surges of Variegated Glacier, Alaska, USA. *Journal of Glaciology*, 32(111), 195-207.
- Huss, M., Farinotti, D., Bauder, A., & Funk, M. (2008). Modelling runoff from highly glacierized alpine drainage basins in a changing climate. *Hydrological processes*, 22(19), 3888-3902.
- Huss, M., Funk, M., & Ohmura, A. (2009). Strong Alpine glacier melt in the 1940s due to enhanced solar radiation. *Geophysical Research Letters*, 36(23).
- Huss, M., Jouvett, G., Farinotti, D., & Bauder, A. (2010). Future high-mountain hydrology: a new parameterization of glacier retreat. *Hydrology and Earth System Sciences*, 14(5), 815-829.
- Huss, M. (2011). Present and future contribution of glacier storage change to runoff from macroscale drainage basins in Europe. *Water Resources Research*, 47(7).
- Huss, M., Zemp, M., Joerg, P. C., & Salzmann, N. (2014). High uncertainty in 21st century runoff projections from glacierized basins. *Journal of Hydrology*, 510, 35-48.
- Irvine-Fynn, T. D. L., Moorman, B. J., Willis, I. C., Sjogren, D. B., Hodson, A. J., Mumford, P. N., ... & Williams, J. L. M. (2005a). Geocryological processes linked to High Arctic proglacial stream suspended sediment dynamics: examples from Bylot Island, Nunavut, and Spitsbergen, Svalbard. *Hydrological Processes*, 19(1), 115-135.
- Irvine-Fynn, T. D. L., Hodson, A. J., Kohler, J., Porter, P., & Vatne, G. (2005b). Dye tracing experiments at Midtre Lovénbreen, Svalbard: preliminary results and interpretations. *Proceedings of the 7th glacier caves and glacial karst in high mountains and polar regions. Institute of the Russian Academy of Sciences, Moscow*, 36-43.
- Irvine-Fynn, T. D. L., Moorman, B. J., Williams, J. L. M., & Walter, F. S. A. (2006). Seasonal changes in ground-penetrating radar signature observed at a polythermal glacier, Bylot Island, Canada. *Earth Surface Processes and Landforms*, 31(7), 892-909.

- Irvine-Fynn, T. D. (2008). *Modelling runoff from the maritime arctic cryosphere: Water storage and routing at Midtre Lovénbreen*. Doctoral thesis, University of Sheffield.
- Irvine-Fynn, T. D., Hanna, E., Barrand, N. E., Porter, P. R., Kohler, J., & Hodson, A. J. (2014). Examination of a physically based, high-resolution, distributed Arctic temperature-index melt model, on Midtre Lovénbreen, Svalbard. *Hydrological Processes*, 28(1), 134-149.
- Iverson, N. R., Hanson, B., Hooke, R. L., & Jansson, P. (1995). Flow mechanism of glaciers on soft beds. *Science*, 267(5194), 80.
- Ivy-Ochs, S., Kerschner, H., Maisch, M., Christl, M., Kubik, P. W., & Schlüchter, C. (2009). Latest Pleistocene and Holocene glacier variations in the European Alps. *Quaternary Science Reviews*, 28(21), 2137-2149.
- Jansson, M. B. (2002). Determining sediment source areas in a tropical river basin, Costa Rica. *Catena*, 47(1), 63-84.
- Jansson, P., Hock, R., & Schneider, T. (2003). The concept of glacier storage: a review. *Journal of Hydrology*, 282(1), 116-129.
- Jobard, S., & Dzikowski, M. (2006). Evolution of glacial flow and drainage during the ablation season. *Journal of Hydrology*, 330(3), 663-671.
- Johannesson, T., Sigurdsson, O., Laumann, T., & Kennett, M. (1995). Degree-day glacier mass-balance modelling with applications to glaciers in Iceland, Norway and Greenland. *Journal of Glaciology*, 41(138), 345-358.
- Juen, M., Mayer, C., Lambrecht, A., Han, H., & Liu, S. (2014). Impact of varying debris cover thickness on ablation: a case study for Koxkar Glacier in the Tien Shan. *The Cryosphere*, 8(2), 377-386.
- Kamb, B. (1987). Glacier surge mechanism based on linked cavity configuration of the basal water conduit system. *Journal of Geophysical Research B*, 92(B9), 9083-9100.
- Kane, D. L., Gieck, R. E., & Hinzman, L. D. (1997). Snowmelt modeling at small Alaskan Arctic watershed. *Journal of Hydrologic Engineering*, 2(4), 204-210.
- Kargel, J.S., Leonard, G.J., Bishop, M.P., Kaab, A. & Raup B. (Eds). (2014). *Global Land Ice Measurements from Space*. Springer-Praxis
- Kayastha, R. B., Takeuchi, Y., Nakawo, M., & Ageta, Y. (2000). Practical prediction of ice melting beneath various thickness of debris cover on Khumbu Glacier, Nepal, using a positive degree-day factor. *IAHS Publication*, 71-82.
- Kellerer-Pirklbauer, A. (2008). The supraglacial debris system at the Pasterze Glacier, Austria: spatial distribution, characteristics and transport of debris. *Zeitschrift für Geomorphologie, Supplementary Issues*, 52(1), 3-25.

- Kettner, A. J., & Syvitski, J. P. (2008). HydroTrend v. 3.0: A climate-driven hydrological transport model that simulates discharge and sediment load leaving a river system. *Computers & Geosciences*, *34*(10), 1170-1183.
- Khadka, D., Babel, M. S., Shrestha, S., & Tripathi, N. K. (2014). Climate change impact on glacier and snow melt and runoff in Tamakoshi basin in the Hindu Kush Himalayan (HKH) region. *Journal of Hydrology*, *511*, 49-60.
- Kido, D., Chikita, K. A., & Hirayama, K. (2007). Subglacial drainage system changes of the Gulkana Glacier, Alaska: discharge and sediment load observations and modelling. *Hydrological Processes*, *21*(3), 399-410.
- Kirkbride, M. P., & Warren, C. R. (1999). Tasman Glacier, New Zealand: 20th-century thinning and predicted calving retreat. *Global and Planetary Change*, *22*(1), 11-28.
- Klok, E. J., Jasper, K., Roelofsma, K. P., Gurtz, J., & Badoux, A. (2001). Distributed hydrological modelling of a heavily glaciated Alpine river basin. *Hydrological Sciences Journal*, *46*(4), 553-570.
- Knight, J., & Harrison, S. (2009). Periglacial and paraglacial environments: a view from the past into the future. *Geological Society, London, Special Publications*, *320*(1), 1-4.
- Knudsen, N. T., Yde, J. C., & Gasser, G. (2007). Suspended sediment transport in glacial meltwater during the initial quiescent phase after a major surge event at Kuannersuit Glacier, Greenland. *Geografisk Tidsskrift-Danish Journal of Geography*, *107*(1), 1-7.
- Koboltschnig, G. R., Schöner, W., Zappa, M., Kroisleitner, C., & Holzmann, H. (2008). Runoff modelling of the glacierized Alpine Upper Salzach basin (Austria): Multi - criteria result validation. *Hydrological Processes*, *22*(19), 3950-3964.
- Konya, K., Matsumoto, T., & Naruse, R. (2004). Surface heat balance and spatially distributed ablation modelling at Koryto Glacier, Kamchatka peninsula, Russia. *Geografiska Annaler: Series A, Physical Geography*, *86*(4), 337-348.
- Korup, O. (2002). Recent research on landslide dams-a literature review with special attention to New Zealand. *Progress in Physical Geography*, *26*(2), 206-235.
- Korup, O., & Tweed, F. (2007). Ice, moraine, and landslide dams in mountainous terrain. *Quaternary Science Reviews*, *26*(25), 3406-3422.
- Krause, P., Boyle, D. P., & Bäse, F. (2005). Comparison of different efficiency criteria for hydrological model assessment. *Advances in Geosciences*, *5*, 89-97.
- Kühni, A., & Pfiffner, O. A. (2001). The relief of the Swiss Alps and adjacent areas and its relation to lithology and structure: topographic analysis from a 250-m DEM. *Geomorphology*, *41*(4), 285-307.

- Lang, H., Schädler, B., & Davidson, G. (1977). Hydroglaciological investigations on the Ewigschneefeld-Grosser Aletschgletscher. *Zeitschrift für Gletscherkunde und Glazialgeologie*, 12(2), 109-124.
- Lang, H. (1986). Forecasting meltwater runoff from snow-covered areas and from glacier basins. In *River flow modelling and forecasting* (pp. 99-127). Springer Netherlands.
- Laumann, T., & Reeh, N. (1993). Sensitivity to climate change of the mass balance of glaciers in southern Norway. *Journal of Glaciology*, 39, 656-665.
- Legates, D. R., & McCabe Jr, G. J. (1999). Evaluating the use of "goodness-of-fit" measures in hydrologic and hydroclimatic model validation. *Water resources research*, 35(1), 233-241.
- Leggat, M. S., Owens, P. N., Stott, T. A., Forrester, B. J., Déry, S. J., & Menounos, B. (2015). Hydro-meteorological drivers and sources of suspended sediment flux in the proglacial zone of the retreating Castle Creek glacier, Cariboo Mountains, British Columbia, Canada. *Earth Surface Processes and Landforms*.
- Lenzi, M. A., & Marchi, L. (2000). Suspended sediment load during floods in a small stream of the Dolomites (northeastern Italy). *Catena*, 39(4), 267-282.
- Lenzi, M. A., Mao, L., & Comiti, F. (2003). Interannual variation of suspended sediment load and sediment yield in an alpine catchment. *Hydrological Sciences Journal*, 48(6), 899-915.
- Liermann, S., Beylich, A. A., & van Welden, A. (2012). Contemporary suspended sediment transfer and accumulation processes in the small proglacial Sætrevatnet sub-catchment, Bødalen, western Norway. *Geomorphology*, 167, 91-101.
- Lønne, I., & Lyså, A. (2005). Deglaciation dynamics following the Little Ice Age on Svalbard: Implications for shaping of landscapes at high latitudes. *Geomorphology*, 72(1), 300-319.
- Lukas, S., Nicholson, L. I., Ross, F. H., & Humlum, O. (2005). Formation, meltout processes and landscape alteration of high-Arctic ice-cored moraines—Examples from Nordenskiöld Land, central Spitsbergen. *Polar Geography*, 29(3), 157-187
- Lukas, S., Nicholson, L. I., & Humlum, O. (2007). Comment on Lønne and Lyså (2005):“Deglaciation dynamics following the Little Ice Age on Svalbard: Implications for shaping of landscapes at high latitudes”, *Geomorphology* 72, 300–319. *Geomorphology*, 84(1), 145-149.
- Lukas, S., Graf, A., Coray, S., & Schlüchter, C. (2012). Genesis, stability and preservation potential of large lateral moraines of Alpine valley glaciers—towards a unifying theory based on Findelengletscher, Switzerland. *Quaternary Science Reviews*, 38, 27-48.

- Lutz, S., Anesio, A. M., Villar, S. E. J., & Benning, L. G. (2014). Variations of algal communities cause darkening of a Greenland glacier. *FEMS microbiology ecology*, 89(2), 402-414.
- MacDougall, A. H., & Flowers, G. E. (2011). Spatial and temporal transferability of a distributed energy-balance glacier melt model. *Journal of Climate*, 24(5), 1480-1498.
- Magnusson, J., Farinotti, D., Jonas, T., & Bavay, M. (2011). Quantitative evaluation of different hydrological modelling approaches in a partly glacierized Swiss watershed. *Hydrological Processes*, 25(13), 2071-2084.
- Mair, D. W., Sharp, M. J., & Willis, I. C. (2002). Evidence for basal cavity opening from analysis of surface uplift during a high-velocity event: Haut Glacier d'Arolla, Switzerland. *Journal of Glaciology*, 48(161), 208-216.
- Mair, D., Willis, I., Fischer, U. H., Hubbard, B., Nienow, P., & Hubbard, A. (2003). Hydrological controls on patterns of surface, internal and basal motion during three "spring events": Haut Glacier d'Arolla, Switzerland. *Journal of Glaciology*, 49(167), 555-567.
- Maisch, M., Wipf, A., Denneler, B., Battaglia, J., & Benz, C. (2000). Die Gletscher der Schweizer Alpen: Gletscherschwund 1850, Aktuelle Vergletscherung, Gletscherschwund-Szenarien 21. Jahrhundert.
- Maizels, J. K. (1979). Proglacial aggradation and changes in braided channel patterns during a period of glacier advance: an Alpine example. *Geografiska Annaler. Series A. Physical Geography*, 87-101.
- Marcus, M. G., Moore, R. D., & Owens, I. F. (1985). Short-term estimates of surface energy transfers and ablation on the lower Franz Josef Glacier, South Westland, New Zealand. *New Zealand Journal of Geology and Geophysics*, 28(3), 559-567.
- Marren, P. M. (2002). Fluvial-lacustrine interaction on Skeiðarársandur, Iceland: implications for sandur evolution. *Sedimentary Geology*, 149(1), 43-58.
- Marren, P. M., Russell, A. J., & Knudsen, O. S. K. A. R. (2002). Discharge magnitude and frequency as a control on proglacial fluvial sedimentary systems. *IAHS Publication*, (276), 297-303.
- Marren, P. M. (2005). Magnitude and frequency in proglacial rivers: a geomorphological and sedimentological perspective. *Earth-Science Reviews*, 70(3), 203-251.
- Marren, P. M., & Toomath, S. C. (2014). Channel pattern of proglacial rivers: topographic forcing due to glacier retreat. *Earth Surface Processes and Landforms*, 39(7), 943-951.
- Marshall, S. J., & Clarke, G. K. (1999). Modeling North American freshwater runoff through the last glacial cycle. *Quaternary Research*, 52(3), 300-315.

- Megnounif, A., Terfous, A., & Ouillon, S. (2013). A graphical method to study suspended sediment dynamics during flood events in the Wadi Sebdou, NW Algeria (1973–2004). *Journal of Hydrology*, 497, 24-36.
- Mercier, D. (2000). From glacial to paraglacial: the metamorphosis of polar landscapes in Svalbard. *Annales de Géographie*. 109(616), 580-596.
- Mercier, D., & Laffly, D. (2005). Actual paraglacial progradation of the coastal zone in the Kongsfjorden area, western Spitsbergen (Svalbard). *Geological Society, London, Special Publications*, 242(1), 111-117.
- Mercier, D. (2009). Paraglacial and paraperiglacial landsystems: concepts, temporal scales and spatial distribution. *Géomorphologie: relief, processus, environnement*, (4/2008), 223-233.
- Mercier, D., Étienne, S., Sellier, D., & André, M. F. (2009). Paraglacial gullying of sediment-mantled slopes: a case study of Colletthøgda, Kongsfjorden area, West Spitsbergen (Svalbard). *Earth Surface Processes and Landforms*, 34(13), 1772-1789.
- Mihalcea, C., Mayer, C., Diolaiuti, G., Lambrecht, A., Smiraglia, C., & Tartari, G. (2006). Ice ablation and meteorological conditions on the debris-covered area of Baltoro glacier, Karakoram, Pakistan. *Annals of Glaciology*, 43(1), 292-300.
- Mohammadi, Z., & Raeisi, E. (2007). Hydrogeological uncertainties in delineation of leakage at karst dam sites, the Zagros Region, Iran. *Journal of Cave and Karst Studies*, 69(3), 305-317.
- Moore, R. D. (2004). Introduction to salt dilution gauging for streamflow measurement: Part 1. *Streamline Watershed Management Bulletin*, 7(4), 20-23.
- Morehead, M. D., Syvitski, J. P., Hutton, E. W., & Peckham, S. D. (2003). Modeling the temporal variability in the flux of sediment from ungauged river basins. *Global and Planetary Change*, 39(1), 95-110.
- Moss, R. H., Babiker, M., Brinkman, S., Calvo, E., Carter, T., Edmonds, J. A., ... & Jones, R. (2008). *Towards new scenarios for analysis of emissions, climate change, impacts, and response strategies* (No. PNNL-SA-63186). Pacific Northwest National Laboratory (PNNL), Richland, WA (US).
- Murray, R. W., Leinen, M., & Isern, A. R. (1993). Biogenic flux of Al to sediment in the central equatorial Pacific Ocean: Evidence for increased productivity during glacial periods. *Paleoceanography*, 8(5), 651-670.
- Murray, T., Stuart, G. W., Fry, M., Gamble, N. H., & Crabtree, M. D. (2000). Englacial water distribution in a temperate glacier from surface and borehole radar velocity analysis. *Journal of Glaciology*, 46(154), 389-398.
- Nicholson, L., & Benn, D. I. (2006). Calculating ice melt beneath a debris layer using meteorological data. *Journal of Glaciology*, 52(178), 463-470.

- Nienow, P., Sharp, M., & Willis, I. (1996). Temporal switching between englacial and subglacial drainage pathways: dye tracer evidence from the Haut Glacier d'Arolla, Switzerland. *Geografiska Annaler. Series A. Physical Geography*, 51-60.
- Nienow, P., Sharp, M., & Willis, I. (1998). Seasonal changes in the morphology of the subglacial drainage system, Haut Glacier d'Arolla, Switzerland. *Earth Surface Processes and Landforms*, 23(9), 825-843.
- Oerlemans, J., & Reichert, B. K. (2000). Relating glacier mass balance to meteorological data by using a seasonal sensitivity characteristic. *Journal of Glaciology*, 46(152), 1-6.
- Oerlemans, J., Giesen, R. H., & Van den Broeke, M. R. (2009). Retreating alpine glaciers: increased melt rates due to accumulation of dust (Vadret da Morteratsch, Switzerland). *Journal of Glaciology*, 55(192), 729-736.
- Ohmura, A. (2001). Physical basis for the temperature-based melt-index method. *Journal of Applied Meteorology*, 40(4), 753-761.
- Orheim, O. (1970). Glaciological Investigations of Store Supphellebre, West-Norway. *Journal of Glaciology*, 38(130), 397-411.
- Orwin, J. F., & Smart, C. C. (2004a). Short-term spatial and temporal patterns of suspended sediment transfer in proglacial channels, Small River Glacier, Canada. *Hydrological Processes*, 18(9), 1521-1542.
- Orwin, J. F., & Smart, C. C. (2004b). The evidence for paraglacial sedimentation and its temporal scale in the deglaciating basin of Small River Glacier, Canada. *Geomorphology*, 58(1), 175-202.
- Orwin, J. F., & Smart, C. C. (2005). An inexpensive turbidimeter for monitoring suspended sediment. *Geomorphology*, 68(1), 3-15.
- Orwin, J. F., Lamoureux, S. F., Warburton, J., & Beylich, A. (2010). A framework for characterizing fluvial sediment fluxes from source to sink in cold environments. *Geografiska Annaler: Series A, Physical Geography*, 92(2), 155-176.
- Östrem, G. (1959). Ice melting under a thin layer of moraine, and the existence of ice cores in moraine ridges. *Geografiska Annaler*, 228-230.
- Østrem, G., & Olsen, H. C. (1987). Sedimentation in a glacier lake. *Geografiska Annaler. Series A. Physical Geography*, 123-138.
- Østrem, D. & Brugman, M. (1991). *Glacier mass balance measurements: a manual for field and office work*. Science Report 4. National Hydrology Research Institute/Norwegian Water Resources and Electricity Board, 224 pp.
- Pachauri, R. K., Allen, M. R., Barros, V. R., Broome, J., Cramer, W., Christ, R., ... & Dasgupta, P. (Eds.). (2014). *Climate Change 2014: Synthesis Report. Contribution of Working Groups I, II and III to the Fifth Assessment Report of*

the Intergovernmental Panel on Climate Change. Intergovernmental Panel on Climate Change.

- Paul, F., Kääb, A., Maisch, M., Kellenberger, T., & Haeberli, W. (2004). Rapid disintegration of Alpine glaciers observed with satellite data. *Geophysical research letters*, 31(21).
- Paul, F., Machguth, H., & Kääb, A. (2005). On the impact of glacier albedo under conditions of extreme glacier melt: the summer of 2003 in the Alps. *EARSeL eProceedings*, 4(2), 139-149.
- Paul, F., Kääb, A., & Haeberli, W. (2007). Recent glacier changes in the Alps observed by satellite: Consequences for future monitoring strategies. *Global and Planetary Change*, 56(1), 111-122.
- Pellicciotti, F., Brock, B., Strasser, U., Burlando, P., Funk, M., & Corripio, J. (2005). An enhanced temperature-index glacier melt model including the shortwave radiation balance: development and testing for Haut Glacier d'Arolla, Switzerland. *Journal of Glaciology*, 51(175), 573-587.
- Pellicciotti, F., Helbing, J., Rivera, A., Favier, V., Corripio, J., Araos, J., ... & Carenzo, M. (2008). A study of the energy balance and melt regime on Juncal Norte Glacier, semi-arid Andes of central Chile, using melt models of different complexity. *Hydrological Processes*, 22(19), 3980-3997.
- Pettersson, R., Jansson, P., & Blatter, H. (2004). Spatial variability in water content at the cold-temperate transition surface of the polythermal Storglaciären, Sweden. *Journal of Geophysical Research: Earth Surface* (2003–2012), 109(F2).
- Porter, P. R., Vatne, G., Ng, F., & Irvine-Fynn, T. D. (2010). Ice-marginal sediment delivery to the surface of a high-Arctic glacier: Austre Brøggerbreen, Svalbard. *Geografiska Annaler: Series A, Physical Geography*, 92(4), 437-449.
- Pralong, M. R., Turowski, J. M., Rickenmann, D., & Zappa, M. (2015). Climate change impacts on bedload transport in alpine drainage basins with hydropower exploitation. *Earth Surface Processes and Landforms*.
- Ramillien, G., Lombard, A., Cazenave, A., Ivins, E. R., Llubes, M., Remy, F., & Biancale, R. (2006). Interannual variations of the mass balance of the Antarctica and Greenland ice sheets from GRACE. *Global and Planetary Change*, 53(3), 198-208.
- Raiswell, R., Tranter, M., Benning, L. G., Siegert, M., De'ath, R., Huybrechts, P., & Payne, T. (2006). Contributions from glacially derived sediment to the global iron (oxyhydr) oxide cycle: implications for iron delivery to the oceans. *Geochimica et Cosmochimica Acta*, 70(11), 2765-2780.
- Raup, B., Racoviteanu, A., Khalsa, S. J. S., Helm, C., Armstrong, R., & Arnaud, Y. (2007). The GLIMS geospatial glacier database: a new tool for studying glacier change. *Global and Planetary Change*, 56(1), 101-110.

- Rees, H. G., & Collins, D. N. (2006). Regional differences in response of flow in glacier-fed Himalayan rivers to climatic warming. *Hydrological processes*, 20(10), 2157-2169.
- Reid, T. D., & Brock, B. W. (2010). An energy-balance model for debris-covered glaciers including heat conduction through the debris layer. *Journal of Glaciology*, 56(199), 903-916.
- Richards, G., & Moore, R. D. (2003). Suspended sediment dynamics in a steep, glacier-fed mountain stream, Place Creek, Canada. *Hydrological Processes*, 17(9), 1733-1753.
- Richards, K. (1984). Some observations on suspended sediment dynamics in Storbregrova, Jotunheimen. *Earth Surface Processes and Landforms*, 9(2), 101-112.
- Richards, K., Sharp, M., Arnold, N., Gurnell, A., Clark, M., Tranter, M., ... & Lawson, W. (1996). An integrated approach to modelling hydrology and water quality in glacierized catchments. *Hydrological Processes*, 10(4), 479-508.
- Richardson, S. D., & Reynolds, J. M. (2000). An overview of glacial hazards in the Himalayas. *Quaternary International*, 65, 31-47.
- Riedel, J. L., Wilson, S., Baccus, W., Larrabee, M., Fudge, T. J., & Fountain, A. (2015). Glacier status and contribution to streamflow in the Olympic Mountains, Washington, USA. *Journal of Glaciology*, 61(225), 8-16.
- Rignot, E., Bamber, J. L., Van Den Broeke, M. R., Davis, C., Li, Y., Van De Berg, W. J., & Van Meijgaard, E. (2008). Recent Antarctic ice mass loss from radar interferometry and regional climate modelling. *Nature Geoscience*, 1(2), 106-110.
- Roberts, M. J., Russell, A. J., Tweed, F. S., & Knudsen, Ó. (2001). Controls on englacial sediment deposition during the November 1996 jökulhlaup, Skeiðarárjökull, Iceland. *Earth Surface Processes and Landforms*, 26(9), 935-952.
- Rogelj, J., Meinshausen, M., & Knutti, R. (2012). Global warming under old and new scenarios using IPCC climate sensitivity range estimates. *Nature climate change*, 2(4), 248-253.
- Rubensdotter, L., & Rosqvist, G. (2009). Influence of geomorphological setting, fluvial-, glaciofluvial-and mass-movement processes on sedimentation in alpine lakes. *The Holocene*, 19(4), 665-678.
- Rushmer, E. L. (2006). Sedimentological and geomorphological impacts of the jökulhlaup (glacial outburst flood) in January 2002 at Kverkfjöll, northern Iceland. *Geografiska Annaler: Series A, Physical Geography*, 88(1), 43-53.
- Russell, A. J., Roberts, M. J., Fay, H., Marren, P. M., Cassidy, N. J., Tweed, F. S., & Harris, T. (2006). Icelandic jökulhlaup impacts: implications for ice-sheet

- hydrology, sediment transfer and geomorphology. *Geomorphology*, 75(1), 33-64.
- Rutter, N. J. (2005). Impact of subglacial hydrology on the release of water from temporary storage in an Alpine glacier. *Annals of Glaciology*, 40(1), 67-75.
- Rutter, N., Hodson, A., Irvine-Fynn, T., & Solås, M. K. (2011). Hydrology and hydrochemistry of a deglaciating high-Arctic catchment, Svalbard. *Journal of Hydrology*, 410(1), 39-50.
- SAS/VAW, (2009). The Swiss Glaciers, Yearbooks of the Glaciological Commission of the Swiss Academy of Science (SAS). Laboratory of Hydraulics, Hydrology and Glaciology (VAW) of ETH Zürich. No. 1–124 (1881–2002).
- Scherler, D., Bookhagen, B., & Strecker, M. R. (2011). Spatially variable response of Himalayan glaciers to climate change affected by debris cover. *Nature geoscience*, 4(3), 156-159.
- Schmid, S. M., Pfiffner, O. A., Froitzheim, N., Schönborn, G., & Kissling, E. (1996). Geophysical-geological transect and tectonic evolution of the Swiss-Italian Alps. *Tectonics*, 15(5), 1036-1064.
- Schneeberger, C., Blatter, H., Abe-Ouchi, A., & Wild, M. (2003). Modelling changes in the mass balance of glaciers of the northern hemisphere for a transient 2× CO₂ scenario. *Journal of Hydrology*, 282(1), 145-163.
- Schuler, T., Fischer, U. H., Sterr, R., Hock, R., & Gudmundsson, G. H. (2002). Comparison of modeled water input and measured discharge prior to a release event: Unteraargletscher, Bernese Alps, Switzerland. *Nordic Hydrology*, 33(1), 27-46.
- Schytt, V. (1964). Scientific results of the Swedish glaciological expedition to Nordaustlandet, Spitsbergen, 1957 and 1958. *Geografiska Annaler*, 242-281.
- Scott Munro, D. (2011). Delays of supraglacial runoff from differently defined microbasin areas on the Peyto Glacier. *Hydrological Processes*, 25(19), 2983-2994.
- Seeger, M., Errea, M. P., Begueria, S., Arnáez, J., Martí, C., & Garcia-Ruiz, J. M. (2004). Catchment soil moisture and rainfall characteristics as determinant factors for discharge/suspended sediment hysteretic loops in a small headwater catchment in the Spanish Pyrenees. *Journal of Hydrology*, 288(3), 299-311.
- Sharp, M., Richards, K., Willis, I., Arnold, N., Nienow, P., Lawson, W., & Tison, J. L. (1993). Geometry, bed topography and drainage system structure of the Haut Glacier d'Arolla, Switzerland. *Earth Surface Processes and Landforms*, 18(6), 557-571.
- Sharp, M., Richards, K. S., & Tranter, M. (Eds.). (1998). *Glacier hydrology and hydrochemistry*. Wiley.

- Shea, J. M., Anslow, F. S., & Marshall, S. J. (2005). Hydrometeorological relationships on Haig Glacier, Alberta, Canada. *Annals of Glaciology*, 40(1), 52-60.
- Singh, P., & Kumar, N. (1996). Determination of snowmelt factor in the Himalayan region. *Hydrological sciences journal*, 41(3), 301-310.
- Singh, P., Kumar, N., & Arora, M. (2000). Degree-day factors for snow and ice for Dokriani Glacier, Garhwal Himalayas. *Journal of Hydrology*, 235(1), 1-11.
- Singh, P., Ramasatri, K. S., Kumar, N., & Bhatnagar, N. K. (2003). Suspended sediment transport from the Dokriani Glacier in the Garhwal Himalayas. *Nordic hydrology*, 34(3), 221-244.
- Singh, P., Kumar, A., & Kishore, N. (2011). Meltwater storage and delaying characteristics of Gangotri Glacier (Indian Himalayas) during ablation season. *Hydrological Processes*, 25(2), 159-166.
- Sletten, K., Lyså, A., & Lønne, I. (2001). Formation and disintegration of a high - arctic ice - cored moraine complex, Scott Turnerbreen, Svalbard. *Boreas*, 30(4), 272-284.
- Smart, P. L., & Laidlaw, I. M. S. (1977). An evaluation of some fluorescent dyes for water tracing. *Water Resources Research*, 13(1), 15-33.
- Smart, C. C. (1988). Quantitative tracing of the Maligne karst system, Alberta, Canada. *Journal of hydrology*, 98(3), 185-204.
- Smith, N. D. (1981). The effect of changing sediment supply on sedimentation in a glacier-fed lake. *Arctic and Alpine Research*, 75-82.
- Smith, D. I., & Atkinson, T. C. (1977). Underground flow in cavernous limestones with special reference to the Malham area. *Field Studies*, 4, 597-616.
- Solomon, S. (Ed.), IPCC. (2007). *Climate change 2007-the physical science basis: Working group I contribution to the fourth assessment report of the IPCC* (Vol. 4). Cambridge University Press.
- Souchez, R., & Lorrain, R. (1987). The subglacial sediment system. *Glacio-Fluvial Sediment Transfer: An Alpine Perspective*. John Wiley and Sons, New York, 179-184.
- Stahl, K., Moore, R. D., Shea, J. M., Hutchinson, D., & Cannon, A. J. (2008). Coupled modelling of glacier and streamflow response to future climate scenarios. *Water Resources Research*, 44(2).
- Stott, T. A., & Grove, J. R. (2001). Short-term discharge and suspended sediment fluctuations in the proglacial Skeldal River, north - east Greenland. *Hydrological Processes*, 15(3), 407-423.
- Stott, T., & Mount, N. (2007). Alpine proglacial suspended sediment dynamics in warm and cool ablation seasons: Implications for global warming. *Journal of Hydrology*, 332(3), 259-270.

- Strasser, U., Corripio, J., Pellicciotti, F., Burlando, P., Brock, B., & Funk, M. (2004). Spatial and temporal variability of meteorological variables at Haut Glacier d'Arolla (Switzerland) during the ablation season 2001: Measurements and simulations. *Journal of Geophysical Research: Atmospheres (1984–2012)*, *109*(D3).
- Sugden, D. E., McCulloch, R. D., Bory, A. J. M., & Hein, A. S. (2009). Influence of Patagonian glaciers on Antarctic dust deposition during the last glacial period. *Nature Geoscience*, *2*(4), 281-285.
- Sujono, J., Shikasho, S., & Hiramatsu, K. (2004). A comparison of techniques for hydrograph recession analysis. *Hydrological processes*, *18*(3), 403-413.
- Sun, M., Li, Z., Yao, X., Zhang, M., & Jin, S. (2015). Modeling the hydrological response to climate change in a glacierized high mountain region, northwest China. *Journal of Glaciology*, *61*(225), 127-136.
- Swift, D. A., Nienow, P. W., Spedding, N., & Hoey, T. B. (2002). Geomorphic implications of subglacial drainage configuration: rates of basal sediment evacuation controlled by seasonal drainage system evolution. *Sedimentary Geology*, *149*(1), 5-19.
- Swift, D. A., Nienow, P. W., Hoey, T. B., & Mair, D. W. (2005a). Seasonal evolution of runoff from Haut Glacier d'Arolla, Switzerland and implications for glacial geomorphic processes. *Journal of hydrology*, *309*(1), 133-148.
- Swift, D. A., Nienow, P. W., & Hoey, T. B. (2005b). Basal sediment evacuation by subglacial meltwater: suspended sediment transport from Haut Glacier d'Arolla, Switzerland. *Earth Surface Processes and Landforms*, *30*(7), 867-883.
- Syvitski, J. P. (2002). Sediment discharge variability in Arctic rivers: implications for a warmer future. *Polar Research*, *21*(2), 323-330.
- Takeuchi, Y., Kayastha, R. B., & Nakawo, M. (2000). Characteristics of ablation and heat balance in debris-free and debris-covered areas on Khumbu Glacier, Nepal Himalayas, in the pre-monsoon season. *IAHS Publication*, 53-62.
- Takeuchi, N., Kohshima, S., & Seko, K. (2001). Structure, formation, and darkening process of albedo-reducing material (cryoconite) on a Himalayan glacier: a granular algal mat growing on the glacier. *Arctic, Antarctic, and Alpine Research*, 115-122.
- Teller, J. T. (1995). History and drainage of large ice-dammed lakes along the Laurentide Ice Sheet. *Quaternary International*, *28*, 83-92.
- Turowski, J. M., Rickenmann, D., & Dadson, S. J. (2010). The partitioning of the total sediment load of a river into suspended load and bedload: a review of empirical data. *Sedimentology*, *57*(4), 1126-1146.

- Turpin, O. C., Ferguson, R. I., & Clark, C. D. (1997). Remote sensing of snowline rise as an aid to testing and calibrating a glacier runoff model. *Physics and Chemistry of the Earth*, 22(3), 279-283.
- Tweed, F. S., & Russell, A. J. (1999). Controls on the formation and sudden drainage of glacier-impounded lakes: implications for jökulhlaup characteristics. *Progress in Physical Geography*, 23(1), 79-110.
- Uhlmann, M., Korup, O., Huggel, C., Fischer, L., & Kargel, J. S. (2013). Supra-glacial deposition and flux of catastrophic rock-slope failure debris, south-central Alaska. *Earth Surface Processes and Landforms*, 38(7), 675-682.
- Urbini, S., & Baskaradas, J. A. (2010). GPR as an effective tool for safety and glacier characterization: experiences and future development. In *Ground Penetrating Radar (GPR), 2010 13th International Conference on* (pp. 1-6). IEEE.
- van den Broeke, M., Bamber, J., Ettema, J., Rignot, E., Schrama, E., van de Berg, W. J., ... & Wouters, B. (2009). Partitioning recent Greenland mass loss. *science*, 326(5955), 984-986.
- van der Veen, C. J. (2007). Fracture propagation as means of rapidly transferring surface meltwater to the base of glaciers. *Geophysical Research Letters*, 34(1).
- Vatne, G., Etzelmüller, B., Sollid, J. L., & Strand, Ø. R. (1995). Hydrology of a polythermal glacier, Erikbreen, northern Spitsbergen. *Nordic hydrology*, 26(3), 169-190.
- Verbunt, M., Gurtz, J., Jasper, K., Lang, H., Warmerdam, P., & Zappa, M. (2003). The hydrological role of snow and glaciers in alpine river basins and their distributed modeling. *Journal of hydrology*, 282(1), 36-55.
- Walder, J. S. & Fowler, A. (1994). Channelized subglacial drainage over a deformable bed. *Journal of Glaciology*, 40(134). 3-15.
- Warburton, J. (1990). An alpine proglacial fluvial sediment budget. *Geografiska Annaler. Series A. Physical Geography*, 261-272.
- Warburton, J. (2007). Sediment budgets and rates of sediment transfer across cold environments in Europe: a commentary. *Geografiska Annaler: Series A, Physical Geography*, 89(1), 95-101.
- Warburton, J., Beylich, A. A., Etienne, S., Etzelmüller, B., Gordeev, V. V., Käyhkö, J., ... & Tweed, F. S. (2007). Sediment Budgets and Rates of Sediment Transfer across Cold Environments in Europe: Introduction and Background to the European Science Foundation Network 'Sedimentary Source-to-Sink Fluxes in Cold Environments' (Sediflux). *Geografiska Annaler. Series A. Physical Geography*, 1-3.
- Weertman, J. (1973). Can a water-filled crevasse reach the bottom surface of a glacier. *IASH Publication*, 95, 139-145.

- Whalley, W. B. (1979). The relationship of glacier ice and rock glacier at Grubengletscher, Kanton Wallis, Switzerland. *Geografiska Annaler. Series A. Physical Geography*, 49-61.
- Williams, G. P. (1989). Sediment concentration versus water discharge during single hydrologic events in rivers. *Journal of Hydrology*, 111(1), 89-106.
- Willis, I. C., Sharp, M. J., & Richards, K. S. (1990). Configuration of the drainage system of Midtdalsbreen, Norway, as indicated by dye-tracing experiments. *Journal of Glaciology*, 36(122), 89-101.
- Willis, I. C., Richards, K. S., & Sharp, M. J. (1996). Links between proglacial stream suspended sediment dynamics, glacier hydrology and glacier motion at Midtdalsbreen, Norway. *Hydrological Processes*, 10(4), 629-648.
- Willis, I. C., Fitzsimmons, C. D., Melvold, K., Andreassen, L. M., & Giesen, R. H. (2012). Structure, morphology and water flux of a subglacial drainage system, Midtdalsbreen, Norway. *Hydrological Processes*, 26(25), 3810-3829.
- Woo, M. K., & Fitzharris, B. B. (1992). Reconstruction of mass balance variations for Franz Josef Glacier, New Zealand, 1913 to 1989. *Arctic and Alpine Research*, 281-290.
- Young, D. S., Hart, J. K., & Martinez, K. (2015). Image analysis techniques to estimate river discharge using time-lapse cameras in remote locations. *Computers & Geosciences*, 76, 1-10.
- Zemp, M., Haeberli, W., Hoelzle, M., & Paul, F. (2006). Alpine glaciers to disappear within decades?. *Geophysical Research Letters*, 33(13).
- Zhang, Y., Liu, S., & Ding, Y. (2006). Observed degree-day factors and their spatial variation on glaciers in western China. *Annals of Glaciology*, 43(1), 301-306.